Column Flotation Scaling Up
Procedure in Paper De-Inking

Hugo Alberto Hernández – Alvarez

Department of Mining and Metallurgical Engineering

McGill University

Montreal, Quebec, Canada

A thesis submitted to the Faculty of Graduate Studies and Research in partial fulfillment of the requirements of the degree of Doctor of Philosophy.

Advisor:

Prof. James A. Finch

Co - Advisor:

Dr. César Gómez

0-612-70042-9

Abstract

As in mineral processing in the 1980's, column flotation technology has great potential in de-inking of waste paper. Although column flotation shows excellent brightness gain and ink removal efficiency, one problem is the lack of accepted scale-up and design procedure as in mineral flotation. Laboratory and pilot columns were operated on paper pulps to evaluate the effects of gas dispersion and mixing on scale-up. Gas dispersion properties were measured by gas holdup (ε_g), gas rate (J_g) and the derived parameter, bubble surface area flux (S_b). To calculate S_b, bubble size (d_b) was estimated from drift flux analysis. Direct measurement of d_b using a photographic technique supported the estimation. Mixing was modeled by relating the vessel dispersion number (N_d), determined from residence time distribution measurements made using a conductivity technique, to design and operating variables. From the mixing model, the pulp zone flotation rate constant (k_c) was determined from measured ink recovery vs time data. The k_c was correlated with gas dispersion and showed a linear dependence on S_b, supporting recent findings in mineral flotation. A linear relationship was also found with ε_g. The improved reliability of scale-up achieved by incorporating the $k_c \alpha S_b$ relationship is demonstrated.

Résumé

Comme pour le traitement des minéraux des années 1980, la technologie de la colonne de flottation a un grand potentiel pour retirer l'encre du papier. Bien que la colonne de flottation apporte un excellent gain de brillance et une élimination efficace de l'encre, le problème réside sur le fait qu'aucune procédure acceptable à grande échelle et de dimensionnement n'existe, contrairement à la flottation minérale. La colonne de laboratoire et la colonne pilote ont fonctionné avec de la pulpe de papier pour évaluer les effects de la dispersion des gaz et le mélange à grande échelle. Les propriétés de la dispersion des gaz ont été mesurées avec la retenue d'air (ε_g), la vélocité des gaz (J_g) et le paramètre dérivé, qui est l'aire de surface de la bulle (S_b). Pour calculer S_b, la taille de la bulle (d_b) a été estimée en utilisant l'analyse du "drift flux". La mesure directe de d_b, qui est possible grâce à l'utilisation d'une technique photographique, a appuyé l'estimation. La modélisation du mélange a été déterminée selon le nombre de dispersion du récipient (N_d). Celui-ci a été déduit des mesures de temps de résidence en utilisant la conductivité, pour le dimensionnement et les variables d'opération. À partir du modèle de mélange, la constante cinétique de la flottation de la zone pulpe (k_c) a été déterminée par les mesures de récupération de l'encre en fonction du temps. Le k_c a été corrélé avec la dispersion de gaz et a démontré une relation lineaire avec S_b, ce qui confirme les récentes découvertes en flottation de minéraux. Une relation linéaire a également été découverte pour ε_g. On a démontré que l'utilisation de la relation entre k_c et S_b améliorait la fiabilité du dimensionnement.

Resumen

Como en el procesamiento de minerales en los 80's, la tecnología de flotación en columna tiene gran potencial en el destintado de papel. Aunque la columna de flotación muestra una excelente ganancia en brillantez y una eficaz eliminación de tinta, el problema reside en la falta de un aceptable procedimiento para el escalamiento y el diseño como en la flotación de minerales. Columnas de laboratorio y piloto fueron operadas usando pulpa de papel para evaluar los efectos de la dispersión de gas y el mezclado en el escalamiento. Las propiedades de la dispersión de gas fueron medidas con la fracción de aire retenido (ε_g), velocidad de gas (J_g) y el parámetro derivado, area superficial de burbuja (S_b). Para calcular S_b, el tamaño de burbuja (d_b) fue estimado usando el análisis "drift flux". Mediciones directas de d_b usando una técnica fotográfica soportarón la estimación. El mezclado fue modelado con el número de dispersión del recipiente (N_d) determinado a partir de mediciones de tiempo de residencia usando conductividad, para relacionarlo con las variables de operación y diseño. Con el modelo de mezclado, la constante de flotación en la zona de pulpa (k_c) fue determinada con mediciones de recuperación de tinta vs tiempo. La k_c se relacionó con la dispersión de gas y se encontró una dependencia lineal sobre S_b, soportando recientes hallazgos en la flotación de minerales. Una relación lineal también se encontró para ε_g. La ventaja en incorporar la relación $k_c \alpha S_b$ en el procedimiento de escalamiento fue mostrada.

Acknowledgments

I would like to acknowledge my supervisor, Prof. James A. Finch for giving the opportunity to undertake this project and for his enthusiasm, excellent advice and constant support throughout my doctorate studies.

As well, I gratefully acknowledge my co-supervisor Dr. César Gómez for helpful discussions.

I would also like to thank:

My colleagues in the column flotation group (Franklin Cortéz, Ramiro Escudero, Francisco Tavera, Jorge Torrealba, Luis Calzado, Victor Méndez, Claudio Acuña, Jolanda Vergouw, Colin Hardie, Gunther Leichte and Linda Restrepo) for their friendship and help.

The "Mexican Mafia" of the Department of Mining and Metallurgical Engineering (Carlos Léon, Ena Aguilar, David Gloria, Claudia Imperial, José Lemús, María Magaña, Victor Morelos, Juan Hernández and Claudia Rodríguez) for their friendship.

Bowater Pulp and Paper mill for providing equipment and test facilities.

Special thanks are also given to the Consejo Nacional de Ciencia y Tecnología (CONACYT) for the financial support during my PhD studies.

I whish to express my love and appreciation to my parents Francisco Hernández and Ignacia Alvarez who provided the endless support which have allowed me to become the person I am today.

Finally, thanks alone are not sufficient reward for the patience and love that my wife Akiko Hosaka and my baby girl Cecilia Natsumi (born 21/6/2000), have given.

Hugo Hernández

Table of Contents

List of Figures

List of Tables

Nomenclature

ε/d_{pipe} = Relative roughness of the pipe

ρ_{bp} = Density of the bubble-particle aggregate [g/cm^3]

ρ_c = Density of the collection zone [g/cm^3]

ρ_f = Density of the cleaning zone [g/cm^3]

ρ_l = Density of the liquid [g/cm^3]

ρ_{sl} = Density of the pulp [g/cm^3]

μ_l = Viscosity of liquid [Kg/m-s]

μ_{sl} = Viscosity of pulp [Kg/m-s]

ΔL = Distance between two points [cm]

ΔP = Pressure difference [cm of water]

ΔH = Difference in manometer heights [cm]

$E(\theta)$ = Dimensionless concentration

δ = Fraction of the bubble surface covered with solids.

ε_g = Fractional gas holdup

θ = Dimensionless time

τ_l = Liquid residence time [min]

τ_p = Particle residence time [min]

A, B Coefficients or constants

A_c = Cross sectional area of the column [cm^2]

A_s = Sparger surface area [cm^2]

b = Klinkenberg's constant for a given gas and for a given porous medium

C = Concentration of ink [ppm]

C_F = Forchheimer coefficient

C_i = Tracer concentration measured as a function of time [g/L, mol/L]

C_p = Concentration of particles

d_b = Mean bubble diameter [cm]

D_c = Diameter of the column [cm]

d_p = Particle diameter [cm]

d_{pipe} = Inner diameter of the pipe [cm]
E_a = Attachment efficiency [%]
E_c = Collision efficiency [%]
E_k = Collection efficiency [%]
E_l = Liquid axial dispersion coefficient [cm^2/s]
f = Friction factor
g = Gravity acceleration [m/s^2]
J_g = Superficial gas velocity [cm/s]
J_l = Superficial liquid velocity [cm/s]
k_c = Flotation rate constant [1/min]
k_{fc} = Overall flotation rate constant [1/min]
K_g = Permeability of the medium to a gas completely filling the pores of the medium [m^2]
K_l = Permeability of the medium to a single liquid phase completely filling the pores medium [m^2]
L = Level [cm]
L_c = Height of the column [cm]
L_s = Length of the sparger [cm]
M = Mass units of tracer [kg]
n = Number of bubbles per unit time
N_d = Vessel dispersion number
P_m = Algebraic sparger mean pressure [Pa]
Q_g = Gas volumetric flow rate [L/min]
Q_l = Liquid volumetric flow rate [L/min]
Q_{TP} = Flow rate adjusted to temperature and pressure [L/min]
r = Sparger radius
R_c = Fractional collection zone recovery
Re_b = Reynolds number of the bubble
Re_{bs} = Reynolds number of the bubble swarm
R_f = Fractional froth zone recovery
R_{fc} = Fractional overall flotation column recovery

R_{ink} = Fractional ink recovery

S = Consistency of the paper pulp [%]

S_b = Bubble surface area flux [1/s]

T = Temperature [°C]

U_{bt} = Terminal velocity of a bubble [cm/s]

U_l = Interstitial liquid velocity [cm/s]

U_{slip} = Slip velocity between two phases [cm/s]

V_c = Column volume occupied by the liquid [cm^3]

Z = Vertical coordinate directed downward

CHAPTER I

Introduction

1.1 Principles of Paper De-inking

De-inking is defined as any process which removes dispersed ink from wood pulp suspensions. The term also includes non-fibrous materials like coatings, adhesives, resins, glass, rocks, staples and tramp metal (Watson, 1996; Petri, 1994; Smook, 1992; and Dorris, 1989). Crow and Secor (1987) identify ten basic stages in the de-inking process.

1. Pulping
2. Pre-washing
3. Screening
4. Reverse cleaning
5. Forward cleaning
6. Washing
7. Flotation
8. Dispersion
9. Blanching
10. Water re-circulation

A typical de-inking flowsheet is shown in Figure I.1. De-inking plants may have some or all of these steps in various sequences. The most important operations are high-consistency pulping, coarse and fine cleaning and flotation (Stevenson, 1992). Bowater Pulp and Paper Canada in Gatineau, Quebec, is an example of a de-inking plant. Figure I.2 shows the flotation cells at Bowater. The de-inking section processes a mixture of 70% old newspapers (ONP) and 30% old magazines (OMG) and has a recycled capacity of 600 t/d (Veilleux *et al.* 2000).

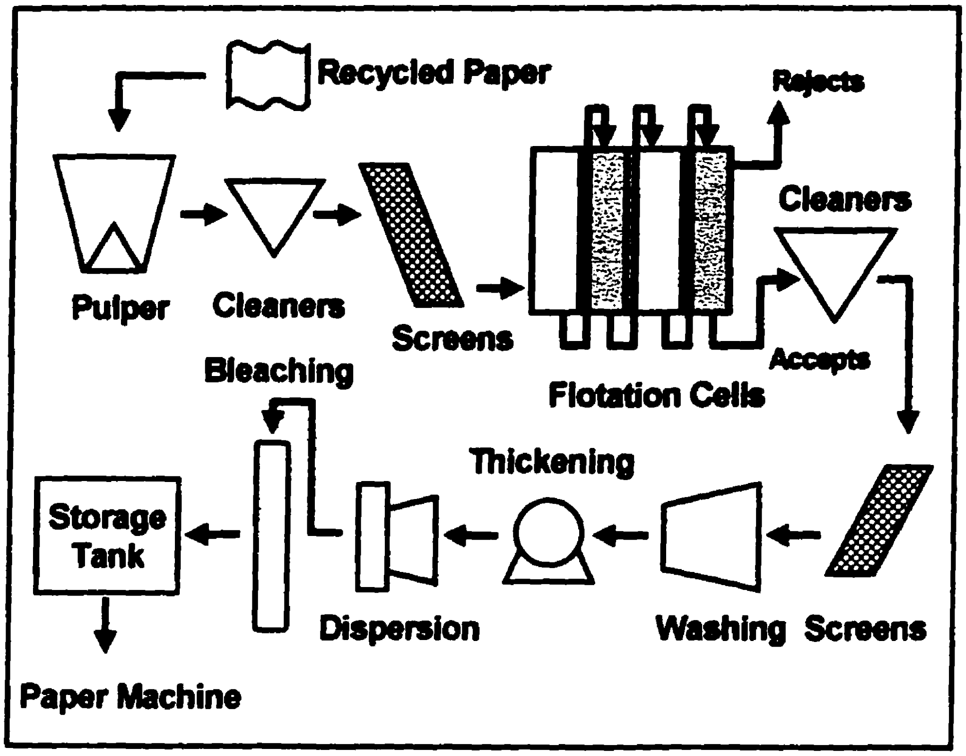

Figure I.1 A typical de-inking mill flowsheet

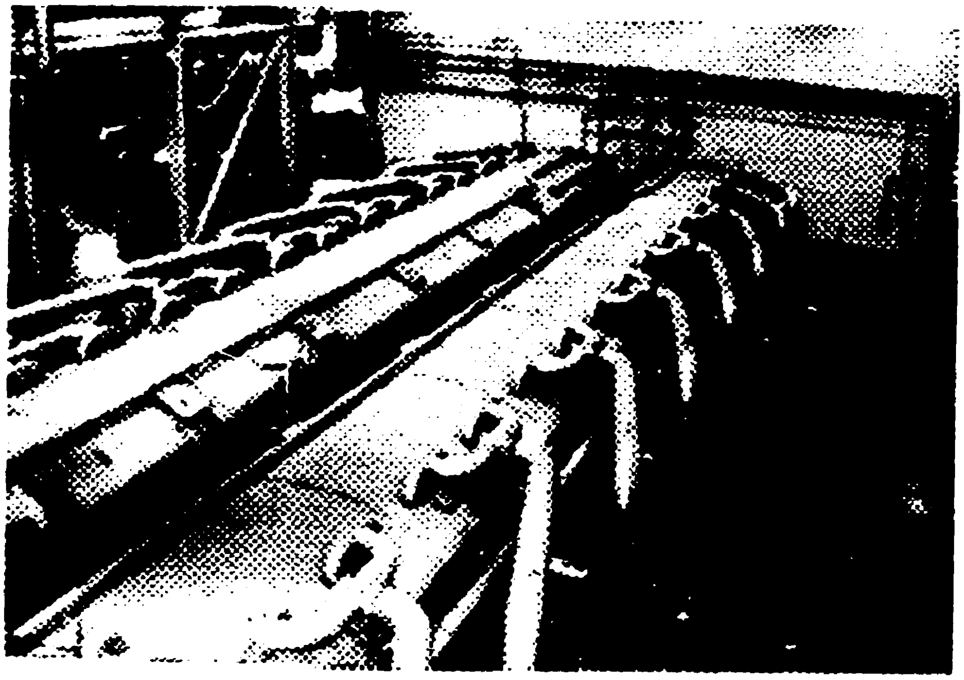

Figure I.2 Flotation cells at Bowater Pulp & Paper, Gatineau Qc.

In mineral processing ore is crushed and ground to liberate minerals to facilitate froth flotation or other separation techniques. **High-consistency** pulping where ink particles are liberated from the fiber is equivalent to comminution in mineral processing. The recycled wastepaper is mixed with water and chemicals in a pulper where shear forces break the mixture into a fibrous pulp which releases the ink. The operation takes place at elevated temperature (40 - 55 °C) and alkaline conditions (pH 9 - 12). The reagents include sodium hydroxide (NaOH) to increase the pH, hydrogen peroxide (H_2O_2) to prevent yellowing of fibers caused by NaOH, and fatty acid soaps (surfactants) which act as both frother and collector (Mak & Stevens, 1993). De-inking involves formation of micro-precipitates of <ink – fatty acid – calcium ions> linked to a fatty acid coated air bubble. Figure I.3 from Putz *et al.* (1993) shows a schematic model of air bubble-ink particle attachment.

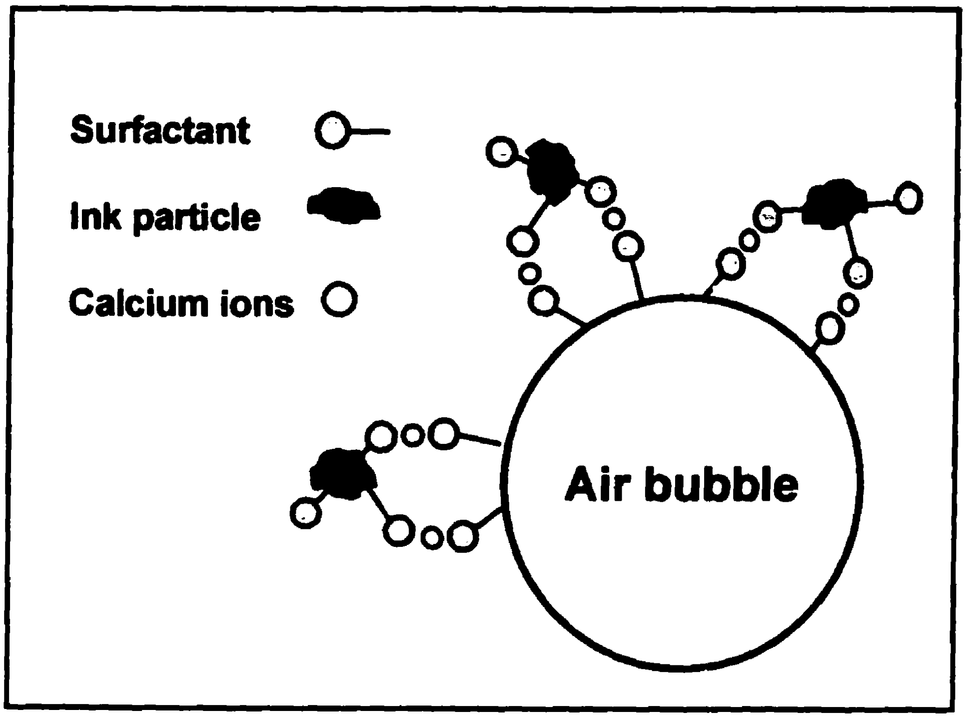

Figure I.3 Model of air bubble-particle attachment in a de-inking system.

In the **Coarse cleaning** stage the accepts from the pulpers are passed through primary, secondary and tertiary screens. The primary screen initially removes large contaminants like plastic bags, cans, wire, etc. The secondary screens consist of high-density cleaners which remove staples, sand, and pieces of glass. Finally the tertiary screens remove large ink particles, plastic, and pieces of glue.

Flotation is one of the most important processes in a waste paper recycling mill, providing a low cost and effective means of removing ink particles (Robertson *et al.*, 1998; Hardie, 1998; Watson *et al.*, 1996; Walmsley, 1992). The ink particles must be large enough to efficiently collide with an air bubble yet small enough that the bubble-particle aggregate can ascend to the flotation cell surface (Ackermann, 1993). Flotation de-inking removes ink particles in the size range roughly 10 - 100 µm (Lindsay & Mostafa, 1995). A schematic of the separation process is shown in Figure I.4.

As in mineral flotation, Zabala and McColl (1968) divided the process into three steps (typical micro processes):

Collision between the ink particle and the air bubble	⇒	Attachment between the ink particle and air bubble	⇒	Rise of the ink particle-bubble aggregate to the surface

The design of a flotation process and selection of equipment aims to maximize ink (contaminant) removal and minimize fiber loss as shown in Figure I.5.

The efficiency of flotation de-inking is measured by brightness gain. Brightness is the fraction of incident light (typically at a wavelength of 457 nm) reflected from a prepared paper sheet.

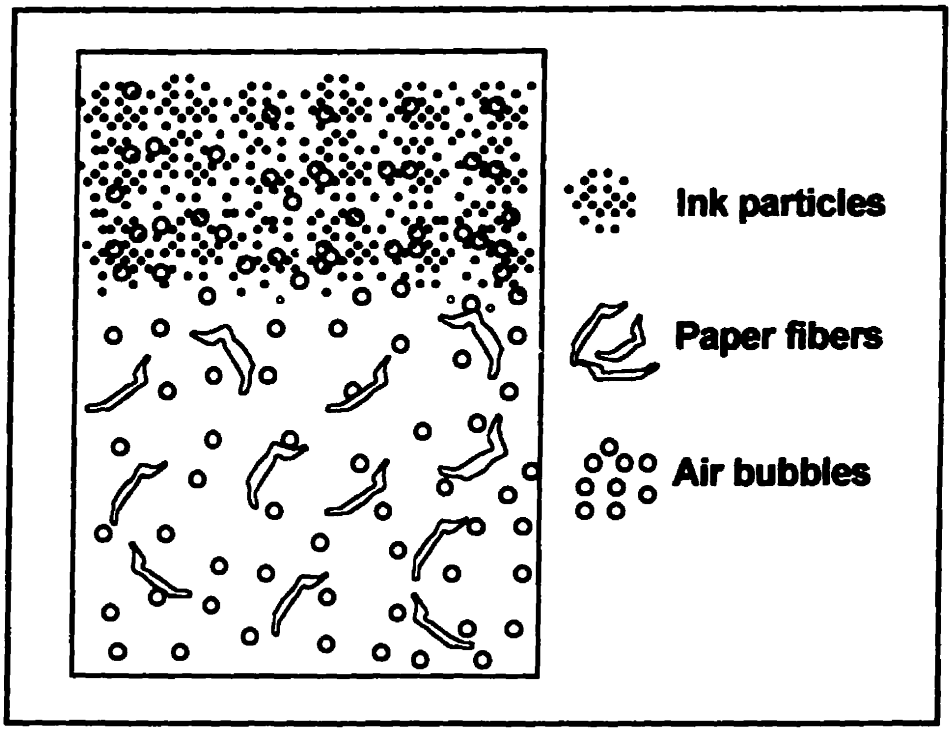

Figure I.4 Basic operating principle of flotation de-inking.

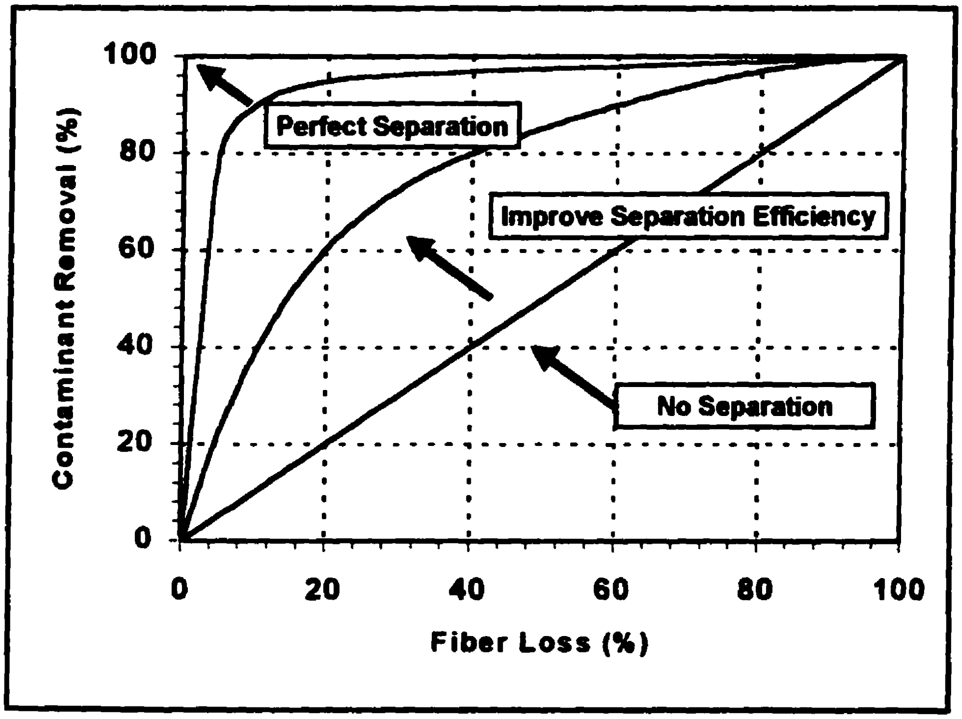

Figure I.5 Separation of fiber and contaminants. (Spangenberg, 1993)

Fine cleaning is a three-step operation designed to maximize the cleaning efficiency at low pulp consistencies. The objective is to remove the lighter contaminants (rejects) such as glue, plastic and light ink compounds from the paper fibers (accepts) using centrifugal lightweight cleaners. The accepts are then treated with five stages of forward cleaners in order to remove sand. Finally, the accepts are passed through three stages of fine (e.g. 0.008 in) screens.

1.2 Flotation of Waste Paper

Paper recycling helps conserve forest resources. To produce one tonne of paper from primary sources requires approximately 1.15 to 1.6 tonnes of waste paper. The demand for recycled paper has been increasing over the past years in North America. The United States and Canada had a recovery rate of 33 and 25%, respectively, in 1990 (Recovery rate is the amount of waste paper recovered for re-use compared with paper consumed.) Countries without forest reserves have recoveries as high as 50% (Smook, 1992).

Flotation has been used in the mineral industry since the late-19th century (AIME, 1962). Kowalewski and Hines (Patent 2005742, 1932) developed the concept for waste paper de-inking in the 1930's and in the 1960's, mineral flotation systems were adapted (Lindsay & Mostafa, 1995).

In the 1980's column flotation was introduced commercially in mineral flotation. There is an interest among some pulp and paper companies in Canada to adapt column flotation technology for waste paper de-inking (Anonymous, 1997; Bailey, 1997; Dessureault *et al.,* 1995; Carabin *et al.*, 1995). Flotation columns have shown excellent results in brightness gain and ink removal (Leichtle, 1998; Watson, 1996; Carabin *et. al.*, 1995; Petri, 1994).

1.3 The Flotation Column

Column flotation is arguably the most important technological innovation in flotation machinery over the last fifty years (Wills, 1992; Pal & Masliyah, 1990; Murdock, 1991; Ynchaustl *et al.*, 1988). A flotation column in a de-inking application is illustrated in Figure I.6. It is a tall vertical reactor with two distinct zones: the collection zone (recovery zone) and the froth zone (cleaning zone). Feed (recycled paper pulp) is introduced to the collection zone below the interface. The descending paper pulp contacts a rising swarm of air bubbles generated by a sparger (bubble generator) system located near the bottom of the column. Hydrophobic ink particles collide with and attach to bubbles, and are transported to the froth zone to form the rejects stream. Hydrophilic fiber and other particles are removed from the bottom of the column to form the accepts stream.

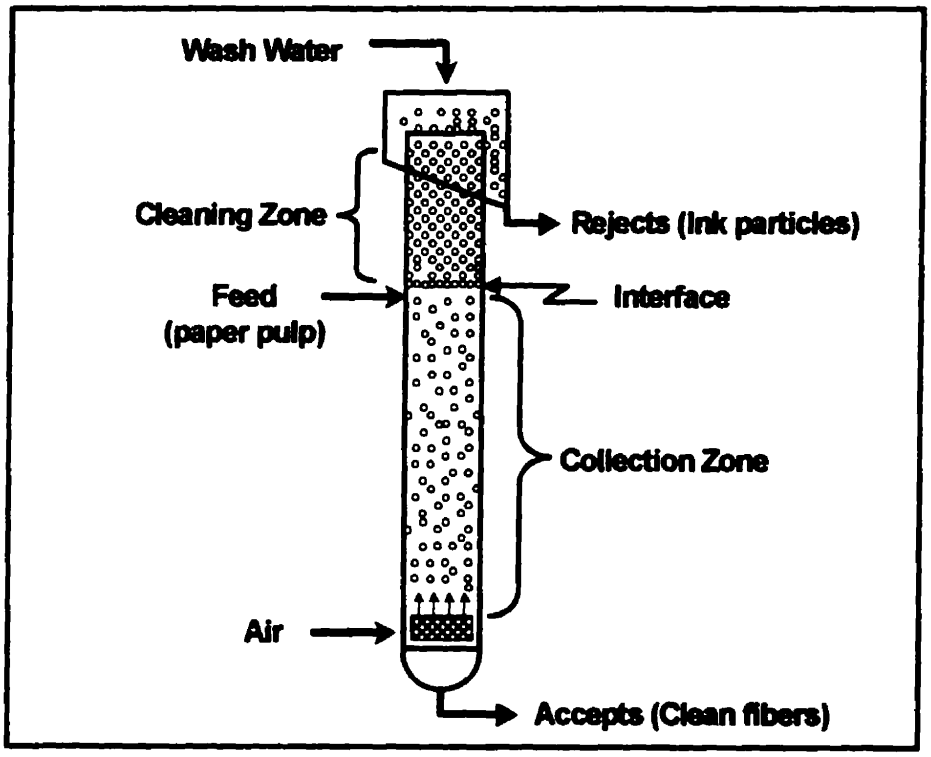

Figure I.6 Schematic diagram of a flotation column in a de-inking process.

De-inking is a reverse flotation process where the non-value component (ink) is floated. Wash water is added at the top to stabilize the froth and to reduce hydraulic entrainment of fibers into the overflow (Robertson *et al.*, 1998). This water replaces the feed water in the froth, which otherwise carries hydrophilic fiber particles into the rejects. The net flow of water moving through the froth zone is called the bias (by convention, bias is positive if the flow is downwards).

Flotation columns have some advantages and disadvantages:

Advantages:

- High ink removal efficiency with low fiber loss, related to use of wash water
- Low floor space requirement
- Low capital and operating costs

Disadvantages:

- Maintenance/reliability of bubble generation devices
- Scale-up requirements adaptation to paper pulp characteristics

Though flotation columns are simple in operation, construction and maintenance, their design for a particular duty can be difficult (Deckwer & Schumpe, 1993; Ityokumbul, 1992b). The design, or scale-up, is the subject of this thesis.

1.4 Research Project Objectives

The general objective is to modify the scaling-up procedure for flotation columns to incorporate gas dispersion characteristics and paper pulp properties in the paper de-inking process. This involves the following specific objectives:

- Determination of the effect of paper pulp consistency on gas dispersion.
- Modelling vessel dispersion number (N_d) for paper pulp systems.
- Relating the flotation rate constant to bubble surface area flux.
- Estimation of paper pulp viscosity.
- Characterization of the bubble generator device.

1.5 Thesis Outline

This work has been organized in a series of chapters and appendixes. In **Chapter I**, the general characteristics of the paper de-inking process are discussed with a short introduction to flotation columns. The objectives of the research project are included. In **Chapter II**, theoretical aspects of the flotation column scale-up procedure are described. This includes using bubble surface area flux as a variable. Mixing and characterization of rigid spargers using the Darcy model are discussed. The chapter includes details on the equipment and instrumentation used. In **Chapter III,** the results of characterization of the spargers are given. In **Chapter IV,** the experimental work and results of estimating paper pulp viscosity are given including a novel back-calculation method employing a direct (photographic) measure of bubble size. **Chapter V** shows the effect of paper pulp consistency on gas dispersion parameters including gas holdup, bubble size and surface area flux. In **Chapter VI**, a mixing model, an expression for vessel dispersion number as a function of design/operating variables, is presented. **Chapter VII** includes the results and discussion of the proposed scale up procedure. In **Chapter VIII**, contributions to knowledge are given. Finally, all experimental data are presented in the **Appendices**.

CHAPTER II
Column Flotation Scale-Up

2.1 Introduction

In this chapter the various components required in scale-up are introduced based on the work of various authors (O'Connor & Mills, 1995; Deckwer & Schumpe, 1993; Luttrel *et al.*, 1993; Ityokumbul, 1992a, 1992b; Wilkinson *et al.*, 1992; Ynchausti *et al.*, 1988; Yianatos *et al.*, 1988a; Dobby & Finch, 1986a; Shah *et al.*, 1982; Flint, 1973). A reliable scale-up procedure must address two important areas: cell geometry (height and diameter), and the air sparging device. As described in **Chapter I**, in a flotation column there are two distinct zones: the collection zone and the cleaning zone. It is necessary to study each zone separately and their interaction as part of the design problem (Dobby & Finch, 1986a). This chapter will start by describing these zones.

2.2 Collection Zone

Particle recovery takes place in this zone. The degree of mixing, the flotation rate constant and residence time of the particles determine the collection zone recovery $\mathbf{R_c}$. For design, the mixing conditions in a flotation column, for example summarized in the vessel dispersion number $\mathbf{N_d}$, must be known. Plug flow ($\mathbf{N_d} \rightarrow 0$) is one condition where all elements of the fluid and particles have the same residence time. The other extreme ($\mathbf{N_d} \rightarrow \infty$) is a perfectly mixed reactor, where the elements show a different residence time. Laboratory column flotation units with large height-to-diameter ratios approach plug flow, while in plant columns the liquid and solids are transported closer to a perfectly mixed condition (Finch & Dobby, 1990). Mixing in practice is between plug flow and perfectly mixed flow.

The vessel dispersion number for the liquid (N_d), is defined as:

$$N_d = \frac{E_l}{U_l * L_c} \qquad (II.1)$$

where:

E_l = Liquid axial dispersion coefficient, cm^2/s

U_l = Interstitial liquid velocity, cm/s and expressed as follows:

$$U_l = \frac{J_l}{(1-\varepsilon_g)} \qquad (II.2)$$

where:

J_l = Superficial liquid velocity, cm/s

ε_g = Fractional gas holdup.

A number of papers have been published on the mixing characteristics of liquids, solid particles and bubbles in columns. Table II.1 is a comprehensive list of vessel dispersion number correlations.

Table II.1 Correlation for liquid phase dispersion number.

Reference	Correlation	Range of Variables
Mavros & Dannilidou (1993)	$N_d = 0.0194 \cdot \exp(0.267 \cdot d_c) \cdot U_l^{-0.56}$	$d_c \le 14$ cm $0.5 \le J_g \le 3.0$ cm/s
Mankosa *et al.* (1992)	$N_d = 1.66 \cdot \left(\frac{d_c}{L_c}\right)^{0.63} \left(\frac{J_g}{U_l}\right)^{0.5}$	$5 \le d_c \le 10$ cm
Xu & Finch (1991)	$N_d = 0.56 \cdot \left(\frac{d_c}{L_c} \cdot \frac{J_g}{J_l} \cdot U_{slip}\right)^{0.41}$	$d_c = 10$ cm, $0.5 \le J_g \le 2.3$ cm/s
Finch & Dobby (1990)	$N_d = \frac{0.063 \cdot D_c \cdot \left(\frac{J_g}{1.6}\right)^{0.3}}{\left(\left(\frac{J_{sl}}{(1-\varepsilon_g)}\right) + U_{ps}\right) \cdot L_c}$	$8 \le d_c \le 100$ cm $0.5 \le J_g \le 2.0$ cm/s
Mankosa (1990)	$N_d = 1.43 \cdot \left(\frac{d_c}{L_c} \cdot \frac{J_g}{U_l}\right)^{0.622}$	$5 \le d_c \le 10$ cm
Luttrell *et al.* (1990)	$N_d = 1.85 \cdot \left(\frac{d_c}{L_c} \cdot \frac{J_g}{J_l}\right)^{0.63}$	$5 \le d_c \le 10$ cm
Matsumoto *et al.* (1989)	$N_d = 9.4 \cdot \left(\frac{1 + 0.55 \cdot (\varepsilon_g \cdot J_l)^{0.75}}{J_l \cdot L_c}\right) \cdot \left[(1-A) \cdot d_c^3 \cdot \varepsilon_g\right]^{0.5}$ $A = \left(\frac{\varepsilon_g \cdot J_l}{(1-\varepsilon_g) \cdot J_g}\right)$	
Laplante *et al.* (1988)	$E_l = 2.98 \cdot d_c^{0.33} \cdot \exp(-0.025 \cdot S)$	S = % sol. Wt $8 \le d_c \le 100$ cm $0.5 \le J_g \le 2.0$ cm/s
Kawase & Moo-Young (1986)	$N_d = 0.342 \cdot n^{-8/3} \cdot Fr^{-1/3}$	$0.625 \le n \le 1$ $2E\text{-}5 \le Fr \le 0.5$
Kelkar *et al.* (1983)	$E_l \cdot (1-\varepsilon_g) = 1.42 \cdot d_c^{1.33} \cdot \left(J_g - \frac{\varepsilon_g \cdot J_l}{1-\varepsilon_g}\right)^{0.73}$	$d_c = 15.4, 30$ $1 \le J_g \le 30$ cm/s $0 \le J_l \le 15$ cm/s
Riquarts (1981)	$N_d = \frac{\left(\frac{J_g \cdot d_c \cdot \rho_l}{\mu_l}\right)^{1/8}}{14.7 \cdot Fr^{3/8}}$	
Joshi (1980) Joshi & Sharma (1979)	$E_l = 0.31 \cdot d_c \cdot [3 \cdot (d_c \cdot (J_g - \varepsilon_g \cdot U_{slip}))]^{0.33}$	$10 \le dc \le 106.7$ cm $1 \le J_g \le 39$ cm/s $0 \le J_l \le 12$ cm/s
Todt *et al.* (1977)	$N_d = 0.166 \cdot (1-\varepsilon_g) \cdot U_{slip} \cdot \frac{d_c}{L_c} \cdot \left(\frac{J_g}{J_l}\right)^{0.31}$	$d_c = 14$ cm
Baid & Rice (1974)	$E_l = 0.35 \cdot d_c^{4/3} \cdot (g \cdot J_g)^{1/3}$	$8.2 \le dc \le 153$ cm $0.3 \le J_g \le 45$ cm/s
Deckwer *et al.* (1974)	$E_l = 0.678 \cdot d_c^{1.4} \cdot J_g^{0.3}$	
Kato & Nishiwaki (1972)	$N_d = \frac{1 + 6.5 \cdot Fr^{0.4}}{13 \cdot Fr^{0.5}}$	$0 \le Fr \le 0.16$ $d_c \ge 12.2$ cm

A relationship between collection zone recovery and residence time assuming first-order kinetics for the particle collection process and particles moving according to the axial dispersion model (Levenspiel, 1999) is:

$$R_c = 1 - \frac{4 * A * \exp\left(\frac{1}{2 * N_d}\right)}{(1+A)^2 * \exp\left(\frac{A}{2 * N_d}\right) - (1-A)^2 * \exp\left(\frac{-A}{2 * N_d}\right)} \quad (II.3)$$

where:

$$A = (1 + 4 * k_c * \tau_p * N_d)^{\frac{1}{2}} \quad (II.4)$$

N_d = Vessel dispersion number and is given by equations in Table II.1.

The particle (τ_p) and liquid (τ_l) retention time can be estimated from:

$$\tau_p = \frac{\tau_l * \left(\frac{J_l}{(1-\varepsilon_g)}\right)}{\frac{J_l}{(1-\varepsilon_g)} + U_{ps}} \quad (II.5)$$

$$\tau_l = \frac{L_c * (1-\varepsilon_g)}{J_l} = \frac{V_c}{Q_l} \quad (II.6)$$

where:

L_c = Height of column recovery zone, cm

Q_l = Volumetric flowrate of the liquid, cm^3/s

V_c = Volume of the column occupied by the liquid, cm^3

J_l is defined as:

$$J_l = \frac{Q_l}{A_c} = \frac{\text{volumetric flowrate of liquid, cm}^3/\text{s}}{\text{column cross-sectional area, cm}^2} \qquad (II.7)$$

Equation II.3 under plug flow conditions ($N_d \rightarrow 0$) reduces to:

$$R_c = 1 - \exp\left(-k_c * \tau_p\right) \qquad (II.8)$$

and for a perfect mixer ($N_d \rightarrow \infty$), recovery is:

$$R_c = 1 - \frac{1}{1 + k_c * \tau_p} \qquad (II.9)$$

A quasi-fundamental interpretation of the rate constant k_c can be derived by introducing the concept of collection efficiency, namely the fraction of all particles swept out by the projected area of the bubble that collide with, attach to and remain attached to a bubble until it reaches the cleaning zone. Ignoring detachment - appropriate for a quiescent system such as a flotation column operating with particle sizes much less than the bubble size (Dobby & Finch, 1986b) - the collection efficiency, E_k, is the product of collision efficiency (E_c) and attachment efficiency (E_a).

$$E_k = E_c * E_a \qquad (II.10)$$

The collection efficiency is a function of three main parameters: particle diameter, bubble size and particle hydrophobicity. The E_k is related to the flotation rate constant, k_c, as follows.

Assuming first-order kinetics Jameson *et al.* (1977) derived:

$$-\frac{dC_p}{dt}=\frac{1.5*J_g*E_k*C_p}{d_b} \qquad (II.11)$$

where:

C_p = Concentration of particles

d_b = Mean bubble diameter, cm

J_g = Superficial gas velocity and is given by:

$$J_g=\frac{Q_g}{A_c}=\frac{\text{volumetric flowrate of air, cm}^3/\text{s}}{\text{column cross - sectional area, cm}^2} \qquad (II.12)$$

The flotation rate constant is:

$$k_c=\frac{1.5*J_g*E_k}{d_b} \qquad (II.13)$$

2.3 Cleaning Zone

The hydrodynamics and particle transport in the cleaning zone are not well understood. They are dependent upon such factors as gas flow rate, bubble size, solid content and bias rate (Dobby & Finch, 1986a). Particles are transported from the collection zone to the froth zone as particle–bubble aggregates. A portion of particles within the froth is dislodged from the bubbles as a result of coalescence and reports back to the collection zone. This phenomena is called froth drop back and, its complement, froth zone recovery, R_f (Finch & Dobby, 1990). Figure II.1 shows the interaction between the collection zone and cleaning zone.

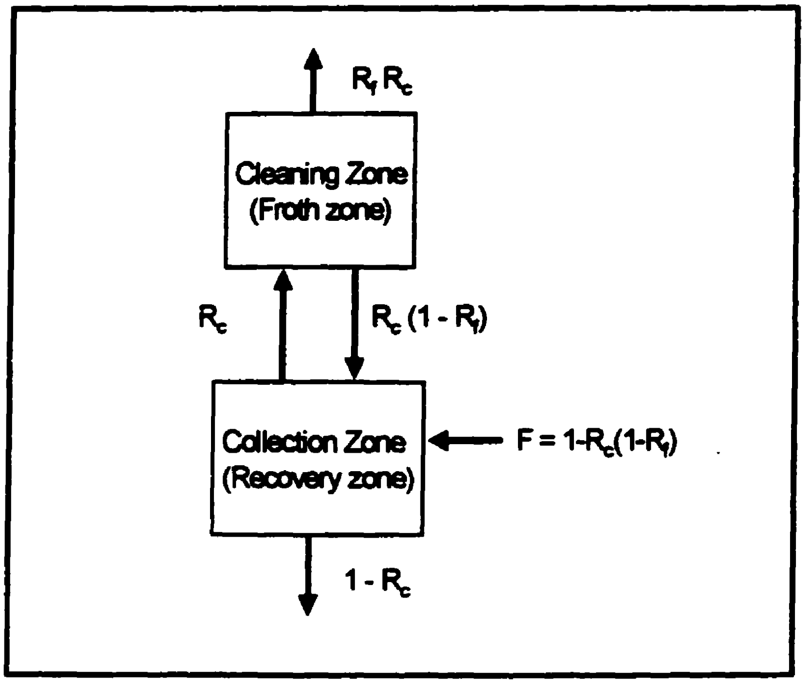

Figure II.1 Conceptual interaction between the collection and cleaning zones.

The overall flotation column recovery (**R_{fc}**), is given by:

$$R_{fc} = \frac{R_f * R_c}{1 - R_c * (1 - R_f)} \qquad (\text{II}.14)$$

Assuming the particle collection process follows first order kinetics and particles move in plug flow, **R_{fc}** can be related to an overall rate constant, **k_{fc}**, (this is a good approximation for a lab column with a large **L_c/D_c** ratio and with no froth layer):

$$R_{fc} = 1 - \exp\left(-k_{fc} * \tau_p\right) \qquad (\text{II}.15)$$

The term **k_{fc}** is related to **k_c** by substituting Equations II.15 and II.8 into II.14 and canceling terms to give:

$$k_{fc} = \frac{1}{\tau_p} * Ln\left[\exp(k_c * \tau_p) * R_f + 1 - R_f\right] \qquad (II.16)$$

when transport is close to perfectly mixed, as approached with small L_c/D_c ratio, R_{fc} is given only if there is no froth layer by:

$$R_{fc} = 1 - \frac{1}{1 + k_{fc} * \tau_p} \qquad (II.17)$$

In this case, substituting Equations II.17 and II.9 into II.13 gives the following:

$$k_{fc} = k_c * R_f \qquad (II.18)$$

Figure II.2 shows the interdependence of the variables on overall flotation recovery.

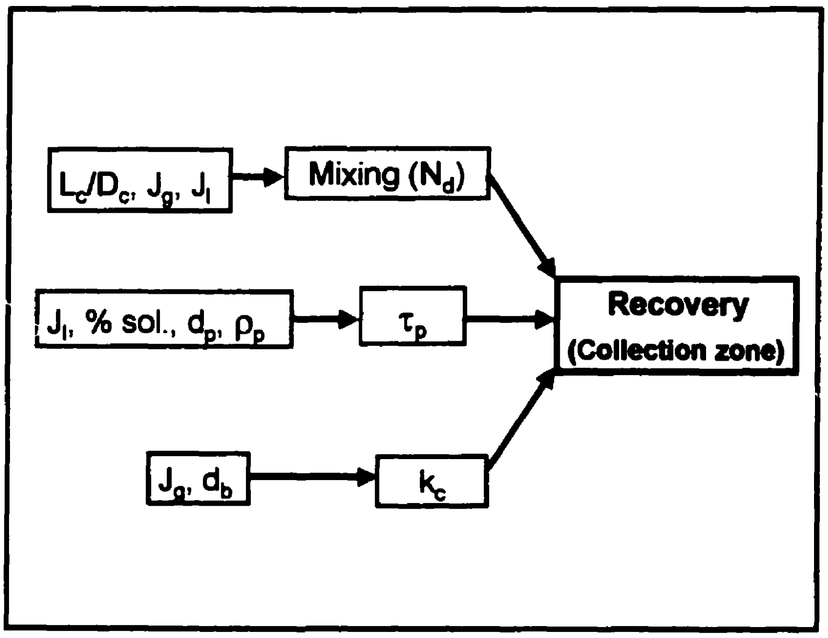

Figure II.2 Interdependence of the variables which control column flotation recovery performance

Following is one scale-up procedure:

1.- Measure k_c and carrying capacity (C_a) in lab unit processing the system of interest
2.- Assume a column diameter (D_c) and calculate cross sectional area (A_c)
3.- Calculate J_l from Equation II.7
4.- Calculate τ_l from Equation II.6 (assume ε_g used in lab test)
5.- Calculate U_{slip} from Masliyah's Equation (Equation II.23, next section)
6.- Calculate τ_p from Equation II.5 then calculate N_d.
7.- Calculate R_c from Equation II.3 and calculate R_{fc} from Equation II.14 (assume R_f)
8.- To have the same R_c in the plant column as obtained in lab units, τ_p must be increased assuming k_c remains constant. The new column geometry can be determined by substituting the corrected τ_p into Equation II.5.

The main problem in step 7 is ensuring k_c remains constant. The criterion claimed for this is that the same gas holdup – gas rate values in the full size unit should be the same as in the laboratory or pilot column used to generate the scale-up data (Finch & Dobby, 1990). A more recent criterion is to preserve the same bubble surface area flux, S_b (Leichtle, 1998). To provide the same S_b is largely the function of the bubble generating system. A method of scaling up spargers to preserve the S_b in a full size column is required (Leichtle, 1998; Escudero *et al.*, 1997). It is postulated in this thesis that it is necessary to incorporate S_b in scaling up a flotation column.

2.4 Bubble Surface Area Flux (S_b)

Bubble surface area flux or bubble surface area generation rate is the surface area of air bubbles generated per unit time per unit cross-sectional area of a flotation cell ($m^2/m^2/s$) (Finch and Dobby, 1990). This variable controls the collection zone rate constant (Gorain *et al.*, 1997; Luttrell *et al.*, 1993). The S_b is not measured directly, but is calculated from the bubble diameter (d_b) and superficial air velocity (J_g):

$$S_b = \frac{6 * J_g}{d_b} \qquad (\text{II.19})$$

Based on Figure II.3, this expression is obtained, as follows:

$$S_b = \frac{n * S}{A_c} = \frac{\left(\dfrac{6 * Q_g}{\pi * d_b{}^3}\right) * \left(\pi * d_b{}^2\right)}{A_c} \qquad (\text{II.20})$$

where:

n = Number of bubbles per unit time of mean size d_b (assumed spherical)

d_b = Mean bubble size, cm

S = Surface area of an individual bubble, cm^2

A_c = Column cross-sectional area, cm^2

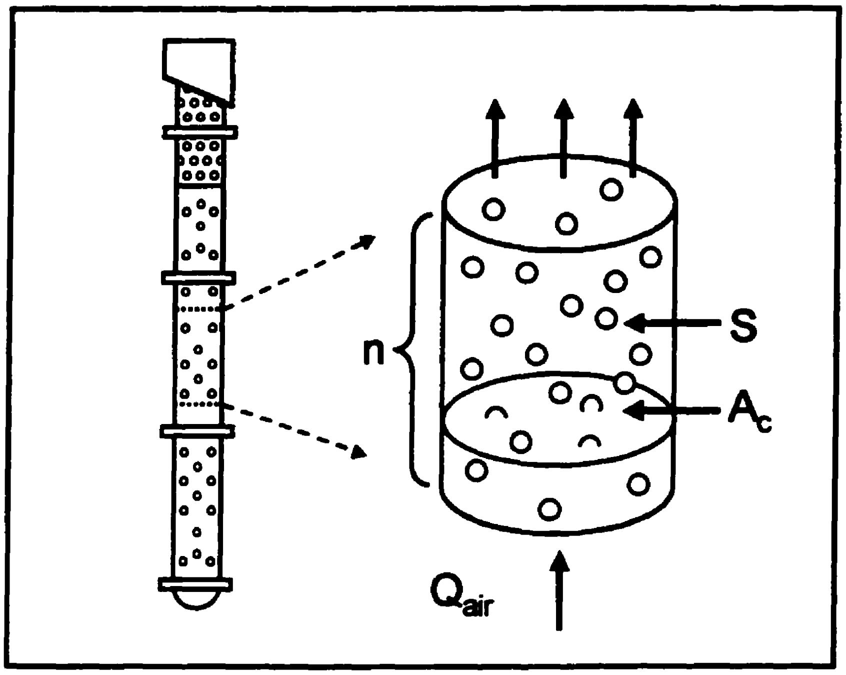

Figure II.3 Diagram representing concept of bubble surface area flux.

Combining, Equations II.13 and II.19 reduce Equation II.8 to:

$$k_c = \frac{E_k * S_b}{4} \qquad (II.21)$$

Equation II.21 gives insight into how to preserve $\mathbf{k_c}$: assuming $\mathbf{E_k}$ is preserved the sparging system in a full-scale column must provide the same $\mathbf{S_b}$ as the laboratory unit to yield the same rate constant. Figure II.4 shows a modified methodology to estimate flotation recovery in the scaling-up procedure. The main problem in estimating $\mathbf{S_b}$ is knowing the size of the bubble ($\mathbf{d_b}$). There are indirect and direct methods to determine the size of the bubble; the former is described next.

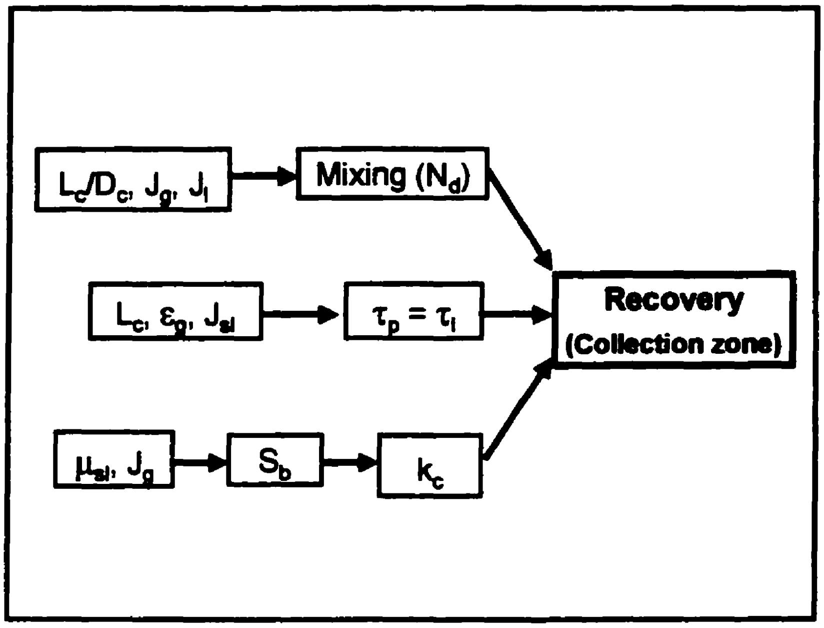

Figure II.4 Modified Figure II.2: Methodology to estimate flotation recovery incorporating $\mathbf{S_b}$.

2.5 Drift Flux Analysis

Drift flux analysis (Wallis, 1969) considers the relative phase velocity (slip velocity) and has been widely used to estimate mean bubble size in flotation columns (Banisi & Finch, 1994; Yianatos *et al.*, 1988b). In the case of a flotation column, the appropriate expression for the relative slip velocity ($\mathbf{U_{slip}}$) between the gas phase and the liquid phase is:

$$U_{slip} = \frac{J_g}{\varepsilon_g} + \frac{J_l}{1-\varepsilon_g} \qquad (\text{II}.22)$$

where:

ε_g = Fractional gas holdup

J_g, J_l = Superficial velocities of the gas and liquid respectively, cm/s

The slip velocity is given in terms of the system properties by an expression due to Masliyah (1979) after Richardson & Zaki (1954):

$$U_{slip} = \frac{g * d_b^2 * (\rho_{sl} - \rho_{bp}) * (1 - \varepsilon_g)^{m-1}}{18 * \mu_{sl} * (1 + 0.15 * Re_{bs}^{0.687})} \qquad (II.23)$$

where:

μ_{sl} = Viscosity of the slurry (pulp), g/cm-s

ρ_{sl}, ρ_{bp} = Densities of the slurry (pulp) and the bubble-particle aggregate receptively, gr/cm^3.

Assuming spherical bubbles and particles, and that a particle occupies a square area of side $\mathbf{d_p}$, the following expression for ρ_{bp} is derived:

$$\rho_{bp} = \frac{\delta * \pi * d_p * \rho_p}{d_b + \delta * \pi * d_p} \qquad (II.24)$$

where δ is the fraction of the bubble surface covered with solids.

The bubble swarm Reynolds number is calculated as:

$$Re_{bs} = \frac{d_b * U_{slip} * \rho_{sl} * (1 - \varepsilon_g)}{\mu_{sl}} \qquad (II.25)$$

and **m** is a function of the Reynolds number of the bubble ($\mathbf{Re_b}$):

$$m = \left(4.45 + 18 * \frac{d_b}{d_c}\right) * Re_b^{-0.1} \qquad 1 < Re_b < 200 \qquad (II.26)$$

$$m = 4.45 * Re_b^{-0.1} \qquad 200 < Re_b < 500 \qquad (II.27)$$

$$Re_b = \frac{U_{bt} * \rho_{sl} * d_b}{\mu_{sl}} \qquad (II.28)$$

The value of **m** in most cases is approximately 3 (Banisi & Finch, 1994). Shah *et al.* (1982) suggest that for ε_g less than 30% the drift flux relationship of Richarson and Zaki (Equation II.21) is the suitable expression for relating slip velocity to terminal velocity U_{bt}:

$$U_{slip} = U_{bt} * (1-\varepsilon_g)^{m-1} \qquad (\text{II.29})$$

Combining Equations II.22 and II.29 and rearranging yields:

$$U_{bt} = \frac{\left(\frac{J_g}{\varepsilon_g} + \frac{J_l}{(1-\varepsilon_g)}\right)}{(1-\varepsilon_g)^{m-1}} \qquad (\text{II.30})$$

Equation II.30 is best reserved for large diameter columns to avoid wall effects (Dobby *et al.*, 1988). Combining Equations II.24 and II.29 and rearranging yields:

$$U_{bt} = \frac{g * d_b^{\,2} * (\rho_{sl} - \rho_{bp})}{18 * \mu_{sl} * \left(1 + 0.15 * Re_{bs}^{\,0.687}\right)} \qquad (\text{II.31})$$

Equation II.31 is one form of the relationship:

$$U_{bt} = \sqrt{\frac{4 * g * d_b}{3 * C_D}} \qquad (\text{II.32})$$

where C_D is the drag coefficient of the gas bubbles.

There have been a variety of expressions proposed for C_D (Table II.2). Zhang *et al.* (1999) recently provided experimental support for the expression of Karamanev *et al.*

Table II.2 Expression given for C_D.

Turton & Levenspiel (1986):	$C_D = \frac{24*(1+0.173*Re_b)^{0.657}}{Re_b} + \frac{0.413}{1+16300*Re_b^{-1.09}}$	$Re_b > 130$ $\rho_s < 300$ kg/m^3	(II.33)
Concha & Almendra (1979):	$C_D = 0.28*(1+9.06*Re_b^{-0.5})^2$	$Re_b < 10^4$	(II.34)
Schiller & Neumann (from Dobby *et al*, 1988)	$C_D = \frac{24}{Re_b}*(1+0.15*Re_b^{0.687})$	$Re_b < 800$	(II.35)
Karamanev *et al.* (1992)	$C_D = 0.95$	$Re_b > 130$	(II.36)

There are several ways to resolve these equations and estimate the bubble size (Banisi & Finch, 1994; Xu & Finch, 1990; Dobby *et al.*, 1988; Yianatos *et al.*, 1988). All of the methods involve an iterative procedure.

Following is the procedure used in this thesis:

1.- Assume initial $\mathbf{d_b}$ and $\mathbf{Re_b}$ (typically 0.1 cm and 100, respectively)
2.- Calculate $\mathbf{U_{bt}}$ using Masliyah expression (Equation II.31)
3.- Calculate $\mathbf{U_{bt}}$ using $\mathbf{Re_b}$ (Equation II.28)
4.- Compare $\mathbf{U_{bt}}$ from step 3 and 4; iterate on $\mathbf{Re_b}$
5.- Calculate **m** from Equation II.26 or II.27
6.- Assume % ε_g (10%)
7.- Calculate $\mathbf{U_{slip}}$ in the swarm using Equation II.23
8.- Calculate $\mathbf{Re_{bs}}$ (Equation II.25)
9.- Calculate $\mathbf{U_{slip}}$ using Masliyah expression (Equation II.24)
10.- Compare $\mathbf{U_{slip}}$ from step 8 and 10; iterate on % ε_g
11.- Match experimental % ε_g iterating on $\mathbf{d_b}$

2.6 Rheology of Paper Pulp

It is evident in the drift flux analysis to estimate d_b that the slurry (pulp) viscosity should be known. The flow behavior of paper pulp is uncertain judging from the evidence (Lindsay & Mostafa, 1995; Duffy *et al.*, 1976). Part of the problem is the complex interaction of the flexible, elastic, asymmetric fibers which leads to unusual non-Newtonian behavior (Leichtle, 1998; Lee & Duffy, 1976; Duffy *et al.*, 1976; Bird *et al.*, 1960). The fibers have a tendency to flocculate and form a network structure. This flocculation can take place at consistencies (i.e. wt% solids) as low as 0.3% (Walmsley, 1992; Bennington *et al.*, 1989). Generally, flotation cells have to operate at low consistency, 0.8 to 1.3%, as performance deteriorates at higher values, which appears to be related to the rapid increase in (apparent) viscosity as pulp fiber concentration (i.e. consistency) increases as shown in Table II.3 (after Ogawa *et al.* 1990).

Table II.3 Apparent viscosity, μ, for various values of pulp fiber consistency.

Consistency, %wt	0.15	0.21	0.43	0.62
Viscosity, $\mu \times 10^3$ Kg/(m-s)	2.40	2.51	6.36	9.70

Figure II.5 shows friction versus velocity in a pipe for paper pulp from Duffy *et al.* (1976). It is clear that the hydrodynamic characteristics of the pulp are different from water. The pertinent question is how find a value for paper pulp viscosity relevant to column flotation.

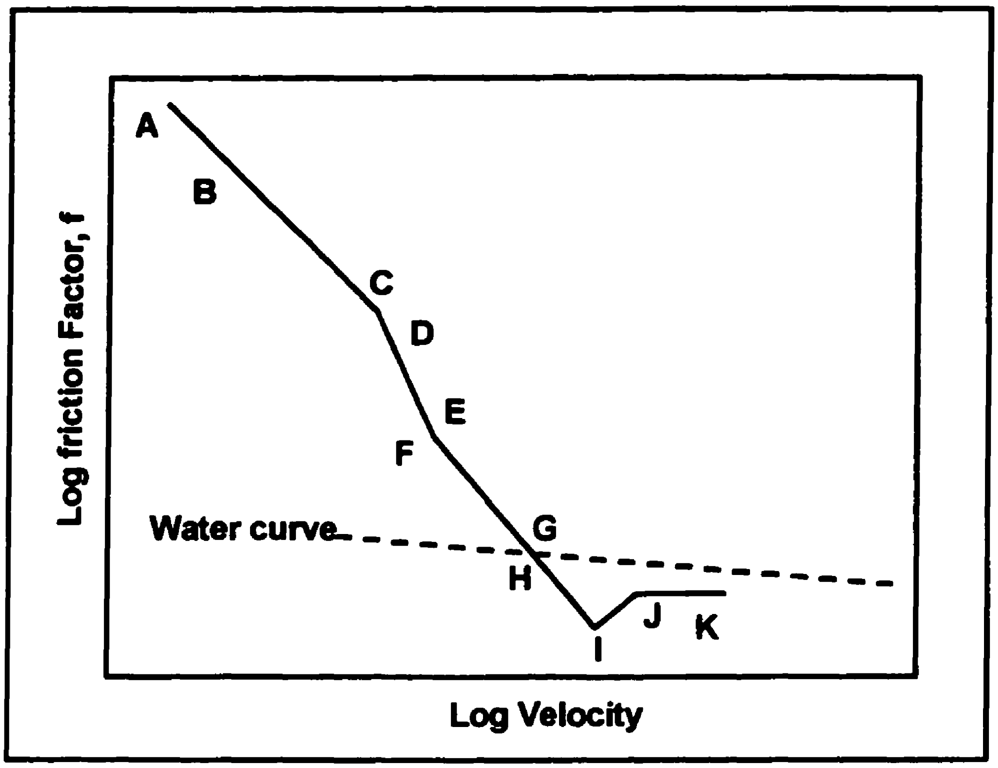

Figure II.5 Friction curve for paper pulp. (Duffy *et al.*, 1976)

The letters refer Figure II.5:

AB: Plug flow where plug-wall contact predominates

BC: Plug flow with combined hydrodynamic shear and plug-wall interaction

C: Plug-wall interaction ceases

DE: Plug flow with water annulus in laminar shear

E: Onset of turbulence in the water annulus

FH: Plug flow with an essentially fiber-free turbulent water annulus

G: Onset of drag reduction

H: Onset of permanent disruption of the plug

HJ: Transition regime characterized by increasing turbulence in the fiber/water annulus and a decreasing size of the plug core with increasing velocity

I: Maximum turbulent drag reduction with the plug core still present

JK: Fully developed turbulence with progressive decrease in drag reduction and damping of turbulence

2.7 Residence Time Distribution

Equation II.3, the key scale-up equation, includes the vessel dispersion number (N_d) as the measure of "mixing". Although there are many correlations to predict N_d (Table II.1), none have been developed for paper pulps. It may be helpful if a correlation could be found for this case.

The elements of a fluid that enter a vessel follow different paths to the discharge. As a result, the different elements reside for different times in a given vessel. The distribution of these times for the fluid elements leaving the vessel is called the exit age distribution (**E**) or the residence time distribution (**RTD**). One method of determining the **RTD** is the stimulus-response method. A tracer is introduced to the inlet stream defining time zero and the outlet stream is monitored continuously to detect the tracer concentration distribution as it leaves. An **RTD** curve is characterized by the mean residence time (τ) and the area under the concentration curve (**A**):

$$\tau = \frac{\int_0^{\infty} t_i * C_i * dt}{\int_0^{\infty} C_i * dt} = \frac{\sum_i t_i * C_i * \Delta t_i}{\sum_i C_i * \Delta t_i} = \frac{V}{Q_l} \qquad (II.37)$$

$$A = \int_0^{\infty} C dt \cong \sum_i C_i * \Delta t_i = \frac{M}{Q_l} \qquad (II.38)$$

where:

C_i = Tracer concentration measured as a funtion of time t_i, g/L, mol/L etc.

V = Volume of the vessel, m^3, L, ml, etc.

Q_l = Flowrate of the liquid, L/min, m^3/s, etc.

M = Mass units of tracer, Kg, g, moles, etc.

Once the mean residence time is obtained from the **RTD** data, the normalized tracer concentration distribution curve **E** vs **t** is computed:

$$E = \frac{C_i}{\sum_i C_i * \Delta t_i} \qquad (II.39)$$

Next, dimensionless time is introduced, defined as:

$$\theta = \frac{t}{\tau} \qquad (II.40)$$

A dimensionless **RTD** curve, **E(θ)** vs. **θ,** with area equal to 1 is obtained by:

$$E(\theta) = E * \tau \qquad (II.41)$$

$$\int_0^\infty E(\theta)_i * d\theta = \sum_i E(\theta)_i * \Delta\theta = 1 \qquad (II.42)$$

Levenspiel (1999) gives the analytical solution to the axial dispersion model:

$$E(\theta) = \left(\frac{1}{4 * \pi * \theta^3 * N_d}\right)^{0.5} * \exp\left[-\frac{(1-\theta)^2}{4 * \theta * N_d}\right] \qquad (II.43)$$

The degree of mixing is quantified by the dimensionless group called the vessel number, $\mathbf{N_d}$. (section 2.2).

2.8 Bubble Generation: Spargers

An essential process in any flotation machine is bubble production. There is a wide variety of sparging devices for columns ranging from rigid porous materials to mechanical systems (Hardie, 1998). An efficient sparger should produce small uniform sized bubbles at the maximum aeration rate with minimum maintenance requirements (Huls *et al.*, 1991; Dobby & Finch, 1986b). An important consideration for scale-up is that the sparger must provide the same bubble surface area flux (S_b) in the full-scale column as in the laboratory column used to obtain the design data (Leichtle, 1998). Internal spargers generate bubbles directly into the slurry/pulp in the column. This is accomplished either at thousands of small holes in a porous material or by disintegration of a gas jet produced at a few fairly large holes (~1mm). In this thesis rigid porous spargers are used made of sintered stainless steel (supplied by Mott Industrial) with different pore sizes. They are commonly employed in small scale experiments but are not favored industrially because of a tendency to plug. Rigid spargers have enjoyed some renewed commercial interest in de-oiling of effluents and, relevant to this work, de-inking of recycled paper. The interest appears to have stemmed from a belief that they produce the small bubbles required to effectively remove the fine ink particles and, because of the low consistency, are less prone to blockage compared to the situation with high density mineral slurries.

2.8.1 Characterization of Rigid Porous Spargers

Escudero (1998) proposed a method to characterize rigid spargers for column flotation applications based on the principle of permeability according with Darcy. The Darcy theory is based on the pressure drop across a porous material being directly proportional to the volume rate of fluid passing through. Thus, for a particular porous material, a given pressure drop corresponds to a given flow rate of the fluid. The particular numerical value of permeability should be a constant, characteristic of the material, and independent of the fluid used (API, 1956).

2.8.1.1 Laminar Flow

Darcy's law represents the laminar flow of fluid through a porous medium in general terms as:

$$J_i = -\frac{K_i}{\mu_i} * \left[\frac{dP}{dS} - \rho_i * g * \frac{dZ}{dS}\right] \qquad (II.44)$$

where:

J_i = Volume flux across a unit area of the porous medium in unit of time, m/s

K_i = Permeability of the medium, m^2

μ_i = Viscosity of the fluid, kg/m-s

dP/dS = Pressure gradient along **S** at the point to which J_i refers.

S = Direction of the flow

ρ_i = Density of the fluid, kg/m^3

g = Gravity acceleration, m/s^2

Z = Vertical coordinate directed downward

In the case of horizontal cylindrical porous medium with outward radial flow, the situation here (Figure II.6), the permeability is:

$$J_i = -\frac{K_i}{\mu_i} * \frac{dP}{dr} \qquad (II.45)$$

$$dP = -\frac{J_i * \mu_i}{K_i} * dr \qquad (II.46)$$

$$dP = -\frac{Q * \mu_i}{2 * \pi * L * K_i} * \frac{dr}{r} \qquad (II.47)$$

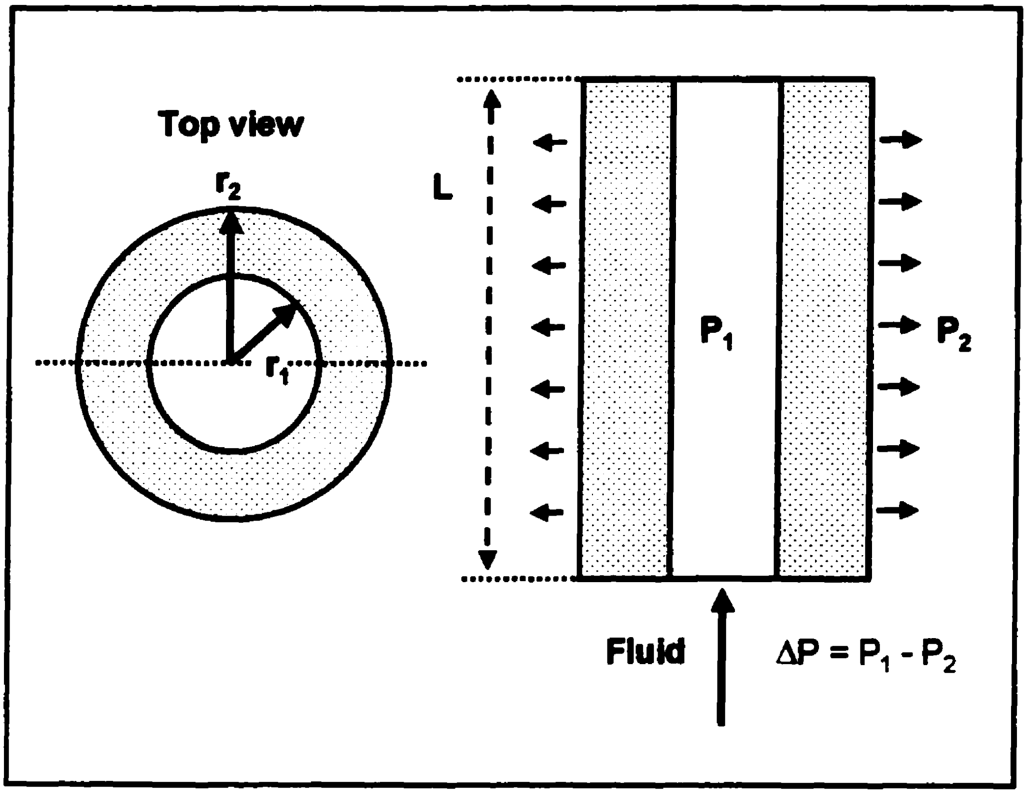

Figure II.6 Geometric characteristics of the stainless steel spargers.

For an incompressible fluid **Q** is a constant radially across the wall of the sparger, and then:

$$\int_{P_1}^{P_2} dP = -\frac{Q * \mu_l}{2 * \pi * L * K_l} * \int_{r_1}^{r_2} \frac{dr}{r} \qquad (II.48)$$

$$\Delta P = \frac{Q * \mu_l}{2 * \pi * L * K_l} * Ln \frac{r_2}{r_1} \qquad (II.49)$$

$$K_l = \frac{Q * \mu_l}{2 * \pi * L * \Delta P} * Ln \frac{r_2}{r_1} \qquad (II.50)$$

For compressible fluids **Q** is not constant, but depends on the pressure gradient along the wall of the sparger and the temperature of the fluid. Air flowrate, referenced to 1 atm and 0°C, was adjusted to the temperature and pressure conditions inside the sparger as follows:

$$Q_{TP} = \frac{\left(\frac{Q_m * T_m}{273.15°K}\right) * 1\,atm}{P_m} \qquad (II.51)$$

where:

Q_{TP} = Flowrate adjusted to temperature and pressure, m^3/s
Q_m = Volume rate of flow at the mean pressure, m^3/s
P_m = Algebraic mean pressure, $(P_1 + P_2) / 2$, atm
T_m = Temperature of the fluid, °K

For compressible fluids Equations II.49 and II.50 become in:

$$\Delta P = \frac{Q_{TP} * \mu_g}{2 * \pi * L * K_g} * Ln \frac{r_2}{r_1} \qquad (II.52)$$

$$K_g = \frac{Q_{TP} * \mu_g}{2 * \pi * L * \Delta P} * Ln \frac{r_2}{r_1} \qquad (II.53)$$

2.8.1.2 Turbulent Flow

In turbulent flow, the unidirectional pressure drop between two locations in a porous medium, fully saturated with a Newtonian incompressible fluid, can be obtained from the Forchheimer extension of the Darcy equation (Joseph *et al.* 1982).

$$\frac{dP}{dS} = \frac{\mu_l}{K_l} J_l + \frac{C_F}{\sqrt{K_l}} * \rho_l * J_l^2 \qquad (II.54)$$

where C_F is the Forchheimer coefficient and is determined experimentally (Givler & Altobelli, 1994).

The equation for radial flow is:

$$\frac{dP}{dr} = \frac{\mu_l * Q}{2 * \pi * L * r * K_l} + \frac{C_F * \rho_l * Q^2}{\sqrt{K_l} * 4 * \pi^2 * L^2 * r^2} \qquad (II.55)$$

On integration:

$$\Delta P = \frac{\mu_l * Q}{2 * \pi * L * K_l} * Ln\frac{r_2}{r_1} + \frac{C_F * \rho_l * Q^2}{\sqrt{K_l} * 4 * \pi^2 * L^2} * \left(\frac{1}{r_1} - \frac{1}{r_2}\right) \qquad (II.56)$$

For turbulent flow using a compressible fluid the relationship **Q - ΔP** displays an exponential behavior (Figure II.7) of the following form (Scheidegger, 1974):

$$\frac{dP}{dr} = A * Q + B * Q^2 \qquad (II.57)$$

$$\frac{dP}{dr} = A * Q^n \qquad (II.58)$$

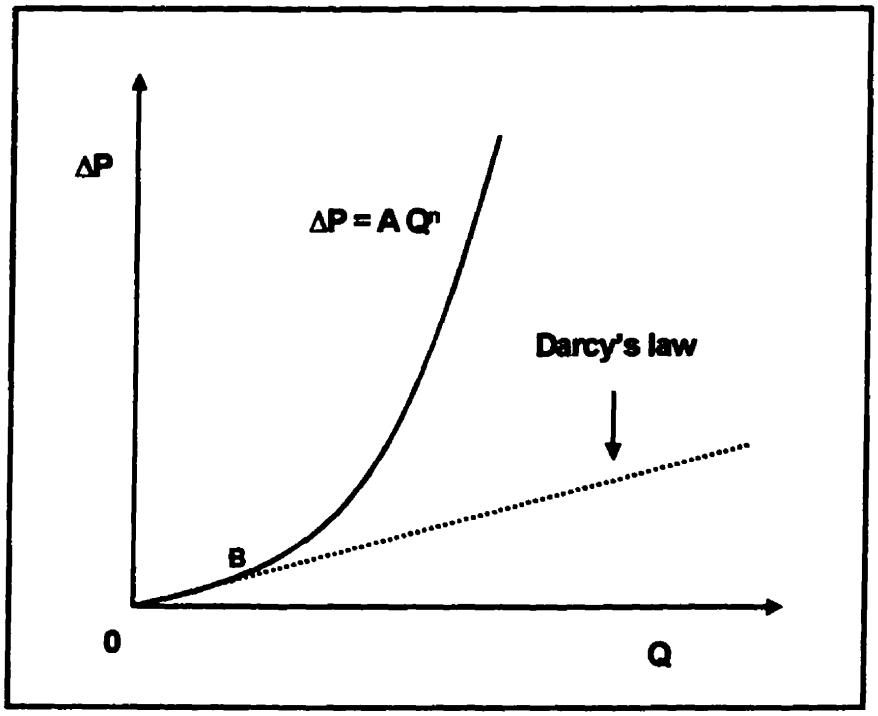

Figure II.7 Representation of linear and non-linear **Q - ΔP** relationships. The *point B indicates a change in the flow regime.*

A modified Darcy's law to calculate the permeability for the sparger with a Newtonian compressible fluid comes from Equation II.52 namely:

$$\Delta P = \frac{Q_{TP}^n * \mu_g}{2 * \pi * L * K_g} * Ln\frac{r_2}{r_1} \qquad (II.59)$$

$$K_g = \frac{Q_{TP}^n * \mu_g}{2 * \pi * L * \Delta P} * Ln\frac{r_2}{r_1} \qquad (II.60)$$

Klinkenberg (1941) found experimentally that the relation between the measurements of permeability of a porous medium with compressible fluids to incompressible fluids is:

$$K_g = K_l + b * K_l * \left(\frac{1}{P_m}\right) \qquad (II.61)$$

where:

K_g = permeability of the medium to a gas completely filling the pores of the medium, m^2

K_l = permeability of the medium to a single liquid phase completely filling the pores medium, m^2

b = Klinkenberg's constant for a given gas and for a given porous medium

P_m = algebraic sparger mean pressure, $(P_1 + P_2) / 2$, Pa

To establish the homogeneity of the SS spargers used in this work the pressure drop was plotted against the quantity **$R_s * J_g$**, where

$$R_s * J_g = \frac{A_c}{A_s} * \frac{Q_m}{A_c} = \frac{Q_m}{A_s} \qquad (II.62)$$

and

A_c = Cross sectional area of the column, cm^2

A_s = Sparger surface area, cm^2

Q_m = Volumetric gas flowrate, cm^3/s

Thus the product **$R_s * J_g$** is equivalent to volumetric gas rate per unit area of sparger (Xu & Finch, 1989).

2.9 The Test Flotation Columns

Three flotation columns were used for this project, two laboratory columns and one pilot unit. Table II.4 shows the characteristics of each. In the text the columns are referred to by the "designated" name.

Table II.4 Characteristics of the flotation columns.

Column (designation)	Inner diameter (cm)	Height (cm)*	Material
4" Lab	10.4	600	Clear acrylic plastic
6" Lab	15.2	400	Clear acrylic plastic & transparent PVC
20" Pilot	50.0	550	Gray PVC

* Up to

The columns can be operated manually or automatically using the digital and analog input/output (I/O) controller OPTOMUX (Figure II.8). This unit is a 16-point rack that accommodates photo-isolated analog or digital power I/O modules. Each OPTOMUX unit consists of a removable brain board and an I/O mounting rack. The brain board contains a microprocessor which communicates with the host computer and controls the plug in I/O modules located on the I/O mounting rack.

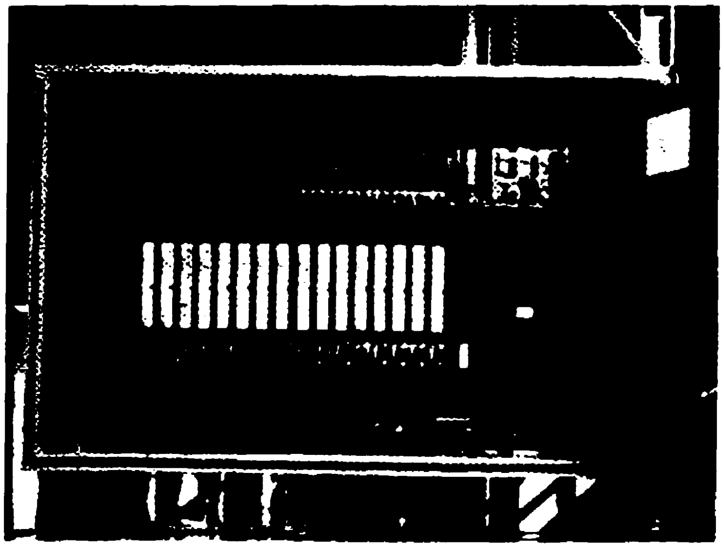

Figure II.8 Analog input/output (I/O) controller OPTOMUX

The peripheral equipment for control and data collection consists of:

- 4 mass air flowmeters, MKS INC model 1162B, ranges 20, 30, 200 & 400 L/m
- 4 magnetic liquid flowmeters, Fischer & Porter model 10D1475
- 3 magnetic liquid flowmeter signal converters, Fischer & Porter model 50XM
- 5 pressure transmitters, Bailey model PTSDDD, ranges 200", 360" & 2078" H_2O
- 3 variable speed peristaltic pumps, Masterflex model 7549-32
- 2 centrifugal pumps, Goulds model 3196 max. range 300 L/m
- 1 centrifugal pump, Franklin electric model 4103007432, 3/4 HP
- 2 control valves, DeZuric
- Temperature ICTD probes, Transduction mod. ICTD P/N1662, range -40 to 150 °C
- 1 Conductivity sensor, Bailey TB1 model TB054
- 1 Conductivity meter, Bailey model 440
- 1 Conductivity meter, VWR Scientific model 2052
- 1 Video camera, Sony handicap model CCD-V801.

The peripherals were attached to the OPTOMUX. This unit digitized the 4-20 mA analog or digital signal which was then transmitted to a Pentium 300 MHz computer. The software used for data acquisition and control was FIX DMMI 32-bit version 6.3 for windows 95/98 by Intellution.

CHAPTER III

Bubble Generators

3.1 Introduction

The bubble generator devices used in this work are stainless steel porous spargers. The first step was to try to characterize the spargers, in particular as a check on their homogeneity. Work by Hardie (1998) and Leichtle (1998) has shown that the sparger type is not important compared to the S_b produced. Therefore, although rigid spargers are not the choice for full scale operation they are adequate to demonstrate the principles at issue here.

3.2 Objective

The objective of this part of the thesis is to establish the homogeneity of the stainless steel spargers (SS spargers) used in this work by determining their permeability according with Darcy's law.

3.3 Experimental

A series of experiments were designed to collect pressure loss data for water and air flowing through rigid SS spargers in the laboratory and pilot units. The characteristics of the spargers are given in Table III.1. A design to allow the installation of different size spargers in the form of porous tubes 0.025 m in diameter was made (Figure III.1), comprising in a SS base where the sparger was maintained in position by a specially designed nut and bolt.

Table III.1 Characteristics of bubble generating devices.

Column	SS Sparger #	Pore Size (μm)	L_s (cm)	R_s
4" Lab	1	0.5	10.5	0.96
	2	2		
	3	5		
	4	10		
	5	20		
	6	40		
	7	100		
6" Lab	1	0.5	28	0.82
20" Pilot	1	0.5	26	9.76
	2		"	"
	3		"	"
	4		"	"
	5		"	"
	6		43	5.90

where:

Pore size is nominal value according with manufacturer

L_s is length of the sparger, cm.

R_s is cross sectional area of the column relative to sparger surface area

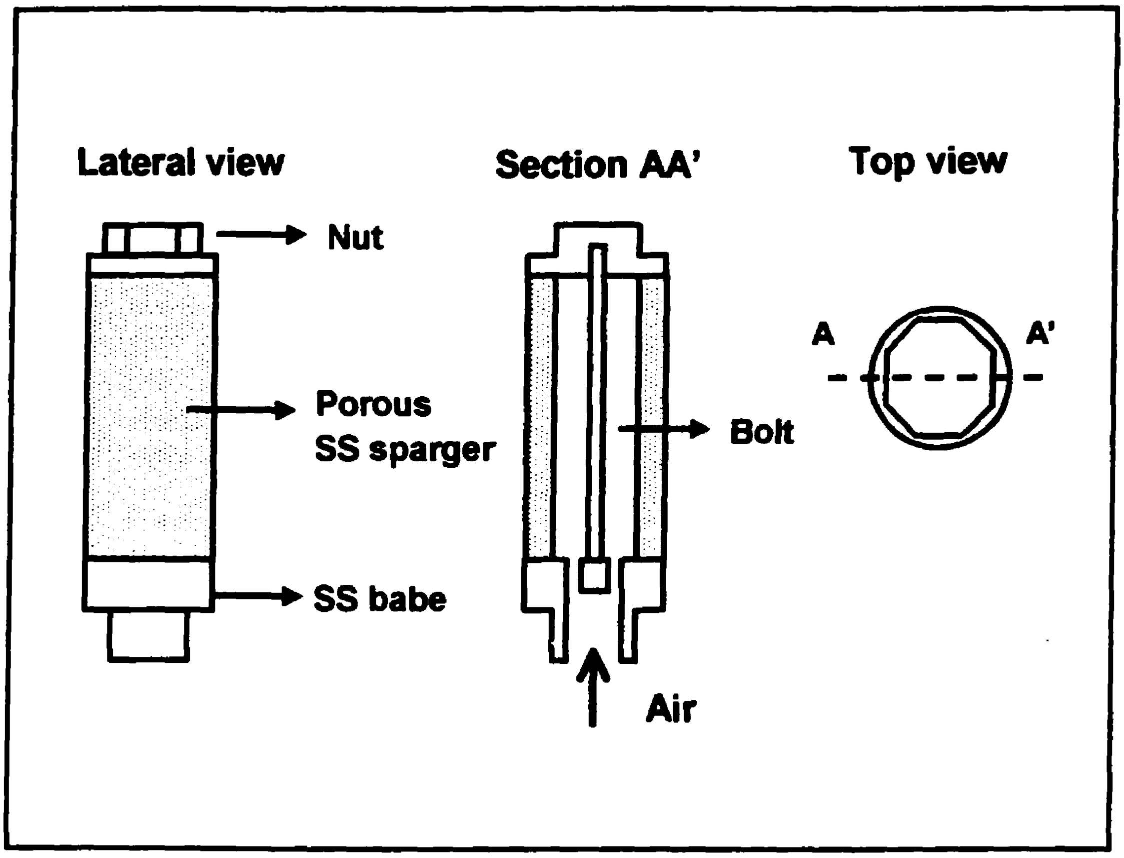

Figure III.1 Sparger construction details.

The set-up used to collect pressure loss data with water as fluid test is depicted in Figure III.2. In the first case, the sparger was installed at the bottom of an acrylic tube (column), 0.105 m in diameter and 1 m in length. Water was delivered using a centrifugal pump and the flowrate was measured using a magnetic flowmeter. The tube, which was completely immersed, was provided with two outlets, one for the water to exit the tube and the other used as a pressure tap. The pressure drop across the sparger was measured with a differential pressure transducer and the temperature of the water was measured using an ICTD probe.

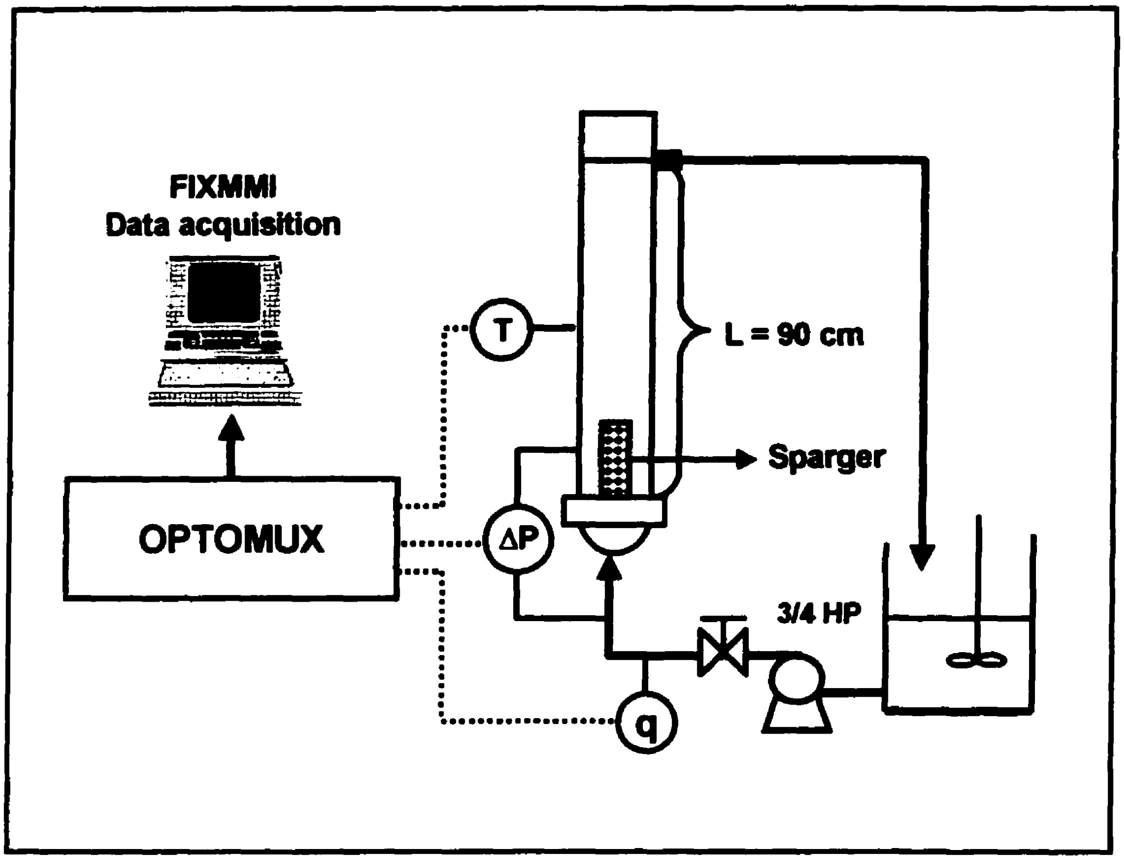

Figure III.2 Experimental set-up to collect pressure loss data with water as test fluid.

In the case of air as test fluid, flowrate was measured and controlled using a mass flowmeter and temperature was measured using an ICTD probe. As in the previous case, the pressure drop across the sparger was measured using a differential pressure transducer. The set-up is described in Figure III.3. The instruments in both cases were linked to the signal conditioning and interface unit, OPTOMUX. Continuous monitoring and registering of the data was performed through a computer running the software FIX-MMI. Table III.2 shows the test fluid and spargers combinations.

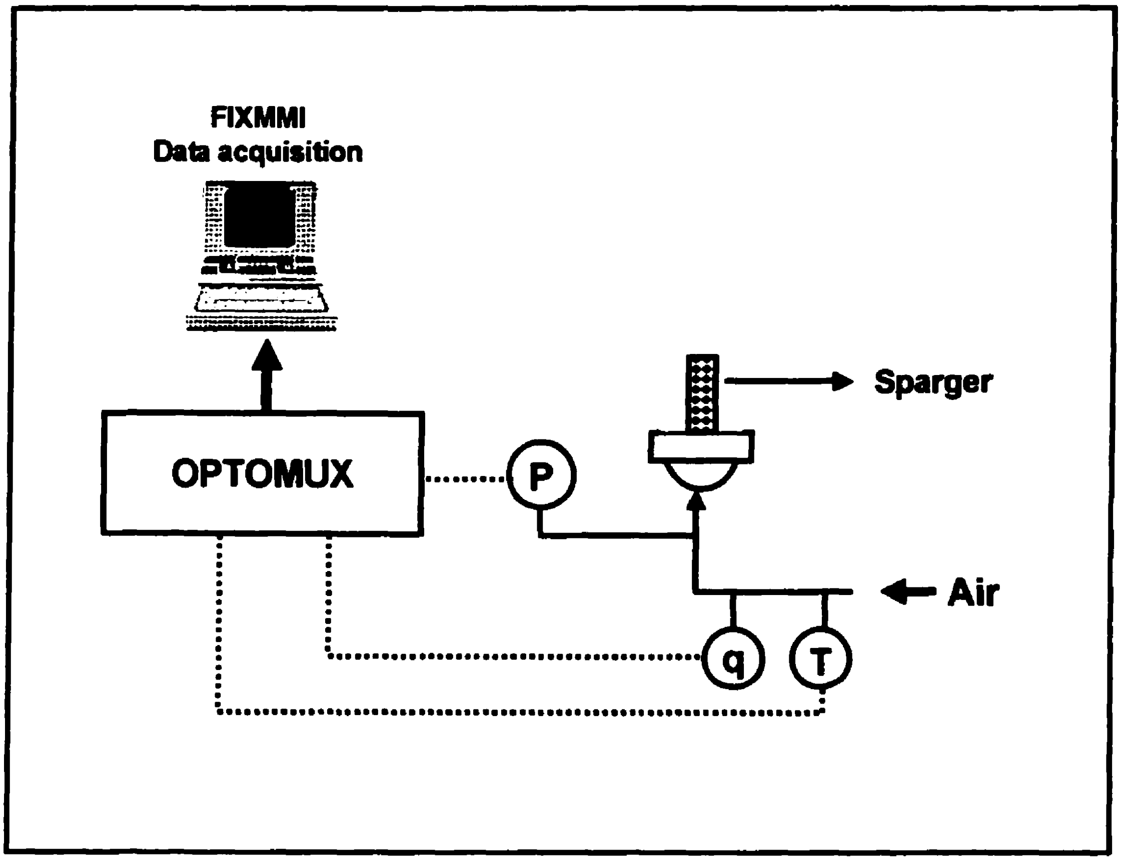

Figure III.3 Experimental set-up to collect pressure loss data with air as test fluid.

Table III.2 Test fluid for each sparger.

Column	SS sparger #	Test Fluid
4" Lab	1, 2, 3, 4, 5, 6, 7	Water
4" Lab	1, 2, 3	Air
6" Lab	1	Air
20" Pilot	1, 2, 3, 4, 5, 6	Air

3.4 Results and Discussion

3.4.1 Water as Test Fluid

Darcy's law represents a relationship between the filtration velocity (Q), and the gradient of pressure (ΔP). Figure III.4 shows the **Q - ΔP** relationships for the set of 7 SS spargers used in the 4" column with different porosity (nominal pore size according to manufacturer see Table III.1) using water as test fluid.

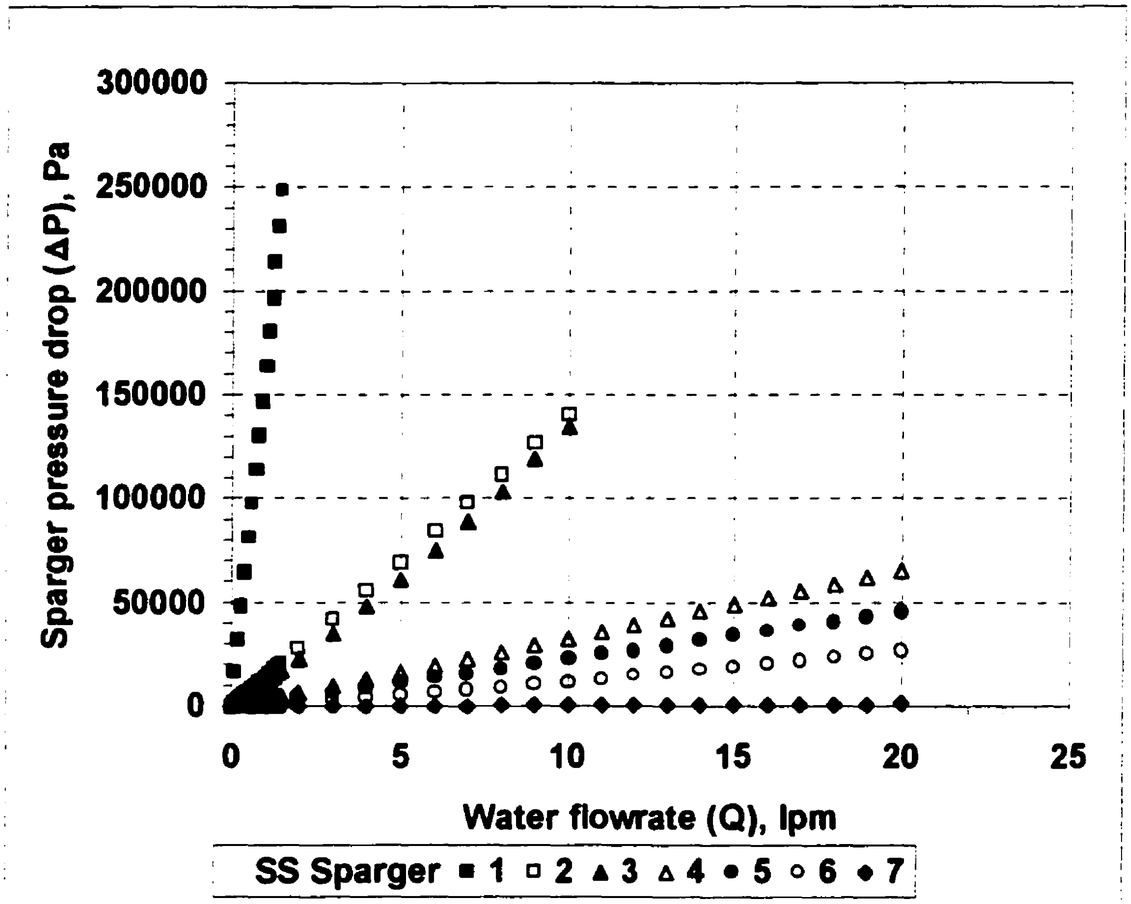

Figure III.4 Q - ΔP relationship for spargers used in 4" lab column with water as test fluid.

Table III.3 shows the calculated values of permeability for water (K_l) and Forchheimer coefficient (C_F) according to Equation II.56, the Forchheimer-extended Darcy equation. According to Figure III.4, the pressure drop decreases when the nominal pore size increases. Sparger 7 has the smallest pressure drop because it has the largest pore size, thus the largest permeability. Spargers 2 and 3 show similar results even though they have different nominal pore size. That is, the results suggest that these two spargers have similar permeability.

Table III.3 Permeability of the spargers used in the 4" lab column with water as test fluid.

SS Sparger #	Nominal Pore Size (μm)	K_l (darcy)	C_F
1	0.5	0.041	43.600
2	2.0	0.480	11.222
3	5.0	0.598	10.849
4	10.0	2.035	0.005
5	20.0	2.937	0.072
6	40.0	6.538	2.460
7	100.0	133.09	0.462

3.4.2 Air as Test Fluid

Figure III.5 shows the **Q** - **ΔP** relationship for three spargers from the set using air as a test fluid. In this case the flowrate was adjusted to temperature and pressure according to Equation II.51. Table III.4 shows the apparent permeability of the spargers (**K_g**) according with Equation II.60 and the permeability corrected (**K_l**) according to Klinkenberg's equation (Eq. II.61).

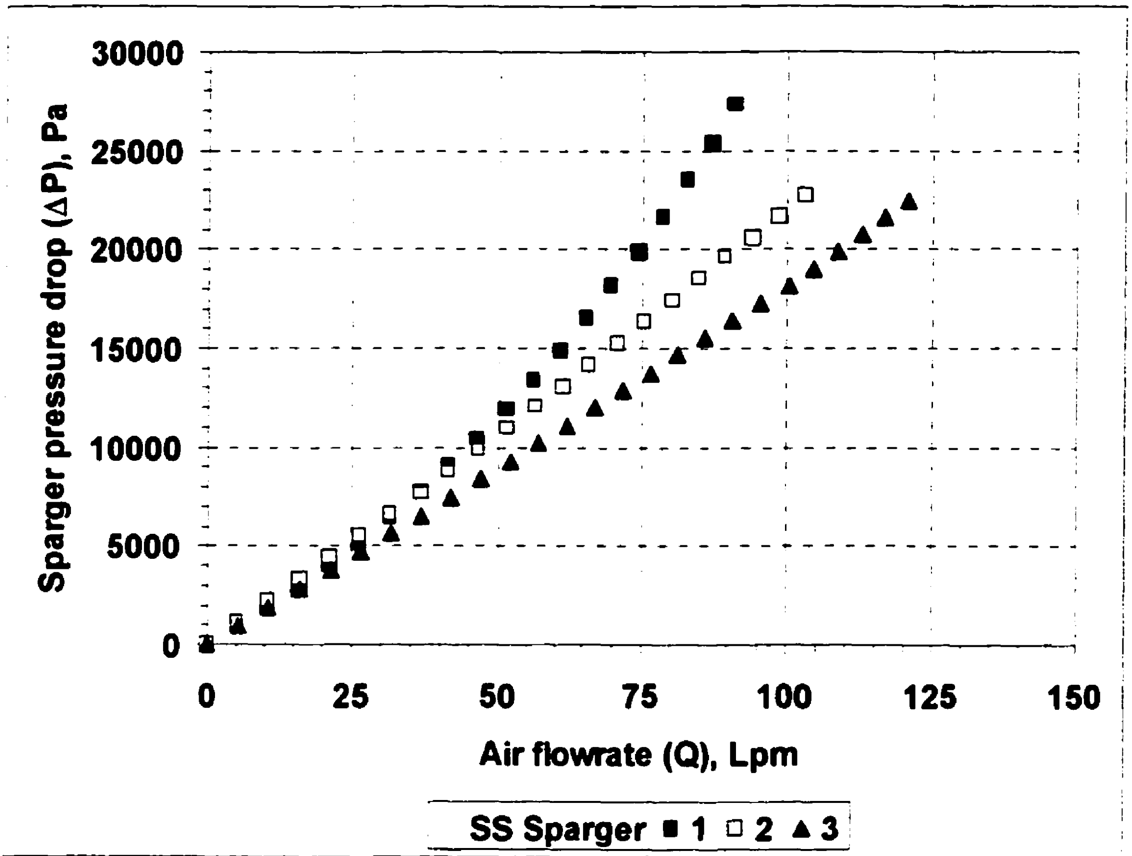

Figure III.5 Q - ΔP relationships for spargers used in 4" lab column with air as test fluid

Table III.4 Permeability of the spargers used in 4" lab column with air as test fluid and permeability corrected according to Klinkenberg's equation.

SS Sparger #	Nominal Pore Size (μm)	K_g (darcy)	n	K_l (darcy)	B
1	0.5	0.131	1.209	0.039	2.436
2	2.0	0.515	1.032	0.458	0.132
3	5.0	0.662	1.020	0.599	0.110

Comparing Tables III.3 and III.4 shows the values of permeability for water and air are in excellent agreement, reinforcing that the fluid conductivity of a porous material does not depend on the test fluid. Figure III.6 shows the **Q - ΔP** relationships for spargers used in the 6" lab column and 20" pilot unit using air as test fluid. As in the previous case the flowrate was adjusted to temperature and pressure according to Equation II.51. Sparger 1 for the 6" column, and 2 and 4 for the 20" pilot unit show different results from other spargers with the same nominal porosity, suggesting a lack of homogeneity in the sparger material. The permeability results are given in Table III.5.

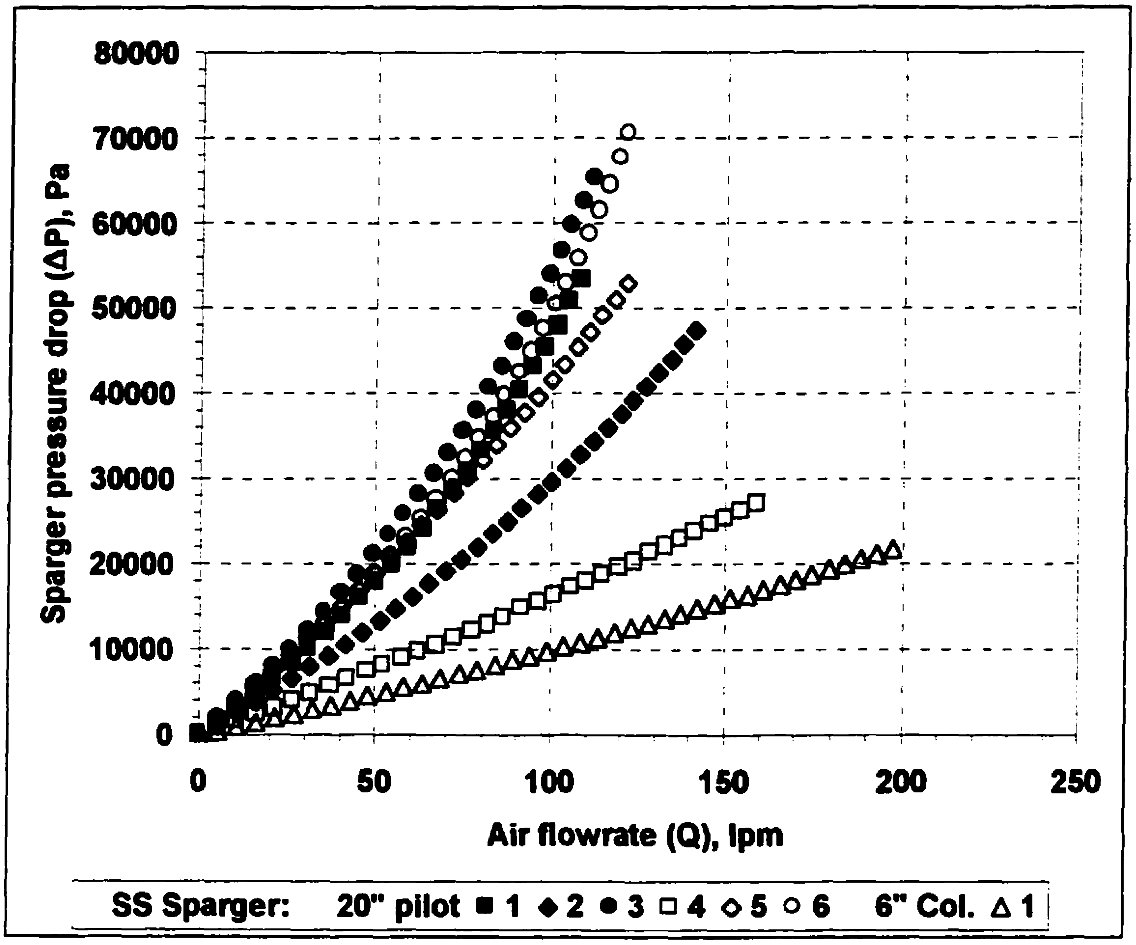

Figure III.6 **Q** - **ΔP** relationships for spargers used in 20" pilot and 6" lab column with air as test fluid.

Table III.5 Permeability of the spargers used in 6" lab column and 20" pilot unit with air as test fluid, nominal pore size 0.5 μm and permeability corrected according to Klinkenberg's equation.

Column	SS Sparger #	K_g (darcy)	n	K_l (darcy)	b
6" Lab.	1	0.336	1.064	0.217	0.126
20" Pilot	1	0.037	1.190	0.022	0.540
	2	0.087	1.118	0.061	0.457
	3	0.034	1.177	0.023	0.527
	4	0.254	1.045	0.210	0.225
	5	0.080	1.080	0.069	0.191
	6	0.016	1.225	0.009	0.802

Figure III.7 shows a comparison between the spargers with the same nominal pore size of 5 μm. All the spargers show different results, proving again that they are not homogeneous even though they have the same nominal pore size. Later it will be shown that the spargers do provide a consistent gas holdup - gas rate relationship despite variations in measured permeability. Escudero (1998), showed this to be the case for spargers of nominal pore size ≤ 2μm (i.e. spargers could be variable in permeability but the gas holdup - gas rate relationship was not affected). The present results suggest that the lack of correlation between sparger permeability and the gas holdup – gas rate relationship is more general. Permeability, while checking sparger material homogeneity, is not an adequate guide to the gas holdup vs gas rate that will be produced.

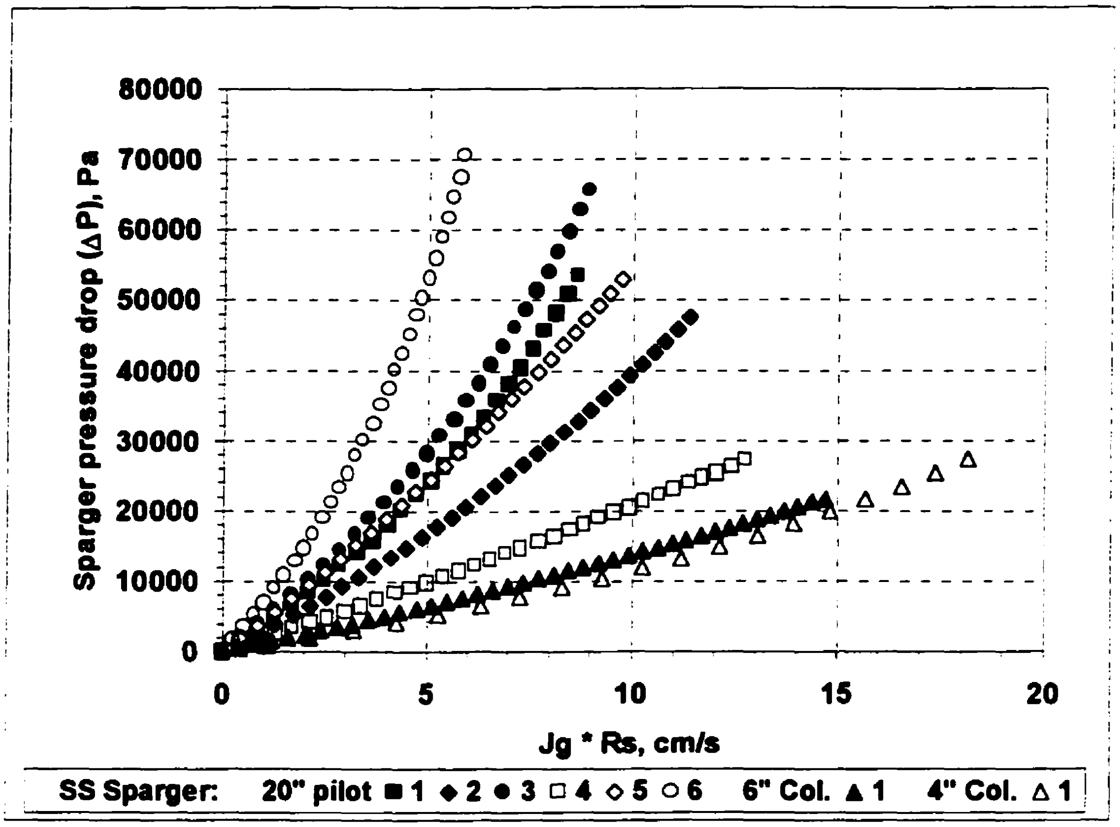

Figure III.7 $\Delta P - (J_g * R_s)$ relationships for all spargers with nominal pore size 0.5 μm with air as test fluid.

3.5 Summary of the Chapter

- Permeability determined with both air and water as test fluid was similar, demonstrating that permeability of a porous material does not depend on the test fluid, but reflects only the nature of the sparger material itself.
- **ΔP - (R_s * J_g)** relationship can be used as a quality check on the homogeneity of the spargers.
- Permeability showed that the spargers are not homogeneous even though they have the same nominal pore size.

The raw data for all these experiments are given in **Appendix A**

CHAPTER IV
Paper Pulp Viscosity

4.1 Introduction

The rheology of paper pulp is evidently complex (Lindsay & Mostafa, 1995; Bennington *et al.*, 1990; Ogawa *et al.*, 1990; Duffy *et al.*, 1976; Lee & Duffy, 1976; Vaseleski & Metzner, 1974; Kerekes, 1970). The interaction of the flexible, elastic, asymmetric fibers leads to unusual non-Newtonian behavior (Leichtle, 1998; Duffy *et al.*, 1976; Lee & Duffy, 1976; Bird *et al.*, 1960). The fibers have the tendency to flocculate and form a network structure. This flocculation can take place at consistencies as low as 0.3% (Walmsley, 1992; Bennington *et al.*, 1989). Flotation cells in de-inking have to operate at low consistency, 0.8 to 1.3%, to limit the impact of viscosity on the process. Paper pulps at this consistency have a density close to that water, but the viscosity is very different. There are many ways to measure viscosity, but they do not necessarily provide a good estimation of viscosity of paper pulp relevant to a flotation column, because most techniques will use shear conditions different from those in flotation. One purpose of this chapter is to obtain a possible relation between the viscosity of paper pulp and consistency under column flotation conditions. One important application of this knowledge is to solve for bubble size using drift flux analysis where viscosity is an input. Two techniques were selected to measure the viscosity. In the first, an experimental analysis of the flowrate and pressure drop relationships for turbulent flow of fiber suspensions through rough pipes was used (Ogawa et al., 1990; Duffy et al., 1976; Kerekes, 1970). While it proved difficult to extrapolate to the shear conditions in the column, the technique gave useful information on the effect of the temperature on viscosity. The second approach used was drift flux analysis itself. Experiments to measure the bubble size photographically and back calculate viscosity by drift flux analysis were performed in the 4" lab column.

4.2 Objective

To determine the apparent viscosity of paper pulp as a function of consistency (% solids) under conditions relevant to column flotation.

4.3 Experimental

4.3.1 Measurement of Viscosity with Moody-Colebrook and Darcy Equations for Turbulent Flow

4.3.1.1 Technique

A series of experiments measuring pressure head loss ($\Delta \mathbf{P}$) as a function of liquid flowrate ($\mathbf{q}$) were performed using paper pulp suspensions pumped continuously through a test loop. The test fluid was pumped at different temperatures through two test sections of galvanized pipe, each 4.5 m long of inside diameter 1.48 and 2.10 cm. For these condition the flow is turbulent. The distance between pressure taps was 3.60 m. Figure IV.1 shows the experimental set-up. The liquid flowrate was measured using a magnetic flowmeter with a signal converter. The pressure head loss data was measured with two differential pressure transmitters and the temperature with an ICTD probe. All the instruments were connected or monitored using a signal conditioning and interface unit and a computer. Outputs were monitored and collected through a software package.

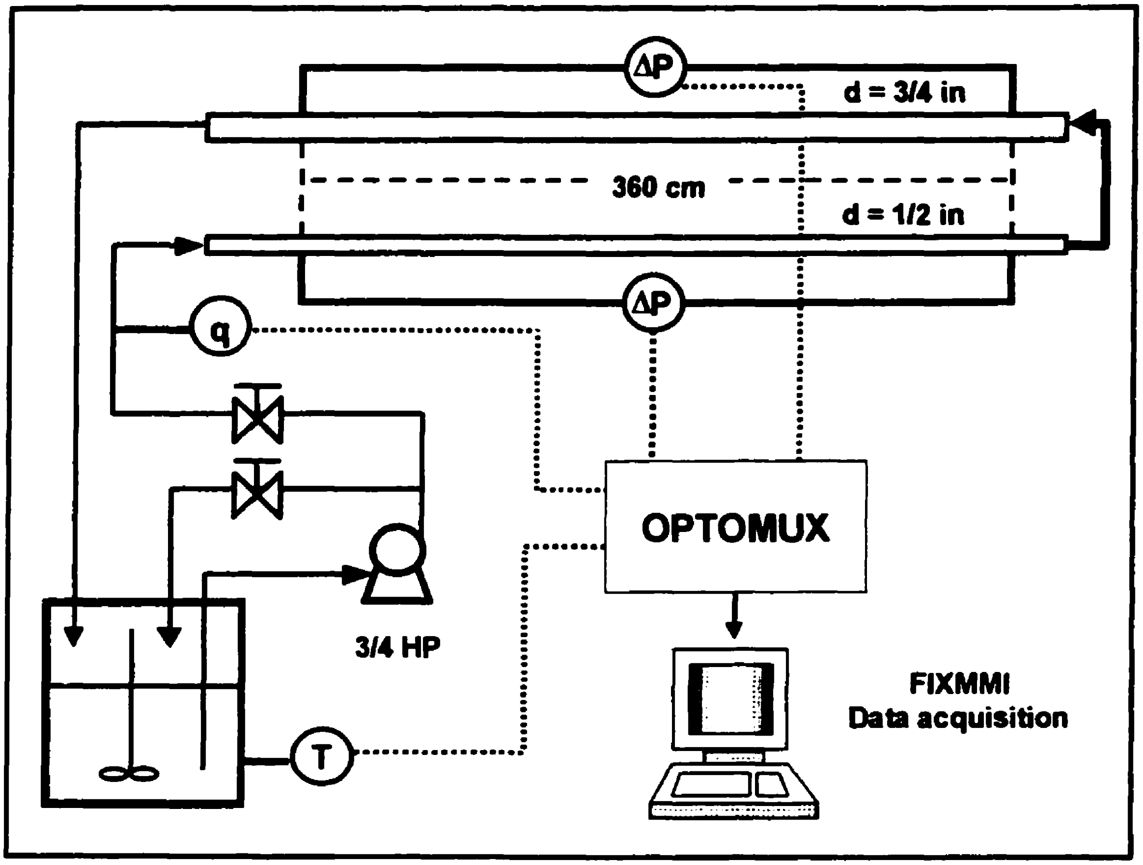

Figure IV.1 Experimental loop used to measure the friction factor and relative roughness.

The friction factor (**f**) and the Reynolds number relationships were determined for water, solutions of polyacrylamine and paper pulp suspensions. The water was used to determine the relative roughness (ε/d_{pipe}) of the pipe and the polyacrylamine solution, with known viscosity, was used to verify the procedure. Reynolds number (**Re**) was estimated as:

$$Re = \frac{\rho_i * \overline{V} * d_{pipe}}{\mu_i} \qquad (IV.1)$$

where:

ρ_l = Density of the fluid, g/cm^3

μ_l = Viscosity of fluid, gr/cm-s

i = Refers to fluid test

d_{pipe} = Inner diameter of the pipe, cm

$\overline{V}$ = Velocity of the flow, cm/s and is given by:

$$\overline{V} = \frac{Q_l}{A_{pipe}} = \frac{\text{Volumetric liquid flowrate, cm}^3\text{/s}}{\text{Pipe cross sectional area, cm}^2} \quad \text{(IV.2)}$$

The friction factor (f) was calculated using Darcy's law for turbulent flow:

$$f = \frac{\Delta P * d_{pipe} * 2}{\rho_i * \Delta L * \overline{V}^2} \quad \text{(IV.3)}$$

$$\frac{1}{f^{0.5}} = -2 * \log\left(\frac{\left(\varepsilon / d_{pipe}\right)}{3.7} + \frac{2.51}{Re * f^{0.5}}\right) \quad \text{(IV.4)}$$

$$\varepsilon / d_{pipe} = \left(10^{\left(-\frac{0.5}{f^{0.5}}\right)} - \frac{2.51}{Re * f^{0.5}}\right) * 3.7 \quad \text{(IV.5)}$$

$$Re = \frac{2.51}{\left(10^{\left(-\frac{0.5}{f^{0.5}}\right)} - \frac{\left(\varepsilon / d_{pipe}\right)}{3.7}\right) * f^{0.5}} \quad \text{(IV.6)}$$

$$\mu_i = \frac{\rho_i * d_{pipe} * \overline{V}}{Re} \qquad (IV.7)$$

where:

ΔP = Pressure head loss, Pascal

ΔL = Distance between two points along the pipe, cm

The relative roughness (ε/d_{pipe}) of the pipe was estimated using the Moody-Colebrook model (Equation IV.5). For the polyacrylamine solutions and paper pulps, knowing the friction factor (**f**) and ε/d, the Reynolds number (**Re**) is calculated from Equation IV.6. The viscosity of the fluid **i** (μ_i) is then found as a function of **Re** (Equation IV.7).

4.3.1.2 Results

Table IV.1 shows the estimation of ε/d for the two pipes using water as a fluid test at three temperatures. They are similar for each temperature and an average value of ε/d was taken for subsequent calculations.

Table IV.1 Values of relative roughness for the galvanized pipes

Diameter [in]	1/2			3/4		
T [°C]	26	35	47	26	35	47
(ε/d_{pipe})	0.00244	0.00248	0.00256	0.00483	0.00484	0.00491
Avg (ε/d_{pipe})	0.00249			0.00486		

Figure IV.2 shows the comparison between the viscosity measured using the pipe set-up and that measured using a Cannon-Fenske viscometer for the 0.03 %wt. polyacrylamine solution (i.e. the viscometer gives the "known" value). The measured values agree closely with the "known" value, therefore, the technique is judged suited to estimate the viscosity of paper pulp.

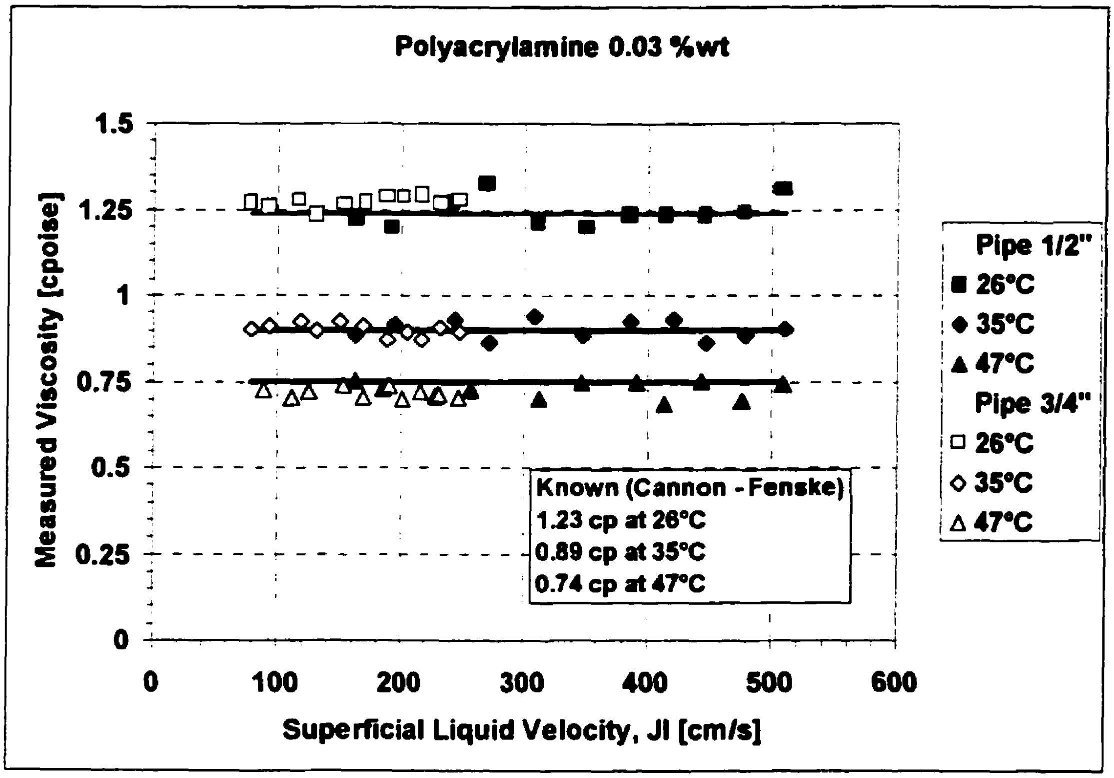

Figure IV.2 Comparison between measured and known viscosity in the pipe loop for a polyacrylamine 0.03 %wt. solution.

To explore the effect of the paper fibers on viscosity, first the fibers were removed from the pulp to generate "grey water" which was circulated in the loop. The comparison between tap water and grey water is shown in Figure IV.3. The figure shows that the viscosity of the grey water is larger than the tap water. Also, the effect of temperature is more evident with grey water - as temperature increases the viscosity increases. Residual clay and reagents in the grey water are likely the cause of this behavior.

The experimental relation between the flowrate and apparent viscosity of the paper pulp for two values of pulp consistency are shown in Figure VIII.4 and VIII.5. The figures show that the flow behavior of the paper pulp is complex. According with the results there is an effect of tube diameter, consistency and temperature. The effect of tube diameter on paper viscosity is observed in all experimental data. Using the smaller diameter pipe (1/2") over all range of flowrates studied, the values of viscosity are smaller than the values from the larger diameter pipe (3/4"). One explanation is that interaction between the free fibers and the wall of the pipe produces high friction losses.

The consistency of paper pulp has a dramatic effect on the apparent viscosity. The value of viscosity increases when the consistency decreases. At low consistency (0.017%), the fibers are free to move with little or no interaction. At the higher consistency (0.91%) the fibers interact to produce flocs. These flocs interlock to form coherent networks which accumulate in the central or core region of the velocity field in the tubes (Kerekes, 1970). This is surrounded by an annulus of the suspending liquid (water), which is nearly fiber free; as a result there is less friction and lower viscosity. As is the case with grey water when the temperature increases, the viscosity increases. Temperature is an important factor in the de-inking process. At high temperature the fibers have a tendency to expand (and the ink particles detach more efficiently). This phenomenon reduces the annulus of water near the pipe wall. As a result friction losses increase and a high value of viscosity results

According with the results and previous attempts to understand paper pulp flow behavior in pipe lines (Bennington *et al.*, 1990; Ogawa *et al.*, 1990; Lee & Duffy, 1976; Duffy *et al.*, 1976; Kerekes, 1970) fiber suspensions are possibly unique. In turbulent flow, the fibers in suspensions are subjected to high shear rates and when there is insufficient volume for the fibers to move freely, they form a network of flocs. As a result the viscosity changes significantly.

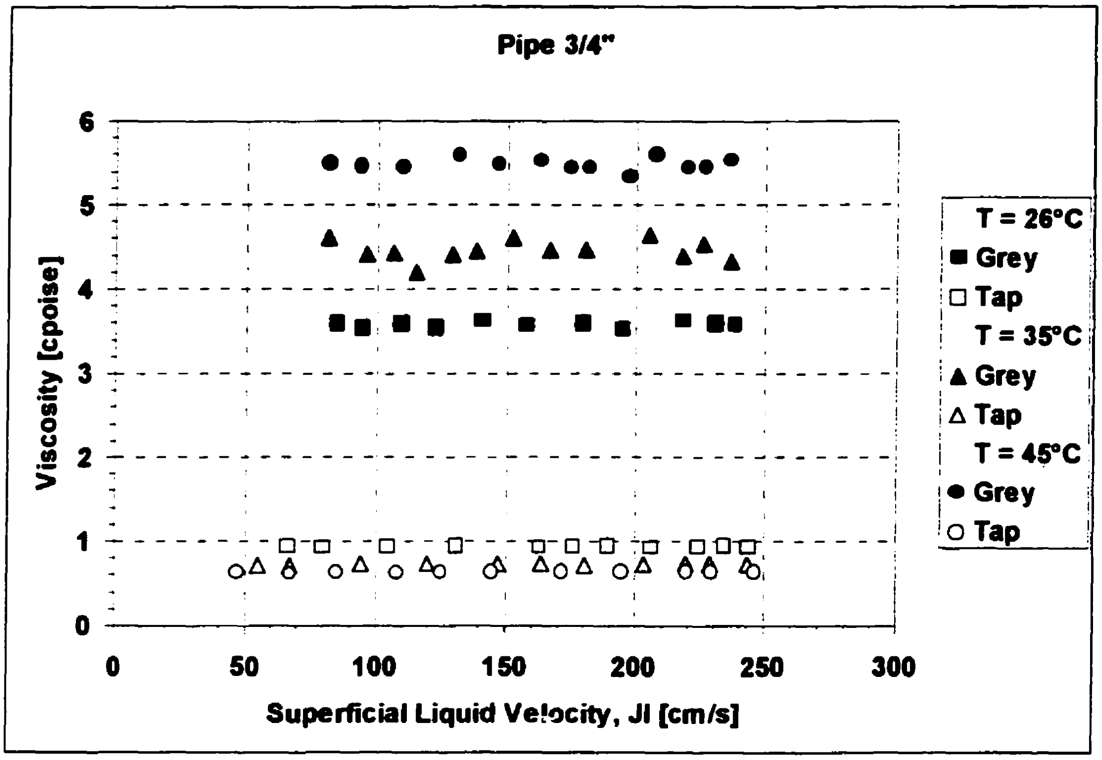

Figure IV.3 Comparison between grey and tap water viscosity for the pipe 3/4"

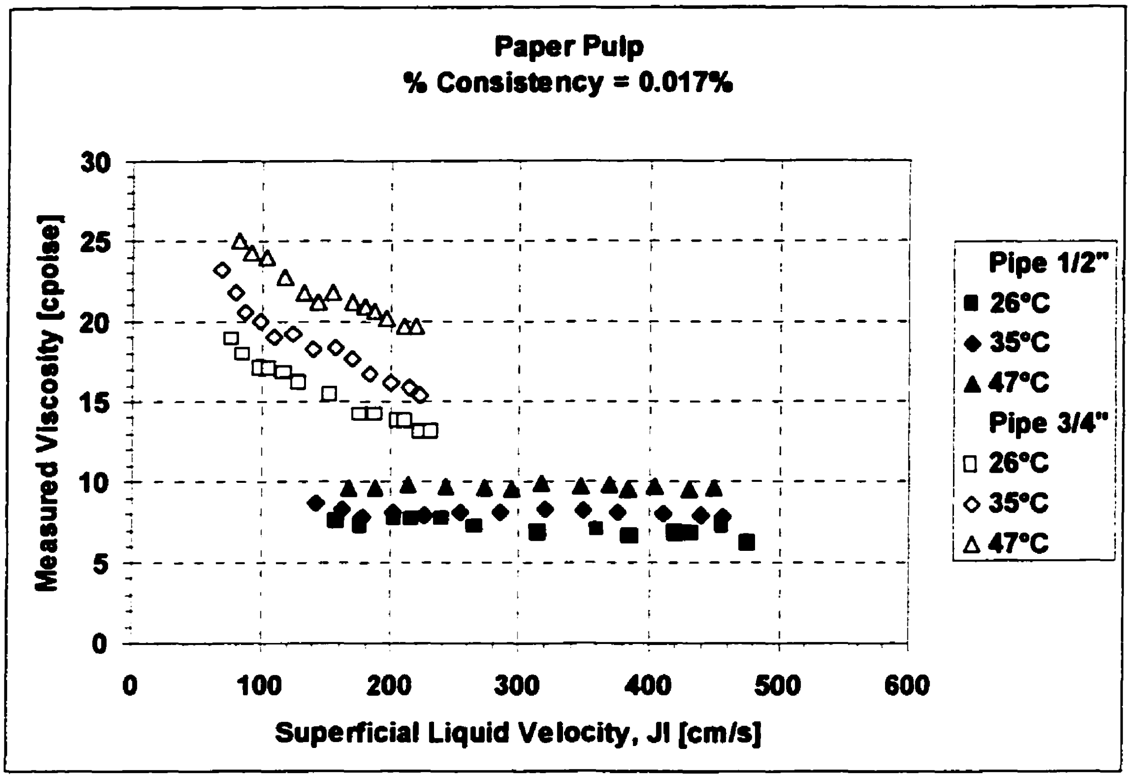

Figure IV.4 Liquid velocity - viscosity relationship (0.017% consistency)

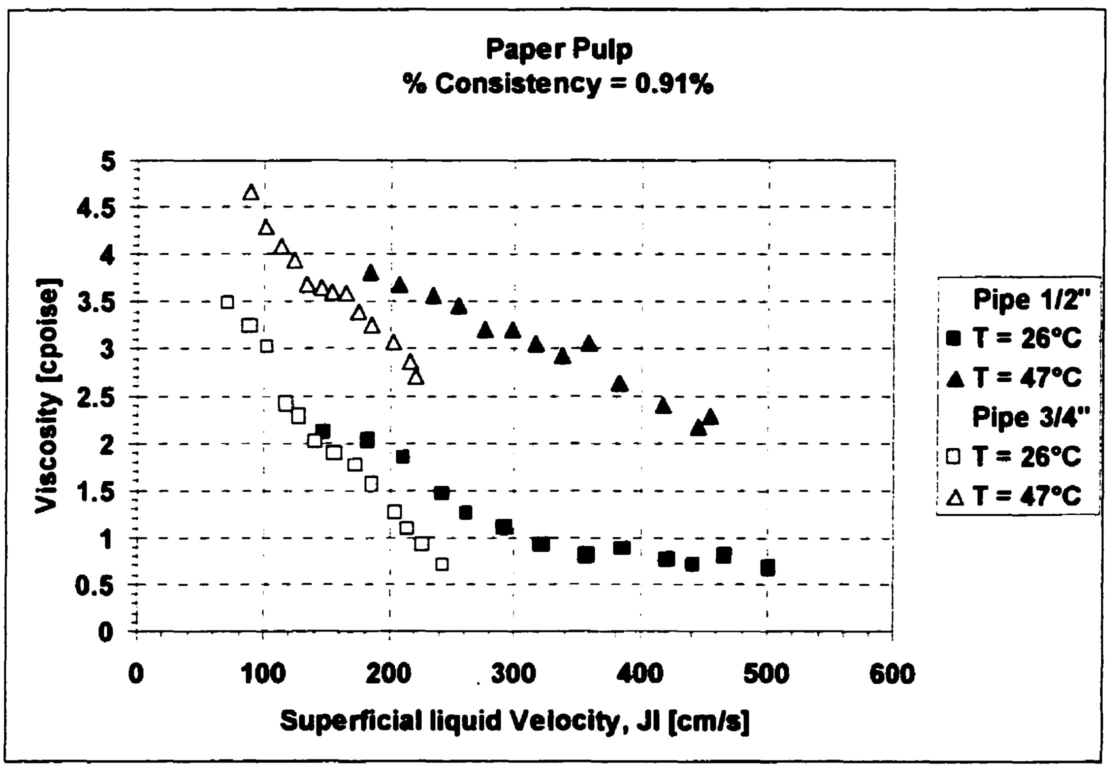

Figure IV.5 Liquid velocity – viscosity relationship (0.91% consistency)

4.3.2 Measurement of Pulp Viscosity by Back Calculation from Direct Bubble Size Measurements

4.3.2.1 Concept

Given the difficulty in estimating viscosity relevant to column flotation a new approach was devised. The proposal is to use bubble size measurements in the flotation column and back calculate viscosity by drift flux analysis. Photographic techniques to measure the bubble size in flotation systems have been reported by many authors (Parthasarathy & Ahmed 1996; Varley, 1995; Miyahara & Hayashino, 1995; Diaz – Peñafiel & Dobby 1994; Tucker *et al.* 1994; Zhou *et al.*, 1992; Dobby *et al.*, 1988; Yianatos *et al.*, 1988b). However, most are for gas – water systems. A device – a so called bubble viewer – to collect a sample of bubbles in slurries has been developed by the mineral processing group at McGill University. A schematic of the viewer is given in Figure IV.6. The chamber and tube are first filled with grey water from the plant (in this case) and inserted in the column. The use of grey water ensures the same chemical environment for the bubble as it enters the viewer. The air bubbles rise through the liquid column in the tube to the angled window of the chamber. Angling the window ensures the formation of a single layer of bubbles whereby overlap of bubbles is minimized and the viewing plane is unambiguous. The bubbles are videotaped and transferred to a computer for image processing. Typically 300 bubbles were sized by hand for each condition. Using the Sauter mean diameter d_s (Eq. IV.8), the viscosity of paper pulp was found by back calculation using drift flux analysis.

$$d_s = \frac{\sum n_i * d_i^3}{\sum n_i * d_i^2} \qquad (IV.8)$$

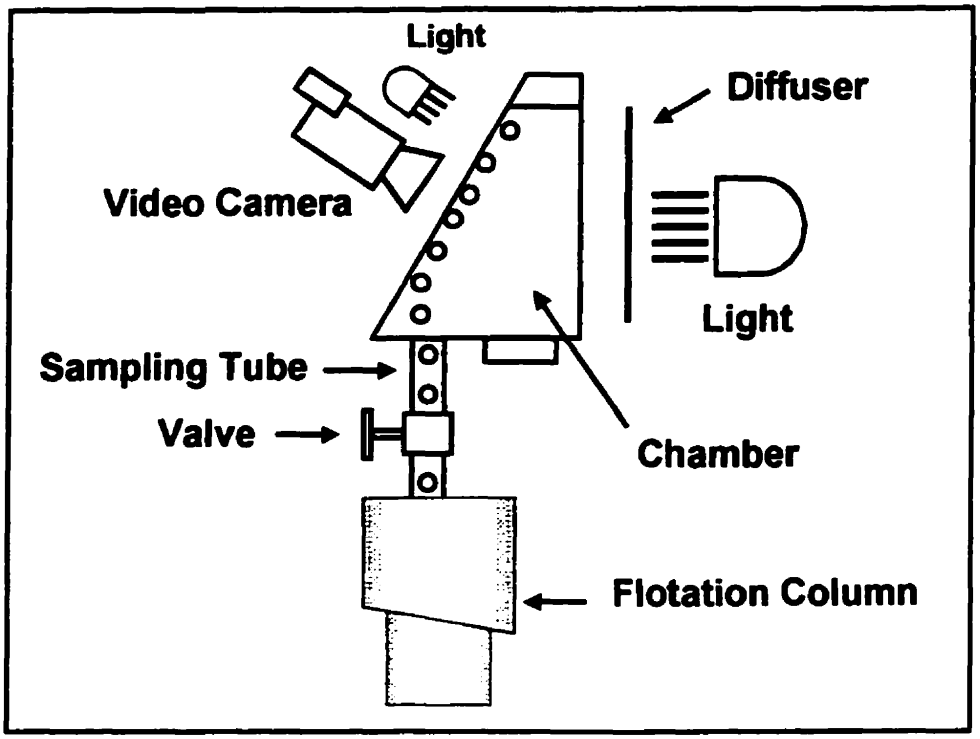

Figure IV.6 Schematic representation of the bubble viewer

The 4" lab column, 450 cm high, was used in this experiment. Air bubbles were produced with the SS sparger # 3 (nominal pore size 5 μm). The column was fed continuously from a 70 L stirred-vessel filled with sample from the plant flotation circuit feed. Three pressure transmitters were installed at intervals along the length of the column both to measure the gas holdup and to control level (position of the pulp/froth interface). Two peristaltic pumps equipped with I/O cards controlled the flow of feed and accepts measured by magnetic flowmeters. The air rate was regulated by a mass flowmeter/controller. The instruments were controlled or monitored using a serial communication interface OPTOMUX and a computer. The software package for data collection and column operation was FIXMMI. The set-up is illustrated in Figure IV.7. The conditions of the experiments are given in Table IV.2.

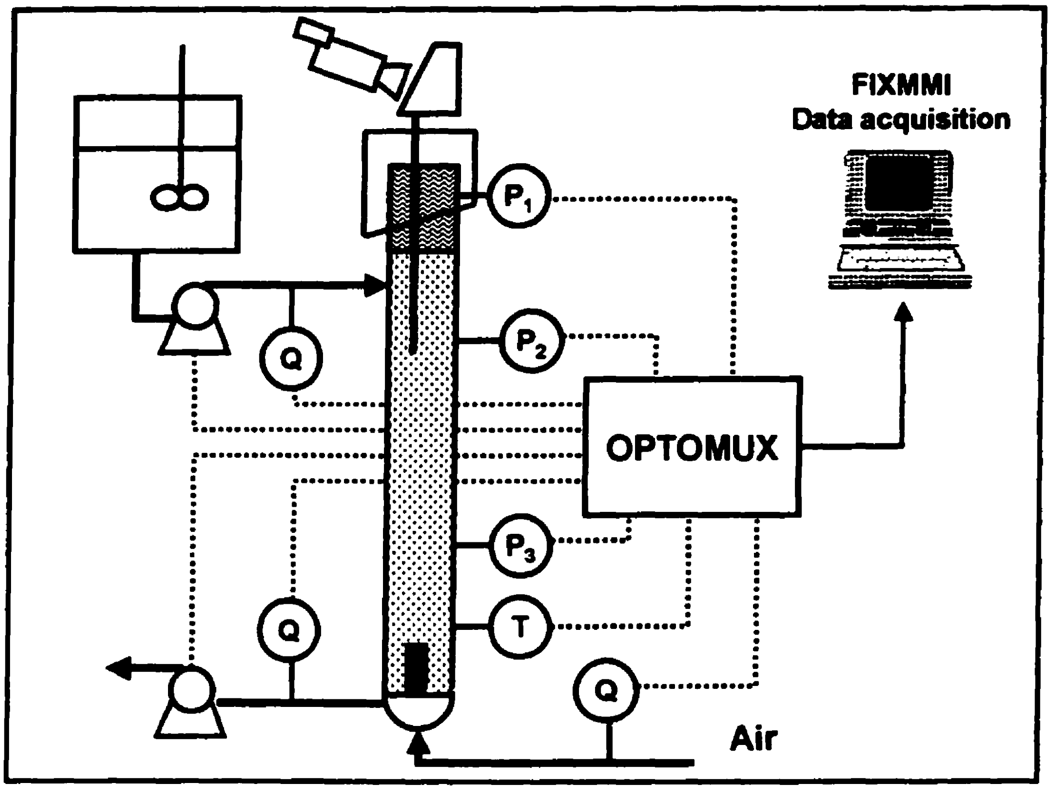

Figure IV.7 Experimental set-up to measure bubble size

Table IV.2 Experimental conditions for direct measurement of bubble size in paper pulp system

Superficial air velocity, J_g (cm/s)	0.5, 1.0, 1.5
Superficial liquid velocity, J_l (cm/s)	1.25
Temperature, **T** (°C)	35 +/- 3 °C
Paper pulp consistency, **S** (%)	~ 0.97

4.3.2.2 Results

Measurement of bubble size distribution was performed for three air velocities up to 1.5 cm/s. At higher velocities large bubbles appeared which were difficult to collect in the viewer (the tube diameter was probably too small). Examples of the bubble images and the measured size distribution are shown for J_g = 0.51 cm/s and 1.5 cm/s in Figures IV.8 through 11; the computed Sauter means are given in Tables IV.3 and 4.

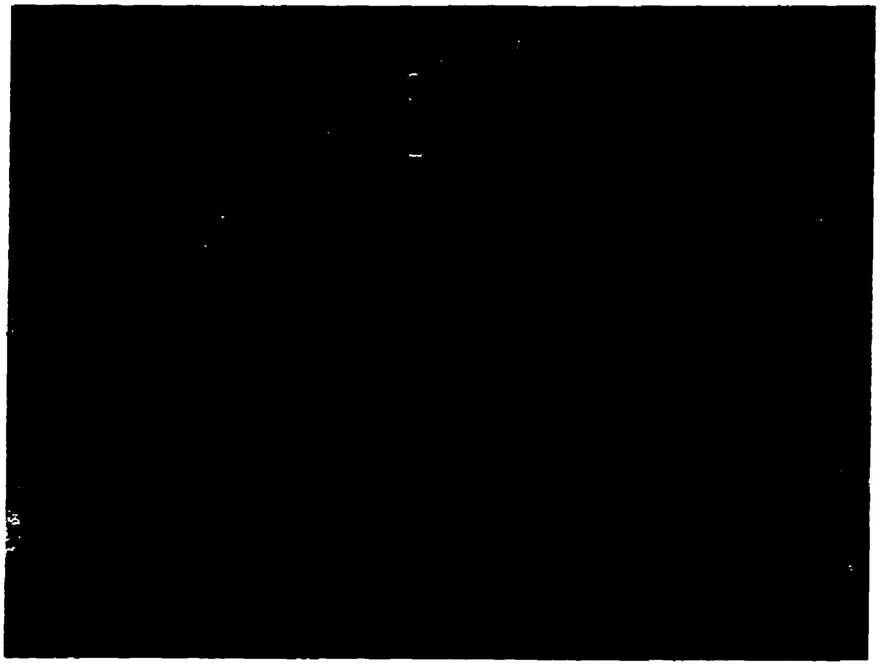

Figure IV.8 Bubbles generated in paper pulp suspension, J_g = 0.51 cm/s

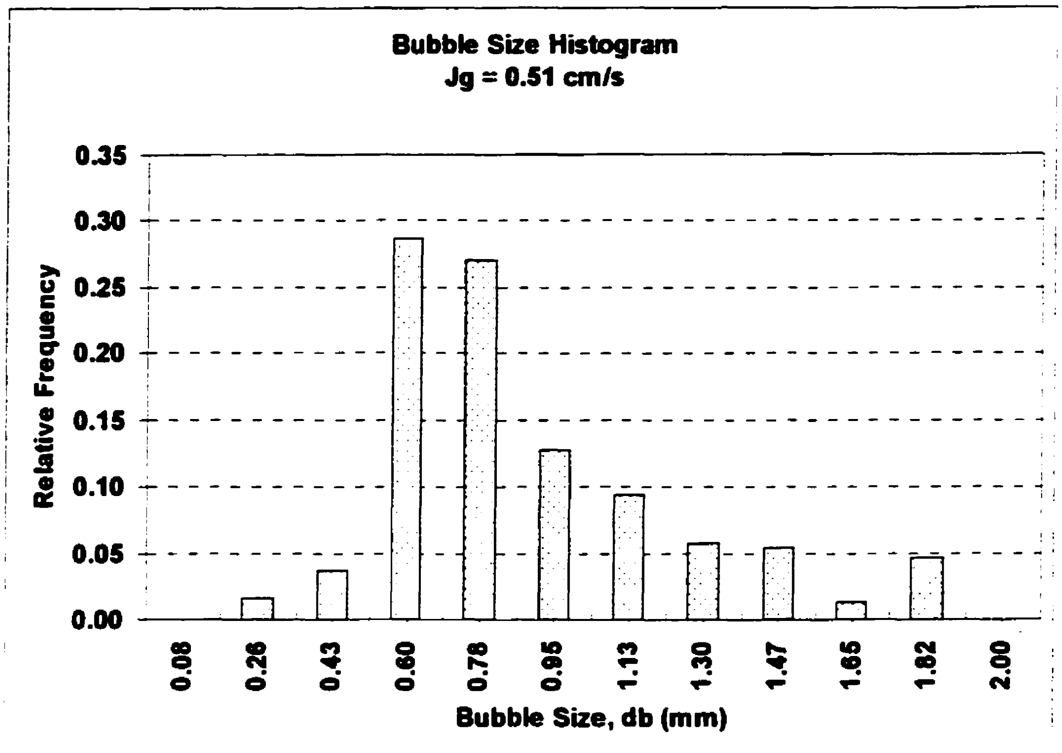

Figure IV.9 Bubble size distribution for paper pulp suspension, J_g = 0.51 cm/s

Table IV.3 Details of bubble size measurement with J_g = 0.51 cm/s

Measurement Class d_b (mm)		Mid point d_b (mm)	Relative Frequency	Frequency
0.00	0.16	0.08	0.00	0
0.17	0.34	0.26	0.02	5
0.35	0.51	0.43	0.04	11
0.52	0.69	0.60	0.29	86
0.70	0.86	0.78	0.27	80
0.87	1.03	0.95	0.13	38
1.04	1.21	1.13	0.09	28
1.22	1.38	1.30	0.06	17
1.39	1.56	1.47	0.05	16
1.57	1.73	1.65	0.01	4
1.74	1.90	1.82	0.05	14
1.91	2.08	2.00	0.00	5
		Sum =	**1.00**	**304**
	Sauter d_b (mm) =		**1.15**	

Figure IV.10 Bubbles generated in paper pulp suspension, J_g = 1.51 cm/s

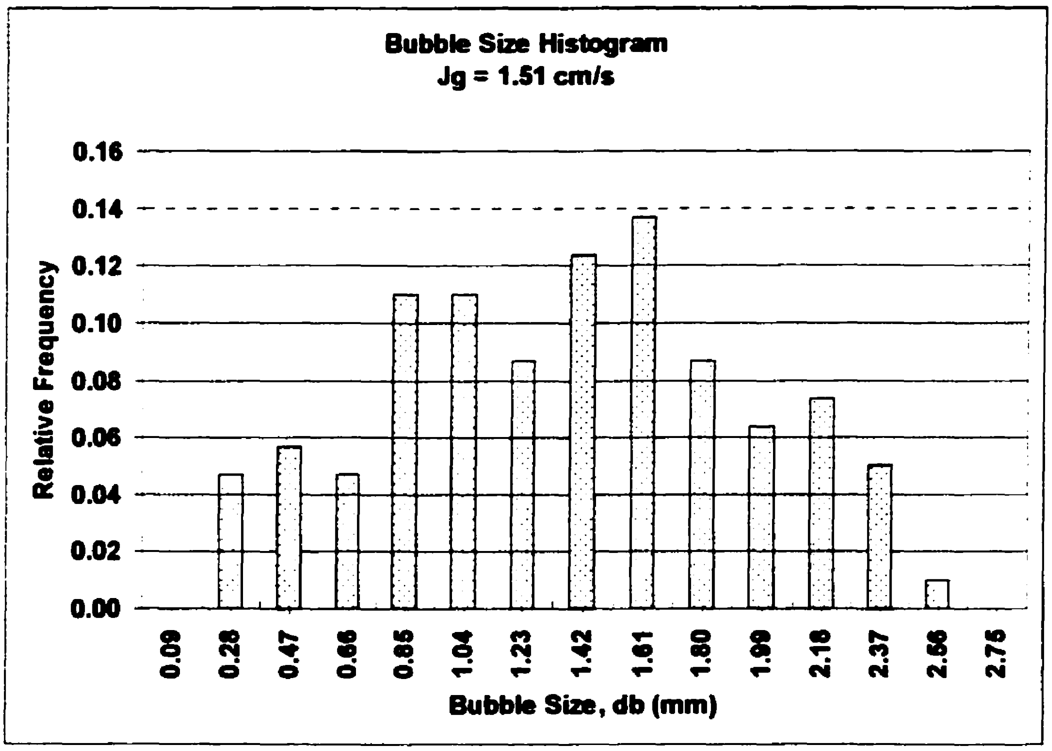

Figure IV.11 Bubble size distribution for paper pulp suspension, J_g = 1.51 cm/s

Table IV.4 Details of bubble size measurement with J_g = 1.51 cm/s

Measurement Class d_b (mm)		Mid point d_b (mm)	Relative Frequency	Frequency
0.00	0.18	0.09	0.00	0
0.19	0.37	0.28	0.05	13
0.38	0.56	0.47	0.06	17
0.57	0.75	0.66	0.05	14
0.76	0.94	0.85	0.11	33
0.95	1.13	1.04	0.11	32
1.14	1.32	1.23	0.09	25
1.33	1.51	1.42	0.12	37
1.52	1.70	1.61	0.14	41
1.71	1.89	1.80	0.09	26
1.90	2.08	1.99	0.06	19
2.09	2.27	2.18	0.07	22
2.28	2.46	2.37	0.05	15
2.47	2.65	2.56	0.01	4
2.66	2.84	2.75	0.00	0
		Sum =	**1.00**	**298**
	Sauter d_b (mm) =		**1.73**	

As can be seen from the histograms, as the air velocity increases, the size distribution widens and moves to larger bubbles. From the Sauter mean bubble size, values of paper pulp viscosity were estimated by back calculation (Table IV.5).

Table IV.5 Estimates of paper pulp viscosity.

J_g (cm/s)	ε_g (%)	Sauter d_b (mm)	μ (cpoise) at 35°C +/- 3°C
0.51	5.10	1.15	1.263
1.03	7.47	1.41	0.861
1.51	11.31	1.73	1.601

The values of viscosity are between those of tap water and grey water namely ca. 0.72 cp and ca. 4.2 cp, respectively (Figure IV.3). This is a potentially significant finding and is the first attempt to support the use of water properties, adapted by Finch *et al.* (2000), for pragmatic purposes. As a further demonstration that water properties are appropriate, Figure IV.12 compares the predicted bubble diameter from drift flux analysis using both tap water (0.72 cp) and grey water (4.2 cp) viscosity compared to the measured. While either value could be used, to a first approximation the trend in the measured d_b is preserved in the estimates using water viscosity. This fact is exploited later to estimate d_b and hence bubble surface area flux in column scale-up.

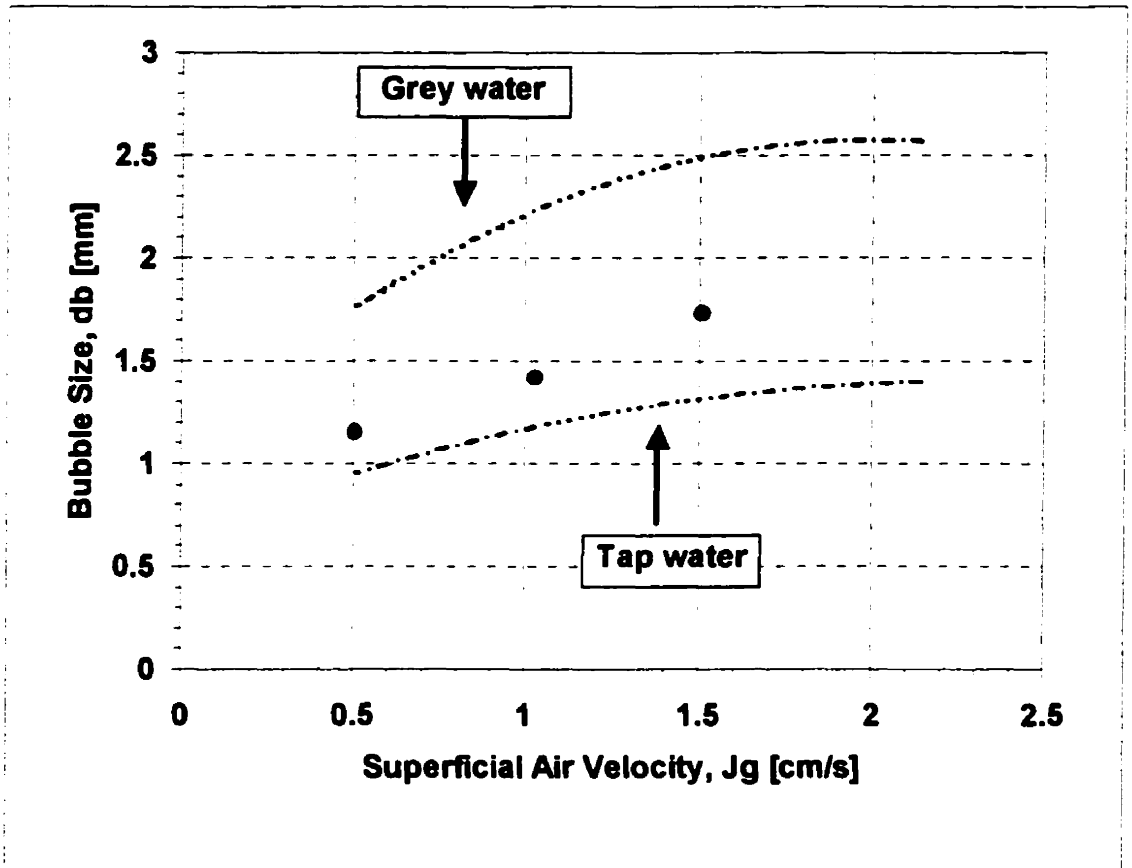

Figure IV.12 Comparison between measured and predicted bubble diameter calculated from drift flux analysis using both tap water and grey water.

4.4 Summary of the Chapter

- Two methods to estimate the apparent viscosity of paper pulp were tested: Fluid flowrate – pressure head loss data in a pipe loop; and a novel approach, measurement of bubble size and back calculation using drift flux analysis.
- The flow behavior of paper pulp is complex: According with the results there is an effect of pipe diameter, consistency and temperature.
- The turbulent flow of fiber in suspension is subject to high shear rates and when there is insufficient volume for the fiber to move freely, they agglomerate and form networks of flocs. As a result the viscosity changes.
- The information obtained from the loop test may not be representative of the behavior in a flotation column.
- The estimate of viscosity using the back calculation procedure suggested values not far different from tap water.

The raw data and calculations for all these experiments are given in **Appendix B**

CHAPTER V

Gas Dispersion in Paper Pulp

5.1 Introduction

The major properties of gas dispersed in a flotation column are gas holdup (ε_g), superficial gas velocity (J_g), bubble size (d_b) and the derived parameter, bubble surface area flux (S_b). Many attempts have been made to understand gas dispersion in paper pulp suspension (Reese *et al.*, 1996; Lidsay *et al.*, 1995; Walmsley, M.R.W. 1992; Pelton & Piette; 1992). However, these studies were conducted under conditions not corresponding to those in a flotation column. In this chapter, the hydrodynamics of gas/pulp systems is reviewed. Experiments were performed in the 4" lab column to explore of the effect of pulp consistency on ε_g.

5.2 Objective

The objective of this chapter is to determine the effect on gas dispersion of sparger type (porosity) and paper pulp consistency: The measure of gas dispersion is gas holdup.

5.3 Experimental

The experiments were performed using the 4" lab column at Bowater's Gatineau de-inking plant. The experimental set-up and the test facility are illustrated in Figures V.1 and 2, respectively. The column was fed continuously with paper pulp from a 70 L stirred-vessel filled from plant flotation circuit feed. Three pressure transmitters were installed at intervals along the length of the column both to measure the gas holdup and to control the position of the pulp/froth interface. The air rate was regulated by a mass flowmeter/controller. Bubble generation used six different porous SS spargers with nominal pore size 0.5, 2, 5, 10, 20, 40 and 100 μm. Two peristaltic pumps equipped with I/O cards, controlled the flow of feed and accepts. Which were measured with two magnetic flowmeters. All instruments were controlled or monitored using a serial communication interface OPTOMUX and a computer. The software package for data collection and column operation was FIXMMI.

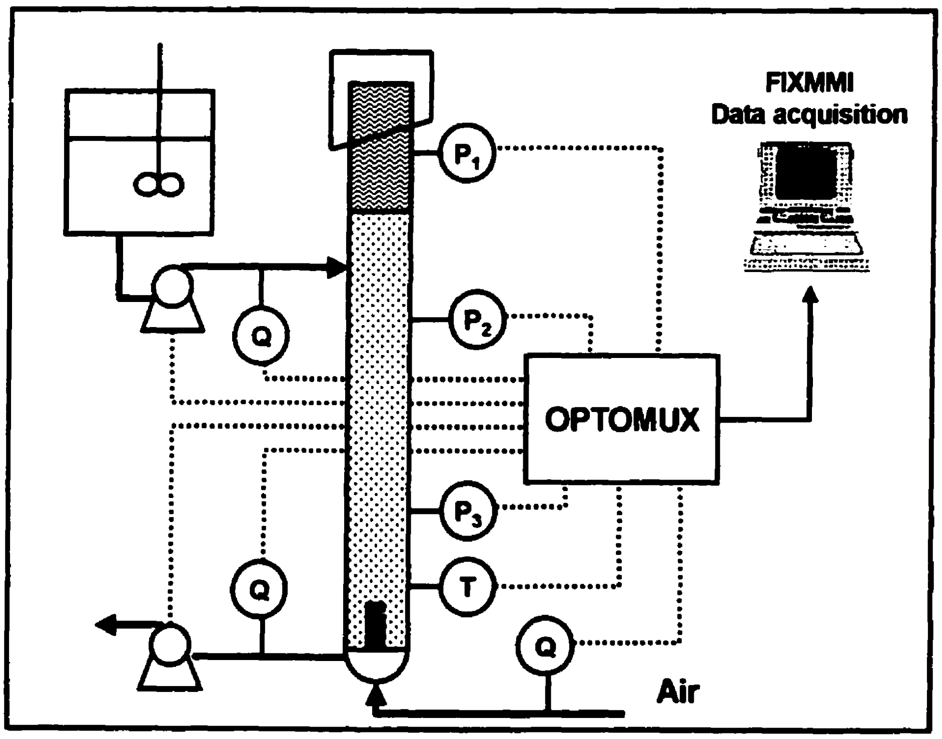

Figure V.1 Experimental set up for measuring gas holdup

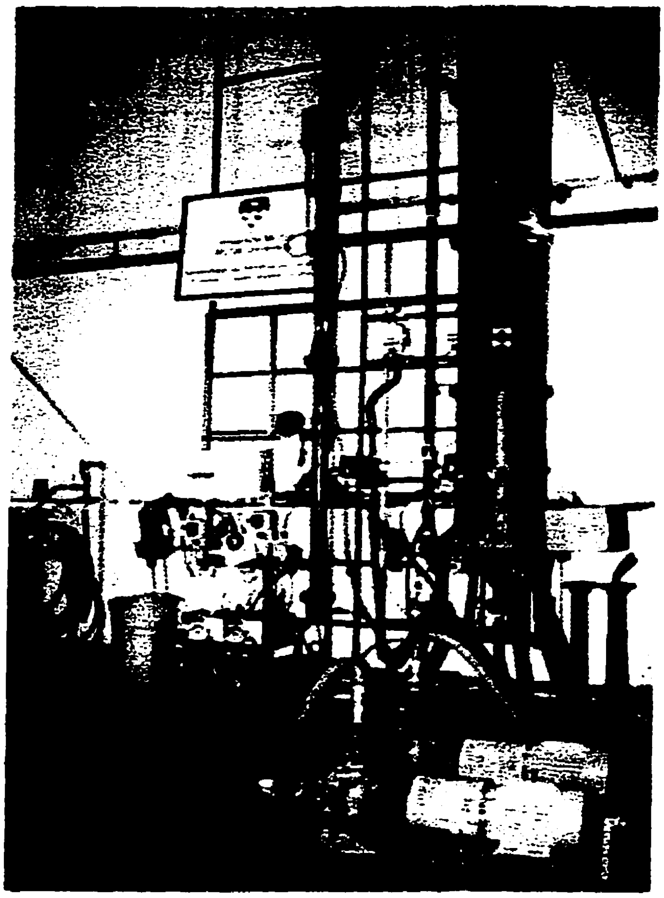

Figure V.2 Column flotation test facility at Bowater's Gatineau plant.

Table V.1 is a summary of the experimental design. The spargers were cleaned with hydrochloric acid before each experiment and the pulp temperature was that of the plant (40°C +/- 5°C). The depth of the froth was maintained at 50 cm (+/- 5 cm) from the top of the column. The pulp dilution water was grey water from the plant thickener.

Table V.1 Experimental design for the 4" lab column.

Sparger	J_g (cm/s)	J_l (cm/s)	% Consistency	T (+/- 5°C)
1 to 7	0.5, 1.0, 1.5, 2.0, 2.5	1.25	1.0	40
1	0.5, 1.0, 1.5, 2.0, 2.5	1.25	0.5, 0.7, 1.0, 1.5	40
6	0.5, 1.0, 1.5, 2.0, 2.5	1.25	0.5, 0.7, 1.0, 1.5	40

5.4 Calculations

5.4.1 Level Control

The froth depth (level) in the column was controlled with the FIX DMMI software package PID routine. The PID block maintains balance in a closed loop by changing the controlled variable (feed flowrate) in response to deviations from a user-defined set point (level in this case). The error or deviation is the difference between the actual value and the set point, calculated using information from the pressure transmitters. In response to this error, the PID block calculates an appropriate control output signal, which attempts to reduce the error to zero. The adjustment that the PID block makes is a function of the difference between the set point and the measurement, in addition to the values of the proportional band, the reset, and the rate. Figure V.3 shows the installation for estimating level in the flotation column. Equation V.1 was used to calculate the level from the three pressure transmitters (Gomez *et al.*, 1997).

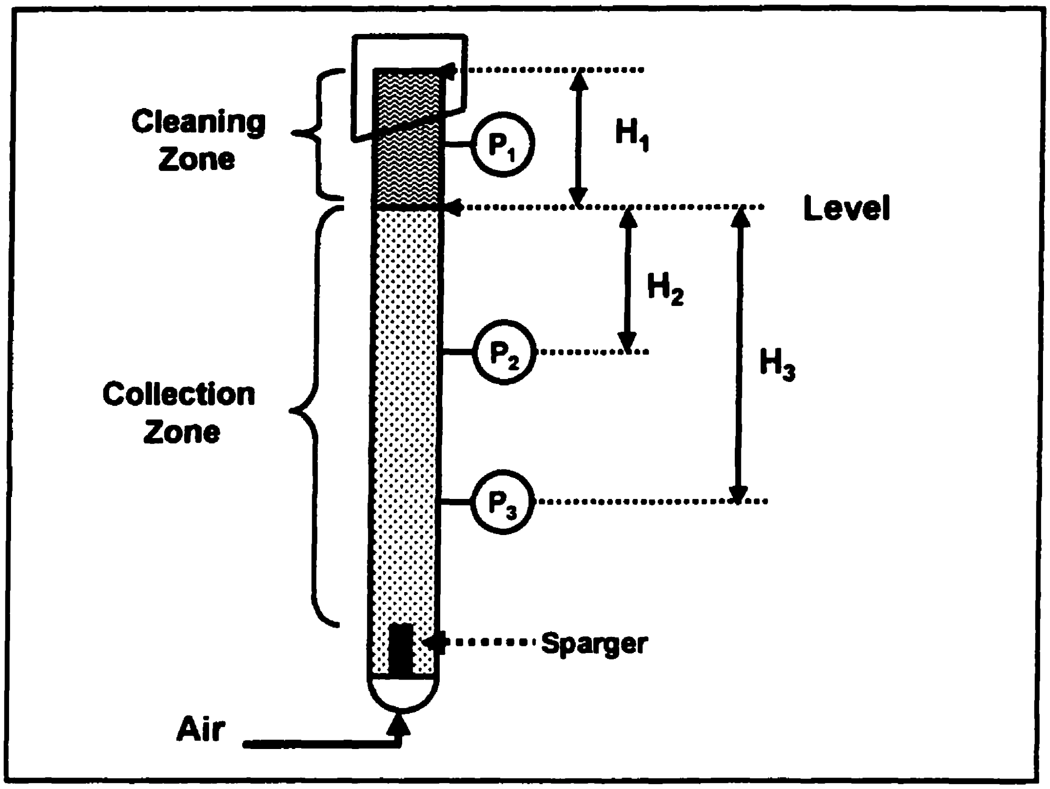

Figure V.3 Schematic of level measurement using three pressure transmitters.

$$\text{Level} = \frac{P_3 - \left(\dfrac{P_3 - P_2}{H_3 - H_2}\right) * H_3}{\dfrac{P_1}{H_1} - \left(\dfrac{P_3 - P_2}{H_3 - H_2}\right)} \qquad (V.1)$$

where:

P_i = Pressure of the point i, m water

H_i = Height i, m

ρ_f = Density of the cleaning zone, Kg/m^3

ρ_c = Density of the collection zone, Kg/m^3

g = Gravity acceleration, 9.81 m/s^2

L = Level, m

Key:

P_1 = $\rho_f * H_1 * g$

P_2 = $\rho_f * L * g + \rho_c * (H_2 - L) * g$

P_3 = $\rho_f * L * g + \rho_c * (H_3 - L) * g$

5.4.2 Gas Holdup

Gas holdup (ε_g) is the fraction of air in a known volume of air + pulp. Provided density is not a factor, as is the case here with such low consistency pulps, ε_g can be measured using the pressure drop between two points along the column (see Figure V.4). Liquid manometers or transducers (as here) can be used to measure the pressure. Gas holdup is then calculated from:

$$\varepsilon_g = \frac{\Delta H}{\Delta L} = 1 - \frac{\Delta P}{\rho_l * g * \Delta L} \qquad (V.2)$$

where:

ΔH = Difference in manometer heights, m

ΔP = Pressure difference, m of water

ΔL = Distance between the pressure transmitters P_2 and P_3, m

ρ_l = Density of the liquid or slurry

g = Gravity acceleration, 9.81 m/s^2

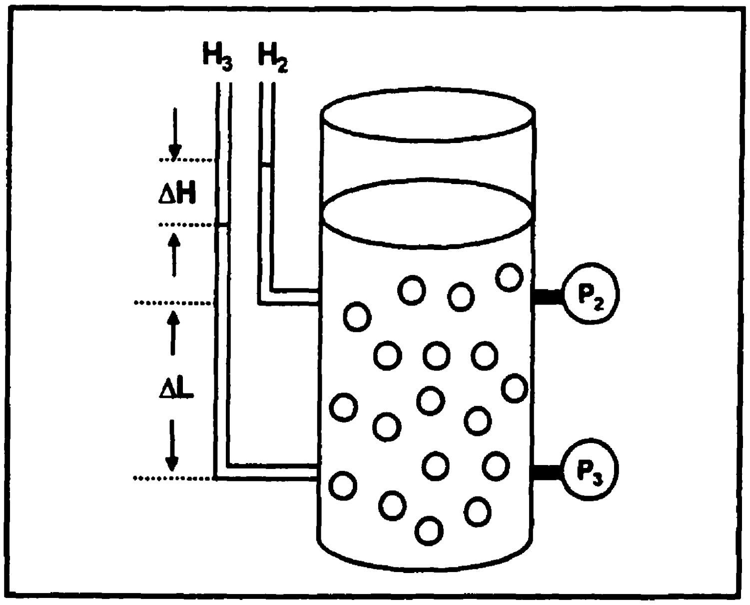

Figure V.4 Schematic of gas holdup measurement.

5.4.3 Paper Pulp Consistency

Consistency of the paper pulp is the dry weight percent solids. Bowater's de-inking process operates with consistencies between 0.80 to 1.35 %. The consistency was measured using the plant procedure as follows:

1. 250 ml of paper pulp suspension was accurately measured
2. The sample was poured into a Buchner funnel and filtered using pre-weighed Ahlstrom filter paper (617 grade, 15 cm diameter, very fast filtration speed)
3. The pad and filter paper were removed from the funnel and any remaining fibers were collected on the inside of the funnel
4. The pad and filter paper were placed in an oven at approximately 150°C until dry
5. After drying, the pad and filter paper were weighed on an electronic balance

The consistency calculation was as follows:

$$\%\,\text{Consistency} = \left[\frac{\left(W_{\text{Pulp dry}} + W_{\text{Filter paper}}\right) - W_{\text{Filter paper}}}{W_{\text{Pulp wet}}}\right] * 100 \qquad (\text{V.3})$$

5.5 Results and Discussion

5.5.1 Effect of Sparger Pore Size

Figure V.5 shows the effect of sparger type (determined by nominal pore diameter) on gas holdup for the same consistency. The sparger # 1 with the finest pore (0.5 μm) gave the highest gas holdup. Sparger # 7 (100 μm), producing large bubbles that rise quickly, as a result gave the lowest gas holdup.

The results are much as expected, confirming the trend with nominal pore size despite uncertainly in permeability (Chapter III).

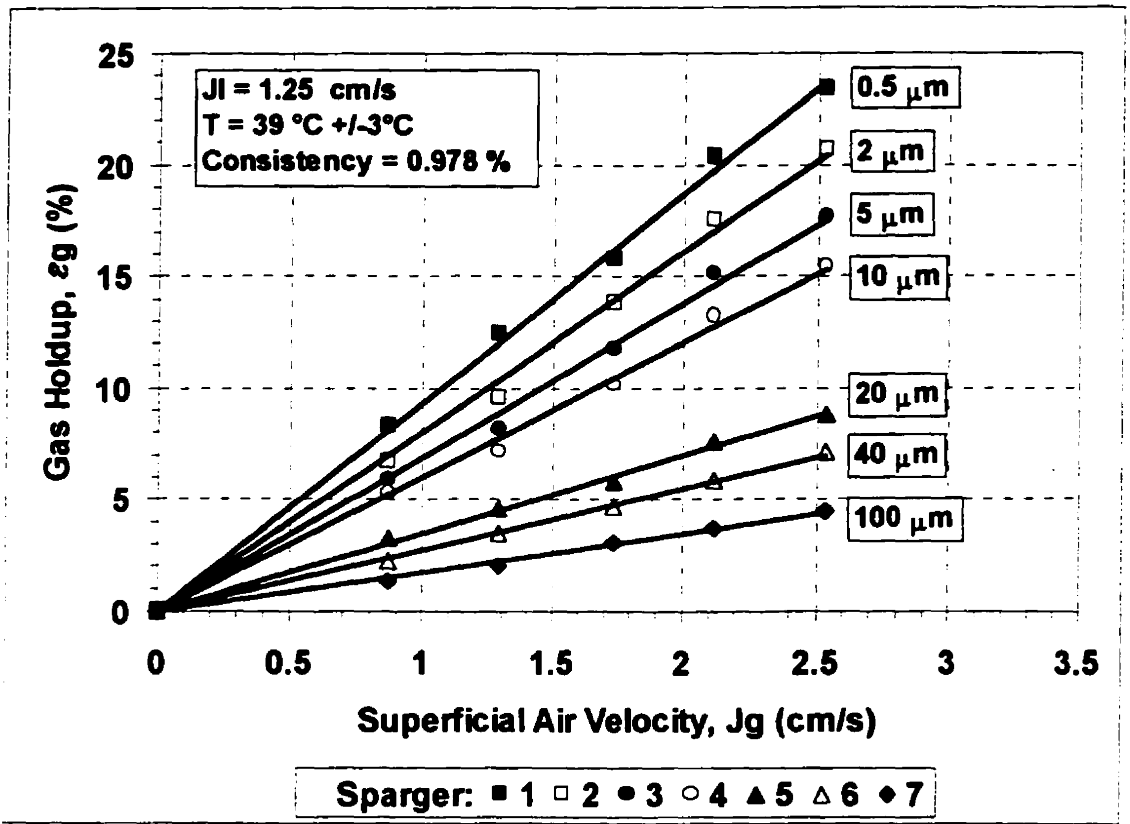

Figure V.5 Effect of sparger nominal pore size on gas holdup.

5.5.2 Effect of Paper Pulp Consistency

Paper pulp consistencies used in this experiment were from 0.50 to 1.35% with dilution to control consistency made using the grey water obtained from the plant thickener. Figures V.6 and V.7 show the effect of the air velocity on gas holdup for the different consistencies using spargers # 1 and # 6. The general trend was that gas holdup decreased with increasing consistency (Figures V.6 - 10). Janse *et al.* (1999) found the same in previous work at Bowater and Lindsay *et al.* (1995) and Reese *et al.* (1996) also report this trend. Some authors suggest the reason is that the fibers promote bubble coalescence. Pelton and Piette (1992) found as the consistency increased, the fibers act as barriers to upward bubble motion resulting in the formation of large bubbles. Walmsley (1992) observed coalescence at 0.10% consistency, where bubbles can still be seen clearly. There is no confirmatory evidence of coalescence in this slurry (partly because at the consistencies used visual inspection is restricted). Banisi (1994) offered a novel interpretation: the presence of solids increased bubble rise velocity through a viscosity-related effect on the bubble wake size and hence reduced gas holdup. The exact cause in the present case remains unknown.

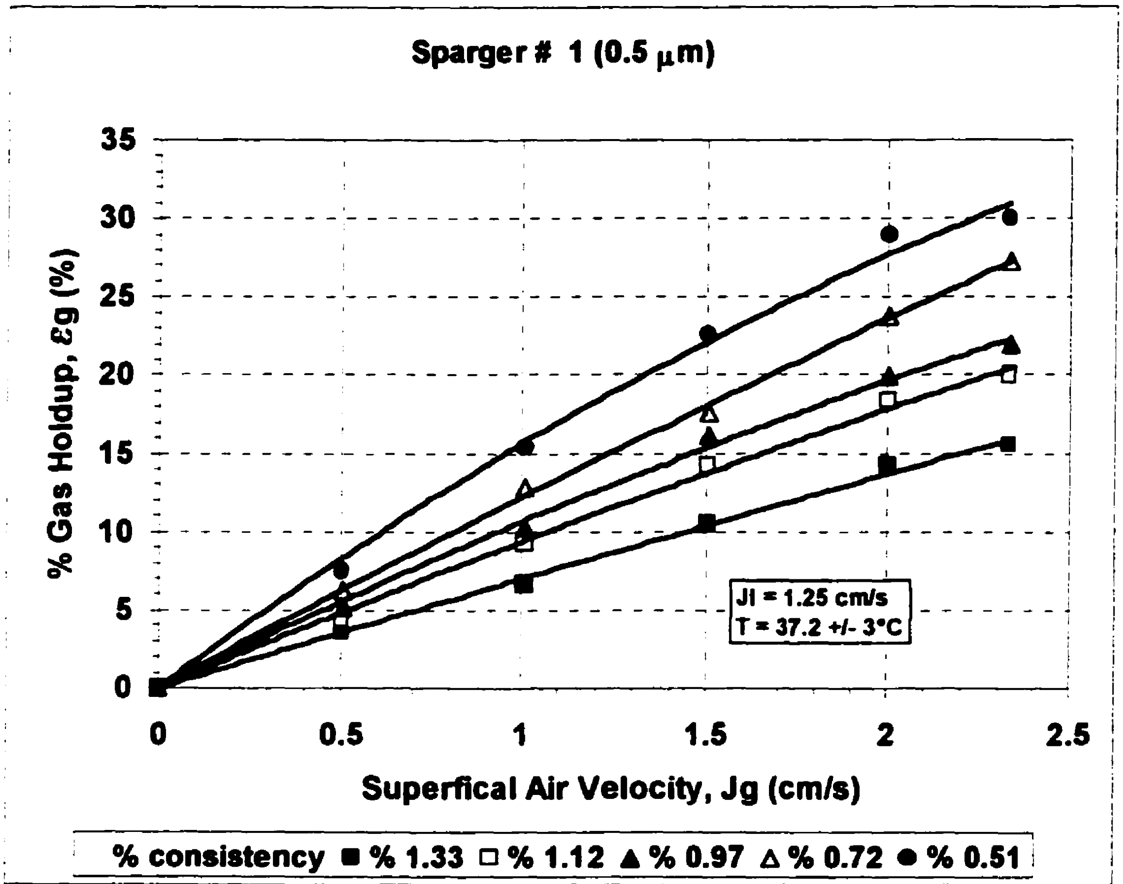

Figure V.6 Gas holdup as a function of superficial air velocity: Effect of pulp consistency for sparger # 1.

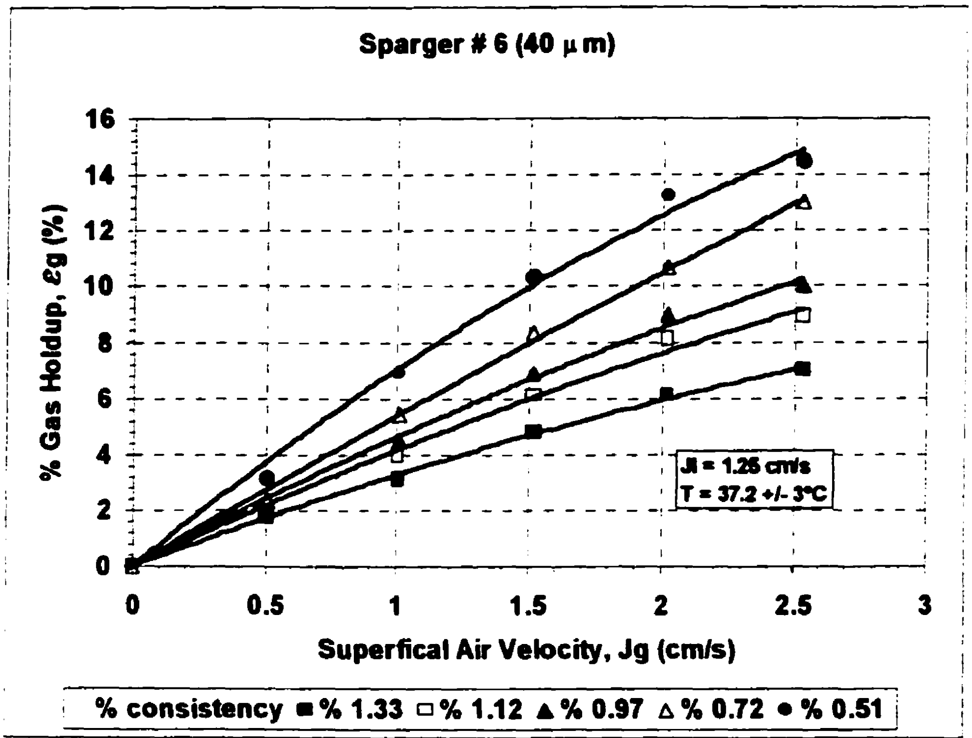

Figure V.7 Gas holdup as a function of superficial air velocity: Effect of pulp consistency for sparger # 6.

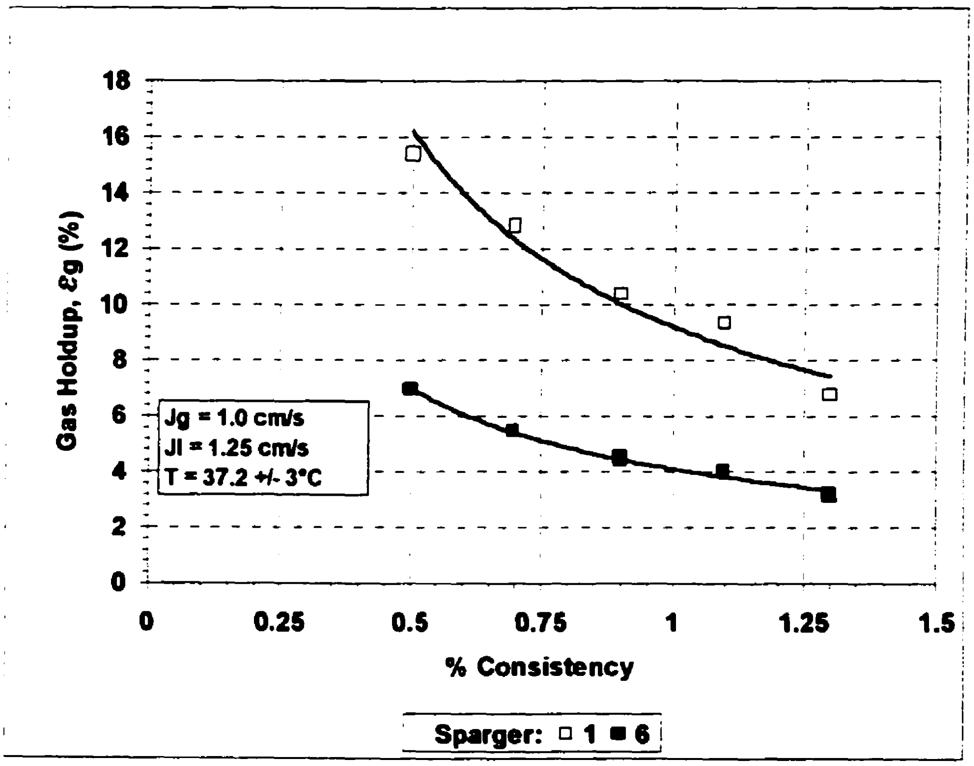

Figure V.8 Gas holdup as a function of pulp consistency for sparger # 1 and # 6.

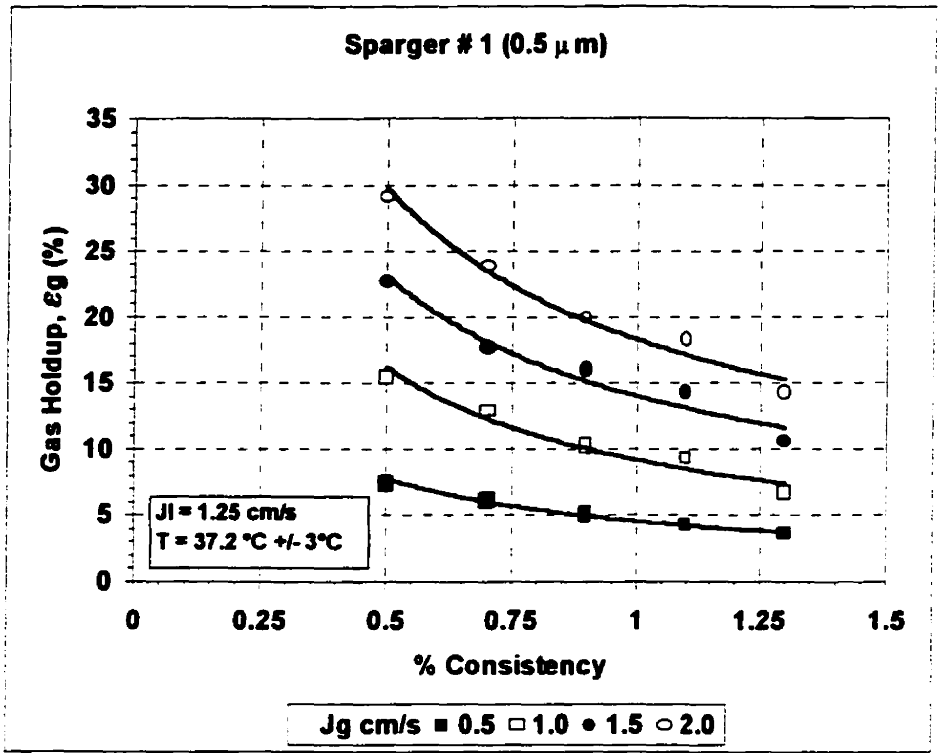

Figure V.9 Gas holdup as a function of pulp consistency for sparger # 1

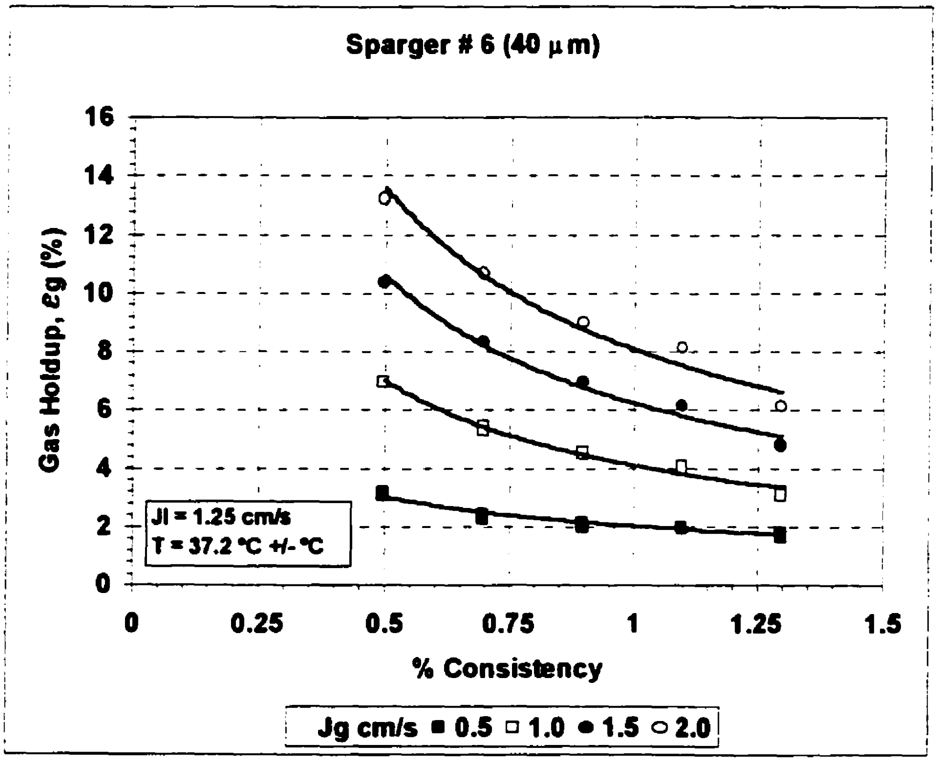

Figure V.10 Gas holdup as a function of pulp consistency for sparger # 6

5.6 Summary of the Chapter

- Gas holdup at a given gas rate increased as nominal pore size decreased, as expected.
- For every air flowrate, gas holdup decreased with increasing consistency. The conventional explanation – fibers cause coalescence and the resulting large bubbles rise rapidly – is assumed here.

The raw data for all these experiments are given in **Appendix C**

CHAPTER VI

Mixing

6.1 Introduction

The degree of mixing is required for scale-up. Column flotation has been the subject of numerous investigations to try to model mixing (or transport) (O'Connor & Mills, 1995; Luttrel *et al.* 1993; Ityokumbul, 1992; Ynchaustl *et al.* 1988; Dobby & Finch, 1986; Shah *et al.* 1982; Flint, 1973). Among the parameters to quantify mixing, one commonly recognized is the dispersion number and/or the axial dispersion coefficient. Joshi and Sharma (1979) linked the axial dispersion coefficient to vessel diameter and velocities of the fluids. Mavros *et al.* (1989) found the axial dispersion coefficient increased (i.e. mixing increased) with gas flow rate up to velocities of 0.1 cm/s, beyond which there was no effect. Conversely, decreased liquid velocities resulted in an increase in mixing. Unfortunately, the range of air velocities is an order of magnitude below typical column operating conditions. Reith *et al.* (1998) measured gas holdup and mixing as a function of air velocity and related the axial dispersion coefficient to the liquid velocity and column geometry. This relationship held as long as the air velocity was in excess of 10 cm/s. Again, these conditions are outside the typical conditions found in column operations.

Several expressions have been developed which relate the dispersion coefficient to various parameters (see Table II.1), although the validity has not been established over a range applicable to column flotation. Columns are rarely operated at gas rates that exceed 2-5 cm/s or designed with height to diameter ratios that exceed 5-8:1 (Finch and Dobby, 1990). It may be helpful if a relationship relevant to column flotation in paper pulp systems could be derived. This is tackled here by determining the residence time distribution (**RTD**) as a function of selected variables from which N_d was estimated by a fitting routine. A conductivity method was employed to determine **RTD** similar to that employed by a number of investigators (Mavros & Danilidou, 1993; Xu & Finch, 1991; Matsumoto *et al.*, 1989; Kato & Nishiwaki, 1972).

6.2 Objective

The objective is to relate the axial dispersion number N_d determined from the **RTD** as a function of column geometry and flow conditions in paper pulp systems.

6.3 Experimental

Liquid residence time distribution (**RTD**) was measured using the stimulus-response technique. A pulse, consisting of an appropriate amount of an aqueous solution of potassium chloride (KCl ~20% weight) was introduced into the incoming liquid (feed) stream, and the response was monitored by recording the change in conductivity of the fluid exiting from the underflow stream. Potassium chloride (**KCl**) was chosen as the tracer because it meets the basic requirements for an **RTD** test as outlined by Shah *et al.* (1978):

1. The tracer should be miscible in and have physical properties similar to the fluid phase of interest, and should not be transferable to the other phase or phases in the system.
2. The tracer should be accurately detectable in small concentrations so that only a small quantity need be injected into the system, thus minimizing

disturbances in the established flow patterns. Also, a concentration range which yields a linear response on the detection system is highly desirable.

3. The tracer detection system should cause the least amount of disturbance to the flow patterns.
4. A sensitive and quick detection response time is needed.

Experiments were conducted in the three columns to give a range in height-to-diameter ratio (L_c/D_c). A summary of the experimental design is given in Table VI.1.

Table VI.1 Experimental design to estimate N_d in paper pulp systems

Column	**4" Lab.**			**6" Lab.**		**20" Pilot**
Diameter (cm)	10.16			15.24		50.00
Height (cm)	243	163	110	258	173	430
L_c/D_c	23.9	16.0	10.8	16.92	11.35	8.6
J_g **(cm/s)**	1.0, 1.5, 2.0			1.0, 1.5, 2.0		1.0, 1.5, 2.0
J_l **(cm/s)**	1.0, 1.5, 2.0			1.0, 1.5		1.5
Consistency (%)	~ 1.0			~ 1.0		~ 1.0
Sparger (μm)	0.5	40		0.5		(6), 0.5

The pulp was fed to the column from a 70 L stirred-vessel filled from the accepts of the plant flotation circuit. The liquid flow rates (feed and underflow) were monitored using two magnetic flow meters with signal converters. The gas flow rate was measured using a mass air flow meter. A porous stainless steel sparger was used to generate the bubbles (1 sparger in the lab units and up to 6 in the pilot column). To determine the interstitial liquid velocity, J_l, it is necessary to measure gas holdup. This was accomplished by means of differential pressure measurements over a section of the collection zone. Each column had three Bailey pressure transmitters for gas holdup measurement (and level control, see Chapter V). Two variable speed peristaltic pumps for the feed and underflow streams in the 4" and 6" columns were used. For the pilot unit, two centrifugal pumps with a maximum capacity of 300 L/m with two valves for flow control were used. Temperature was registered using an ICTD probe. Conductivity was measured using a sensor connected to a Bailey conductivity meter. The input tracer was injected close to the column and the conductivity sensor was placed close to the column in the underflow line, to minimize time delay in collecting the signals. The 0 – 4096 analog/digital output signal was recorded every 2 seconds. The instruments were connected or monitored using a signal conditioning and interface unit OPTOMUX monitored on a Pentium 200 MHz computer. Outputs were monitored and collected through a software package FIXMMI. A schematic diagram of the lab column used in the liquid RTD tests is shown in Figure VI.1.

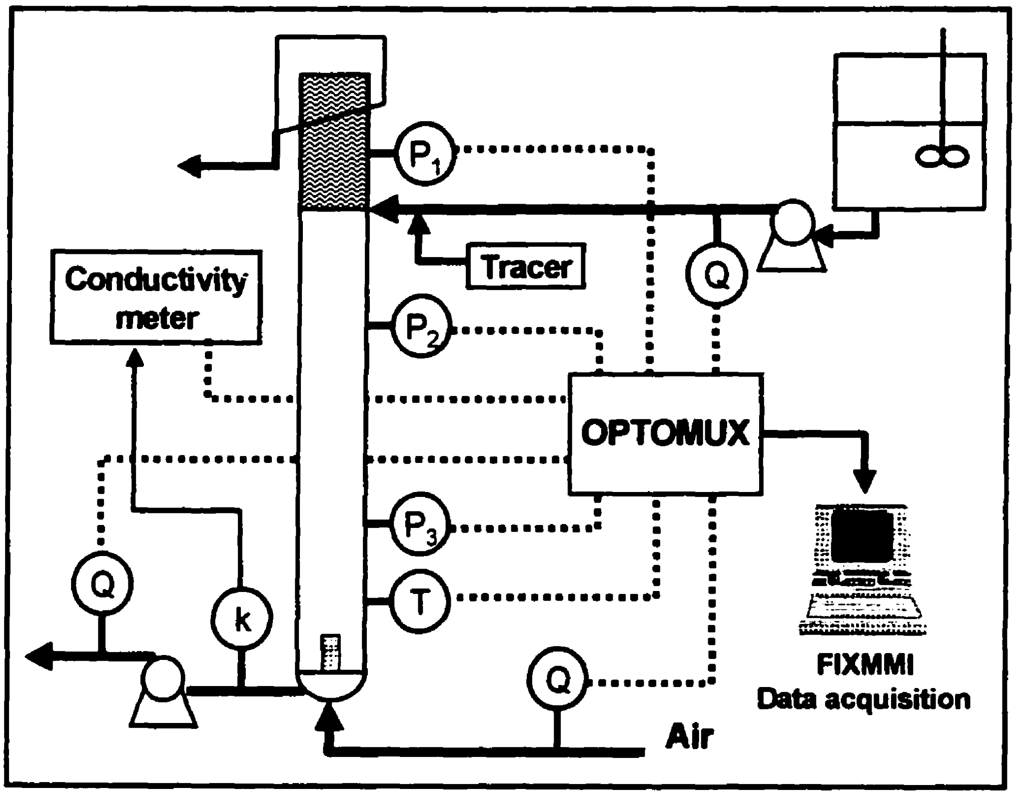

Figure VI.1 Experimental set-up to measure RTD in 4" lab column.

6.4 Calculations

6.4.1 Conductivity Meter Calibration

The **KCl** concentration was detected using the Bailey conductivity meter. The correlation between **KCl** concentration, conductance and conductivity were established for the appropriate range of the conductivity meter. The procedure to calibrate the instrument is described below.

First:

A known resistance (Ω) was connected in the terminals of the conductivity meter, and the **A/D** output signal was monitored using the interface OPTOMUX. A correlation between **A/D** signals vs. conductance (**1/Ω**) was found for three ranges of the conductivity meter. Figure VI.2 shows an example of a calibration curve. The plot is for range 1.

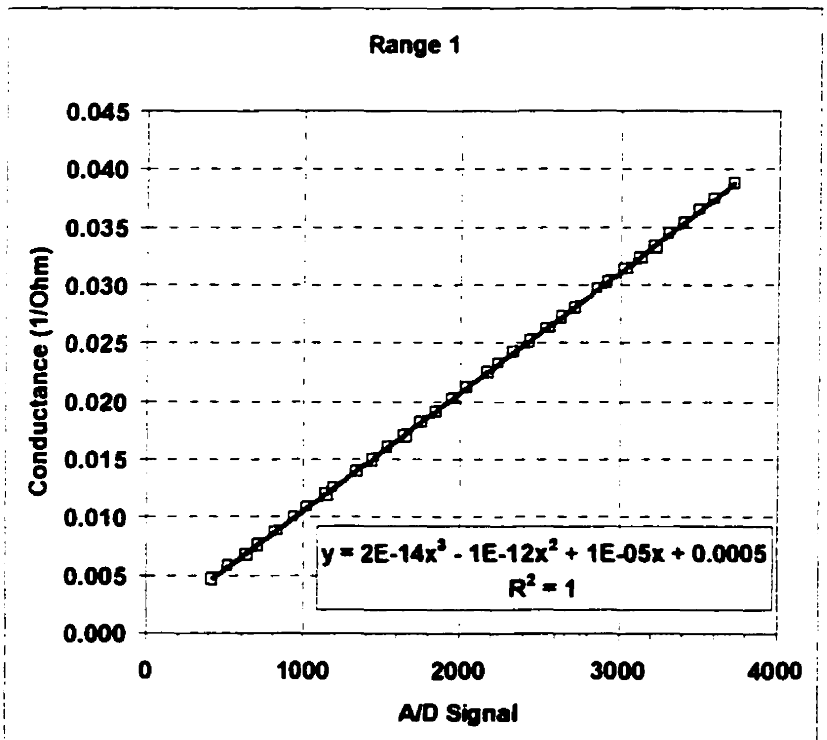

Figure VI.2 Calibration curve of Conductance vs. A/D signal

Second:

The conductivity sensor was connected to the conductivity meter. The **A/D** signal using different solutions of **KCl** with known conductivity and temperature was monitored using OPTOMUX. A peristaltic pump was used to circulate the solution through a PVC pipe of 1/2 inch diameter where the sensor was installed (Figure VI.3). Correlations between conductance vs. conductivity and conductivity vs. **KCl** concentration were found for different temperatures and different ranges of the conductivity meter (Figures VI.4, VI.5 and VI.6).

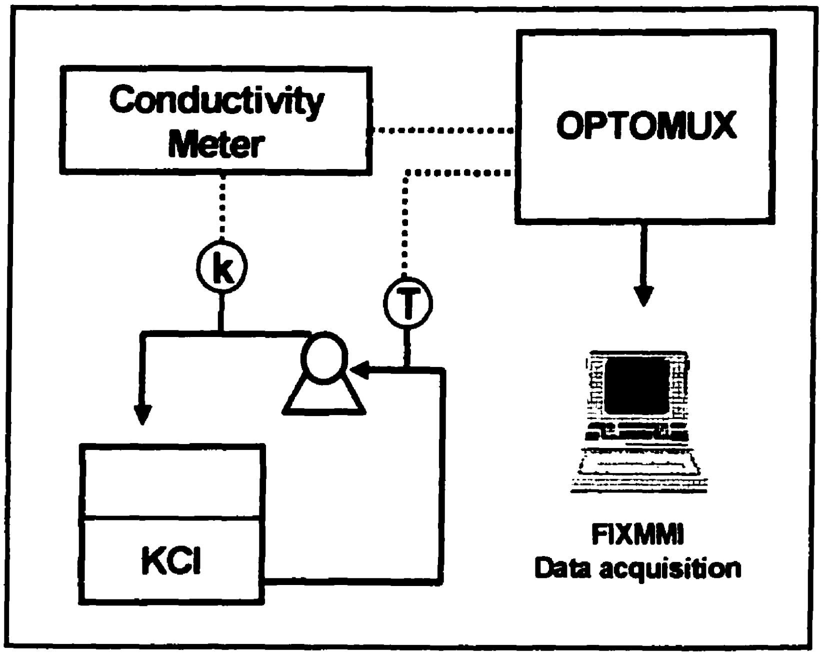

Figure VI.3 Set-up to calibrate the conductivity meter

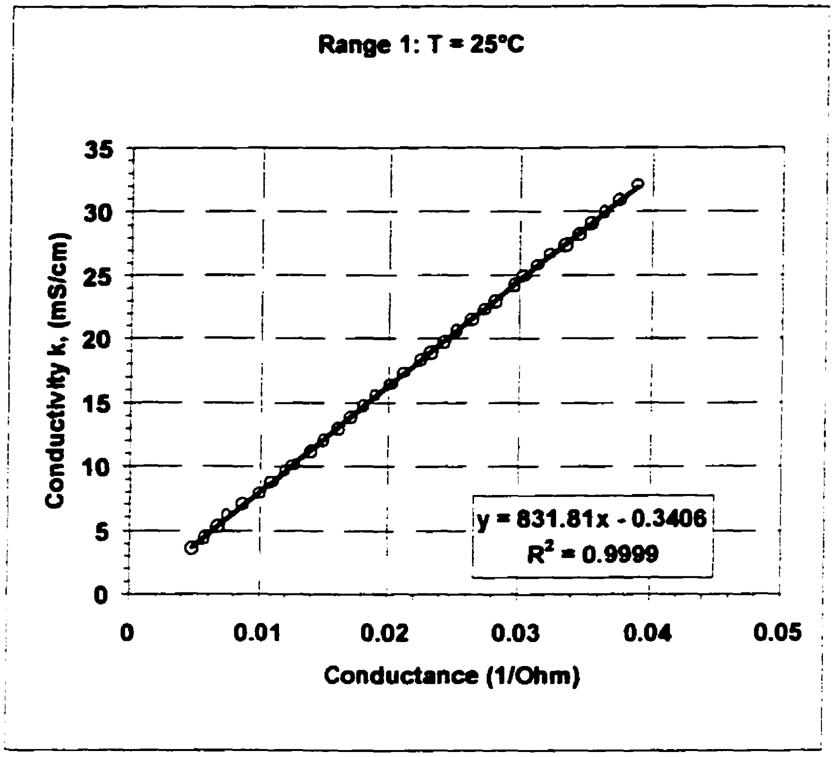

Figure VI.4 Calibration curve of conductivity vs. conductance

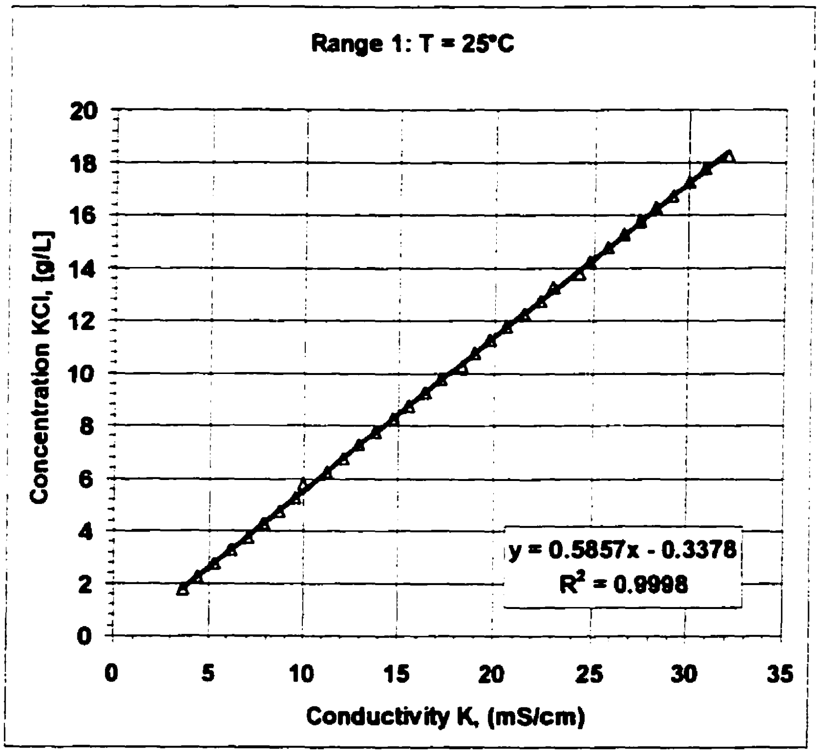

Figure VI.5 Calibration curve of [KCl] vs. Conductivity

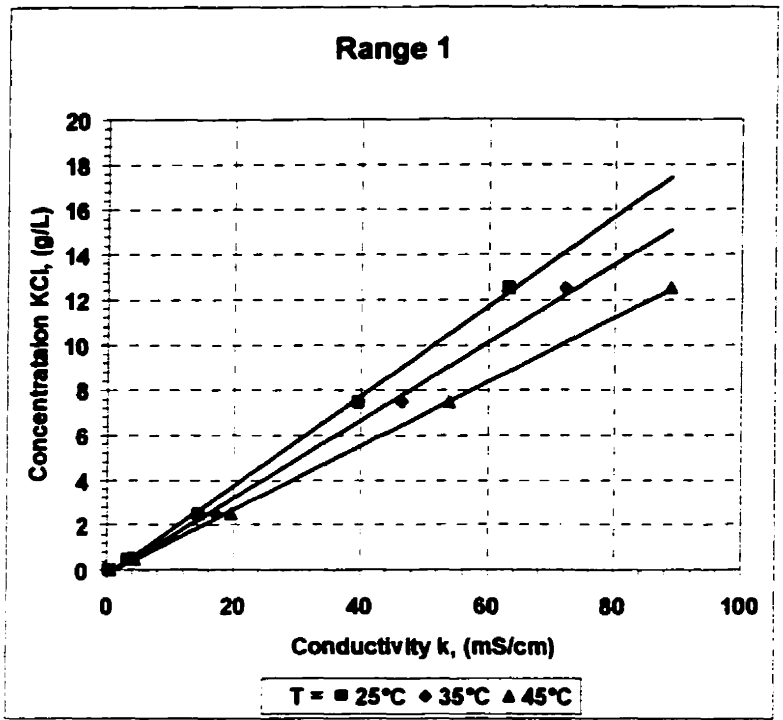

Figure VI.6 Calibration curve of [KCl] vs. conductivity as a function of temperature

6.4.2 Residence Time Distribution

Fitting of experimental residence time distributions (**RTD**) and predicting age distributions from the laboratory and pilot flotation columns using the axial dispersion model were done using the equations described in section 2.7 according with Levenspiel (1999).

6.5 Results and Discussion

A typical residence time distribution (**RTD**) curve is shown in Figure VI.7. One example of fitting the **RTD**, and calculating the mean residence time, mass balance and variance from the **A/D** signal response – time data is given in **Appendix E**.

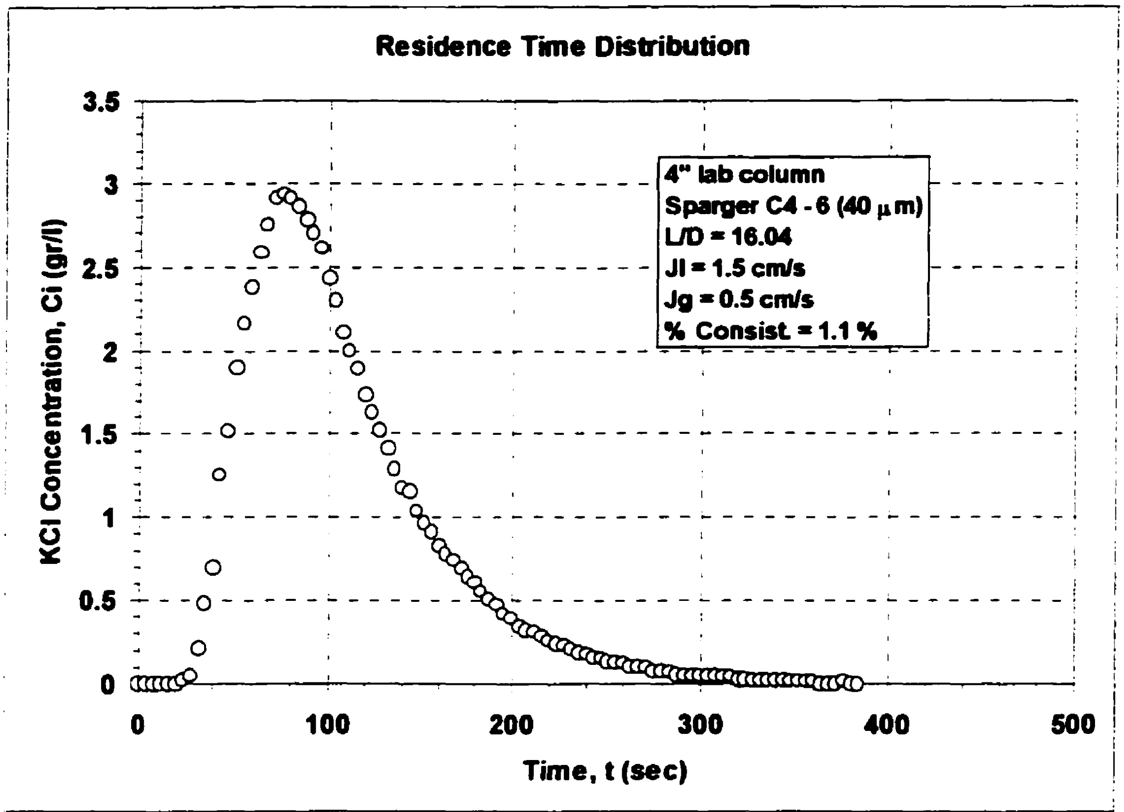

Figure VI.7 Typical RTD curve with L_c/D_c = 16.04

After obtaining the **RTD** curve, the mean residence time **(**τ**)** and the normalized tracer concentration (**E**) were calculated using Equation II.37 and Equation II.39, respectively. The curve with respect to the initial tracer concentration, determined from the total area under the normalized **RTD** curve, is plotted in Figure VI.8.

Fitting the dimensionless **RTD** curve **E(θ)** vs. θ using Equations II.41 and II.40 is illustrated in Figure VI.9. There is a good fit for N_d = 0.0975 (The curve for N_d = 0.9999 is shown for comparison only).

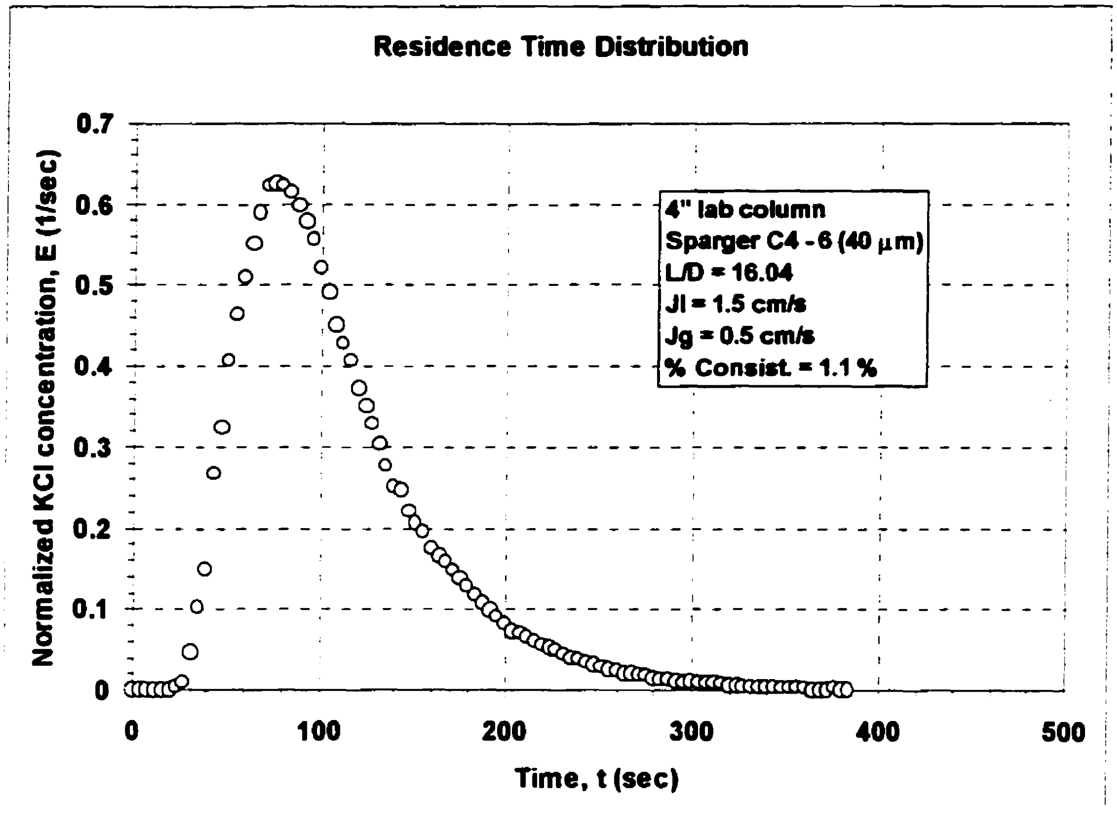

Figure VI.8 Normalized RTD curve with L_c/D_c = 16.04

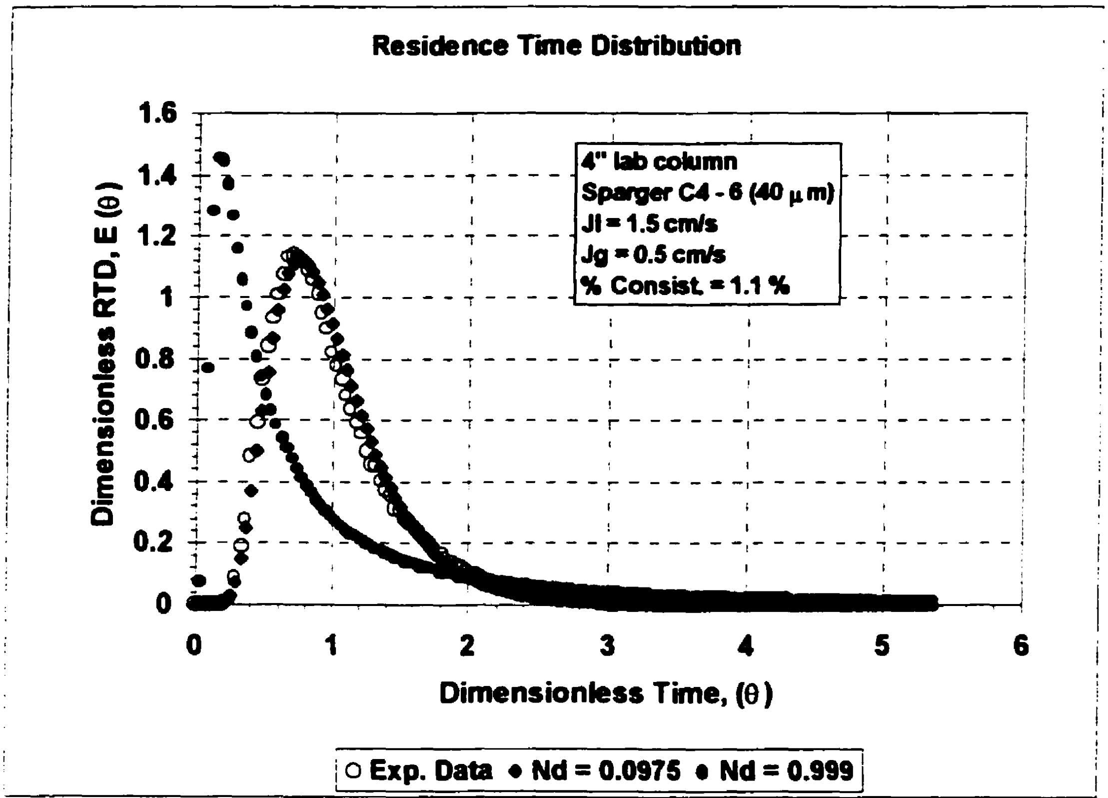

Figure VI.9 Dimensionless RTD curve

6.5.1 Modelling the Vessel Dispersion Number

To model axial mixing, it is necessary to develop an expression which incorporates the variables thought to influence dispersion. These include (but not exclusively): column height and diameter, gas and liquid superficial velocities, and gas holdup. An expression of the following form found in the literature (Mankosa, 1990; Luttrell *et al.*, 1990: Xu & Finch, 1991) was used:

$$N_d = A * \left(\frac{D_c}{L_c} * \frac{J_g}{J_l} * (1 - \varepsilon_g) \right)^B \qquad \text{(VI.1)}$$

where:

N_d = Vessel dispersion number

D_c/L_c = Diameter/height of the column, cm/cm

J_g, J_l = Air and liquid superficial velocities respectively, cm/s

ε_g = Fractional gas holdup

A, B = Constants

The effect of paper pulp consistency and bubble size is included inherently in the expression since these parameters have a direct impact on the gas holdup. Equation V1.1 has the form:

$$Y = A * X^B \quad \text{or} \quad LnY = LnA + B * LnX$$

The least squares method was used to find the parameters **A** and **B**. The solution is:

$$N_d = 1.296 * \left(\frac{D_c}{L_c} * \frac{J_g}{J_l} * (1 - \varepsilon_g) \right)^{0.67} \qquad (VI.2)$$

Figure VI.10 shows the vessel dispersion number (**N_d**), as a function of the expression in the bracket. It shows a reasonable fit: Mixing increases (i.e., **N_d** increases) with both gas flow rate and column diameter, while it decreases with an increase in liquid flow rate and column height. The predicted **N_d** is used in the recovery equation (Equation II.3) in column scale-up as outlined in Chapter VI.

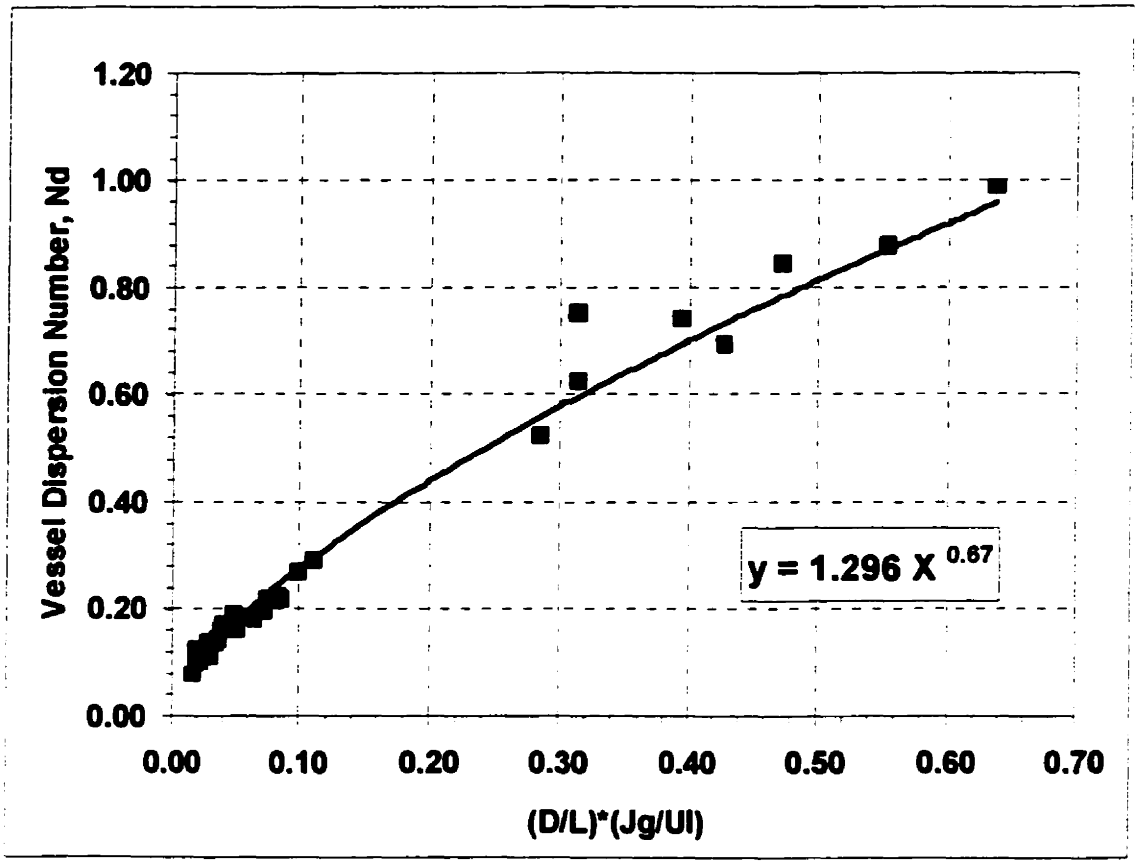

Figure VI.10 Experimentally determined N_d as a function of dimensionless flows and column geometry

6.6 Summary of the Chapter

- An impulse tracer study was used to measure the **RTD** in the three columns as a function of J_g and J_l.
- An expression relating the vessel dispersion number (N_d) to column geometry and flow rates was derived.
- N_d increases with gas flow rate and column diameter, and decreases with an increase in liquid flow rate or column height.

Appendix D summarizes N_d values and tracer mass balances obtained in the experimental work. Some tests were repeated and these are included in the table and show that the reproducibility is good. Also results from the least squares method to find parameters **A** and **B** are given.

CHAPTER VII
Column Scale-Up

7.1 Introduction

Column flotation technology has shown potential in de-inking of waste paper (Watson *et al.* 1996; Carabin *et al.,* 1995; Dessureault, *et al.,* 1995; Petri, 1994). Although column flotation shows excellent brightness gain and ink removal efficiency one problem is that there is no accepted scale-up and design procedure as in mineral processing. Recent work by Leichtle (1998) has indicated that recovery is governed more by the bubble surface area flux (S_b) than any other variable. For this reason it is necessary that S_b be included in any scale-up procedure. The purpose of this chapter is to compare the traditional scale-up procedure with a new proposal including S_b. The relationships presented in previous chapters are incorporated into a comprehensive routine for flotation column scale-up. Laboratory and pilot column tests were conducted at the Bowater paper pulp facilities in Gatineau, Qc. Results from 4" lab column tests were used to scale-up to and compare with the performance in the 20" pilot unit.

7.2 Objective

The objective is to evaluate and compare the traditional scale-up procedure for flotation columns in the paper de-inking process with a new proposal incorporating bubble surface area flux S_b.

7.3 Scale-Up Theory

There are basically three approaches being used in scale-up of flotation columns. These can be classified as scale-up on the basis of column area, scale-up on the basis of column volume and scale-up on the basis of reaching a target recovery (Mankosa, 1990).

First approach

Throughput is assumed to be proportional to the cross-sectional area of the column. This can be expressed mathematically as:

$$D_2 = D_1 * \sqrt{\frac{Q_{f2}}{Q_{f1}}} \qquad (\text{VII.1})$$

where

D_1 and D_2 = Diameters of test and desired column, respectively.

Q_{f1} and Q_{f2} = Volumetric flow rates of feed slurry to test column and full size column.

This approach is valid for data obtained from a laboratory column with a very large L_c/D_c aspect ratio with height similar to the full-scale column. This approach assumes that the change in mixing in the column resulting from the change in aspect ratio on scale-up does not greatly affect the performance of the column. This scale-up generally provides a conservative estimate of column diameter (i.e., larger than actually necessary) (Boutin and Wheeler, 1967; Mathieu, 1972).

Second approach

Scale-up on the basis of volume can be represented mathematically as:

$$V_2 = V_1 * \frac{Q_{f2}}{Q_{f1}} \qquad (\text{VII.2})$$

or, if the aspect ratio of the column remains constant:

$$D_2 = D_1 * \sqrt[3]{\frac{Q_{f2}}{Q_{f1}}} \qquad (\text{VII.3})$$

where $\mathbf{V_1}$ and $\mathbf{V_2}$ represent the volumes of test column and full size column, respectively.

This approach assumes that the slurry residence time is the same in both columns. However, since liquid and air velocities are allowed to change in this type of scale-up, the gas holdup in the column may not necessary remain constant which affects the residence time.

Third approach

In scale-up is on the basis of achieving a target recovery (Dobby & Finch, 1986; Luttrell *et al.*, 1988), it is necessary to study the collection zone and the froth zone separately to understand the overall process (see Chapter II).

The recovery in the collection zone is a function of the flotation rate constant ($\mathbf{k_c}$), mean particle residence time (τ_p), and degree of mixing, represented by the vessel dispersion number ($\mathbf{N_d}$).

A laboratory column with large L_c/D_c ratio tends to exhibit plug flow transport. For a first-order rate process with plug flow the recovery in the collection zone (R_c) is given by:

$$R_c = R_{eq} * [1 - \exp(-k_c * \tau_p)] \qquad \text{(VII.4)}$$

and the recovery in a system exhibiting perfect mixing is:

$$R_c = R_{eq} * \left[1 - \frac{1}{(1 + k_c * \tau_p)}\right] \qquad \text{(VII.5)}$$

where R_{eq} is the equilibrium (or maximum) recovery at long flotation times. Watson (1996) estimated for paper de-inking at Gatineau that the maximum ink recovery was 87 %.

Transport in practice lies plug and perfectly mixed flow. The relationship between recovery and the vessel dispersion number N_d, is given by Levenspiel (1999):

$$R_c = R_{eq} * \left[1 - \frac{4 * A * \exp\left(\frac{1}{2 * N_d}\right)}{(1+A)^2 * \exp\left(\frac{A}{2 * N_d}\right) - (1-A)^2 * \exp\left(\frac{-A}{2 * N_d}\right)}\right] \qquad \text{(VII.6)}$$

where:

$$A = (1 + 4 * k_c * \tau_p * N_d)^{\frac{1}{2}} \qquad \text{(VII.7)}$$

The vessel dispersion number is further defined as:

$$N_d = \frac{E_l}{U_l * L_c} \qquad (VII.8)$$

where

E_l = Liquid axial dispersion coefficient, cm^2/s

L_c = Height of the column recovery zone, cm

U_l = Interstitial liquid velocity expressed as follows:

$$U_l = \frac{J_l}{(1-\varepsilon_g)} \qquad (VII.9)$$

The particle mean residence time is defined as:

$$\tau_p = \frac{L_c * (1-\varepsilon_g)}{J_l} = \frac{V_c}{Q_t} \qquad (VII.10)$$

where

L_c = Height of column recovery zone, cm

Q_t = Tailings volumetric flow rate, cm^3/s

V_c = Volume occupied by the liquid, cm^3

J_l = Superficial liquid velocity, cm/s

As revealed in Equations VII.4 through VII.10, the dependence of flotation recovery on rate constant, residence time and mixing is further complicated since none of these variables are completely independent. For instance, Jameson *et al.* (1977) derived that the first-order flotation rate constant (**k_c**) is a function of bubble size (**d_b**) and air velocity (**J_g**), as follows:

$$k_c = \frac{1.5 * E_k * J_g}{d_b} \qquad (VII.11)$$

where E_k is the collection efficiency

In terms of bubble surface area flux Equation VII.11 becomes:

$$k_c = \frac{E_k * S_b}{4} \qquad (VII.12)$$

Gorain *et al.* (1997) found for shallow froths a relationship between rate constant and bubble surface area flux:

$$k_c = P * S_b \qquad (VII.13)$$

where **P** is a constant that summarizes the operational and chemical factors.
To include froths, Equation VII.13 is modified to:

$$k_c = P * S_b * R_f \qquad (VII.14)$$

where R_f is the froth zone recovery and the overall flotation column recovery (R_{fc}), is given by (Finch & Dobby, 1990):

$$R_{fc} = \frac{R_f * R_c}{R_f * R_c + (1 - R_c)} \qquad (VII.15)$$

The empirical relationship developed in Chapter VI will be used to predict the mixing conditions within the column:

$$N_d = 1.296 * \left(\frac{D_c}{L_c} * \frac{J_g}{J_l} * \left(1 - \varepsilon_g\right) \right)^{0.67} \qquad \text{(VII.16)}$$

The relationships established for flotation rate constant (Equations VII.11 to 13), mean residence time (Equation VII.10) and vessel dispersion number (Equation VII.16) provide the means to calculate recovery for a wide range of conditions.

7.4 Experimental

The first step in selecting a flotation column is to conduct small scale tests. The 4" lab column (D_c = 0.102 m, L_c = 4.40 m) was used to collect scaling-up data at Bowater's Gatineau de-inking plant to compare predicted performance on the 20" pilot unit. A portion of the feed to the plant flotation cells was diverted to feed both columns. The temperature of the pulp was the same as in the plant (40 +/- 5°C). When steady-state conditions were achieved (i.e., gas holdup constant) samples were taken from the reject and feed streams to determine residual ink concentration, consistency, and brightness gain with which to calculate flotation efficiency and ink recovery. Air flowrate and retention time were manipulated, using different sparger porosities in the laboratory column, and using up to six spargers of one porosity in the pilot unit. Both columns were fully automated (Figures VII.1 and VII.2 illustrate the experimental set-up for each). Gas holdup was determined using two pressure transmitters. Two peristaltic pumps equipped with I/O cards, controlled the flow of feed and accepts in the laboratory column. Two centrifugal pumps and two control valves were used in the pilot unit. The rates of the feed and accepts in both columns were measured with two magnetic flowmeters. The air flowrate was regulated by a mass flowmeter/controller. All the instruments were controlled or monitored using a serial communication interface OPTOMUX and a computer. The software package for data collection and column operation was FIXMMI.

To estimate the collection zone flotation rate constant, k_c, the operating conditions in both columns, e.g. the gas rate and pulp retention time, were altered. Details are given in Tables VII.1. and VII.2.

Table VII.1 Experimental details to estimate k_c using 4" lab column.

SS sparger #	1	2	5
Nominal pore size (μm)	0.5	2.0	20.0
J_g (cm/s)	0.5, 1.0, 1.5	1.5, 2.0, 2.5, 3.0	1.0, 1.5
J_l (cm/s)	1.0, 1.5, 2.0, 2.5		
Consistency (%)	~ 1.0		
L_c/D_c	44.0		

Table VII.2 Experimental details to estimate k_c using pilot unit

SS sparger #	1, 2, 3, 4, 5, 6
Nominal pore size (μm)	0.5
J_g (cm/s)	0.5, 1.0, 1.5
J_l (cm/s)	0.5, 1.0
Consistency (%)	~ 1.0
L_c/D_c	10.6

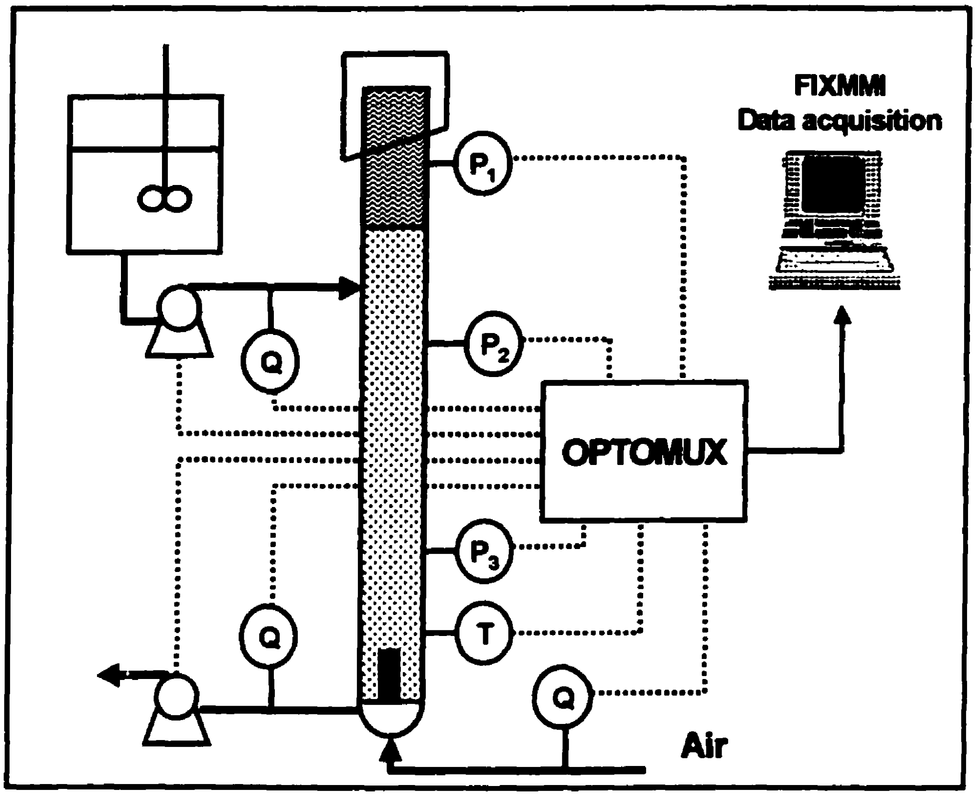

Figure VII.1 Experimental set-up for 4" lab column

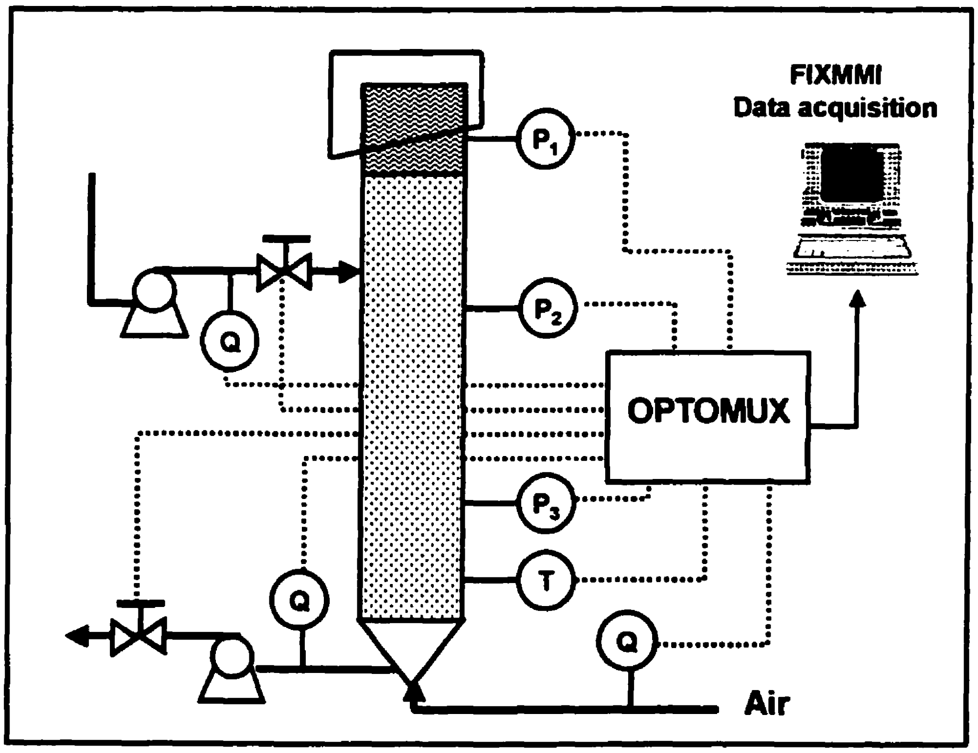

Figure VII.2 Experimental set-up for 20" pilot unit

7.5 Measurements

7.5.1 Effective Residual Ink Concentration (ERIC)

The following procedure was used to make **ERIC** measurements.

1. A sample from the feed and underflow was taken (approximately 1 liter).
2. A 250 ml sample was thoroughly mixed prior to filtering through Ahlstrom filter paper (617 grade, 15 cm diameter, and very fast filtration speed) in a Buchner funnel. The volume of sample filtered was sufficiently large to have a final dry pad weight of approximately 4.0 g.
3. The filter paper was removed and the sample pressed between two blotter sheets using a mechanical roll press and then placed on a fan for room temperature forced air-drying.

The ink concentration in ppm of a dried pad was measured using a Technidyne Micro TB-1C. The instrument measured the reflectance of the pads at a wavelength of 950 nm that is converted into an ink concentration. An average of 10 ERIC values (5 per side) was obtained.

7.5.2 Flotation Efficiency

After the ink concentration (**C** in ppm) of the pad was measured the flotation efficiency (**F.E.**) was calculated with the following equation:

$$F.E. = \frac{\left(C_{Feed} - C_{Accepts}\right)}{C_{Feed}} \qquad (VII.17)$$

7.5.3 Consistency and Ink Recovery

The consistency of the paper pulp was measured using the procedure described in section 5.3.3. and the ink recovery (**R_{ink}**) is defined as:

$$R_{ink} = \frac{(C_i * S_i * Q_i * \rho_i) - (C_o * S_o * Q_o * \rho_o)}{(C_i * S_i * Q_i * \rho_i)} \qquad (\text{VII.18})$$

where

C = Concentration of ink, ppm.

S = Consistency of the pulp

Q = Volumetric flowrate, L/min

ρ = Stream density (g/L) and the subscripts refer to initial (**i**) and final (**o**), values.

7.6 Results and Discussion

7.6.1 Sparger Porosity

The effect of sparger porosity on ink recovery (**R_{ink}**) and brightness gain for spargers # 5 and # 1 (nominal pore size 20 and 0.5 μm, respectively) is shown in Figures VII.3 and VII.4, respectively. The air velocity (**J_g**) was maintained constant at 1.16 cm/s with froth depth close to zero. The lower ink recovery with sparger # 5 can be related to the larger bubbles produced (see Chapter V).

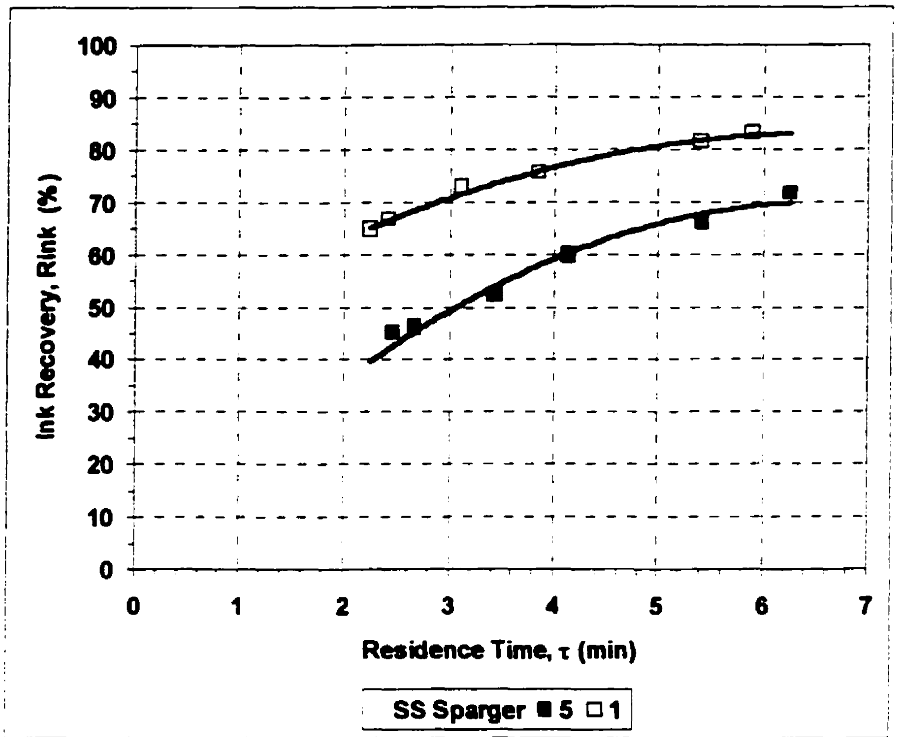

Figure VII.3 Ink recovery as a function of retention time for SS spargers # 5 and # 1 with nominal pore size 20 and 0.5 μm, respectively.

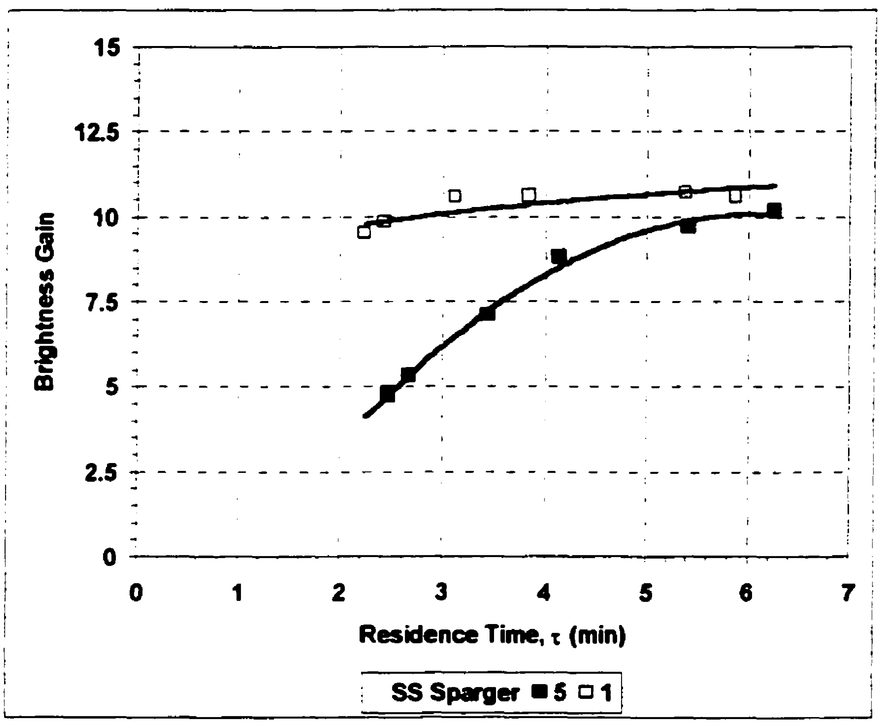

Figure VII.4 Brightness gain as a function of retention time for SS spargers # 5 and # 1 with nominal pore size 20 and 0.5 μm, respectively.

7.6.2 Flotation Rate Constant in 4" Lab Column

In Chapter II it was shown that the laboratory column exhibited close to plug flow transport ($N_d \rightarrow 0$). Assuming this condition the flotation rate constant (k_c) from Equation VII.4 is the slope of the plot $-Ln(1-R_c/R_{eq})$ against residence time (τ). Figure VII.5 is an example of this plot from tests using sparger # 1 (0.5 μm) at three values of superficial air velocity (J_g) in the 4" lab column.

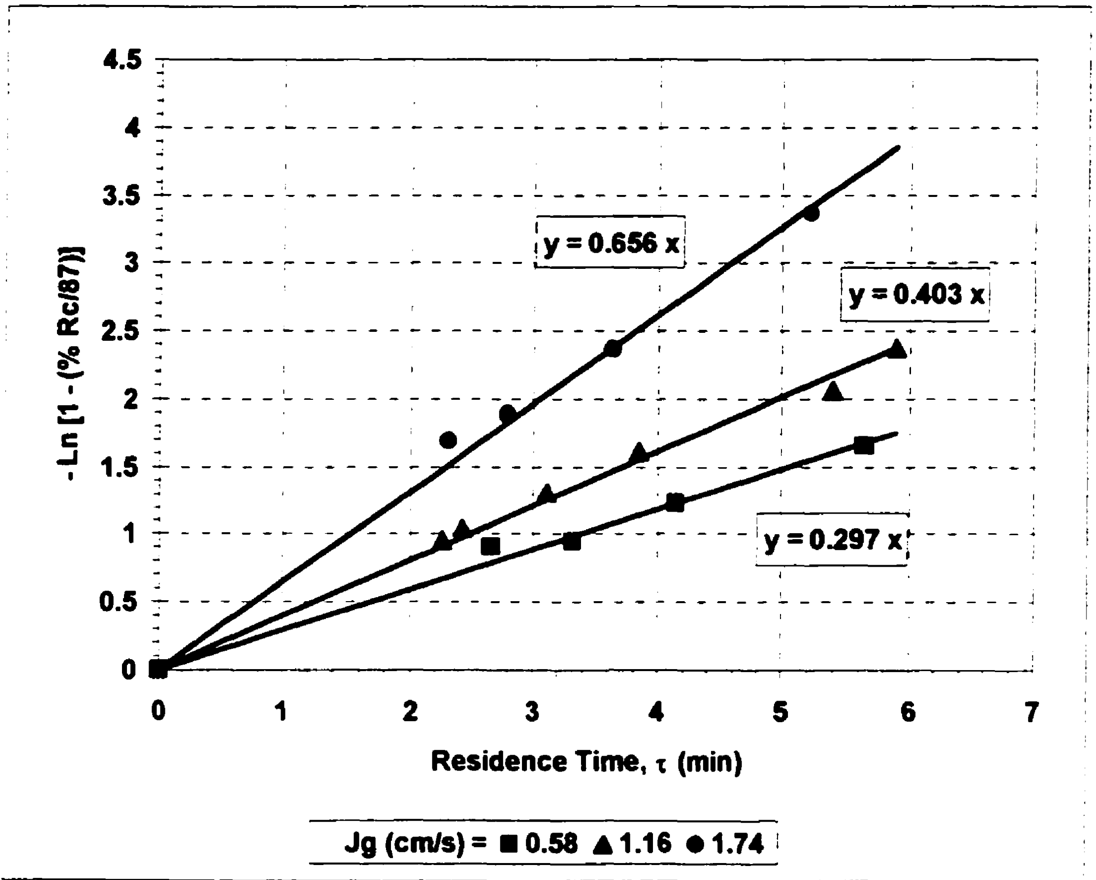

Figure VII.5 Plot to estimate flotation rate constant for sparger # 1 (nominal pore size 0.5 μm) in 4" lab column.

Table VII.3 is a summary of k_c results from testing in the laboratory column, assuming plug flow (Equation VII.4) and using N_d calculated from Equation VII.16 and back calculating k_c from the axial dispersion model (**A.D.M.**) (Equation VII.6). (For interest the k_c assuming perfect mixing (**P.M.**) is included (Equations VII.5)). The estimate from the axial dispersion model is in good agreement with that assuming plug flow because the large L_c/D_c aspect ratio gives N_d close to zero. The **A.D.M.** based results were used subsequently.

Table VII.3 Summary of flotation rate constant estimation in 4" lab column.

SS Sparger	J_g (cm/s)	ε_g (%)	d_b (cm)	S_b (1/s)	k_c (1/min)		
					Plug	A.D.M.	P. M.
1	0.58	5.46	0.0980	35.57	0.2976	0.3204	0.5914
1	1.16	11.12	0.1089	64.12	0.4036	0.4586	1.0534
1	1.74	20.05	0.0989	105.62	0.6563	0.8025	2.9572
2	1.53	13.42	0.1263	72.69	0.4914	0.5676	1.4347
2	2.36	20.68	0.1270	111.48	0.7198	0.8761	2.8050
2	2.83	25.19	0.1315	129.23	0.7588	1.0215	3.4524
2	3.06	27.37	0.1336	137.59	0.7639	0.9898	3.2181
2	3.30	29.40	0.1347	147.06	0.7801	1.0102	3.2091
5	1.16	6.03	0.1503	46.32	0.2770	0.2989	0.5225
5	1.74	8.70	0.1635	63.86	0.3060	0.3414	0.6277

Selecting the **A.D.M.** estimates, k_c is plotted against gas rate (Figure VII.6), bubble size (Figure VII.7), gas holdup (Figure VII.8) and surface area flux (Figure VII.9) following the approach of Gorain (1996). In each plot, the results are for the SS spargers # 1 (0.5 μm), # 2 (2 μm) and # 5 (20 μm). A simple linear correlation was investigated for each case and the R^2 coefficient is shown in Table VII.4.

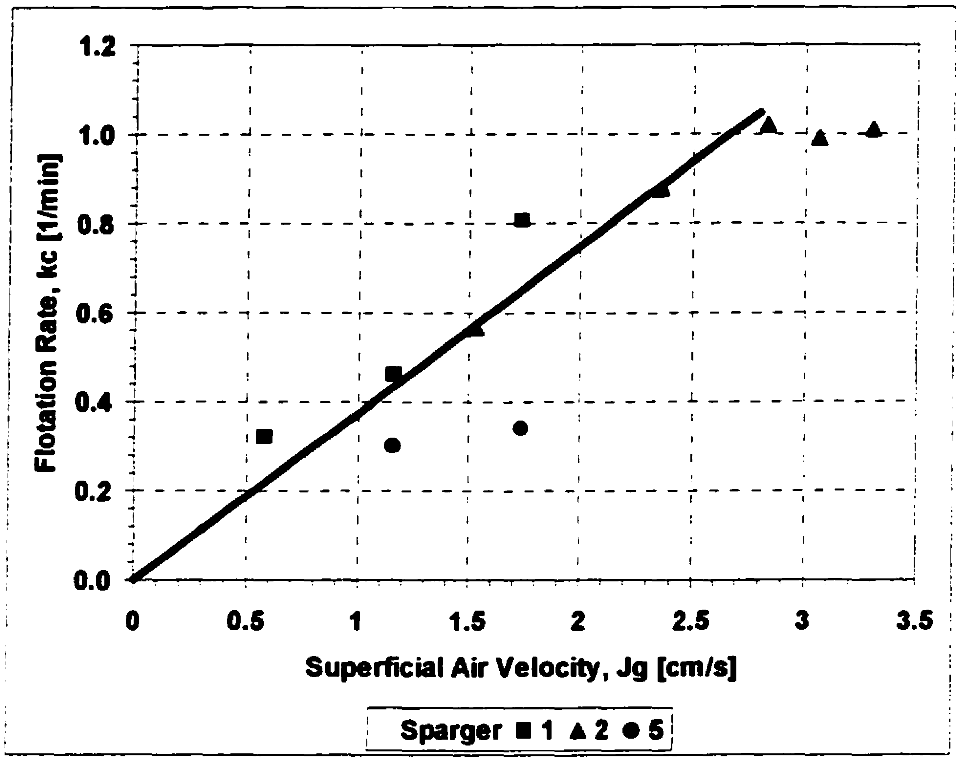

Figure VII.6 Flotation rate constant as a function of superficial air velocity in 4" lab column.

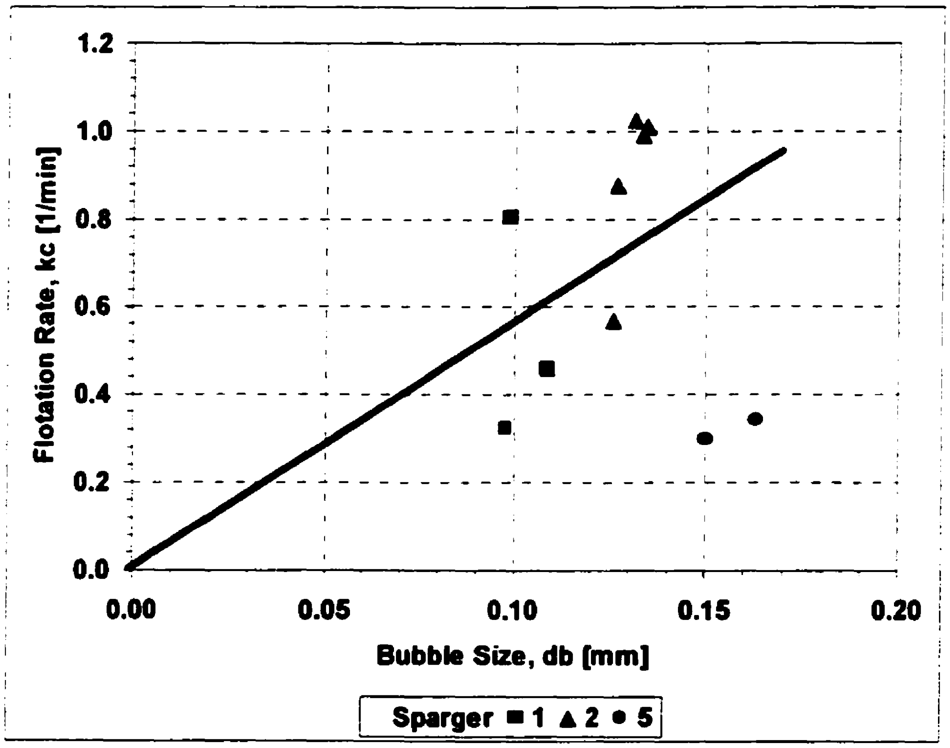

Figure VII.7 Flotation rate constant as a function of bubble size in 4" lab column.

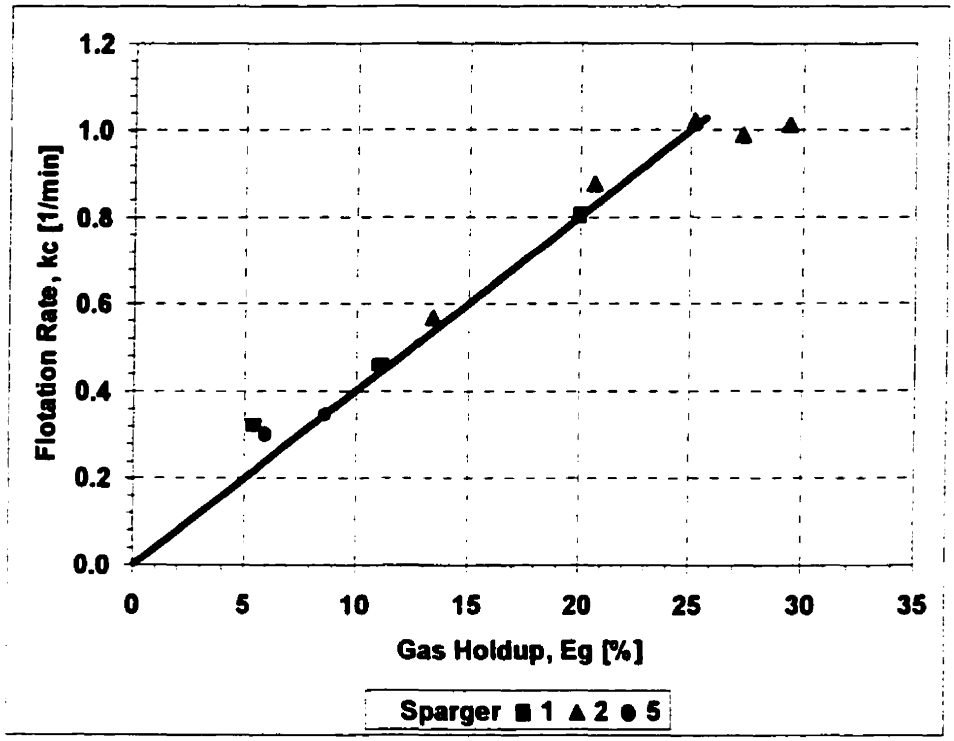

Figure VII.8 Flotation rate constant as a function of gas holdup in 4" lab column.

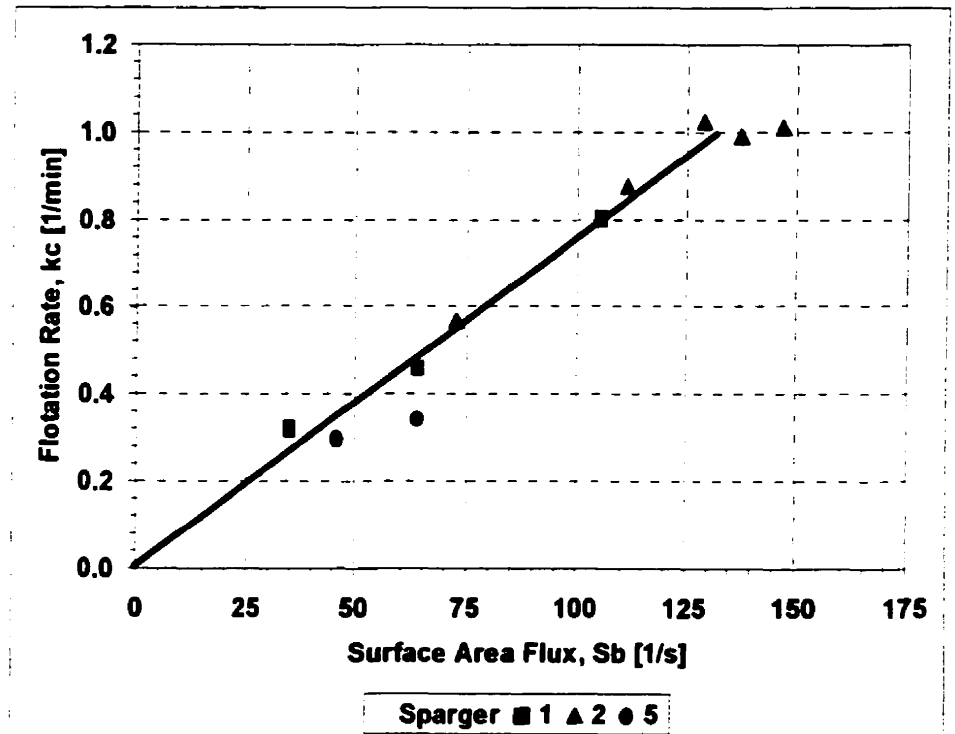

Figure VII.9 Flotation rate constant as a function of surface area flux in 4" lab column.

Table VII.4 Correlation coefficient R^2 and the slope for each plot in Figures VII.6 to VII.9 for the 4" lab column.

Correlation	R^2	Slope
k_c vs. J_g	0.866	0.3369
k_c vs. d_b	0.210	5.1051
k_c vs. ε_g	0.960	0.0386
k_c vs. S_b	0.969	0.0073

Figures VII.6 and 7 show $\mathbf{k_c}$ against $\mathbf{J_g}$ and $\mathbf{d_b}$, respectively. They show a large scatter, the data indicating little correlation between these parameters over the range of operating conditions tested. This observation is supported by the low R^2 values (Table VII.3). Figures VII.8 and VII.9 show the variation of $\mathbf{k_c}$ with ε_g and $\mathbf{S_b}$. There is a linear trend in both plots, supported by the values of R^2 shown in Table VII.3. The results indicate there is a somewhat better correlation between $\mathbf{k_c}$ and $\mathbf{S_b}$ than for ε_g, and is represented by Equation VII.9 where the constant **P** is the slope:

$$K_c = 0.0073 * S_b \qquad (VII.19)$$

Finch *et al.* (2000) demonstrated a linear relationship between $\mathbf{S_b}$ and ε_g over a wide range of cell types and operating regimes. This is supported in Figure VII.10. The $\mathbf{S_b}$ vs. ε_g (%) relationship is:

$$S_b = 5.25 * \%\varepsilon_g \qquad (VII.20)$$

which is similar to that found by Finch *et al.* (2000) (slope ~ 5.5 vs. ~ 5.3 here).

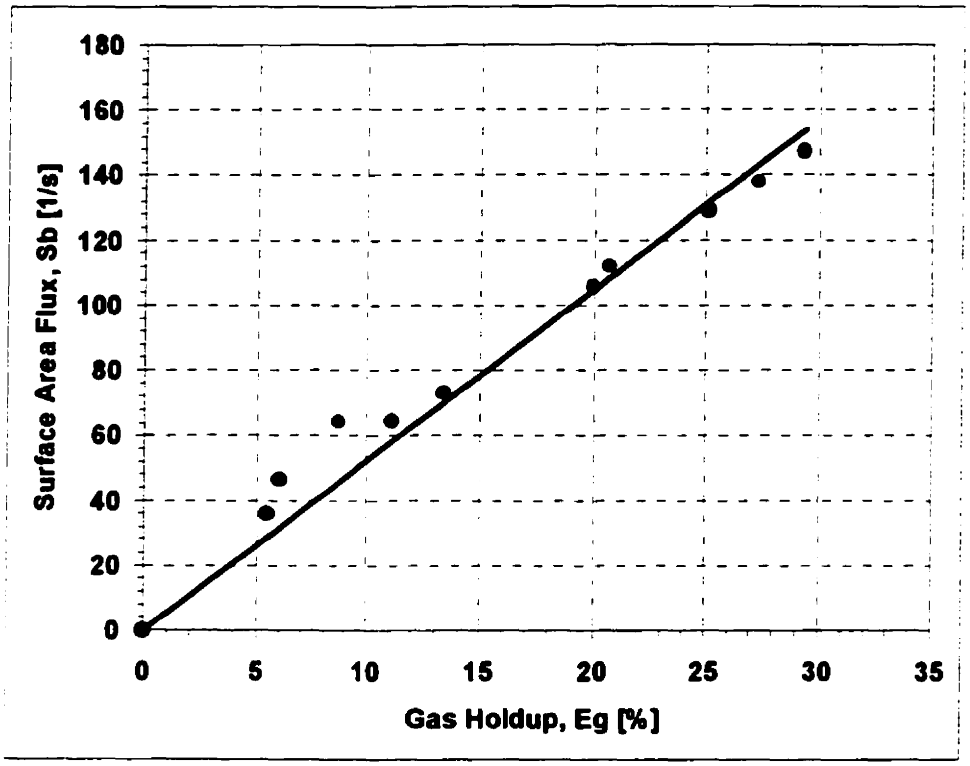

Figure VII.10 Surface area flux as a function of gas holdup in the 4" lab column

7.6.3 Flotation Rate Constant in 20" Pilot Unit

The collection zone flotation constant in the pilot unit was estimated using the axial dispersion model (Equation VII.6) and the vessel dispersion number (Equation VII.16). Table VII.5 is a summary of $\mathbf{k_c}$ results. Figure VII.11 shows a comparison between the flotation rate constant in the 4" lab column and the 20" pilot unit as a function of surface area flux. The model $\mathbf{k_c = P * S_b}$ is supported by both cases; again a linear dependence on ε_g is also evident (Figure VII.12).

Table VII.5 Summary of flotation rate constant estimation in pilot unit.

J_g (cm/s)	J_l (cm/s)	ε_g (%)	S_b (1/s)	N_d	k_c (1/min) A.D.M.
2.64	0.893	10.24	53.81	0.5119	0.2923
2.81	0.622	11.30	59.38	0.6751	0.4469
2.92	0.710	11.56	60.74	0.6317	0.3693
2.97	0.759	11.90	62.53	0.6098	0.3807
3.08	0.493	13.56	71.25	0.8237	0.5203
3.12	1.130	13.84	72.72	0.4753	0.3483
3.16	0.573	14.80	77.77	0.7497	0.5083
3.17	0.951	15.70	82.50	0.5313	0.5017
3.17	0.804	15.45	81.18	0.5968	0.4811
3.22	0.658	15.80	83.02	0.6867	0.4874
3.22	1.002	17.24	90.56	0.5123	0.4839
3.28	0.962	17.12	89.96	0.5341	0.5172
3.28	1.091	17.72	93.11	0.4884	0.4907

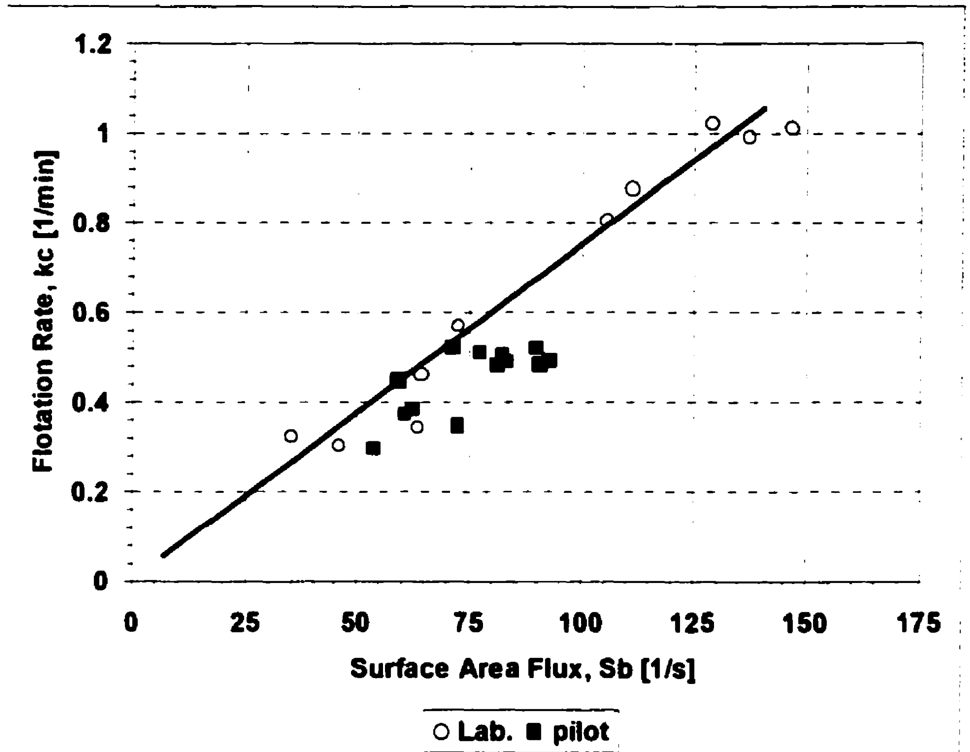

Figure VII.11 Flotation rate constant as a function of surface area flux in 4" lab column and 20" pilot unit.

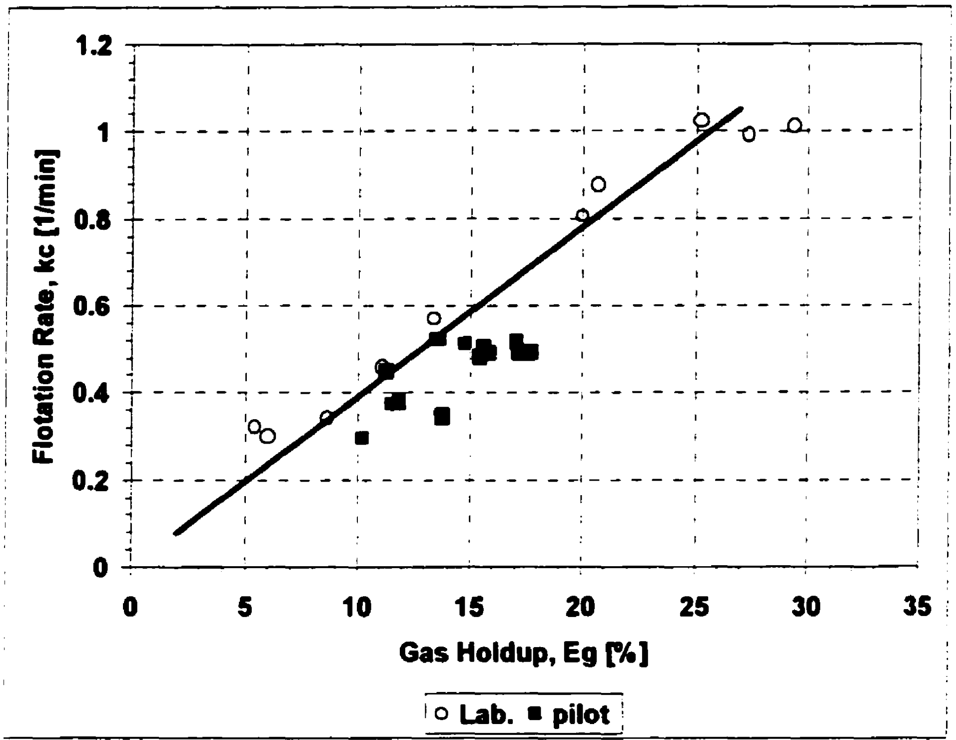

Figure VII.12 Flotation rate constant as a function of gas holdup in 4" lab column and 20" pilot unit.

7.6.4 Classical and New Scale-up

The classical column design procedure, using the axial dispersion model and assuming flotation to be a first order process, has been used to predict the performance of the pilot unit using a rate constant determined in a laboratory column. Although alternatives have been proposed (e.g. Ityokumbul, 1992a & b), most commercial scale-up procedures are based on this classical reactor design approach. Procedures to use laboratory column data in the design of large units have been extensively treated in the literature (Deckwer & Schumpe, 1993; Luttrell *et al*, 1993c; Ityokumbul, 1992a; Mankosa, 1990; Dobby & Finch, 1986a).

In the present work, the following assumptions are made:

1. Transport in the column follows the axial dispersion model.
2. Carrying capacity is not a limitation.
3. The particle residence time is equal to liquid residence time.

Following is the step-by-step classical column flotation scaling-up procedure:

Classical scale-up procedure

Step 1: Conduct a laboratory column flotation test as a function of superficial liquid velocity (**J_l**) to control retention time. Use a flotation column with a large **L_c/D_c** aspect ratio to give close to plug flow and hence a simply determination of rate constant, **k_c**. In the case of an existing plant, use samples from the operating plant at the point in the process where flotation is being considered.

Step 2: Determine the following parameters from the scale-up test:

a) Gas holdup ε_g, (Eq. V.2).

b) Superficial air and liquid velocities **J_l** and **J_g**, (Eq. II.7 & II.10).

c) Wash water flowrate, **J_w**.

d) % Consistency **S**, (Eq. V.3).

e) Ink recovery **R_{ink}**, (Eq. VII.18).

f) Particle retention time τ_p, (Eq. VII.10).

g) Vessel dispersion number **N_d**, (Eq. VII.16).

Step 3: Assume a first-order rate process with plug flow transport (**N_d** $\rightarrow$ 0) and calculate a flotation rate constant **k_c**, (Eq. VII.4).

Step 4: Assume that the new column has the same **k_c**.

Step 5: Plot **R_{ink}** as a function of τ_p and determine a **J_l** require to achieve the target recovery, **R'_{ink}**.

Step 6: Select a design column geometry, **D_c** and **L_c** (respecting building dimensions (height) if necessary).

Step 7: Calculate cross section area A_c.

Step 8: Assume that the ε_g is equal in the laboratory and design column at the same J_g.

Step 9: Calculate a τ_p, (Eq. VII.10)

Step 10: Calculate N_d, (Eq. VII.16).

Step 11: Knowing k_c from step 4 and N_d from step 10, determine a new R_{ink} with the axial dispersion model (Eq. VII.6).

Step 12: To have the same R'_{ink} as in step 5, τ_p must be increased or decreased. The new column geometry can be determined by fitting J_l or D_c in order to have the same R'_{ink}

The main problem with this method is in steps 4 and 8. According with the previous section k_c is a function of S_b (or ε_g). While efforts are made to ensure S_b is the same in the full size units lack of measurement techniques are a handicap. This handicap is being overcome and knowing how k_c varies with S_b can be brought into the scale-up procedure. Following is a proposal for scale-up of a flotation column incorporating in step 5 S_b estimated from Equation VII.19.

New Scale-up procedure

Steps 1 to 4: Same as previous method

Step 5: Estimate S_b (Eq. VII.19).

Step 6: Estimate % ε_g (Eq. VII.20).

Step 7: Plot R_{ink} as a function of τ_p and determine a J_l required to achieve the target recovery, R'_{ink}.

Step 8: Select a new column geometry D_c and L_c.

Step 9: Calculate cross section area A_c.

Step 10: Calculate τ_p (Eq. VII.10) and N_d (Eq. VII.16).

Step 11, 12: Same as previous method.

To test the new method, ink recovery in the pilot unit was predicted and compared to the measured ink recovery (R_{ink}) in tests with zero froth depth. Table VII.6 gives the details of one test and the comparison of classical and new procedure is presented in Table VII.7.

Table VII.6 Summary of operating conditions and results in the 20" pilot unit.

L_c (cm) =	540	ε_g (%) =	11.90
D_c (cm) =	50.8	τ_p (min) =	10.45
J_g (cm/s) =	2.97	N_d =	0.606
J_l (cm/s) =	0.76	R_{ink} (%) =	77.31

Table VII.7 Summary of operating conditions and comparison of scale-up predictions.

Parameter	Classical	New proposal
L_c/D_c	10.63	10.63
Area, A_c (cm^2)	2026.83	2026.83
Air velocity, J_g (cm/s)	2.97	2.97
Liquid velocity, J_l (cm/s)	0.76	0.76
Gas holdup, ε_g (%)	11.90	11.90
Residence time, τ_p (min)	10.45	10.45
Ink recovery (target), R'_{ink} (%)	**77.31**	**77.31**
Max ink recovery, R_{eq} (%)	87.00	87.00
Surface area flux, S_b (1/s)	N/A	62.47
Rate constant, k_c (1/min)	**0.989***	**0.456**
Dispersion number, N_d	0.606	0.606
Ink recovery (prediction), R_{ink} (%)	**85.38**	**79.64**

* From Table VII.3

Following with the classical procedure, k_c is the same in both columns. The predicted and experimental R_{ink} in the pilot unit were 85.38% and 79.64%, respectively. This large difference is because the surface area flux in the laboratory unit is higher than in the pilot unit. The sparging system in the laboratory column produced S_b = 129 1/s with J_g = 2.8 cm/s and in the pilot unit gave S_b = 62.5 1/s with J_g = 2.9 cm/s. Assuming the same k_c, the target R_{ink} would be matched by increasing J_l from 0.76 to 2.43 cm/s or decreasing L_c from 540 to 241 cm. Either way the capacity of the column is being over estimated with potentially disastrous results.

For a successful scale-up, knowledge of the true k_c in the design column is required. In the new proposal k_c is predicted from S_b. For S_b = 62.5 1/s the value of k_c is 0.456 1/min. Using this value there is a close agreement between the estimated and the actual recovery (77.30% vs. 79.64%, respectively). This calculation illustrates that care must be taken to account for differences in S_b between the laboratory and full size columns. It is necessary to ensure that the required S_b is achieved in the full size column. The results indicate that the new procedure incorporating S_b gives improved scale-up predictions. It is appreciated that the froth zone recovery is not included, the improvement in the modelling applying only the collection zone.

7.7 Summary of the Chapter

- The traditional scale-up procedure has been compared with a new proposal, which incorporates the flotation rate constant k_c as a function of bubble surface area flux S_b.
- Improved scale-up predictions are made using the new procedure.
- A linear relationship between the flotation rate constant k_c and gas holdup ε_g and between k_c and bubble surface area flux S_b were obtained for the 4" lab and 20" pilot column

The raw data and calculations experiments are given in **Appendix E**

CHAPTER VIII
Conclusions

8.1 Overall Conclusions

A number of conclusions can be drawn from the tests performed during this thesis. They are described as follows:

- The column flotation scale-up procedure was reviewed with regard to paper de-inking.
- A new scale-up procedure has been developed incorporating bubble surface area flux.
- The permeability of rigid porous spargers calculated according to Darcy's law for turbulent flow (Eq. II.56) does not depend on the fluid, but reflects only the nature of the sparger material itself.
- Determining the **ΔP - (R_s * J_g)** relationship can be used as a quality check on sparger material homogeneity.
- Permeability, while checking homogeneity, is not a sufficient guide to the gas holdup – air rate relationship that will be produced.
- Rigid spargers are not homogeneous even though they have the same nominal porosity.
- Pulp viscosity estimation using a pipe test loop test may not be representative of behavior in a flotation column.
- Gas holdup at a given air rate increased as nominal pore size decreased (as expected).
- Increasing pulp consistency decreased gas holdup.

- An expression which relates the vessel dispersion number as a function of flowrates and column geometry was developed.

$$N_d = 1.296 * \left(\frac{D_c}{L_c} * \frac{J_g}{J_l} * (1 - \varepsilon_g) \right)^{0.67}$$

- Predictions can be made for large scale columns based on laboratory column flotation test results using the new procedure that incorporates a k_c - S_b relationship.
- Linear relationships between flotation rate constant k_c and gas holdup ε_g and between k_c and bubble surface area flux S_b were obtained for the 4" lab column and pilot unit.
- The model $k_c = P * S_b$ is supported by the de-inking case study.
- The scale-up procedure was validated by testing predicted vs measured ink recovery in the 20" pilot unit.

8.2 Contributions to Knowledge

1) A new scaling-up procedure for flotation columns incorporating a linear relationship between collection zone rate constant and bubble surface area flux.
2) A novel approach to estimate viscosity using bubble size measurements and back calculation from drift flux analysis.
3) An expression to correlate vessel dispersion number as a function of flow rates and column geometry for paper pulps.

8.3 Suggestion for Future Work

- Sparger characterization should be revisited to study the effect of permeability on the gas holdup – gas rate relationship.
- Study relationship between pressure drop and air flowrate for each sparger working simultaneously in the pilot unit.
- Study plugging effect of porous sparger.
- Extend the pulp viscosity measurement using bubble size measurements procedure to more consistencies and to mineral systems.
- Investigate the possible effect of froth zone recovery (R_f) on flotation rate constant and determine the overall kinetics.
- Evaluate froth recovery effect on scale-up.

References

Ackerman, C. Deinkability of Waterborn Flexo Inks by Flotation. *2nd Research Forum on Recycling*. CPPA, 1993, pp. 201 – 215.

AIME. Froth Flotation: 50th Anniversary Volume. *Society of Mining Engineers of AIME. Minerals Beneficiation Division*. 1962.

Ajerstch, M. & Pelton R. Mechanisms of Pulp loss in Flotation Deinking. *Journal of Pulp and Paper Science*. Vol. 22, No. 9, September 1996, pp. 338 – 345.

Anonymous. Annual Report 96 - 97. Mechanical Wood - Pulps Network of Canada. 1998.

API (American Petroleum Institute). Recommended Practice for Determining Permeability of Porous Media. *Third Edition*, 1956, pp. 3 – 27

Bailey, J. Recycling Forum Looks for a Balance. *Pulp & Paper Canada*, Vol. 98 No. 12, 1997.

Banisi, S. & Finch J. Reconciliation of Bubble Size Estimation Methods Using Drift Flux Analysis. (Technical Note). *Minerals Engineering*. Vol. 7, No. 12, 1994, pp. 1555 – 1559.

Banisi, S. On-Line Phase Holdup Measurement and Analysis in Flotation Columns. *PhD Thesis*. McGill University, Montreal, Qc. Canada 1994.

Bennington, C.P.J., Kerekes, R.J. & Grace, J.R. Mixing in Pulp Bleaching. *Journal of Pulp and Paper Science*. Vol. 15, 1989, pp. 186.

Bennington, C.P.J., Kerekes, R.J. & Grace, J.R. The Yield Stress of Fibre Suspensions. *The Canadian Journal of Chemical Engineering*. Vol. 68, 1990, pp. 748 - 757.

Bird, R.B., Stewart, W.E. & Lightfoot, E.N. Transport Phenomena. *John Wiley and Sons Inc*, New York, 1960

Boutin, P and Wheeler, D.A. Column Flotation Development Using an 18-inch Pilot Unit. *Canadian Mining Journal.* Vol. 88, No. 3, 1967, pp. 94 - 101.

Carabin, P., Dessureault S., Kleuser, J. & Ward, K. Flotation Column De-inking of MOW. *4TH Research Forum on Recycling* 1995, pp. 67 – 77.

Concha, F. & Almendra, E.R. *International Journal of Mineral Processing*. Vol. 5, 1979, pp. 349.

Crow, D.R. & Secor, R.F. The Ten Steps of Deinking. *TAPPI Journal* Vol. 70 No. 7, 1987, pp. 101 – 106.

Deckwer, W.D. & Schumpe, A. Improved Tools for Bubble Column Reactor Design and Scale-up. *Chemical Engineering Science*. Vol. 48, No. 5, 1993, pp. 889 – 910.

Deckwer, W.D., Burckhart, R. & Zoll, G. Mixing and Mass Transfer in Tall Bubble Columns. *Chemical Engineering Science*. Vol. 29, 1974, pp. 2177 – 2188.

Dessureault, S., Barbe, M.C. & Lévesque, M. Column Flotation: A New Technology for De-inking Recycled Pulp. *TAPPI Symposium*, New Orleans, USA, 1995.

Diaz-Peñafiel, P. & Dobby, G.S. Kinetic Studies in Flotation Columns: Bubble Size Effect. *Minerals Engineering*, Vol. 7, No. 4, 1994, pp. 465 – 478.

Dobby, G. & Finch, J. Flotation Column Scale-up and Modeling. *CIM Bulletin* Vol. 78, 1986a, pp. 89 – 96.

Dobby, G. & Finch, J. Particle Collection in Columns – Gas Rate and Bubble Size Effects, *Canadian Metallurgical Quarterly*, Vol. 25, No. 1, 1986b, pp. 9 - 13.

Dobby, G., Yianatos, J. & Finch, J. Estimation of Bubble Diameter in Flotation Columns from Drift Flux Analysis. *Canadian Metallurgical Quarterly*, Vol. 27, No. 2, 1988, pp. 85 – 90.

Dorris, G. Deinking and Wet End Chemistry. *Recycling and the Canadian Pulp and*

Paper Industry. Research Program Committee of Paprican Report, 1989, pp. 1 – 35.

Duffy, G.G., Titchener, A.L., Lee. P.F. & Moller, K. The Mechanism of Flow of Pulp Suspensions in Pipes. *APPITA Journal,* Vol. 29, 1976, pp. 363 – 370.

Escudero, R. Characterization of Rigid Spargers and Their Selection for Flotation Columns. *PhD Thesis*. McGill University, Montreal, Qc. Canada 1998.

Finch, J. & Dobby, G. Column Flotation. *Pergamon Press*, 1990.

Finch, J., Xiao, J., Hardie, C. & Gomez, C. Gas Dispersion Properties: Bubble Surface Area Flux and Gas Holdup. *Minerals Engineering*, Vol. 13. No. 4, 2000, pp. 365 – 372.

Flint, L. Factors Influencing the Design of Flotation Equipment. *Miner. Sci. Eng.*, Vol. 5, No. 3, July 1973, pp. 232 - 241.

Givler, R.C., & Altobelli, S.A. A Determination of the Effective Viscosity for the Brinlman - Forchheimer Flow Model. *Journal of Fluids Mechanics*. Vol. 258, 1994, pp. 335 – 370.

Gomez, C., Fernandez, J. & Finch J. Observations on Level Measurements in Flotation Column from Pressure Readings. *Proceedings of the 2nd UNC-McGill Bi-Annual International Symposium on Fundamentals of Mineral Processing and Environment*. Sudbury, On, Canada. 1997, pp. 21 – 31.

Gorain, B.K. The Effect of Bubble Surface Area Flux on The Kinetics of Flotation and Its Relevance. *PhD Thesis*. University of Queensland. 1997.

Gorain, B.K., Franzidis, J.P. & Manlapig. Studies On Impeller Type Speed and Air Flow Rate in an Industrial Scale Flotation Cell. Part: 3 Effect on Superficial Gas Velocity. *Minerals Engineering*, Vol. 9, No. 6, 1996, pp. 639 -654

Hardie, C. In Plant Comparison of Internal and External Spargers for Flotation Column De-inking. *Master Thesis*. McGill University, Montreal, Qc., Canada 1998.

Huls, B.J., LaChance, C.D. & Dobby, G. Bubble Generation Assessment for an Industrial Flotation Column. *Minerals Engineering* Vol. 4, No. 1, 1991, pp. 37 – 42

Ityokumbul, M.T. What Really Determines the Height in Column Flotation?. *Minerals and Metallurgical Processing*. February 1996, pp. 36 – 40.

Ityokumbul, M.T. A Mass Transfer Approach to Flotation Column Design. *Chemical Engineering Science*. Vol. 47, No. 13/14, 1992a, pp. 3605-3612.

Ityokumbul, M.T. A New Modelling Approach to Flotation Column Design. *Minerals Engineering*. Vol. 5, No. 6, 1992b, pp. 685 – 693.

Jameson, G., Nam, S. & Young, M. Physical Factors Affecting Recovery Rates in Flotation. *Miner. Sci. Eng*. Vol. 9, No. 3, 1977, pp. 103 - 108.

Janse, P., Gomez, C. & Finch J. Effect of Pulp Fibres in a Flotation Column. *The Canadian Journal of Chemical Engineering*, Vol. 77, 1999, pp. 22 – 25.

Joseph, D.D., Nield, D.A. & Papanicolaou, G. Nonlinear Equation Governing Flow in a Saturate Porous Medium. *Water Resources Research*, Vol. 18, 1982, pp. 1049 – 1052.

Joshi, J.B. Axial Mixing in Multiphase Contactors – A Unified Correlation-. *Trans. Instn. Chem. Engrs*. Vol. 58, 1980, pp. 155 – 165.

Joshi, J.B., & Sharma, M.M. A Circulation Cell Model for Bubble Columns. *Trans. Instn. Chem. Engrs*. Vol. 57, 1979, pp. 244 – 251.

Joshi, J.B., & Sharma, M.M. Liquid Phase Back Mixing in Sparged Contactors. *The Canadian Journal of Chemical Engineering*, Vol. 56, 1978, pp. 115 - 225

Karamanev, D.G. & Nikolov, L.N. Freely Rising Spheres Do Not Obey Newton's Law for Free settling. *A.I.Ch.E. Journal*. Vol. 38, 1992, pp. 1843 – 1846.

Kato, Y. & Nishiwaki, A. Longitudinal Dispersion Coefficient of a Liquid in a Bubble Column. *International Chemical Engineering*, Vol. 12, No. 1, 1972, pp. 182 – 187.

Kawase, Y. & Moo-Young, M. Liquid Phase Mixing in Bubble Columns with Newtonian and Non-Newtonian Fluids. *Chemical Engineering Science,* Vol. 41, No. 8, 1986, pp. 1969 – 1977.

Kaya, M. & Oz, D. Waste Paper De-inking by Froth Flotation. *Proceedings of the XIX IMPC.* San Francisco, Cal., E.U. Vol. 4, Chapter 34, 1993, pp. 167 – 170.

Kelkar, B.G., Godbole, S.P., Honath, M.F., Shah, Y.T. Carr, N.L. & Deckwer, W.D. Effect of Addition of Alcohols on Gas Holdup and Back Mixing in Bubble Columns. *A.I.Ch.E. Journal,* Vol. 29, 1983, pp. 361 – 369.

Kerekes, R.J.E. Turbulent Drag Reduction in Pipe Flow of Ideal Fibre Suspensions. *PhD Thesis,* McGill University, Montreal, Qc, Canada. 1970.

Klinkenberg, L.J. The Permeability of Porous Media to Liquids and Gases. *American Petroleum Institute. Drilling and Production Practice.* 1941, pp. 200 – 213.

Laplante, A., Yianatos, J. & Finch, J. On the Mixing Characteristics of the Collection Zone in Flotation Columns. *Column '88,* Chapter 9, Ed. Sastry, K.V.S., pp. 69 – 79.

Lee, P.F. & Duffy, G.G. Relationships Between Velocity Profiles and Drag Reduction in Turbulence Fiber Suspension Flow. *A.I.Ch.E. Journal,* Vol. 22, 1976, pp. 750 – 753.

Leichtle, G.F. Analysis of Bubble Generating Devices in a De-inking Column. *Master Thesis.* McGill University, 1998.

Levenspiel, O. Chemical Reaction Engineering. 3rd Edition. *John Wiley and Sons, Inc.* New York, 1999. Chapter 13.

Lindsay, J.D. & Mostafa, S. Macroscopic Flow Structures in Bubbling Paper Pulp-Water Slurry. *Ind. Eng. Chem. Res.* Num. 34, 1995, pp. 3342 – 3353.

Luttrell, G.H., Mankosa, M.J. & Yoon, R-H. Design and Scale-Up Criteria for Column Flotation. *XVIII Int. Min. Proc. Congress*, Sydney, Australia, 1993.

Luttrell, G.H., Weber, A.T., Adel G.T. and Yoon R.H. Microbubble Flotation of Fine Coal. *Column Flotation '88*. Sastry, K.V.S. Ed. Society of Mining Engineers, Inc., Littleton, Colorado, USA, 1988, pp. 205 - 211.

Luttrell, G.H., Yan, S., Adel, G.T. & Yoon, R.H. A Computer-aided Design Package for Column Flotation. *SME Annual Meeting*. Salt Lake City, USA, 1990, pp. 90 - 173.

Mak, N. & Stevens, J. Characteristics of Fatty Acids as an Effective Flotation De-inking Collector. *2nd Research Forum on Recycling*, 1993, pp. 145 – 152.

Mankosa, M.J. Scale-up of Column Flotation. *PhD Thesis*. Virginia Polytechnic Institute and State University, 1990.

Mankosa, M.J., Lutrell, G.H., Adel, G.T. & Yoon, R.H. A Study of Axial Mixing in Column Flotation. *International Journal of Mineral Processing*. Vol. 35, 1992.

Masliyah, J.H. Hindered Settling in a Multi-Species Particle System. *Chemical Engineering Science*, Vol. 34, 1979, pp. 1166 – 1168.

Mathieu, G.I. Comparison of Flotation Column with Conventional Flotation for Concentration of Molybdenum Ore. *CIM Bull.* May 1972, pp. 41 - 45.

Matsumoto, T., Hidaka, N. & Morooka, S. Axial Distribution of Solid Holdup in Bubble Column for Gas-Liquid –Solid Systems *A.I.Ch.E. Journal*, Vol. 35, 1989, pp. 1701 - 1708.

Mavros, P. & Daniilidou, A. Mixing in Flotation Columns. Part II. Liquid-Phase Residence Time Distributions Studies. *Minerals Engineering*. Vol. 6, No. 7, 1993, pp. 707 – 718.

Mavros, P. Lazaridis, N.K. & Matis, K.A. A Study and Modelling of Liquid – Phase Mixing in a Flotation Column. *International Journal of Mineral Processing*, Vol. 26, 1989, pp. 1.

Miyahara, T. & Hayashino, T. Size of Bubble Generated from Perfored Plates in Non-Newtonian Liquids. *Journal of Chemical Engineering of Japan*. Vol. 28, No. 5, 1995, pp. 596 - 600

Murdock, D.J. Technology Development - An Overview of Column Flotation. *Journal of the South African Institute of Mining and Metallurgy*. March 1991.

O'Connor, C.T. & Mills, P.J.T. The Influence of Bubble Size on Scale-up of Column Flotation Cells. *Minerals Engineering*, Vol. 8, No 10, 1995, pp. 1185 – 1195.

Ogawa, K., Yoshikawa, S., Ikeda, J. & Ogawa H. Pressure Loss and Velocity Profile of Pulp Flow in a Circular Pipe. *TAPPI Journal*. April 1990, pp. 217 - 221

Pal, R. & Masliyah, J. Flow in Froth Zone of a Flotation Column. *Canadian Metallurgical Quarterly*. Vol. 29, No. 2, 1990, pp. 97 – 103.

Parthasarathy, R. & Ahmed, N. Size Distribution of Bubbles Generated by Fine Pore Spargers. *Journal of Chemical Engineering of Japan*. Vol. 29, No. 6, 1996, pp. 1030 - 1034

Patent No. 2005742, 1932.

Pelton, R & Piette, R. Air Bubble in Quiescent Wood Pulp Suspensions. *The Canadian Journal of Chemical Engineering*. Vol. 70, 1992, pp. 660 – 663.

Petri, B. De-inking Wastepaper in an Open and Packed Flotation Column. *Master Thesis*. University of Toronto, 1994.

Putz, H.J., Shaffrath, H.J. & Göttsching, L. De-inking of Oil and Water-Borne Printing Inks: A New Flotation De-inking Model. *Pulp & Paper Canada*, Vol. 94 No. 7, 1993, pp. 193 – 198.

Reese, J., Jiang, P. & Fan, S. Bubble Characteristics in Three – Phase Systems Used for Paper Pulp Processing. *Chemical Engineering Science*. Vol. 51, 1996, pp. 2501 - 2510.

Reith, T., Renken, S. & Israel B.A. Gas Holdup and Axial Mixing in Fluids Phase of Bubble Columns. *Chemical Engineering Science*, Vol. 23, 1998, pp. 619 – 623.

Richarson, J.F. & Zaki, W.M. Sedimentation and Fluidization: Part I. *Trans. Inst. Chem. Engrs*. Vol. 32, 1954, pp. 35 – 53.

Riquarts, H.P. A Physical Model for Axial Mixing of the Liquid Phase for Heterogeneous Flow Regime in Bubble Columns. *Ger. Chem. Eng*. Vol. 4, 1981, pp. 18.

Robertson, N., Patton, M. & Pelton, R. Washing the Fibers from Foams for Higher Yields in Flotation De-inking. *TAPPI Journal*. June1998, pp. 138 – 142.

Scheidegger, A.E. The Physics of Flow Through Porous Media. *Third Edition*. University of Toronto Press. 1974

Shah, Y.T., Kelkar, B.G., Godbole, S.P. & Decker, W.D. Design Parameters Estimations for Bubble Column Reactors. *A.I.Ch.E. Journal*, Vol. 18, No. 3, 1982, pp. 353 – 379.

Shah, Y.T., Stiegel, G.J. & Sharma, M.M. Back Mixing in Gas-Liquid Reactors. *A.I.Ch.E. Journal*, Vol. 24, 1978, pp. 369 – 375.

Smook, G.A. Handbook for Pulp and Paper Technologists, *Angus Wilde Publications*, 1992.

Spangenberg, J. Secondary Fiber Recycling. *TAPPI Press*, Chapter 15, 1993.

Stevenson, S. De-inking is CP Forest's News at Gatineau. *Pulp & Paper Canada*. Vol. 93, No. 5, 1992, pp. 28 – 32.

Todt, J., Lücke, J., Schügerl, K. & Renken, A. Gas Holdup and Longitudinal Dispersion in Different Types of Multiphase Reactors and Their Possible Application for Microbial Processes. *Chemical Engineering Science*. Vol. 32, 1977, pp. 369 – 375.

Tucker, J.P., Deglon, D.A., Franzidis, J.P., Harris, M.C. & O'Connor, C.T. An Evaluation of a Direct Method of Bubble Size Distribution Measurement in a Laboratory Batch Flotation Cell. *Minerals Engineering*. Vol. 7, No. 5/6, 1994, pp. 667 – 680.

Turton, R. & Levenspiel, O. A Short Note on the Drag Correlation for Spheres. *Powder Technology,* Vol. 47, 1986.

Varley, J. Submerged Gas – Liquid Jets: Bubble Size Prediction. *Chemical Engineering Science*. Vol. 50, No. 5, 1995, pp. 901 - 905

Vaseleski, R.C. & Metzner, A.B. Drag Reduction in the Turbulent Flow of Fiber Suspensions. *A.I.Ch.E Journal*, Vol. 20, No. 2, 1974, pp. 301 – 306.

Veilleux, S., Chabot, B., Daneault, C. Quantification of Macro Stickies and Optimization of the Wastepaper Deinking Process. *Pulp and paper Canada*. Vol. 101, No. 12, December 2000, pp. 130 –133.

Wallis, G.B. One Dimensional Two - Phase Flow. *McGraw-Hill,* New York. Chapter 9. 1969.

Walmsley, M.R.W. Air Bubble Motion in Wood Pulp Fibre Suspension. *APPITA Journal,* Vol. 45, 1992, pp. 509 – 515.

Watson, J. De-inking Recycled Paper Using Column Flotation. *Master Thesis*. McGill University, Montreal, Qc., Canada 1996.

Watson, J., Gomez, C.O. & Finch, J. De-inking Recycled Paper Using Column Flotation. *Column 96*. Montreal, Qc. Canada, 1996, pp. 195 – 207. Ed. C.O. Gomez & J.A. Finch.

Wilkinson, P., Spek A. & Van Dierendock, L. Design Parameters Estimation for Scale-Up of High-Pressure Bubble Columns. *A.I.Ch.E. Journal*, Vol. 38, No. 4 April 1992, pp. 544 - 554

Wills, B.A. Mineral Processing Technology, *Pergamon Press*, 1992.

Xu, M. & Finch J. Effect of Spargers Surface Area on Bubble Diameter in Flotation Columns. *Canadian Metallurgical Quarterly*, Vol. 28, No. 1, 1989 pp. 1 - 6.

Xu, M. & Finch, J. Estimating Vessel Dispersion Number in Flotation Columns. *Column '91*. CIM, Sudbury, Ontario. Vol. 2, Eds. Agar, G.E., Huls, B.J. & Hyma, D.B., 1991, pp. 437 – 454.

Xu, M. & Finch, J. Simplification of Bubble Size Estimation in a Bubble Swarm. *Journal of Colloid and Interface Science*. Vol. 140, No. 1, 1990, pp. 298 – 299.

Xu, M. & Finch, J. The Axial Dispersion Model in Flotation Columns Studies. *Minerals Engineering*, Vol. 4, No. 5/6, 1991, pp. 553 – 562.

Yianatos, J., Espinosa, R., Finch, J., Laplante, A. & Dobby, G. Effect of Column Height on Flotation Column Performance. *Minerals and Metallurgical Processing*. February, 1988a. pp. 11 – 14.

Yianatos, J., Finch, J., Dobby, G. & Xu, M. Bubble Size Estimation in a Bubble Swarm. *Journal of Colloid Interface*. Vol. 126, No. 1, 1988b, pp. 37 – 44.

Ynchaustl, R.A., McKay, J.D. & Foot, D.G. Jr. Column Flotation Parameters - Their Effects. *Column Flotation '88*. Chapter 17, Ed. Sastry, K.V.S., 1988, pp. 157 – 171.

Zabala, J.M. & McColl, M.A. De-inking at Papelera Peninsular and the Philosophy of De-inking System Design, *TAPPI Journal*. September 1968, pp. 62 – 68.

Zhou, Z.A., Egiebor, N.O. & Plitt, L.R. Frother Effects on Bubble Size Estimation in a Flotation Column. *Minerals Engineering*. Vol. 6, No. 1, 1993, pp. 55 – 67.

Appendix A: Bubble Generators

Fluid Test: Water. Spargers for 4" lab column

T = 21 °C	ΔP (Pa)	ΔP (Pa)	ΔP (Pa)	ΔP (Pa)	ΔP (Pa)	ΔP (Pa)	ΔP (Pa)
Q (lpm)	SS # 1	SS # 2	SS # 3	SS # 4	SS # 5	SS # 6	SS # 7
0.0	0	0	0	0	0	0	0
0.1	16002	1377	1108	325	221	101	5
0.2	32078	2755	2221	650	451	203	10
0.3	48226	4133	3339	975	677	305	15
0.4	64446	5512	4461	1301	902	407	20
0.5	80740	6892	5588	1626	1128	510	25
0.6	97106	8272	6720	1951	1354	613	30
0.7	113545	9652	7857	2276	1579	716	35
0.8	130057	11033	8999	2601	1805	820	40
0.9	146641	12415	10145	2926	2030	924	45
1.0	163299	13797	11296	3251	2251	1028	50
1.1	180029	15180	12452	3576	2482	1133	56
1.2	196832	16563	13612	3902	2707	1238	61
1.3	213707	17947	14778	4227	2933	1343	66
1.4	230656	19332	15948	4552	3158	1449	71
1.5	247677	20717	17123	4877	3384	1555	76
2.0		27650	23069	6503	4512	2089	102
3.0		41557	35318	9754	6768	3183	155
4.0		55519	48043	13005	9028	4309	210
5.0		69537	61245	16257	11280	5469	266
6.0		83609	74923	19508	13536	6660	323
7.0		97736	89078	22759	15792	7885	381
8.0		111918	103709	26010	18048	9142	441
9.0		126156	118817	29262	20394	10432	502
10.0		140448	134401	32513	22660	11754	565
11.0				35764	24926	13109	629
12.0				39028	27192	14509	694
13.0				42280	29458	15918	761
14.0				45532	31724	17371	829
15.0				48785	33990	18857	899
16.0				52037	36256	20371	969
17.0				55289	38522	21926	1042
18.0				58541	40788	23510	1115
19.0				61794	43054	25127	1190
20.0				65046	45320	26789	1266

Fluid Test: Air

T = 24°C	ΔP (Pa)
Q (lpm)	SS # 1
0.0	0
5.4	932
10.8	1921
16.1	2965
21.4	4065
26.6	5221
31.7	6433
36.8	7701
41.8	9025
46.7	10405
51.6	11841
56.3	13332
61.0	14880
65.6	16483
70.1	18142
74.6	19857
78.9	21628
83.1	23455
87.3	25338
91.4	27277

T = 24°C	ΔP (Pa)
Q (lpm)	SS # 2
0.0	0
5.4	1098
10.8	2195
16.1	3290
21.4	4384
26.6	5476
31.7	6566
36.8	7655
41.9	8742
46.8	9828
51.8	10912
56.7	11994
61.5	13075
66.3	14155
71.1	15232
75.8	16309
80.4	17383
85.0	18456
89.6	19528
94.1	20598
98.6	21666
103.0	22733

T = 24°C	ΔP (Pa)
Q (lpm)	SS # 3
0.0	0
5.4	946
10.8	1887
16.1	2825
21.4	3759
26.7	4689
31.9	5616
37.0	6538
42.1	7456
47.2	8371
52.2	9282
57.2	10189
62.1	11091
67.0	11991
71.8	12886
76.6	13777
81.4	14664
86.2	15548
90.9	16427
95.5	17303
100.3	18175
104.5	19043
108.6	19907
112.7	20767
116.7	21624
120.7	22476

Fluid Test: Air. Sparger for 6 " lab column

T = 23°C	ΔP (Pa)
Q (lpm)	SS # 1
0.0	0
5.4	492
10.7	986
16.0	1483
21.1	1983
26.2	2486
31.2	2991
36.1	3498
41.0	4009
45.7	4522
50.4	5038
55.0	5556
59.5	6077
64.0	6601
68.4	7128
72.7	7657
77.0	8189
81.1	8723
85.2	9260
89.3	9800
93.3	10343
97.2	10888
101.1	11435
104.8	11986
108.6	12539
112.3	13095
115.9	13654
119.4	14215
122.9	14779
126.4	15345
129.8	15914
133.1	16486
136.4	17061
139.6	17638
142.8	18218
145.9	18800
149.0	19385
152.0	19973
155.0	20564
157.9	21157
160.8	21753

Fluid Test: Air. Spargers for 20" pilot unit

T = 23°C	ΔP (Pa)
Q (lpm)	SS # 1
0.0	0
5.4	1585
10.7	3217
16.0	4894
21.1	6617
26.2	8385
31.2	10200
36.1	12061
40.8	13967
45.5	15919
50.1	17917
54.6	19961
59.1	22051
63.4	24186
67.6	26368
71.7	28595
75.8	30868
79.7	33187
83.6	35552
87.3	37963
91.0	40419
94.6	42922
98.1	45470
101.5	48064
104.8	50704
108.0	53390

T = 23°C	ΔP (Pa)
Q (lpm)	SS # 2
0.0	0
5.4	1287
10.8	2587
16.1	3899
21.3	5224
26.4	6561
31.5	7911
36.5	9273
41.5	10648
46.4	12035
51.2	13435
55.9	14848
60.6	16273
65.2	17710
69.8	19160
74.3	20623
78.7	22098
83.1	23586
87.4	25086
91.7	26599
95.8	28124
100.0	29662
104.0	31212
108.0	32775
112.0	34350
115.9	35938
119.7	37539
123.5	39152
127.2	40777
130.9	42415
134.5	44066
138.0	45729
141.5	47405

T = 23°C	ΔP (Pa)
Q (lpm)	SS # 3
0.0	0
5.4	1946
10.7	3929
15.9	5949
21.0	8006
26.0	10099
30.9	12229
35.7	14396
40.4	16600
44.9	18841
49.4	21119
53.8	23433
58.1	25784
62.3	28172
66.4	30597
70.4	33059
74.3	35557
78.1	38093
81.8	40665
85.4	43274
89.0	45919
92.4	48602
95.8	51321
99.1	54078
102.3	56871
105.4	59700
108.4	62567
111.4	65471

Fluid Test: Air

T = 23°C	ΔP (Pa)
Q (lpm)	SS # 4
0.0	0
5.4	811
10.8	1623
16.2	2435
21.5	3249
26.8	4062
32.0	4877
37.2	5692
42.3	6508
47.4	7324
52.5	8141
57.5	8959
62.5	9778
67.4	10597
72.3	11417
77.2	12237
82.0	13058
86.8	13880
91.6	14702
96.3	15525
101.0	16349
105.6	17174
110.3	17999
114.8	18825
119.4	19651
123.9	20478
128.4	21306
132.8	22135
137.3	22964
141.6	23794
146.0	24624
150.3	25455
154.6	26287
158.8	27119

T = 23°C	ΔP (Pa)
Q (lpm)	SS # 5
0.0	0
5.4	1890
10.7	3780
15.9	5670
21.0	7560
26.1	9451
31.0	11341
35.9	13231
40.6	15121
45.3	17011
49.9	18901
54.4	20791
58.9	22681
63.3	24571
67.6	26461
71.8	28352
76.0	30242
80.1	32132
84.1	34022
88.1	35912
92.0	37802
95.8	39692
99.6	41582
103.3	43472
107.0	45362
110.6	47253
114.2	49143
117.7	51033
121.2	52923

T = 24°C	ΔP (Pa)
Q (lpm)	SS # 6
0.0	0
5.4	1673
10.7	3392
16.0	5159
21.1	6972
26.1	8832
31.1	10738
35.9	12692
40.7	14692
45.4	16739
49.9	18833
54.4	20974
58.8	23162
63.0	25396
67.2	27677
71.3	30005
75.3	32380
79.2	34802
83.0	37270
86.7	39786
90.3	42348
93.8	44957
97.2	47612
100.6	50315
103.8	53065
107.0	55861
110.0	58704
113.0	61593
115.9	64530
118.7	67513
121.4	70544

Fluid Test: Air. Spargers for 4" lab column

T = 23°C	ΔP (Pa)
Jg * Rs (cm/s)	SS # 1
0.0	0
1.08	932
2.15	1921
3.21	2965
4.26	4065
5.29	5221
6.31	6433
7.32	7701
8.31	9025
9.29	10405
10.26	11841
11.20	13332
12.14	14880
13.05	16483
13.95	18142
14.83	19857
15.69	21628
16.54	23455
17.37	25338
18.18	27277

T = 25°C	ΔP (Pa)
Jg * Rs (cm/s)	SS # 2
0.0	0
1.08	1098
2.15	2195
3.20	3290
4.25	4384
5.28	5476
6.31	6566
7.32	7655
8.33	8742
9.32	9828
10.30	10912
11.27	11994
12.24	13075
13.19	14155
14.14	15232
15.07	16309
16.00	17383
16.91	18456
17.82	19528
18.72	20598
19.61	21666
20.50	22733

T = 25°C	ΔP (Pa)
Jg * Rs (cm/s)	SS # 3
0.0	0
1.08	946
2.15	1887
3.21	2825
4.26	3759
5.30	4689
6.34	5616
7.36	6538
8.38	7456
9.38	8371
10.38	9282
11.37	10189
12.35	11091
13.32	11991
14.29	12886
15.25	13777
16.20	14664
17.14	15548
18.07	16427
19.00	17303
19.96	18175
20.79	19043
21.61	19907
22.42	20767
23.22	21624
24.00	22476

Fluid Test: Air. Sparger 6" lab column.

T = 23°C	ΔP (Pa)
Jg * Rs (cm/s)	SS # 1
0.00	0
0.38	492
0.76	986
1.13	1483
1.51	1983
1.88	2486
2.25	2991
2.61	3498
2.98	4009
3.34	4522
3.71	5038
4.07	5556
4.43	6077
4.78	6601
5.14	7128
5.49	7657
5.84	8189
6.19	8723
6.54	9260
6.89	9800
7.23	10343
7.57	10888
7.91	11435
8.25	11986
8.59	12539
8.92	13095
9.25	13654
9.59	14215
9.92	14779

T = 23°C	ΔP (Pa)
Jg * Rs (cm/s)	SS # 1
10.24	15345
10.57	15914
10.89	16486
11.21	17061
11.53	17638
11.85	18218
12.17	18800
12.48	19385
12.80	19973
13.11	20564
13.42	21157
13.72	21753

Fluid Test: Air. Spargers for 20" pilot unit

T = 24°C	ΔP (Pa)
Jg * Rs (cm/s)	SS # 1
0.00	0
0.43	1585
0.86	3217
1.28	4894
1.70	6617
2.10	8385
2.50	10200
2.90	12061
3.28	13967
3.66	15919
4.03	17917
4.39	19961
4.74	22051
5.09	24186
5.43	26368
5.76	28595
6.09	30868
6.40	33187
6.71	35552
7.02	37963
7.31	40419
7.60	42922
7.88	45470
8.15	48064
8.42	50704
8.67	53390

T = 24°C	ΔP (Pa)
Jg * Rs (cm/s)	SS # 2
0.00	0
0.44	1287
0.87	2587
1.29	3899
1.71	5224
2.12	6561
2.53	7911
2.93	9273
3.33	10648
3.72	12035
4.11	13435
4.49	14848
4.87	16273
5.24	17710
5.61	19160
5.97	20623
6.32	22098
6.68	23586
7.02	25086
7.36	26599
7.70	28124
8.03	29662
8.36	31212
8.68	32775
9.00	34350
9.31	35938
9.62	37539
9.92	39152
10.22	40777
10.51	42415
10.80	44066
11.09	45729
11.37	47405

T = 24°C	ΔP (Pa)
Jg * Rs (cm/s)	SS # 3
0.00	0
0.43	1946
0.86	3929
1.28	5949
1.69	8006
2.09	10099
2.48	12229
2.87	14396
3.24	16600
3.61	18841
3.97	21119
4.32	23433
4.67	25784
5.00	28172
5.33	30597
5.65	33059
5.97	35557
6.27	38093
6.57	40665
6.86	43274
7.15	45919
7.43	48602
7.70	51321
7.96	54078
8.22	56871
8.47	59700
8.71	62567
8.95	65471

Fluid Test: Air

T = 24°C	ΔP (Pa)
Jg * Rs (cm/s)	SS # 4
0.00	0
0.44	811
0.87	1623
1.30	2435
1.73	3249
2.15	4062
2.57	4877
2.98	5692
3.40	6508
3.81	7324
4.21	8141
4.62	8959
5.02	9778
5.42	10597
5.81	11417
6.20	12237
6.59	13058
6.97	13880
7.36	14702
7.74	15525
8.11	16349
8.49	17174
8.86	17999
9.23	18825
9.59	19651
9.95	20478
10.31	21306
10.67	22135
11.03	22964
11.38	23794
11.73	24624
12.07	25455
12.42	26287
12.76	27119

T = 24°C	ΔP (Pa)
Jg * Rs (cm/s)	SS # 5
0.00	0
0.43	1890
0.86	3780
1.28	5670
1.69	7560
2.09	9451
2.49	11341
2.88	13231
3.26	15121
3.64	17011
4.01	18901
4.37	20791
4.73	22681
5.08	24571
5.43	26461
5.77	28352
6.10	30242
6.43	32132
6.76	34022
7.08	35912
7.39	37802
7.70	39692
8.00	41582
8.30	43472
8.60	45362
8.89	47253
9.17	49143
9.46	51033
9.73	52923

T = 24°C	ΔP (Pa)
Jg * Rs (cm/s)	SS # 6
0.00	0
0.26	1672
0.52	3392
0.78	5158
1.03	6971
1.27	8831
1.51	10738
1.75	12692
1.98	14692
2.20	16739
2.43	18833
2.64	20974
2.85	23162
3.06	25396
3.27	27677
3.46	30005
3.66	32380
3.85	34802
4.03	37270
4.21	39786
4.39	42348
4.56	44957
4.72	47612
4.88	50315
5.04	53065
5.19	55861
5.34	58704
5.49	61593
5.63	64530
5.77	67513
5.90	70544

Permeability Calculations
Fluid Test: Air. Sparger # 1 for 4" lab column

Sparger C4 - 1
Experimental data

Q	DP	Pm	Q (TP)	Q (TP)	Ln Q (TP)	Ln DP	1/Pm	Kg	Kg lin
lpm	Pa	atm	lpm	[m^3/s]			1/atm	Darcy	Darcy
5	932	1.00	5.43	9.05E-05	-9.310	6.838	0.99542	0.1145	0.1364
10	1921	1.01	10.81	1.80E-04	-8.621	7.561	0.99061	0.1277	0.1359
15	2965	1.01	16.14	2.69E-04	-8.221	7.995	0.98558	0.1342	0.1354
20	4065	1.02	21.40	3.57E-04	-7.939	8.310	0.98033	0.1377	0.1349
25	5221	1.03	26.60	4.43E-04	-7.721	8.561	0.97488	0.1395	0.1344
30	6433	1.03	31.74	5.29E-04	-7.545	8.769	0.96923	0.1401	0.1338
35	7701	1.04	36.80	6.13E-04	-7.397	8.949	0.96339	0.1400	0.1333
40	9025	1.04	41.80	6.97E-04	-7.269	9.108	0.95736	0.1393	0.1327
45	10405	1.05	46.72	7.79E-04	-7.158	9.250	0.95116	0.1382	0.1321
50	11841	1.06	51.56	8.59E-04	-7.059	9.379	0.94480	0.1369	0.1315
55	13332	1.07	56.32	9.39E-04	-6.971	9.498	0.93827	0.1353	0.1308
60	14880	1.07	61.01	1.02E-03	-6.891	9.608	0.93160	0.1335	0.1302
65	16483	1.08	65.61	1.09E-03	-6.818	9.710	0.92478	0.1316	0.1295
70	18142	1.09	70.12	1.17E-03	-6.752	9.806	0.91783	0.1295	0.1288
75	19857	1.10	74.55	1.24E-03	-6.691	9.896	0.91076	0.1274	0.1282
80	21628	1.11	78.90	1.31E-03	-6.634	9.982	0.90356	0.1253	0.1275
85	23455	1.12	83.15	1.39E-03	-6.581	10.063	0.89626	0.1231	0.1268
90	25338	1.13	87.31	1.46E-03	-6.533	10.140	0.88886	0.1209	0.1260
95	27277	1.13	91.39	1.52E-03	-6.487	10.214	0.88137	0.1186	0.1253
								Avg =	0.1312
								STD =	0.0035

Ln DP = Ln A + n Ln Q			Klikenberg Effect		
n =	1.2085		Kg = Kl + b Kl * (1/Pm)		
RSQ =	0.9957		Y = A + B X		
A =	17.9543		Kl (A) =	0.0398	Darcy
Kg =	1.3E-13	m^2	b Kl (B) =	0.0188	
Kg =	0.1310	Darcy	b =	0.4733	
			RQS =	0.1955	
			Kg =	0.0576	Darcy
			STD =	0.0007	

Fluid Test: Air. Sparger # 2 for 4" lab column

Sparger C4 - 2
Experimental data

Q	DP	Pm	Q (TP)	Q (TP)	Ln Q (TP)	Ln DP	1/Pm	Kg	Kg lin
lpm	Pa	atm	lpm	[m^3/s]			1/atm	Darcy	Darcy
5	1098	1.01	5.43	9.05E-05	-9.311	7.001	0.99461	0.5039	0.5184
10	2195	1.01	10.80	1.80E-04	-8.623	7.694	0.98928	0.5126	0.5181
15	3290	1.02	16.11	2.69E-04	-8.223	8.099	0.98402	0.5168	0.5178
20	4384	1.02	21.37	3.56E-04	-7.940	8.386	0.97883	0.5191	0.5175
25	5476	1.03	26.57	4.43E-04	-7.722	8.608	0.97369	0.5203	0.5172
30	6566	1.03	31.72	5.29E-04	-7.545	8.790	0.96862	0.5209	0.5169
35	7655	1.04	36.81	6.14E-04	-7.396	8.943	0.96360	0.5210	0.5166
40	8742	1.04	41.85	6.98E-04	-7.268	9.076	0.95865	0.5208	0.5163
45	9828	1.05	46.84	7.81E-04	-7.155	9.193	0.95375	0.5204	0.5160
50	10912	1.05	51.78	8.63E-04	-7.055	9.298	0.94891	0.5197	0.5157
55	11994	1.06	56.68	9.45E-04	-6.965	9.392	0.94412	0.5190	0.5154
60	13075	1.06	61.52	1.03E-03	-6.883	9.478	0.93939	0.5181	0.5151
65	14155	1.07	66.31	1.11E-03	-6.808	9.558	0.93471	0.5171	0.5148
70	15232	1.08	71.06	1.18E-03	-6.739	9.631	0.93009	0.5161	0.5145
75	16309	1.08	75.76	1.26E-03	-6.675	9.699	0.92552	0.5149	0.5143
80	17383	1.09	80.42	1.34E-03	-6.615	9.763	0.92100	0.5138	0.5140
85	18456	1.09	85.03	1.42E-03	-6.559	9.823	0.91653	0.5126	0.5137
90	19528	1.10	89.60	1.49E-03	-6.507	9.880	0.91211	0.5113	0.5135
95	20598	1.10	94.12	1.57E-03	-6.458	9.933	0.90774	0.5100	0.5132
100	21666	1.11	98.60	1.64E-03	-6.411	9.983	0.90341	0.5087	0.5129
105	22733	1.11	103.04	1.72E-03	-6.367	10.032	0.89914	0.5074	0.5127
								Avg =	0.5154
								STD =	0.0018

Ln DP = Ln A + n Ln Q			Klikenberg Effect		
n =	1.0317		Kg = Kl + b Kl * (1/Pm)		
RSQ =	0.9999		Y = A + B X		
A =	16.5845		Kl (A) =	0.4583	Darcy
Kg =	5.1E-13	m^2	b Kl (B) =	0.0604	
Kg =	0.5154	Darcy	b =	0.1319	
			RQS =	0.1276	
			Kg =	0.5154	Darcy
			STD =	0.0018	

Fluid Test: Air. Sparger # 3 for 4" lab column

Sparger C4 - 3
Experimental data

Q	DP	Pm	Q (TP)	Q (TP)	Ln Q (TP)	Ln DP	1/Pm	Kg	Kg lin
lpm	Pa	atm	lpm	[m^3/s]			1/atm	Darcy	Darcy
5	946	1.00	5.43	9.05E-05	-9.310	6.852	0.99536	0.6506	0.6654
10	1887	1.01	10.81	1.80E-04	-8.621	7.543	0.99077	0.6581	0.6651
15	2825	1.01	16.15	2.69E-04	-8.220	7.946	0.98625	0.6619	0.6648
20	3759	1.02	21.43	3.57E-04	-7.937	8.232	0.98179	0.6641	0.6645
25	4689	1.02	26.67	4.44E-04	-7.719	8.453	0.97738	0.6654	0.6642
30	5616	1.03	31.86	5.31E-04	-7.541	8.633	0.97304	0.6663	0.6639
35	6538	1.03	37.01	6.17E-04	-7.391	8.785	0.96875	0.6667	0.6637
40	7456	1.04	42.11	7.02E-04	-7.262	8.917	0.96451	0.6670	0.6634
45	8371	1.04	47.17	7.86E-04	-7.148	9.033	0.96033	0.6670	0.6631
50	9282	1.05	52.18	8.70E-04	-7.047	9.136	0.95620	0.6669	0.6628
55	10189	1.05	57.16	9.53E-04	-6.956	9.229	0.95213	0.6667	0.6626
60	11091	1.05	62.09	1.03E-03	-6.874	9.314	0.94811	0.6664	0.6623
65	11991	1.06	66.98	1.12E-03	-6.798	9.392	0.94414	0.6660	0.6620
70	12886	1.06	71.83	1.20E-03	-6.728	9.464	0.94022	0.6656	0.6618
75	13777	1.07	76.65	1.28E-03	-6.663	9.531	0.93634	0.6651	0.6615
80	14664	1.07	81.42	1.36E-03	-6.602	9.593	0.93252	0.6646	0.6613
85	15548	1.08	86.16	1.44E-03	-6.546	9.652	0.92874	0.6641	0.6610
90	16427	1.08	90.86	1.51E-03	-6.493	9.707	0.92502	0.6636	0.6608
95	17303	1.09	95.53	1.59E-03	-6.443	9.759	0.92133	0.6630	0.6605
100.2	18175	1.09	100.32	1.67E-03	-6.394	9.808	0.91770	0.6636	0.6603
104.8	19043	1.09	104.52	1.74E-03	-6.353	9.854	0.91410	0.6603	0.6600
109.3	19907	1.10	108.65	1.81E-03	-6.314	9.899	0.91055	0.6571	0.6598
113.8	20767	1.10	112.71	1.88E-03	-6.277	9.941	0.90705	0.6540	0.6596
118.3	21624	1.11	116.72	1.95E-03	-6.242	9.982	0.90358	0.6509	0.6594
122.8	22476	1.11	120.66	2.01E-03	-6.209	10.020	0.90016	0.6478	0.6591
								Avg =	0.6629
								STD =	0.0015

Ln DP = Ln A + n Ln Q			Klikenberg Effect		
n =	1.0204		Kg = Kl + b Kl * (1/Pm)		
RSQ =	0.9999		Y = A + B X		
A =	16.3341		Kl (A) =	0.5997	Darcy
Kg =	6.5E-13	m^2	b Kl (B) =	0.0660	
Kg =	0.6621	Darcy	b =	0.1100	
			RQS =	0.1127	
			Kg =	0.6629	Darcy
			STD =	0.0015	

Fluid Test: Air. Sparger # 1 for 6" lab column

sparger C6 - 1
Experimental data

Q	DP	Pm	Q (TP)	Q (TP)	Ln Q (TP)	Ln DP	1/Pm	Kg	Kg lin
lpm	Pa	atm	lpm	[m^3/s]			1/atm	Darcy	Darcy
5	492	1.00	5.44	9.07E-05	-9.308	6.198	0.99758	0.2915	0.3196
10	986	1.00	10.86	1.81E-04	-8.617	6.894	0.99516	0.3032	0.3193
15	1483	1.01	16.25	2.71E-04	-8.214	7.302	0.99273	0.3095	0.3190
20	1983	1.01	21.62	3.60E-04	-7.929	7.592	0.99031	0.3136	0.3187
25	2486	1.01	26.96	4.49E-04	-7.708	7.818	0.98788	0.3165	0.3184
30	2991	1.01	32.27	5.38E-04	-7.528	8.003	0.98546	0.3186	0.3182
35	3498	1.02	37.55	6.26E-04	-7.376	8.160	0.98303	0.3200	0.3179
40	4009	1.02	42.81	7.14E-04	-7.245	8.296	0.98060	0.3211	0.3176
45	4522	1.02	48.04	8.01E-04	-7.130	8.417	0.97817	0.3218	0.3173
50	5038	1.02	53.25	8.87E-04	-7.027	8.525	0.97574	0.3223	0.3170
55	5556	1.03	58.43	9.74E-04	-6.934	8.623	0.97331	0.3226	0.3167
60	6077	1.03	63.58	1.06E-03	-6.850	8.712	0.97088	0.3227	0.3164
65	6601	1.03	68.71	1.15E-03	-6.772	8.795	0.96845	0.3226	0.3162
70	7128	1.04	73.81	1.23E-03	-6.701	8.872	0.96602	0.3224	0.3159
75	7657	1.04	78.88	1.31E-03	-6.634	8.943	0.96359	0.3222	0.3156
80	8189	1.04	83.92	1.40E-03	-6.572	9.010	0.96116	0.3218	0.3153
85	8723	1.04	88.94	1.48E-03	-6.514	9.074	0.95873	0.3213	0.3150
90	9260	1.05	93.94	1.57E-03	-6.459	9.133	0.95630	0.3208	0.3147
95	9800	1.05	98.90	1.65E-03	-6.408	9.190	0.95387	0.3202	0.3144
100	10343	1.05	103.85	1.73E-03	-6.359	9.244	0.95144	0.3196	0.3142
105	10888	1.05	108.76	1.81E-03	-6.313	9.295	0.94901	0.3189	0.3139
110	11435	1.06	113.65	1.89E-03	-6.269	9.344	0.94658	0.3182	0.3136
115	11986	1.06	118.51	1.98E-03	-6.227	9.391	0.94416	0.3174	0.3133
120	12539	1.06	123.34	2.06E-03	-6.187	9.437	0.94173	0.3166	0.3130
125	13095	1.06	128.15	2.14E-03	-6.149	9.480	0.93930	0.3158	0.3127
130	13654	1.07	132.93	2.22E-03	-6.112	9.522	0.93688	0.3149	0.3125
135	14215	1.07	137.69	2.29E-03	-6.077	9.562	0.93445	0.3140	0.3122
140	14779	1.07	142.42	2.37E-03	-6.043	9.601	0.93203	0.3131	0.3119
145	15345	1.08	147.12	2.45E-03	-6.011	9.639	0.92961	0.3121	0.3116
150	15914	1.08	151.80	2.53E-03	-5.980	9.675	0.92719	0.3111	0.3113
155	16486	1.08	156.45	2.61E-03	-5.949	9.710	0.92477	0.3101	0.3110
160	17061	1.08	161.07	2.68E-03	-5.920	9.745	0.92235	0.3091	0.3107
165	17638	1.09	165.67	2.76E-03	-5.892	9.778	0.91993	0.3081	0.3105
170	18218	1.09	170.24	2.84E-03	-5.865	9.810	0.91752	0.3071	0.3102
175	18800	1.09	174.79	2.91E-03	-5.839	9.842	0.91510	0.3060	0.3099
180	19385	1.10	179.31	2.99E-03	-5.813	9.872	0.91269	0.3050	0.3096
185	19973	1.10	183.80	3.06E-03	-5.788	9.902	0.91028	0.3039	0.3093
190	20564	1.10	188.27	3.14E-03	-5.764	9.931	0.90787	0.3028	0.3090
195	21157	1.10	192.71	3.21E-03	-5.741	9.960	0.90547	0.3017	0.3088
200	21753	1.11	197.13	3.29E-03	-5.718	9.988	0.90306	0.3006	0.3085
								Avg =	0.3140
								STD =	0.0033

Ln DP = Ln A + n Ln Q			Klikenberg Effect		
n =	1.0644		Kg = Kl + b Kl * (1/Pm)		
RSQ =	0.9992		Y = A + B X		
A =	16.0306		Kl (A) =	0.2170	Darcy
Kg =	3.32E-13	m^2	b Kl (B) =	0.1257	
Kg =	0.3363	Darcy	b =	0.5792	
			RQS =	0.1812	
			Kg =	0.3365	Darcy
			STD =	0.0036	

Fluid Test: Air. Sparger # 1 for 20" pilot unit

Sparger C20 - 1

Experimental data

Q	DP	Pm	Q (TP)	Q (TP)	Ln Q (TP)	Ln DP	1/Pm	Kg	Kg ln
lpm	Pa	atm	lpm	[m^3/s]			1/atm	Darcy	Darcy
5	1585	1.01	5.41	9.02E-05	-9.313	7.37	0.9922	0.0321	0.0394
10	3217	1.02	10.74	1.79E-04	-8.628	8.08	0.9844	0.0358	0.0392
15	4894	1.02	15.99	2.66E-04	-8.230	8.50	0.9764	0.0378	0.0391
20	6617	1.03	21.14	3.52E-04	-7.951	8.80	0.9684	0.0390	0.0390
25	8385	1.04	26.20	4.37E-04	-7.736	9.03	0.9603	0.0397	0.0388
30	10200	1.05	31.17	5.20E-04	-7.563	9.23	0.9521	0.0401	0.0387
35	12061	1.06	36.06	6.01E-04	-7.417	9.40	0.9438	0.0403	0.0385
40	13967	1.07	40.84	6.81E-04	-7.292	9.54	0.9355	0.0404	0.0384
45	15919	1.08	45.54	7.59E-04	-7.184	9.68	0.9272	0.0404	0.0383
50	17917	1.09	50.14	8.36E-04	-7.087	9.79	0.9188	0.0402	0.0381
55	19961	1.10	54.65	9.11E-04	-7.001	9.90	0.9103	0.0400	0.0380
60	22051	1.11	59.06	9.84E-04	-6.924	10.00	0.9019	0.0397	0.0378
65	24186	1.12	63.38	1.06E-03	-6.853	10.09	0.8934	0.0394	0.0377
70	26368	1.13	67.61	1.13E-03	-6.788	10.18	0.8849	0.0390	0.0375
75	28595	1.14	71.74	1.20E-03	-6.729	10.26	0.8763	0.0386	0.0374
80	30868	1.15	75.77	1.26E-03	-6.674	10.34	0.8678	0.0382	0.0373
85	33187	1.16	79.72	1.33E-03	-6.624	10.41	0.8593	0.0377	0.0371
90	35552	1.18	83.57	1.39E-03	-6.576	10.48	0.8507	0.0372	0.0370
95	37963	1.19	87.33	1.46E-03	-6.532	10.54	0.8422	0.0367	0.0368
100	40419	1.20	91.00	1.52E-03	-6.491	10.61	0.8337	0.0362	0.0367
105	42922	1.21	94.57	1.58E-03	-6.453	10.67	0.8252	0.0357	0.0365
110	45470	1.22	98.06	1.63E-03	-6.417	10.72	0.8167	0.0352	0.0364
115	48064	1.24	101.45	1.69E-03	-6.382	10.78	0.8083	0.0347	0.0362
120	50704	1.25	104.76	1.75E-03	-6.350	10.83	0.7999	0.0342	0.0361
125	53390	1.26	107.98	1.80E-03	-6.320	10.89	0.7915	0.0336	0.0360
								Avg =	0.0377
								STD =	0.0010

Ln DP = Ln A + n Ln Q			Klinkenberg Effect		
n =	1.1902		Kg = Kl + b Kl * (1/Pm)		
RSQ =	0.9949		Y = A + B X		
A =	18.2957		Kl (A) =	0.0225	Darcy
Kg =	3.71E-14	m^2	b Kl (B) =	0.0169	
Kg =	0.0376	Darcy	b =	0.7516	
			RQS =	0.1887	
			Kg =	0.0377	Darcy
			STD =	0.0010	

Fluid Test: Air. Sparger # 2 for 20" pilot unit

Sparger C20 - 2
Experimental data

Q lpm	DP Pa	Pm atm	Q (TP) lpm	Q (TP) [m^3/s]	Ln Q (TP)	Ln DP	1/Pm 1/atm	Kg Darcy	Kg lin Darcy
5	1287	1.01	5.42	9.04E-05	-9.311	7.160	0.99369	0.0774	0.0897
10	2587	1.01	10.78	1.80E-04	-8.625	7.858	0.98740	0.0830	0.0896
15	3899	1.02	16.06	2.68E-04	-8.226	8.268	0.98112	0.0861	0.0894
20	5224	1.03	21.28	3.55E-04	-7.944	8.561	0.97487	0.0880	0.0892
25	6561	1.03	26.43	4.41E-04	-7.728	8.789	0.96864	0.0893	0.0890
30	7911	1.04	31.51	5.25E-04	-7.552	8.976	0.96243	0.0902	0.0889
35	9273	1.05	36.53	6.09E-04	-7.404	9.135	0.95624	0.0907	0.0887
40	10648	1.05	41.48	6.91E-04	-7.277	9.273	0.95008	0.0911	0.0885
45	12035	1.06	46.36	7.73E-04	-7.166	9.396	0.94394	0.0913	0.0883
50	13435	1.07	51.18	8.53E-04	-7.067	9.506	0.93782	0.0913	0.0882
55	14848	1.07	55.93	9.32E-04	-6.978	9.606	0.93173	0.0912	0.0880
60	16273	1.08	60.62	1.01E-03	-6.897	9.697	0.92567	0.0911	0.0878
65	17710	1.09	65.24	1.09E-03	-6.824	9.782	0.91963	0.0909	0.0877
70	19160	1.09	69.80	1.16E-03	-6.756	9.861	0.91362	0.0906	0.0875
75	20623	1.10	74.30	1.24E-03	-6.694	9.934	0.90763	0.0902	0.0873
80	22098	1.11	78.73	1.31E-03	-6.636	10.003	0.90168	0.0899	0.0871
85	23586	1.12	83.10	1.39E-03	-6.582	10.068	0.89575	0.0894	0.0870
90	25086	1.12	87.41	1.46E-03	-6.531	10.130	0.88985	0.0890	0.0868
95	26599	1.13	91.66	1.53E-03	-6.484	10.189	0.88397	0.0885	0.0866
100	28124	1.14	95.84	1.60E-03	-6.439	10.244	0.87813	0.0880	0.0865
105	29662	1.15	99.97	1.67E-03	-6.397	10.298	0.87232	0.0874	0.0863
110	31212	1.15	104.04	1.73E-03	-6.357	10.349	0.86654	0.0869	0.0862
115	32775	1.16	108.04	1.80E-03	-6.320	10.397	0.86078	0.0863	0.0860
120	34350	1.17	111.99	1.87E-03	-6.284	10.444	0.85506	0.0857	0.0858
125	35938	1.18	115.88	1.93E-03	-6.250	10.490	0.84937	0.0851	0.0857
130	37539	1.19	119.71	2.00E-03	-6.217	10.533	0.84371	0.0845	0.0855
135	39152	1.19	123.49	2.06E-03	-6.186	10.575	0.83808	0.0839	0.0853
140	40777	1.20	127.21	2.12E-03	-6.156	10.616	0.83249	0.0833	0.0852
145	42415	1.21	130.87	2.18E-03	-6.128	10.655	0.82692	0.0826	0.0850
150	44066	1.22	134.48	2.24E-03	-6.101	10.693	0.82139	0.0820	0.0849
155	45729	1.23	138.03	2.30E-03	-6.075	10.730	0.81589	0.0814	0.0847
160	47405	1.23	141.53	2.36E-03	-6.050	10.766	0.81042	0.0807	0.0846
								Avg =	0.0871
								STD =	0.0016

Ln DP = Ln A + n Ln Q			Klinkenberg Effect		
n =	1.1183		Kg = Kl + b Kl * (1/Pm)		
RSQ =	0.9976		Y = A + B X		
A =	17.4567		Kl (A) =	0.0617	Darcy
Kg =	8.59E-14	m^2	b Kl (B) =	0.0282	
Kg =	0.0870	Darcy	b =	0.4572	
			RQS =	0.1744	
			Kg =	0.0871	Darcy
			STD =	0.0016	

Fluid Test: Air. Sparger # 3 for 20" pilot unit

Sparger C20 - 3
Experimental data

Q	DP	Pm	Q (TP)	Q (TP)	Ln Q (TP)	Ln DP	1/Pm	Kg	Kg lin
lpm	Pa	atm	lpm	[m^3/s]			1/atm	Darcy	Darcy
5	1946	1.01	5.41	9.01E-05	-9.315	7.574	0.99049	0.0294	0.0359
10	3929	1.02	10.71	1.78E-04	-8.631	8.276	0.98098	0.0326	0.0358
15	5949	1.03	15.90	2.65E-04	-8.235	8.691	0.97148	0.0343	0.0357
20	8006	1.04	21.00	3.50E-04	-7.958	8.988	0.96200	0.0354	0.0355
25	10099	1.05	25.99	4.33E-04	-7.744	9.220	0.95253	0.0360	0.0354
30	12229	1.06	30.88	5.15E-04	-7.572	9.412	0.94309	0.0364	0.0353
35	14396	1.07	35.67	5.94E-04	-7.428	9.575	0.93367	0.0367	0.0352
40	16600	1.08	40.35	6.73E-04	-7.304	9.717	0.92429	0.0368	0.0351
45	18841	1.09	44.94	7.49E-04	-7.197	9.844	0.91494	0.0368	0.0350
50	21119	1.10	49.42	8.24E-04	-7.102	9.958	0.90562	0.0367	0.0348
55	23433	1.12	53.81	8.97E-04	-7.017	10.062	0.89635	0.0366	0.0347
60	25784	1.13	58.10	9.68E-04	-6.940	10.158	0.88713	0.0364	0.0346
65	28172	1.14	62.29	1.04E-03	-6.870	10.246	0.87795	0.0361	0.0345
70	30597	1.15	66.38	1.11E-03	-6.807	10.329	0.86882	0.0359	0.0344
75	33059	1.16	70.38	1.17E-03	-6.748	10.406	0.85975	0.0356	0.0343
80	35557	1.18	74.28	1.24E-03	-6.694	10.479	0.85073	0.0352	0.0342
85	38093	1.19	78.09	1.30E-03	-6.644	10.548	0.84177	0.0349	0.0340
90	40665	1.20	81.81	1.36E-03	-6.598	10.613	0.83287	0.0345	0.0339
95	43274	1.21	85.44	1.42E-03	-6.554	10.675	0.82404	0.0341	0.0338
100	45919	1.23	88.98	1.48E-03	-6.514	10.735	0.81527	0.0337	0.0337
105	48602	1.24	92.43	1.54E-03	-6.476	10.791	0.80656	0.0333	0.0336
110	51321	1.25	95.80	1.60E-03	-6.440	10.846	0.79792	0.0329	0.0335
115	54078	1.27	99.08	1.65E-03	-6.406	10.898	0.78936	0.0325	0.0334
120	56871	1.28	102.27	1.70E-03	-6.374	10.949	0.78086	0.0321	0.0333
125	59700	1.29	105.39	1.76E-03	-6.344	10.997	0.77244	0.0317	0.0332
130	62567	1.31	108.42	1.81E-03	-6.316	11.044	0.76409	0.0312	0.0331
135	65471	1.32	111.37	1.86E-03	-6.289	11.089	0.75582	0.0308	0.0330
								Avg =	0.0344
								STD =	0.0009

Ln DP = Ln A + n Ln Q			Klinkenberg Effect		
n =	1.17743		Kg = Kl + b Kl * (1/Pm)		
RSQ =	0.9951		Y = A + B X		
A =	18.3867		Kl (A) =	0.0236	Darcy
Kg =	3.39E-14	m^2	b Kl (B) =	0.0124	
Kg =	0.0343	Darcy	b =	0.5266	
			RQS =	0.1777	
			Kg =	0.0344	Darcy
			STD =	0.0009	

Fluid Test: Air. Sparger # 4 for 20" pilot unit

Sparger C20 - 4
Experimental data

Q	DP	Pm	Q (TP)	Q (TP)	Ln Q (TP)	Ln DP	1/Pm	Kg	Kg lin
lpm	Pa	atm	lpm	[m^3/s]			1/atm	Darcy	Darcy
5	811	1.00	5.44	9.06E-05	-9.309	6.698	0.99601	0.2434	0.2575
10	1623	1.01	10.83	1.80E-04	-8.620	7.392	0.99206	0.2500	0.2573
15	2435	1.01	16.18	2.70E-04	-8.218	7.798	0.98812	0.2535	0.2572
20	3249	1.02	21.48	3.58E-04	-7.935	8.086	0.98422	0.2556	0.2570
25	4062	1.02	26.75	4.46E-04	-7.716	8.310	0.98035	0.2570	0.2568
30	4877	1.02	31.97	5.33E-04	-7.537	8.492	0.97650	0.2580	0.2566
35	5692	1.03	37.16	6.19E-04	-7.387	8.647	0.97268	0.2586	0.2564
40	6508	1.03	42.30	7.05E-04	-7.257	8.781	0.96889	0.2590	0.2562
45	7324	1.04	47.40	7.90E-04	-7.143	8.899	0.96512	0.2593	0.2561
50	8141	1.04	52.46	8.74E-04	-7.042	9.005	0.96138	0.2593	0.2559
55	8959	1.04	57.49	9.58E-04	-6.951	9.100	0.95766	0.2593	0.2557
60	9778	1.05	62.47	1.04E-03	-6.867	9.188	0.95397	0.2592	0.2555
65	10597	1.05	67.42	1.12E-03	-6.791	9.268	0.95031	0.2589	0.2554
70	11417	1.06	72.33	1.21E-03	-6.721	9.343	0.94667	0.2587	0.2552
75	12237	1.06	77.20	1.29E-03	-6.656	9.412	0.94305	0.2583	0.2550
80	13058	1.06	82.03	1.37E-03	-6.595	9.477	0.93946	0.2579	0.2549
85	13880	1.07	86.83	1.45E-03	-6.538	9.538	0.93590	0.2575	0.2547
90	14702	1.07	91.59	1.53E-03	-6.485	9.596	0.93236	0.2571	0.2545
95	15525	1.08	96.31	1.61E-03	-6.435	9.650	0.92884	0.2566	0.2544
100	16349	1.08	101.00	1.68E-03	-6.387	9.702	0.92535	0.2561	0.2542
105	17174	1.08	105.65	1.76E-03	-6.342	9.751	0.92187	0.2555	0.2540
110	17999	1.09	110.27	1.84E-03	-6.299	9.798	0.91843	0.2549	0.2539
115	18825	1.09	114.85	1.91E-03	-6.258	9.843	0.91500	0.2544	0.2537
120	19651	1.10	119.40	1.99E-03	-6.220	9.886	0.91160	0.2537	0.2535
125	20478	1.10	123.91	2.07E-03	-6.183	9.927	0.90822	0.2531	0.2534
130	21306	1.11	128.39	2.14E-03	-6.147	9.967	0.90486	0.2525	0.2532
135	22135	1.11	132.84	2.21E-03	-6.113	10.005	0.90153	0.2518	0.2531
140	22964	1.11	137.25	2.29E-03	-6.080	10.042	0.89822	0.2512	0.2529
145	23794	1.12	141.63	2.36E-03	-6.049	10.077	0.89493	0.2505	0.2527
150	24624	1.12	145.98	2.43E-03	-6.019	10.111	0.89166	0.2498	0.2526
155	25455	1.13	150.30	2.50E-03	-5.989	10.145	0.88841	0.2492	0.2524
160	26287	1.13	154.58	2.58E-03	-5.961	10.177	0.88518	0.2485	0.2523
165	27119	1.13	158.83	2.65E-03	-5.934	10.208	0.88197	0.2478	0.2521
								Avg =	0.2547
								STD =	0.0016

Ln DP = Ln A + n Ln Q			Klinkenberg Effect		
n =	1.0452		Kg = Kl + b Kl * (1/Pm)		
RSQ =	0.9996		Y = A + B X		
A =	16.3827		Kl (A) =	0.2104	Darcy
Kg =	2.51E-13	m^2	b Kl (B) =	0.0473	
Kg =	0.2547	Darcy	b =	0.2247	
			RQS =	0.1544	
			Kg =	0.2547	Darcy
			STD =	0.0016	

Fluid Test: Air. Sparger # 5 for 20" pilot unit

Sparger C20 - 5
Experimental data

Q	DP	Pm	Q (TP)	Q (TP)	Ln Q (TP)	Ln DP	1/Pm	Kg	Kg lin
lpm	Pa	atm	lpm	[m^3/s]			1/atm	Darcy	Darcy
5	1890	1.01	5.41	9.01E-05	-9.314	7.544	0.99076	0.0752	0.0820
10	3780	1.02	10.71	1.79E-04	-8.630	8.238	0.98169	0.0787	0.0819
15	5670	1.03	15.93	2.65E-04	-8.234	8.643	0.97278	0.0805	0.0818
20	7560	1.04	21.04	3.51E-04	-7.955	8.931	0.96403	0.0816	0.0817
25	9451	1.05	26.07	4.35E-04	-7.741	9.154	0.95544	0.0823	0.0816
30	11341	1.06	31.01	5.17E-04	-7.568	9.336	0.94700	0.0827	0.0814
35	13231	1.07	35.86	5.98E-04	-7.422	9.490	0.93871	0.0829	0.0813
40	15121	1.07	40.63	6.77E-04	-7.298	9.624	0.93057	0.0830	0.0812
45	17011	1.08	45.31	7.55E-04	-7.189	9.742	0.92256	0.0830	0.0811
50	18901	1.09	49.92	8.32E-04	-7.092	9.847	0.91469	0.0829	0.0810
55	20791	1.10	54.44	9.07E-04	-7.005	9.942	0.90695	0.0828	0.0809
60	22681	1.11	58.90	9.82E-04	-6.926	10.029	0.89934	0.0826	0.0808
65	24571	1.12	63.27	1.05E-03	-6.855	10.109	0.89186	0.0824	0.0807
70	26461	1.13	67.58	1.13E-03	-6.789	10.183	0.88450	0.0822	0.0806
75	28352	1.14	71.81	1.20E-03	-6.728	10.252	0.87727	0.0819	0.0805
80	30242	1.15	75.98	1.27E-03	-6.672	10.317	0.87015	0.0816	0.0804
85	32132	1.16	80.08	1.33E-03	-6.619	10.378	0.86314	0.0813	0.0803
90	34022	1.17	84.11	1.40E-03	-6.570	10.435	0.85625	0.0809	0.0803
95	35912	1.18	88.08	1.47E-03	-6.524	10.489	0.84946	0.0806	0.0802
100	37802	1.19	91.99	1.53E-03	-6.480	10.540	0.84279	0.0802	0.0801
105	39692	1.20	95.83	1.60E-03	-6.440	10.589	0.83621	0.0799	0.0800
110	41582	1.21	99.62	1.66E-03	-6.401	10.635	0.82974	0.0795	0.0799
115	43472	1.21	103.35	1.72E-03	-6.364	10.680	0.82337	0.0791	0.0798
120	45362	1.22	107.02	1.78E-03	-6.329	10.722	0.81710	0.0787	0.0797
125	47253	1.23	110.63	1.84E-03	-6.296	10.763	0.81092	0.0783	0.0797
130	49143	1.24	114.20	1.90E-03	-6.264	10.802	0.80483	0.0780	0.0796
135	51033	1.25	117.70	1.96E-03	-6.234	10.840	0.79883	0.0776	0.0795
140	52923	1.26	121.16	2.02E-03	-6.205	10.877	0.79292	0.0772	0.0794
								Avg =	0.0806
								STD =	0.0008

Ln DP = Ln A + n Ln Q			Klinkenberg Effect		
n =	1.080		Kg = Kl + b Kl * (1/Pm)		
RSQ =	0.999		Y = A + B X		
A =	17.533		Kl (A) =	0.0690	Darcy
Kg =	7.95E-14	m^2	b Kl (B) =	0.0132	
Kg =	0.0806	Darcy	b =	0.1909	
			RQS =	0.1397	
			Kg =	0.0806	Darcy
			STD =	0.0008	

Fluid Test: Air. Sparger # 6 for 20" pilot unit

Sparger C20 - 6 L = 0.43 m

Experimental data

Q	DP	Pm	Q (TP)	Q (TP)	Ln Q (TP)	Ln DP	1/Pm	Kg	Kg lin
lpm	Pa	atm	lpm	[m^3/s]			1/atm	Darcy	Darcy
5	1673	1.01	5.41	9.02E-05	-9.313	7.422	0.99181	0.0134	0.0175
10	3392	1.02	10.73	1.79E-04	-8.629	8.129	0.98354	0.0152	0.0175
15	5159	1.03	15.97	2.66E-04	-8.232	8.548	0.97518	0.0163	0.0174
20	6972	1.03	21.10	3.52E-04	-7.953	8.850	0.96674	0.0170	0.0173
25	8832	1.04	26.15	4.36E-04	-7.738	9.086	0.95824	0.0174	0.0173
30	10738	1.05	31.10	5.18E-04	-7.565	9.282	0.94968	0.0177	0.0172
35	12692	1.06	35.95	5.99E-04	-7.420	9.449	0.94106	0.0179	0.0171
40	14692	1.07	40.71	6.78E-04	-7.296	9.595	0.93240	0.0180	0.0171
45	16739	1.08	45.37	7.56E-04	-7.187	9.726	0.92370	0.0180	0.0170
50	18833	1.09	49.93	8.32E-04	-7.091	9.843	0.91497	0.0180	0.0169
55	20974	1.10	54.40	9.07E-04	-7.006	9.951	0.90621	0.0180	0.0168
60	23162	1.11	58.77	9.79E-04	-6.928	10.050	0.89743	0.0179	0.0168
65	25396	1.13	63.04	1.05E-03	-6.858	10.142	0.88864	0.0178	0.0167
70	27677	1.14	67.22	1.12E-03	-6.794	10.228	0.87983	0.0177	0.0166
75	30005	1.15	71.30	1.19E-03	-6.735	10.309	0.87103	0.0175	0.0166
80	32380	1.16	75.29	1.25E-03	-6.681	10.385	0.86223	0.0173	0.0165
85	34802	1.17	79.18	1.32E-03	-6.630	10.457	0.85344	0.0172	0.0164
90	37270	1.18	82.97	1.38E-03	-6.584	10.526	0.84466	0.0170	0.0164
95	39786	1.20	86.67	1.44E-03	-6.540	10.591	0.83589	0.0168	0.0163
100	42348	1.21	90.28	1.50E-03	-6.499	10.654	0.82715	0.0166	0.0162
105	44957	1.22	93.79	1.56E-03	-6.461	10.713	0.81844	0.0164	0.0162
110	47612	1.23	97.22	1.62E-03	-6.425	10.771	0.80975	0.0161	0.0161
115	50315	1.25	100.55	1.68E-03	-6.391	10.826	0.80110	0.0159	0.0160
120	53065	1.26	103.80	1.73E-03	-6.360	10.879	0.79249	0.0157	0.0160
125	55861	1.28	106.95	1.78E-03	-6.330	10.931	0.78391	0.0155	0.0159
130	58704	1.29	110.02	1.83E-03	-6.301	10.980	0.77539	0.0152	0.0158
135	61593	1.30	113.00	1.88E-03	-6.275	11.028	0.76691	0.0150	0.0158
140	64530	1.32	115.90	1.93E-03	-6.249	11.075	0.75848	0.0148	0.0157
145	67513	1.33	118.71	1.98E-03	-6.225	11.120	0.75010	0.0145	0.0156
150	70544	1.35	121.44	2.02E-03	-6.203	11.164	0.74178	0.0143	0.0156
								Avg =	0.0165
								STD =	0.0006

Ln DP = Ln A + n Ln Q			Klinkenberg Effect		
n =	1.2245		Kg = Kl + b Kl * (1/Pm)		
RSQ =	0.9925		Y = A + B X		
A =	18.6173		Kl (A) =	0.00976	Darcy
Kg =	1.63E-14	m^2	b Kl (B) =	0.00782	
Kg =	0.01648	Darcy	b =	0.80158	
			RQS =	0.20528	
			Kg =	0.01654	Darcy
			STD =	0.000598	

Appendix B: Paper Pulp Viscosity

Measuremets of viscosity with Moddy-Colebrook and Darcy Equations for turbulent Flow uisng a galvanized loop.

Results for 1/2" galvanized pipe (D_{int} = 0.01480 m)
Fluid Test: Water

T =	23.5	°C		
Density =	997.22	kg/m^3		
Viscosity =	0.9216	cpoise		
Q [L/min]	DP [cm H2O]	Re	Friction Factor	E/D
13.90	62.91	21557	0.0301	0.00240
16.70	88.47	25899	0.0294	0.00238
22.00	148.60	34118	0.0284	0.00239
27.60	229.00	42803	0.0278	0.00242
34.40	350.20	53349	0.0274	0.00248
37.10	402.90	57536	0.0271	0.00241
39.90	465.00	61878	0.0273	0.00257
43.30	543.00	67151	0.0268	0.00243
47.10	643.00	73044	0.0270	0.00257
49.30	702.70	76456	0.0268	0.00251
51.20	751.60	79403	0.0265	0.00244
			Avg =	0.00245

T =	35.5	°C		
Density =	993.73	kg/m^3		
Viscosity =	0.7123	cpoise		
Q [L/min]	DP [cm H2O]	Re	Friction Factor	E/D
8.10	22.30	16197	0.0316	0.00247
11.50	42.78	22996	0.0301	0.00251
14.10	62.70	28195	0.0293	0.00253
19.80	118.96	39593	0.0282	0.00251
25.20	187.20	50391	0.0274	0.00242
30.90	277.00	61789	0.0270	0.00243
34.40	341.20	68787	0.0268	0.00244
37.90	413.78	75786	0.0268	0.00251
42.70	521.40	85384	0.0266	0.00251
46.10	603.20	92183	0.0264	0.00247
48.10	655.40	96182	0.0263	0.00248
51.10	736.80	102181	0.0262	0.00247
			Avg =	0.00248

T =	47.2	°C		
Density =	989.27	kg/m^3		
Viscosity =	0.5738	cpoise		
Q [L/min]	DP [cm H2O]	Re	Friction Factor	E/D
5.80	11.67	14332	0.0324	0.00257
9.80	30.74	24217	0.0299	0.00253
14.20	61.74	35090	0.0286	0.00252
17.80	94.80	43986	0.0279	0.00251
22.70	150.90	56094	0.0273	0.00251
26.40	200.54	65237	0.0269	0.00243
30.50	264.78	75369	0.0266	0.00242
36.10	369.89	89207	0.0265	0.00250
40.90	470.93	101068	0.0263	0.00249
46.30	599.10	114412	0.0261	0.00247
48.20	648.74	119107	0.0261	0.00248
51.80	747.12	128003	0.0260	0.00249
			Avg =	0.00249

Fluid Test: Polyacrylamide 0.03% wt

T =	26.5	°C		
Density =	996.46	kg/m^3		
E/D =	0.00248			
Q [L/min]	DP [cm H2O]	Friction Factor	Re	Viscosity [cpoise]
16.60	91.40	0.0308	19194	1.2351
19.60	124.00	0.0299	23234	1.2048
24.80	194.10	0.0293	27636	1.2816
27.50	236.90	0.0290	29371	1.3372
31.90	310.56	0.0283	37067	1.2291
35.80	386.14	0.0279	42123	1.2138
39.30	459.25	0.0276	48577	1.1554
42.60	540.30	0.0276	47884	1.2706
45.60	615.00	0.0274	51678	1.2602
48.80	696.10	0.0271	59830	1.1649
51.80	789.00	0.0273	55456	1.3340

T =	35.5	°C		
Density =	993.73	kg/m^3		
E/D =	0.0024/8			
Q [L/min]	DP [cm H2O]	Friction Factor	Re	Viscosity [cpoise]
16.60	87.20	0.0294	26459	0.8936
19.80	122.89	0.0291	28554	0.9876
24.90	189.60	0.0284	35439	1.0007
27.70	229.10	0.0278	45007	0.8766
31.50	292.30	0.0274	52455	0.8553
35.50	366.64	0.0270	61409	0.8234
39.50	451.20	0.0269	66690	0.8436
43.00	532.00	0.0268	71787	0.8531
45.60	597.40	0.0267	73396	0.8849
48.80	684.90	0.0267	72252	0.9620
52.00	769.30	0.0265	85910	0.8621

T =	47.2	°C		
Density =	989.27	kg/m^3		
E/D =	0.00248			
Q [L/min]	DP [cm H2O]	Friction Factor	Re	Viscosity [cpoise]
16.60	85.20	0.0289	30855	0.7628
18.80	107.40	0.0284	36053	0.7394
23.30	161.10	0.0277	45834	0.7208
26.20	202.10	0.0275	50080	0.7418
31.90	294.10	0.0270	63179	0.7159
35.40	361.20	0.0269	65577	0.7654
39.90	455.20	0.0267	73720	0.7674
42.20	504.84	0.0265	84598	0.7073
45.30	582.40	0.0265	82992	0.7739
48.50	662.30	0.0263	95439	0.7205
51.90	758.45	0.0263	95353	0.7717

Fluid Test: Polyacrylamine 0.3%

T =	26.5	°C		
Density =	996.46	kg/m^3		
E/D =	0.00248			
Q [L/min]	DP [cm H2O]	Friction Factor	Re	Viscosity [cpoise]
14.70	89.40	0.0384	6015	3.4905
18.10	127.90	0.0362	7825	3.3037
21.50	174.30	0.0350	9264	3.3146
24.20	212.10	0.0336	11420	3.0266
26.60	256.80	0.0337	11290	3.3649
32.50	369.90	0.0325	13780	3.3682
35.80	439.52	0.0318	15615	3.2743
39.60	528.40	0.0312	17438	3.2433
44.90	671.40	0.0309	18826	3.4062
47.50	745.30	0.0306	19893	3.4102
51.50	863.80	0.0302	21966	3.3483

T =	35.5	°C		
Density =	993.73	kg/m^3		
E/D =	0.00248			
Q [L/min]	DP [cm H2O]	Friction Factor	Re	Viscosity [cpoise]
19.10	133.80	0.0341	10525	2.5847
23.20	190.45	0.0329	12787	2.5841
27.40	259.41	0.0321	14675	2.6594
31.20	328.45	0.0314	16986	2.6160
35.30	412.32	0.0308	19300	2.6050
39.10	498.10	0.0303	21482	2.5924
42.80	590.40	0.0300	23235	2.6236
44.20	625.30	0.0298	24475	2.5721
47.80	726.10	0.0295	25860	2.6326
51.41	829.40	0.0292	28614	2.5589
54.30	918.60	0.0290	30407	2.5434

T =	47.2	°C		
Density =	989.27	kg/m^3		
E/D =	0.00248			
Q [L/min]	DP [cm H2O]	Friction Factor	Re	Viscosity [cpoise]
16.70	103.40	0.0346	9725	2.4347
19.50	136.80	0.0336	11384	2.4288
24.90	215.60	0.0325	13766	2.5647
28.50	273.50	0.0314	16726	2.4160
32.60	349.09	0.0307	19674	2.3494
36.00	415.90	0.0300	23204	2.1998
39.80	507.60	0.0299	23454	2.4060
42.60	584.32	0.0301	22643	2.6675
46.00	665.80	0.0294	26995	2.4161
49.60	764.00	0.0290	30077	2.3382
53.00	869.00	0.0289	31080	2.4178

Fluid Test: Grey Water

T =	26.5	°C		
Density =	996.46	kg/m^3		
E/D =	0.00248			
Q [L/min]	DP [cm H2O]	Friction Factor	Re	Viscosity [cpoise]
17.90	113.40	0.0328	12970	1.9711
19.90	137.10	0.0321	14745	1.9275
23.00	178.80	0.0313	17097	1.9213
25.80	221.60	0.0309	18872	1.9525
29.60	284.10	0.0301	22678	1.8641
33.20	351.50	0.0296	25714	1.8440
37.70	449.90	0.0293	27266	1.9747
41.00	525.30	0.0290	30336	1.9303
45.70	642.20	0.0285	35013	1.8641
48.41	721.30	0.0285	34710	1.9919
50.20	772.30	0.0284	36133	1.9842

T =	35.5	°C		
Density =	993.73	kg/m^3		
E/D =	0.00248			
Q [L/min]	DP [cm H2O]	Friction Factor	Re	Viscosity [cpoise]
17.10	108.90	0.0346	9726	2.5041
20.20	146.10	0.0333	11972	2.4031
22.40	176.80	0.0328	13094	2.4365
24.20	202.20	0.0321	14742	2.3380
27.10	251.60	0.0319	15451	2.4981
29.10	284.10	0.0312	17618	2.3525
32.00	339.60	0.0308	19009	2.3976
35.00	404.80	0.0307	19475	2.5596
37.90	470.30	0.0304	20751	2.6013
43.00	600.20	0.0302	22056	2.7767
45.80	671.30	0.0298	24500	2.6625
47.50	721.00	0.0297	24776	2.7306
49.70	784.30	0.0295	26034	2.7190

T =	47.2	°C		
Density =	989.27	kg/m^3		
E/D =	0.00248			
Q [L/min]	DP [cm H2O]	Friction Factor	Re	Viscosity [cpoise]
17.10	113.90	0.0364	7643	3.1722
19.80	148.20	0.0353	8826	3.1809
23.10	195.98	0.0343	10208	3.2086
27.80	274.20	0.0331	12283	3.2091
31.00	334.50	0.0325	13689	3.2110
34.20	399.26	0.0319	15368	3.1554
36.70	455.30	0.0316	16320	3.1885
38.30	492.30	0.0313	17080	3.1794
41.50	571.20	0.0310	18442	3.1906
43.60	625.40	0.0307	19465	3.1759
46.20	697.10	0.0305	20465	3.2009
47.70	738.56	0.0303	21363	3.1659
49.70	798.60	0.0302	21980	3.2061

Fluid Test: Paper Pulp 0.017% Wt.

T =	26.5	°C		
Density =	996.46	kg/m^3		
E/D =	0.00248			
Q [L/min]	DP [cm H2O]	Friction Factor	Re	Viscosity [cpoise]
16.10	127.30	0.0455	3040	7.5636
18.00	152.78	0.0437	3538	7.2668
20.70	197.63	0.0428	3851	7.6770
22.10	221.50	0.0420	4113	7.6738
24.50	264.80	0.0409	4593	7.6181
27.10	311.30	0.0393	5419	7.1422
32.10	415.90	0.0374	6710	6.8320
36.80	532.60	0.0365	7559	6.9530
39.20	589.10	0.0355	8537	6.5578
42.80	696.50	0.0353	8889	6.8765
44.10	732.80	0.0349	9297	6.7743
46.60	818.60	0.0350	9277	7.1742
48.60	858.90	0.0337	11174	6.2119

T =	35.5	°C		
Density =	993.73	kg/m^3		
E/D =	0.00248			
Q [L/min]	DP [cm H2O]	Friction Factor	Re	Viscosity [cpoise]
14.50	110.30	0.0488	2379	8.6798
16.60	137.50	0.0464	2841	8.3229
18.10	156.80	0.0445	3310	7.7876
20.60	198.30	0.0434	3624	8.0968
23.00	239.00	0.0420	4130	7.9317
26.00	298.10	0.0410	4550	8.1395
29.20	365.10	0.0398	5133	8.1018
32.70	448.60	0.0390	5596	8.3223
35.70	521.80	0.0381	6221	8.1734
38.40	592.50	0.0374	6763	8.0864
42.00	693.80	0.0366	7460	8.0184
44.90	780.60	0.0360	8031	7.9626
46.60	831.90	0.0356	8454	7.8508

T =	47.2	°C		
Density =	989.27	kg/m^3		
E/D =	0.00248			
Q [L/min]	DP [cm H2O]	Friction Factor	Re	Viscosity [cpoise]
17.10	150.30	0.0480	2515	9.6388
19.10	181.70	0.0465	2814	9.6252
21.70	227.60	0.0451	3139	9.8022
24.80	286.40	0.0435	3610	9.7410
27.80	348.20	0.0421	4102	9.6091
30.00	396.80	0.0412	4471	9.5131
32.40	459.10	0.0408	4620	9.9439
35.50	536.70	0.0398	5154	9.7663
37.60	595.30	0.0393	5405	9.8634
39.10	633.10	0.0387	5804	9.5513
41.20	697.90	0.0384	5988	9.7556
43.90	776.50	0.0376	6547	9.5070
45.90	843.10	0.0374	6751	9.6405

Fluid Test: Paper Pulp 0.91% Wt.

T =	26.5	°C		
Density =	996.46	kg/m^3		
E/D =	0.00248			
Q [L/min]	**DP [cm H2O]**	**Friction Factor**	**Re**	**Viscosity [cpoise]**
15.10	84.35	0.0343	10208	2.1126
18.70	123.40	0.0327	13188	2.0251
21.70	159.40	0.0314	16933	1.8303
24.80	197.40	0.0298	24472	1.4473
26.90	225.60	0.0289	30944	1.2415
29.80	269.87	0.0282	39206	1.0855
32.90	321.00	0.0275	51053	0.9204
36.40	385.60	0.0270	64989	0.7999
39.30	449.60	0.0270	64766	0.8666
42.90	528.00	0.0266	80683	0.7594
45.20	581.90	0.0264	91399	0.7063
47.70	651.20	0.0265	83972	0.8113
51.20	739.90	0.0262	108927	0.6713

T =	**35.5**	**°C**		
Density =	**993.73**	**kg/m^3**		
E/D =	**0.00248**			
Q [L/min]	**DP [cm H2O]**	**Friction Factor**	**Re**	**Viscosity [cpoise]**
19.50	145.90	0.0357	8390	3.3104
22.20	179.80	0.0339	10823	2.9215
24.00	204.70	0.0330	12479	2.7393
26.30	241.30	0.0324	13869	2.7008
28.50	276.70	0.0317	15996	2.5376
31.40	324.50	0.0306	20017	2.2342
34.30	378.60	0.0299	23501	2.0787
37.10	436.20	0.0295	26429	1.9993
40.10	499.54	0.0289	31167	1.8325
42.80	550.40	0.0279	42812	1.4239
44.70	601.70	0.0280	41822	1.5223
46.80	650.40	0.0276	48694	1.3689
48.50	697.30	0.0276	49675	1.3906

T =	**47.2**	**°C**		
Density =	**989.27**	**kg/m^3**		
E/D =	**0.00248**			
Q [L/min]	**DP [cm H2O]**	**Friction Factor**	**Re**	**Viscosity [cpoise]**
18.80	140.32	0.0371	6998	3.8088
21.20	172.60	0.0359	8175	3.6769
23.90	217.40	0.0355	8538	3.9691
26.00	246.30	0.0340	10642	3.4641
28.20	281.20	0.0330	12515	3.1949
30.50	324.40	0.0326	13542	3.1934
32.30	357.70	0.0320	14964	3.0604
34.50	400.70	0.0314	16747	2.9210
36.60	449.80	0.0314	17024	3.0484
39.00	495.10	0.0304	20946	2.6400
42.50	573.30	0.0296	25213	2.3900
45.40	641.30	0.0291	29601	2.1746
46.40	672.20	0.0292	28752	2.2881

Results for 3/4" galvanized pipe (D_{int} = 0.0210 m)
Fluid Test: Water

T =	23.5	°C		
Density =	996.46	kg/m^3		
Viscosity =	0.9216	cpoise		
Q [L/min]	DP [cm H2O]	Re	Friction Factor	E/D
13.90	12.87	15181	0.0354	0.00490
16.70	18.15	18239	0.0346	0.00485
22.00	30.61	24027	0.0336	0.00484
27.60	47.35	30143	0.0330	0.00488
34.40	72.10	37569	0.0324	0.00480
37.10	83.51	40518	0.0323	0.00481
39.90	96.32	43576	0.0322	0.00484
43.30	112.60	47289	0.0319	0.00479
47.10	132.68	51439	0.0318	0.00480
49.30	145.20	53842	0.0318	0.00482
51.20	156.10	55917	0.0317	0.00480
			Avg =	0.00483

T =	35.5	°C		
Density =	993.73	kg/m^3		
Viscosity =	0.7123	cpoise		
Q [L/min]	DP [cm H2O]	Re	Friction Factor	E/D
11.50	8.72	16207	0.0352	0.00491
14.10	12.79	19871	0.0343	0.00486
19.80	24.46	27903	0.0333	0.00489
25.20	38.85	35513	0.0326	0.00486
30.90	57.61	43546	0.0322	0.00484
34.40	70.92	48479	0.0320	0.00483
37.90	85.53	53411	0.0317	0.00480
42.70	107.96	60176	0.0316	0.00481
46.10	125.40	64967	0.0315	0.00481
48.10	136.20	67786	0.0314	0.00480
51.10	153.40	72013	0.0313	0.00480
			Avg =	0.00484

T =	47.2	°C		
Density =	989.27	kg/m^3		
Viscosity =	0.5738	cpoise		
Q [L/min]	DP [cm H2O]	Re	Friction Factor	E/D
9.80	6.32	17067	0.0352	0.00513
14.15	12.71	24643	0.0340	0.00514
17.75	19.60	30912	0.0333	0.00510
22.60	31.29	39359	0.0328	0.00512
26.27	41.86	45750	0.0325	0.00510
30.35	55.45	52856	0.0322	0.00510
36.04	77.50	62765	0.0320	0.00508
40.90	99.50	71229	0.0319	0.00511
45.99	125.21	80094	0.0317	0.00510
48.06	136.60	83699	0.0317	0.00511
51.59	157.00	89846	0.0316	0.00511
			Avg =	0.00511

Fluid Test: Polyacrylamine 0.03 %Wt.

T =	26.5	°C		
Density =	996.46	kg/m^3		
E/D =	0.00493			
Q [L/min]	DP [cm H2O]	Friction Factor	Re	Viscosity [cpoise]
16.60	18.36	0.0354	15256	1.0952
19.60	25.13	0.0348	17871	1.1039
24.80	39.08	0.0338	23835	1.0473
27.50	47.68	0.0335	26015	1.0640
31.90	63.35	0.0331	30379	1.0569
35.80	79.11	0.0328	34080	1.0573
39.30	94.66	0.0326	37814	1.0461
42.40	109.65	0.0324	40800	1.0460
45.60	126.02	0.0322	45421	1.0105
48.80	143.76	0.0321	48776	1.0070
51.80	161.34	0.0320	52616	0.9909

T =	35.5	°C		
Density =	993.73	kg/m^3		
E/D =	0.00493			
Q [L/min]	DP [cm H2O]	Friction Factor	Re	Viscosity [cpoise]
16.60	17.80	0.0344	19589	0.8506
19.80	24.90	0.0339	23243	0.8551
24.90	38.45	0.0331	30814	0.8111
27.70	47.28	0.0329	33594	0.8277
31.50	60.48	0.0325	39464	0.8012
35.50	75.98	0.0321	47477	0.7506
39.50	93.60	0.0320	52159	0.7601
43.00	110.21	0.0318	59616	0.7240
45.60	123.81	0.0317	61025	0.7501
48.80	141.20	0.0316	67324	0.7276
52.00	159.90	0.0315	71942	0.7255

T =	47.2	°C		
Density =	989.27	kg/m^3		
E/D =	0.00493			
Q [L/min]	DP [cm H2O]	Friction Factor	Re	Viscosity [cpoise]
16.60	17.32	0.0337	24810	0.6686
18.80	21.90	0.0332	29403	0.6389
23.30	33.12	0.0327	36349	0.6405
26.20	41.60	0.0325	40260	0.6503
31.90	60.69	0.0319	53592	0.5948
35.40	74.50	0.0318	57240	0.6180
39.90	93.80	0.0316	70404	0.5663
42.20	104.80	0.0315	72595	0.5809
45.30	120.30	0.0314	80550	0.5620
48.50	137.40	0.0313	89652	0.5406
51.90	156.96	0.0312	96905	0.5352

Fluid Test: Polyacrylamine 0.3 %wt.

T =	26.5	°C		
Density =	996.46	kg/m^3		
E/D =	0.00493			
Q [L/min]	DP [cm H2O]	Friction Factor	Re	Viscosity [cpoise]
18.10	25.80	0.0419	5402	3.3723
21.50	34.54	0.0397	7116	3.0410
24.20	43.46	0.0395	7396	3.2934
26.60	51.21	0.0385	8561	3.1274
32.50	74.50	0.0375	10068	3.2490
35.80	88.57	0.0367	11564	3.1160
39.60	106.58	0.0361	13052	3.0537
44.90	135.21	0.0357	14465	3.1244
47.50	150.31	0.0354	15272	3.1306
51.50	174.18	0.0349	17254	3.0042

T =	35.5	°C		
Density =	993.73	kg/m^3		
E/D =	0.00493			
Q	DP	Friction	Re	Viscosity
[L/min]	[cm H2O]	Factor		[cpoise]
19.10	26.87	0.0393	7599	2.5230
23.20	38.10	0.0377	9663	2.4099
27.40	51.83	0.0368	11425	2.4074
31.20	65.85	0.0361	13246	2.3644
35.30	83.23	0.0356	14623	2.4231
39.10	100.47	0.0350	16742	2.3442
42.80	119.43	0.0348	17968	2.3909
44.20	126.75	0.0346	18795	2.3606
47.80	146.85	0.0343	20572	2.3323
51.41	168.54	0.0340	22279	2.3162
54.30	187.30	0.0339	23203	2.3490

T =	47.2	°C		
Density =	989.27	kg/m^3		
E/D =	0.00493			
Q	DP	Friction	Re	Viscosity
[L/min]	[cm H2O]	Factor		[cpoise]
16.70	20.62	0.0396	7249	2.3019
19.50	27.31	0.0385	8584	2.2700
24.90	42.78	0.0370	11116	2.2384
28.50	54.75	0.0361	13153	2.1651
32.60	70.50	0.0355	14904	2.1858
36.00	84.60	0.0350	17070	2.1073
39.80	102.50	0.0347	18473	2.1529
42.60	116.69	0.0344	19604	2.1714
46.00	134.57	0.0341	21870	2.1018
49.60	155.90	0.0339	22699	2.1835
53.00	176.89	0.0337	24294	2.1800

Fluid Test: Grey Water

T =	26.5	°C		
Density =	996.46	kg/m^3		
E/D =	0.00493			
Q [L/min]	DP [cm H2O]	Friction Factor	Re	Viscosity [cpoise]
17.90	25.50	0.0423	5130	3.5121
18.80	27.75	0.0417	5484	3.4503
19.90	30.75	0.0413	5799	3.4537
23.00	40.05	0.0403	6623	3.4956
25.80	49.22	0.0393	7548	3.4404
29.60	63.45	0.0385	8530	3.4926
33.20	78.15	0.0377	9734	3.4331
37.70	98.90	0.0370	11024	3.4422
41.00	115.20	0.0364	12277	3.3613
45.70	141.50	0.0360	13366	3.4415
48.41	157.41	0.0357	14295	3.4086

T =	35.5	°C		
Density =	993.73	kg/m^3		
E/D =	0.00493			
Q	DP	Friction	Re	Viscosity
[L/min]	[cm H2O]	Factor		[cpoise]
17.10	24.80	0.0452	3781	4.5398
20.20	33.00	0.0431	4689	4.3246
22.40	39.75	0.0422	5176	4.3438
24.20	45.15	0.0411	5932	4.0947
27.10	55.95	0.0406	6312	4.3095
29.10	63.75	0.0401	6727	4.3419
32.00	76.20	0.0397	7171	4.4793
35.00	89.25	0.0388	8095	4.3401
37.90	103.20	0.0383	8804	4.3210
43.00	130.95	0.0378	9632	4.4810
45.80	145.80	0.0371	10902	4.2169
47.50	156.75	0.0370	10937	4.3593
49.70	169.28	0.0365	12034	4.1454

T =	47.2	°C		
Density =	989.27	kg/m^3		
E/D =	0.00493			
Q	**DP**	**Friction**	**Re**	**Viscosity**
[L/min]	**[cm H2O]**	**Factor**		**[cpoise]**
17.10	25.78	0.0472	3148	5.4273
19.80	33.33	0.0455	3669	5.3922
23.10	43.75	0.0439	4310	5.3559
27.80	61.20	0.0424	5074	5.4744
31.00	74.15	0.0413	5773	5.3662
34.20	88.61	0.0406	6349	5.3827
36.70	100.40	0.0399	6928	5.2933
38.30	108.45	0.0396	7252	5.2777
41.50	125.10	0.0389	8025	5.1677
43.60	138.11	0.0389	8015	5.4359
46.20	152.70	0.0383	8791	5.2516
47.70	162.00	0.0381	9054	5.2645
49.70	175.10	0.0380	9306	5.3369

Fluid Test: Paper Pulp 0.017 %wt

T =	26.5	°C		
Density =	996.46	kg/m^3		
E/D =	0.00493			
Q	DP	Friction	Re	Viscosity
[L/min]	[cm H2O]	Factor		[cpoise]
16.10	33.50	0.0687	867	18.6933
18.00	39.70	0.0651	1018	17.7992
20.70	49.50	0.0614	1224	17.0229
22.10	55.12	0.0600	1320	16.8562
24.50	65.40	0.0579	1482	16.6397
27.10	76.80	0.0556	1704	16.0073
32.10	101.40	0.0523	2116	15.2727
36.80	125.61	0.0493	2645	14.0019
39.20	140.20	0.0485	2823	13.9786
42.80	162.45	0.0472	3167	13.6047
44.10	171.23	0.0468	3262	13.6062
46.60	186.43	0.0456	3630	12.9225
48.60	200.56	0.0451	3807	12.8500

T =	35.5	°C		
Density =	993.73	kg/m^3		
E/D =	0.00493			
Q	DP	Friction	Re	Viscosity
[L/min]	[cm H2O]	Factor		[cpoise]
16.60	37.00	0.0716	769	21.6652
18.10	41.90	0.0682	887	20.4844
20.60	51.50	0.0647	1040	19.8904
23.00	61.00	0.0615	1220	18.9184
26.00	75.30	0.0594	1365	19.1208
29.20	90.30	0.0565	1616	18.1364
32.70	109.70	0.0547	1804	18.1921
35.70	126.30	0.0528	2042	17.5514
38.40	141.10	0.0510	2323	16.5902
42.00	163.20	0.0493	2643	15.9489
44.90	182.50	0.0483	2881	15.6462
46.60	193.40	0.0475	3077	15.2027

T =	47.2	°C		
Density =	989.27	kg/m^3		
E/D =	0.00493			
Q	DP	Friction	Re	Viscosity
[L/min]	[cm H2O]	Factor		[cpoise]
17.10	40.70	0.0745	685	24.9344
19.10	48.30	0.0709	791	24.1388
21.70	59.50	0.0677	907	23.8996
24.80	73.10	0.0637	1094	22.6602
27.80	87.40	0.0606	1280	21.6956
30.00	98.60	0.0587	1420	21.1042
32.40	113.20	0.0578	1497	21.6213
35.50	131.20	0.0558	1688	21.0176
37.60	144.20	0.0546	1813	20.7287
39.10	153.70	0.0538	1908	20.4819
41.20	167.00	0.0527	2062	19.9645
43.90	185.10	0.0514	2253	19.4705
45.90	200.00	0.0508	2354	19.4854

Fluid Test: Paper Pulp 0.91 %wt.

T =	26.5	°C		
Density =	996.46	kg/m^3		
E/D =	0.00493			
Q	DP	Friction	Re	Viscosity
[L/min]	[cm H2O]	Factor		[cpoise]
15.10	18.69	0.0436	4460	3.4076
18.70	27.00	0.0411	5971	3.1525
21.70	34.87	0.0394	7486	2.9177
24.80	42.94	0.0371	10776	2.3163
26.90	49.51	0.0364	12422	2.1797
29.80	58.96	0.0353	15708	1.9095
32.90	70.40	0.0346	18842	1.7575
36.40	84.65	0.0340	22482	1.6296
39.30	96.87	0.0333	27673	1.4294
42.90	112.54	0.0325	39167	1.1025
45.20	123.30	0.0321	49011	0.9283
47.70	135.60	0.0317	63623	0.7546
51.20	153.70	0.0312	100498	0.5128

T =	35.5	°C		
Density =	993.73	kg/m^3		
E/D =	0.00493			
Q	DP	Friction	Re	Viscosity
[L/min]	[cm H2O]	Factor		[cpoise]
19.50	30.00	0.0421	5282	3.7058
22.20	37.84	0.0409	6060	3.6774
24.00	43.54	0.0403	6581	3.6608
26.30	50.94	0.0393	7604	3.4717
28.50	58.96	0.0387	8274	3.4576
31.40	69.54	0.0376	9892	3.1863
34.30	80.43	0.0364	12249	2.8108
37.10	92.58	0.0359	13838	2.6911
40.10	106.98	0.0355	15098	2.6659
42.80	118.90	0.0346	18718	2.2952
44.70	128.12	0.0342	21058	2.1307
46.80	138.00	0.0336	25396	1.8497
48.50	147.54	0.0334	26762	1.8191

T =	47.2	°C		
Density =	989.27	kg/m^3		
E/D =	0.00493			
Q	DP	Friction	Re	Viscosity
[L/min]	[cm H2O]	Factor		[cpoise]
18.80	29.30	0.0444	4100	4.5822
21.20	35.26	0.0420	5311	3.9887
23.90	43.78	0.0410	5974	3.9975
26.00	50.60	0.0401	6773	3.8361
28.20	57.67	0.0388	8102	3.4780
30.50	66.78	0.0384	8609	3.5403
32.30	74.00	0.0380	9272	3.4812
34.50	83.47	0.0376	9971	3.4576
36.60	92.30	0.0369	11223	3.2588
39.00	103.20	0.0363	12525	3.1115
42.50	120.20	0.0356	14529	2.9229
45.40	134.78	0.0350	16815	2.6980
46.40	139.45	0.0347	18308	2.5326

Results for bubble size measurements using a bubble viewer

Sparger # 3 (5 μm) for 4" lab column.

Jg = 0.51 cm/s Eg = 5.1 %		JL = 1.25 cm/s Paper Pulp = 0.97 % wt		
Measurement Class		Mid point	Relative Freq.	Frequency
0.00	0.16	0.08	0.00	0
0.17	0.34	0.26	0.02	5
0.35	0.51	0.43	0.04	11
0.52	0.69	0.60	0.29	86
0.70	0.86	0.78	0.27	80
0.87	1.03	0.95	0.13	38
1.04	1.21	1.13	0.09	28
1.22	1.38	1.30	0.06	17
1.39	1.56	1.47	0.05	16
1.57	1.73	1.65	0.01	4
1.74	1.90	1.82	0.05	14
1.91	2.08	2.00	0.00	5
		Sum =	1.00	304
	d suater =	1.155		

Jg = 1.03 cm/s Eg = 10.47 %		JL = 1.25 cm/s Paper Pulp = 0.97 % wt		
Measurement Class		Mid point	Relative Freq.	Frequency
0.00	0.19	0.09	0.00	0
0.20	0.39	0.29	0.01	4
0.40	0.59	0.49	0.03	10
0.60	0.79	0.69	0.08	25
0.80	0.99	0.89	0.25	75
1.00	1.18	1.09	0.23	70
1.19	1.38	1.29	0.17	50
1.39	1.58	1.49	0.03	8
1.59	1.78	1.69	0.05	16
1.79	1.98	1.89	0.13	39
1.99	2.18	2.08	0.00	1
2.19	2.38	2.28	0.00	1
		Sum =	1.00	300
	d suater =	1.414		

Jg = 1.51 cm/s Eg = 16.3 %		JL = 1.25 cm/s Paper Pulp = 0.97 % wt		
Measurement Class		**Mid point**	**Measurement Class**	**Mid point**
0.00	0.18	0.09	0.00	0
0.19	0.37	0.28	0.04	13
0.38	0.56	0.47	0.06	17
0.57	0.75	0.66	0.05	14
0.76	0.94	0.85	0.11	33
0.95	1.13	1.04	0.11	32
1.14	1.32	1.23	0.06	25
1.33	1.51	1.42	0.17	37
1.52	1.70	1.61	0.11	41
1.71	1.89	1.80	0.09	26
1.90	2.08	1.99	0.06	19
2.09	2.27	2.18	0.08	22
2.28	2.46	2.37	0.06	15
2.47	2.65	2.56	0.00	4
		Sum =	**1.00**	**298**
	d suater =	**1.73**		

APPENDIX C: Gas Dispersion on Paper Pulp

4 " lab column **Sparger # 1 (0.5 μm)** **% Consistency: 1.3 %**

Jg cm/s	% Eg	db mm	Sb 1/s
0.00	0.00	0.000	0.00
0.50	3.60	0.080	37.86
1.01	6.70	0.132	45.77
1.51	10.50	0.155	58.31
2.00	14.25	0.170	70.70
2.33	17.00	0.171	81.85

4 " lab column **Sparger # 1 (0.5 μm)** **% Consistency: 1.1 %**

Jg (cm/s)	% Eg	db mm	Sb 1/s
0.00	0.00	0.000	0.00
0.50	4.22	0.075	40.39
1.01	9.26	0.120	50.35
1.51	14.25	0.137	65.97
2.00	18.31	0.145	82.89
2.33	22.14	0.149	93.94

4 " lab column **Sparger # 1 (0.5 μm)** **% Consistency: 0.9 %**

Jg cm/s	% Eg	db mm	Sb 1/s
0.00	0.00	0.000	0.00
0.50	5.20	0.074	40.93
1.01	10.29	0.102	59.23
1.51	16.10	0.118	76.60
2.00	19.89	0.124	96.93
2.51	23.78	0.128	117.57

4 " lab column **Sparger # 1 (0.5 μm)** **% Consistency: 0.7 %**

Jg cm/s	% Eg	db mm	Sb 1/s
0.00	0.00	0.000	0.00
0.50	6.25	0.072	42.07
1.01	12.80	0.098	61.65
1.51	17.64	0.110	82.17
2.00	23.80	0.117	102.73
2.51	27.30	0.118	127.54

4 " lab column **Sparger # 1 (0.5 μm)** **% Consistency: 0.5 %**

Jg cm/s	% Eg	db mm	Sb 1/s
0.00	0.00	0.000	0.00
0.50	7.50	0.060	50.48
1.01	15.40	0.070	86.56
1.51	22.56	0.076	119.58
2.00	29.47	0.084	142.86
2.51	33.31	0.087	172.98

4 " lab column **Sparger # 6 (40 μm)** **% Consistency: 1.3 %**

Jg (cm/s)	% Eg	db (mm)	Sb (1/s)
0.00	0.00	0.000	0.00
0.51	1.75	0.138	22.00
1.01	3.16	0.250	24.28
1.52	4.80	0.320	28.44
2.02	6.10	0.350	34.65
2.54	7.24	0.378	40.26

4 " lab column **Sparger # 6 (40 μm)** **% Consistency: 1.1 %**

Jg (cm/s)	% Eg	db (mm)	Sb (1/s)
0.00	0.00	0.000	0.00
0.51	2.10	0.125	24.29
1.01	4.50	0.190	31.94
1.52	6.89	0.220	41.36
2.02	8.95	0.242	50.16
2.54	11.50	0.266	57.11

4 " lab column **Sparger # 6 (40 μm)** **% Consistency: 0.9 %**

Jg (cm/s)	% Eg	db (mm)	Sb (1/s)
0.00	0.00	0.000	0.00
0.51	1.96	0.130	23.35
1.01	4.01	0.238	25.50
1.52	6.10	0.280	32.50
2.02	8.10	0.300	40.42
2.54	9.98	0.320	47.56

4 " lab column **Sparger # 6 (40 μm)** **% Consistency: 0.7 %**

Jg (cm/s)	% Eg	db (mm)	Sb (1/s)
0.00	0.00	0.000	0.00
0.51	2.35	0.120	25.30
1.01	5.42	0.160	37.93
1.52	8.30	0.190	47.89
2.02	10.67	0.210	57.75
2.54	13.47	0.230	66.17

4 " lab column **Sparger # 6 (40 μm)** **Consistency: 0.5 %**

Jg (cm/s)	% Eg	db (mm)	Sb (1/s)
0.00	0.00	0.000	0.00
0.51	3.14	0.098	30.98
1.01	6.90	0.110	55.17
1.52	10.32	0.130	70.00
2.02	13.20	0.140	86.62
2.54	16.50	0.148	102.83

APPENDIX D: Mixing

Vessel dispersion number obtained at various conditions.

4 " lab column

Lc (cm)	Jl (cm/s)	Jg (cm/s)	% Eg	τ* (min)	τ** (min)	N_d	KCl, (gr-min/l)	
							in	out
243	1.12	1.10	14.10	4.10	3.49	0.1349	3.85	3.01
243	0.98	1.49	21.52	2 40	3.19	0.1590	3.85	3.41
243	0.99	2.14	27.24	2.08	2.94	0.1853	3.85	3.66
243	2.20	1.11	15.36	1.32	1.67	0.0756	3.50	3.47
243	2.14	1.48	23.85	1.14	1.50	0.1013	3.50	3.44
243	1.98	2.14	30.80	1.00	1.36	0.1146	3.50	3.46
163	1.02	0.48	2.45	2.40	2.58	0.1342	6.00	5.92
163	1.11	1.10	4.70	2.20	2.60	0.1819	6.00	6.00
163	1.14	1.48	7.10	2.04	2.46	0.2187	6.00	5.84
163	1.48	0.48	3.18	1.75	1.75	0.0975	4.79	4.67
163	1.54	0.97	6.23	1.52	1.70	0.1423	5.48	5.05
163	1.53	1.48	8.69	1.43	1.65	0.1829	5.48	5.51
110	0.98	0.48	2.80	1.65	1.73	0.1593	8.00	7.75
110	0.97	1.10	5.10	1.56	1.69	0.2678	9.00	9.27
110	1.12	1.47	8.46	1.47	1.62	0.2888	10.00	10.30
110	1.54	0.51	3.02	1.17	1.18	0.1354	6.85	6.87
110	1.47	1.12	6.10	1.07	1.15	0.1792	6.85	6.61
110	1.53	1.52	9.48	0.99	1.10	0.2250	6.16	5.57

* Nominal time, Volume of the column / liquid flowrate

** RTD data

Dimensionless RTD curve E(θ) vs. θ using 4" lab column

Nd =	0.1349	0.1590	0.1853	0.0756	0.1013	0.1146	0.1342	0.1819	0.2187
(θ)	E (θ)	E (θ))	E (θ)	E (θ)	E (θ)	E (θ)	E (θ)	E (θ)	E (θ)
0.000	0.000	0.000	0.000	0.000	0.000	0.000	0.000	0.000	0.000
0.037	0.000	0.000	0.000	0.000	0.000	0.000	0.000	0.000	0.000
0.073	0.000	0.000	0.000	0.000	0.000	0.000	0.000	0.000	0.000
0.110	0.000	0.000	0.001	0.000	0.000	0.000	0.000	0.001	0.005
0.147	0.002	0.006	0.017	0.000	0.000	0.000	0.002	0.015	0.042
0.184	0.013	0.034	0.069	0.000	0.002	0.005	0.013	0.063	0.131
0.220	0.050	0.097	0.165	0.001	0.011	0.022	0.049	0.156	0.264
0.257	0.119	0.198	0.293	0.008	0.038	0.065	0.117	0.281	0.416
0.294	0.220	0.323	0.434	0.026	0.092	0.139	0.217	0.420	0.562
0.330	0.343	0.458	0.570	0.067	0.175	0.241	0.339	0.557	0.690
0.367	0.474	0.588	0.692	0.134	0.284	0.362	0.470	0.679	0.793
0.404	0.601	0.705	0.791	0.230	0.409	0.492	0.598	0.782	0.870
0.441	0.717	0.803	0.869	0.350	0.540	0.620	0.715	0.861	0.922
0.477	0.817	0.880	0.924	0.484	0.668	0.737	0.814	0.919	0.954
0.514	0.897	0.937	0.959	0.624	0.785	0.839	0.895	0.957	0.968
0.551	0.957	0.974	0.978	0.759	0.886	0.923	0.956	0.978	0.969
0.587	0.998	0.995	0.982	0.883	0.968	0.987	0.998	0.984	0.958
0.624	1.022	1.002	0.975	0.990	1.030	1.031	1.022	0.978	0.939
0.661	1.031	0.996	0.958	1.076	1.072	1.058	1.032	0.963	0.914
0.698	1.028	0.981	0.935	1.140	1.096	1.069	1.029	0.941	0.884
0.734	1.014	0.959	0.907	1.181	1.104	1.066	1.015	0.913	0.851
0.771	0.991	0.930	0.875	1.202	1.098	1.052	0.993	0.881	0.816
0.808	0.963	0.898	0.840	1.205	1.081	1.029	0.965	0.847	0.780
0.845	0.929	0.862	0.804	1.191	1.054	0.999	0.931	0.811	0.744
0.881	0.892	0.825	0.767	1.164	1.019	0.962	0.894	0.773	0.708
0.918	0.852	0.786	0.729	1.126	0.979	0.922	0.854	0.736	0.672
0.955	0.811	0.747	0.692	1.080	0.934	0.879	0.813	0.699	0.638
0.991	0.769	0.708	0.656	1.027	0.887	0.834	0.771	0.662	0.604
1.028	0.727	0.670	0.621	0.970	0.839	0.789	0.729	0.626	0.571
1.065	0.686	0.633	0.586	0.911	0.790	0.743	0.688	0.592	0.540
1.102	0.646	0.596	0.553	0.851	0.741	0.698	0.647	0.558	0.510
1.138	0.606	0.561	0.522	0.791	0.693	0.654	0.608	0.526	0.482
1.175	0.569	0.528	0.491	0.732	0.646	0.612	0.570	0.496	0.455
1.212	0.532	0.495	0.463	0.675	0.601	0.571	0.534	0.466	0.429
1.248	0.498	0.465	0.435	0.620	0.558	0.531	0.499	0.439	0.405
1.285	0.465	0.436	0.409	0.567	0.516	0.494	0.466	0.412	0.381
1.322	0.433	0.408	0.384	0.518	0.477	0.459	0.434	0.387	0.359
1.359	0.404	0.382	0.361	0.472	0.440	0.425	0.405	0.364	0.339
1.395	0.376	0.357	0.339	0.429	0.406	0.394	0.377	0.341	0.319
1.432	0.350	0.334	0.318	0.388	0.373	0.364	0.350	0.320	0.301
1.469	0.325	0.312	0.299	0.351	0.343	0.336	0.326	0.300	0.283
1.505	0.302	0.292	0.280	0.317	0.315	0.311	0.303	0.282	0.267
1.542	0.281	0.272	0.263	0.286	0.289	0.287	0.281	0.264	0.252
1.579	0.261	0.254	0.247	0.258	0.265	0.264	0.261	0.248	0.237
1.616	0.242	0.238	0.232	0.231	0.242	0.243	0.242	0.232	0.223
1.652	0.224	0.222	0.217	0.208	0.222	0.224	0.224	0.218	0.211

1.689	0.208	0.207	0.204	0.186	0.203	0.206	0.208	0.204	0.198
1.726	0.193	0.193	0.191	0.167	0.185	0.190	0.193	0.191	0.187
1.762	0.179	0.180	0.179	0.149	0.169	0.174	0.178	0.179	0.176
1.799	0.165	0.168	0.168	0.133	0.154	0.160	0.165	0.168	0.166
1.836	0.153	0.157	0.158	0.119	0.141	0.147	0.153	0.158	0.157
1.873	0.142	0.146	0.148	0.106	0.128	0.135	0.142	0.148	0.148
1.909	0.131	0.136	0.139	0.095	0.117	0.124	0.131	0.139	0.139
1.946	0.122	0.127	0.130	0.085	0.106	0.114	0.121	0.130	0.131
1.983	0.113	0.119	0.122	0.075	0.097	0.104	0.112	0.122	0.124
2.019	0.104	0.111	0.115	0.067	0.088	0.096	0.104	0.114	0.117
2.056	0.096	0.103	0.107	0.060	0.080	0.088	0.096	0.107	0.110
2.093	0.089	0.096	0.101	0.053	0.073	0.081	0.089	0.100	0.104
2.130	0.083	0.090	0.095	0.047	0.066	0.074	0.082	0.094	0.098
2.166	0.076	0.084	0.089	0.042	0.060	0.068	0.076	0.088	0.093
2.203	0.071	0.078	0.083	0.037	0.055	0.062	0.070	0.083	0.088
2.240	0.065	0.073	0.078	0.033	0.050	0.057	0.065	0.078	0.083
2.276	0.060	0.068	0.073	0.029	0.045	0.052	0.060	0.073	0.078
2.313	0.056	0.063	0.069	0.026	0.041	0.048	0.056	0.068	0.074
2.350	0.052	0.059	0.065	0.023	0.037	0.044	0.052	0.064	0.070
2.387	0.048	0.055	0.061	0.020	0.034	0.040	0.048	0.060	0.066
2.423	0.044	0.051	0.057	0.018	0.031	0.037	0.044	0.056	0.062
2.460	0.041	0.048	0.054	0.016	0.028	0.034	0.041	0.053	0.059
2.497	0.038	0.045	0.050	0.014	0.026	0.031	0.038	0.050	0.055
2.534	0.035	0.042	0.047	0.013	0.023	0.028	0.035	0.047	0.052
2.570	0.032	0.039	0.044	0.011	0.021	0.026	0.032	0.044	0.050
2.607	0.030	0.036	0.042	0.010	0.019	0.024	0.030	0.041	0.047
2.644	0.028	0.034	0.039	0.009	0.017	0.022	0.028	0.039	0.044
2.680	0.026	0.032	0.037	0.008	0.016	0.020	0.025	0.036	0.042
2.717	0.024	0.029	0.035	0.007	0.014	0.018	0.024	0.034	0.040
2.754	0.022	0.028	0.033	0.006	0.013	0.017	0.022	0.032	0.037
2.791	0.020	0.026	0.031	0.005	0.012	0.015	0.020	0.030	0.035
2.827	0.019	0.024	0.029	0.005	0.011	0.014	0.019	0.028	0.034
2.864	0.017	0.022	0.027	0.004	0.010	0.013	0.017	0.026	0.032
2.901	0.016	0.021	0.025	0.004	0.009	0.012	0.016	0.025	0.030
2.937	0.015	0.019	0.024	0.003	0.008	0.011	0.015	0.023	0.028
2.974	0.014	0.018	0.022	0.003	0.007	0.010	0.014	0.022	0.027
3.011	0.013	0.017	0.021	0.003	0.007	0.009	0.013	0.021	0.025
3.048	0.012	0.016	0.020	0.002	0.006	0.008	0.012	0.019	0.024
3.084	0.011	0.015	0.019	0.002	0.005	0.008	0.011	0.018	0.023
3.121	0.010	0.014	0.018	0.002	0.005	0.007	0.010	0.017	0.022
3.158	0.009	0.013	0.017	0.002	0.004	0.006	0.009	0.016	0.020
3.194	0.009	0.012	0.016	0.001	0.004	0.006	0.009	0.015	0.019
3.231	0.008	0.011	0.015	0.001	0.004	0.005	0.008	0.014	0.018
3.268	0.007	0.011	0.014	0.001	0.003	0.005	0.007	0.013	0.017
3.305	0.007	0.010	0.013	0.001	0.003	0.004	0.007	0.013	0.016
3.341	0.006	0.009	0.012	0.001	0.003	0.004	0.006	0.012	0.016
3.378	0.006	0.009	0.011	0.001	0.002	0.004	0.006	0.011	0.015
3.415	0.005	0.008	0.011	0.001	0.002	0.003	0.005	0.010	0.014
3.451	0.005	0.008	0.010	0.001	0.002	0.003	0.005	0.010	0.013
3.488	0.005	0.007	0.010	0.001	0.002	0.003	0.005	0.009	0.013
3.525	0.004	0.007	0.009	0.000	0.002	0.003	0.004	0.009	0.012

3.562	0.004	0.006	0.008	0.000	0.002	0.002	0.004	0.008	0.011
3.598	0.004	0.006	0.008	0.000	0.001	0.002	0.004	0.008	0.011
3.635	0.003	0.005	0.008	0.000	0.001	0.002	0.003	0.007	0.010
3.672	0.003	0.005	0.007	0.000	0.001	0.002	0.003	0.007	0.010
3.708	0.003	0.005	0.007	0.000	0.001	0.002	0.003	0.006	0.009
3.745	0.003	0.004	0.006	0.000	0.001	0.002	0.003	0.006	0.009
3.782	0.003	0.004	0.006	0.000	0.001	0.001	0.002	0.006	0.008
3.819	0.002	0.004	0.006	0.000	0.001	0.001	0.002	0.005	0.008
3.855	0.002	0.004	0.005	0.000	0.001	0.001	0.002	0.005	0.007
3.892	0.002	0.003	0.005	0.000	0.001	0.001	0.002	0.005	0.007
3.929	0.002	0.003	0.005	0.000	0.001	0.001	0.002	0.004	0.007
3.966	0.002	0.003	0.004	0.000	0.001	0.001	0.002	0.004	0.006
4.002	0.002	0.003	0.004	0.000	0.000	0.001	0.002	0.004	0.006
4.039	0.001	0.003	0.004	0.000	0.000	0.001	0.001	0.004	0.006
4.076	0.001	0.002	0.004	0.000	0.000	0.001	0.001	0.004	0.005
4.112	0.001	0.002	0.003	0.000	0.000	0.001	0.001	0.003	0.005
4.149	0.001	0.002	0.003	0.000	0.000	0.001	0.001	0.003	0.005
4.186	0.001	0.002	0.003	0.000	0.000	0.001	0.001	0.003	0.005
4.223	0.001	0.002	0.003	0.000	0.000	0.001	0.001	0.003	0.004
4.259	0.001	0.002	0.003	0.000	0.000	0.000	0.001	0.003	0.004
4.296	0.001	0.002	0.003	0.000	0.000	0.000	0.001	0.002	0.004
4.333	0.001	0.002	0.002	0.000	0.000	0.000	0.001	0.002	0.004
4.369	0.001	0.001	0.002	0.000	0.000	0.000	0.001	0.002	0.004
4.406	0.001	0.001	0.002	0.000	0.000	0.000	0.001	0.002	0.003
4.443	0.001	0.001	0.002	0.000	0.000	0.000	0.001	0.002	0.003
4.480	0.001	0.001	0.002	0.000	0.000	0.000	0.001	0.002	0.003
4.516	0.001	0.001	0.002	0.000	0.000	0.000	0.001	0.002	0.003
4.553	0.001	0.001	0.002	0.000	0.000	0.000	0.001	0.002	0.003
4.590	0.000	0.001	0.002	0.000	0.000	0.000	0.000	0.002	0.003
4.626	0.000	0.001	0.002	0.000	0.000	0.000	0.000	0.001	0.003
4.663	0.000	0.001	0.001	0.000	0.000	0.000	0.000	0.001	0.002
4.700	0.000	0.001	0.001	0.000	0.000	0.000	0.000	0.001	0.002
4.737	0.000	0.001	0.001	0.000	0.000	0.000	0.000	0.001	0.002
4.773	0.000	0.001	0.001	0.000	0.000	0.000	0.000	0.001	0.002
4.810	0.000	0.001	0.001	0.000	0.000	0.000	0.000	0.001	0.002
4.847	0.000	0.001	0.001	0.000	0.000	0.000	0.000	0.001	0.002
4.883	0.000	0.001	0.001	0.000	0.000	0.000	0.000	0.001	0.002
4.920	0.000	0.001	0.001	0.000	0.000	0.000	0.000	0.001	0.002
4.957	0.000	0.000	0.001	0.000	0.000	0.000	0.000	0.001	0.002
4.994	0.000	0.000	0.001	0.000	0.000	0.000	0.000	0.001	0.002
5.030	0.000	0.000	0.001	0.000	0.000	0.000	0.000	0.001	0.001

Nd =	0.0975	0.1423	0.1829	0.1593	0.2678	0.2888	0.1354	0.1792	0.2250
(θ)	E (θ)	E (θ))	E (θ)	E (θ)	E (θ)	E (θ)	E (θ)	E (θ)	E (θ)
0.000	0.000	0.000	0.000	0.000	0.000	0.000	0.000	0.000	0.000
0.037	0.000	0.000	0.000	0.000	0.000	0.000	0.000	0.000	0.000
0.073	0.000	0.000	0.000	0.000	0.001	0.001	0.000	0.000	0.000
0.110	0.000	0.000	0.001	0.000	0.021	0.032	0.000	0.001	0.007
0.147	0.000	0.003	0.015	0.006	0.104	0.139	0.002	0.014	0.048
0.184	0.001	0.018	0.065	0.034	0.250	0.306	0.014	0.059	0.145
0.220	0.009	0.063	0.158	0.098	0.421	0.486	0.050	0.148	0.284
0.257	0.032	0.142	0.284	0.199	0.583	0.647	0.121	0.271	0.438
0.294	0.080	0.252	0.424	0.325	0.719	0.775	0.222	0.409	0.584
0.330	0.157	0.379	0.561	0.460	0.823	0.867	0.345	0.546	0.710
0.367	0.261	0.511	0.683	0.590	0.896	0.927	0.476	0.670	0.809
0.404	0.384	0.636	0.785	0.706	0.941	0.960	0.604	0.774	0.881
0.441	0.516	0.747	0.864	0.804	0.964	0.973	0.720	0.856	0.930
0.477	0.646	0.839	0.921	0.881	0.969	0.970	0.818	0.916	0.958
0.514	0.767	0.912	0.958	0.937	0.962	0.955	0.898	0.956	0.969
0.551	0.873	0.964	0.978	0.975	0.944	0.931	0.957	0.978	0.966
0.587	0.960	0.998	0.983	0.995	0.919	0.902	0.998	0.986	0.953
0.624	1.027	1.016	0.977	1.001	0.889	0.869	1.022	0.981	0.932
0.661	1.075	1.021	0.962	0.996	0.856	0.834	1.030	0.967	0.906
0.698	1.104	1.013	0.939	0.981	0.821	0.797	1.027	0.945	0.875
0.734	1.115	0.996	0.911	0.958	0.784	0.760	1.013	0.918	0.842
0.771	1.112	0.971	0.879	0.930	0.748	0.724	0.990	0.887	0.806
0.808	1.097	0.941	0.845	0.897	0.712	0.688	0.961	0.852	0.770
0.845	1.071	0.907	0.809	0.861	0.676	0.653	0.927	0.816	0.734
0.881	1.037	0.869	0.771	0.824	0.642	0.619	0.890	0.779	0.698
0.918	0.997	0.830	0.734	0.785	0.609	0.586	0.850	0.741	0.663
0.955	0.952	0.790	0.697	0.746	0.577	0.555	0.809	0.704	0.629
0.991	0.904	0.749	0.660	0.708	0.546	0.526	0.768	0.667	0.595
1.028	0.855	0.708	0.625	0.669	0.517	0.497	0.726	0.631	0.563
1.065	0.805	0.668	0.590	0.632	0.489	0.471	0.685	0.596	0.533
1.102	0.754	0.629	0.557	0.596	0.462	0.445	0.644	0.562	0.503
1.138	0.705	0.591	0.525	0.561	0.437	0.421	0.605	0.530	0.475
1.175	0.657	0.555	0.494	0.527	0.413	0.399	0.568	0.499	0.449
1.212	0.610	0.520	0.465	0.495	0.391	0.377	0.531	0.470	0.423
1.248	0.566	0.487	0.438	0.464	0.369	0.357	0.497	0.441	0.399
1.285	0.523	0.455	0.411	0.435	0.349	0.338	0.464	0.415	0.377
1.322	0.483	0.425	0.386	0.408	0.330	0.320	0.433	0.389	0.355
1.359	0.445	0.397	0.363	0.382	0.312	0.302	0.403	0.366	0.335
1.395	0.409	0.370	0.341	0.357	0.295	0.286	0.376	0.343	0.316
1.432	0.376	0.345	0.320	0.334	0.279	0.271	0.350	0.322	0.298
1.469	0.345	0.321	0.300	0.312	0.264	0.257	0.325	0.302	0.281
1.505	0.316	0.299	0.281	0.292	0.250	0.243	0.302	0.283	0.265
1.542	0.289	0.278	0.264	0.272	0.236	0.231	0.281	0.265	0.250
1.579	0.265	0.259	0.248	0.254	0.224	0.219	0.260	0.249	0.235
1.616	0.242	0.241	0.232	0.237	0.212	0.207	0.242	0.233	0.222
1.652	0.221	0.224	0.218	0.222	0.201	0.196	0.224	0.218	0.209
1.689	0.201	0.208	0.204	0.207	0.190	0.186	0.208	0.205	0.197
1.726	0.183	0.193	0.191	0.193	0.180	0.177	0.193	0.192	0.186

1.762	0.167	0.179	0.179	0.180	0.170	0.168	0.179	0.180	0.176
1.799	0.152	0.167	0.168	0.168	0.162	0.159	0.166	0.168	0.166
1.836	0.138	0.155	0.158	0.157	0.153	0.151	0.153	0.158	0.156
1.873	0.126	0.144	0.148	0.146	0.145	0.144	0.142	0.148	0.148
1.909	0.114	0.133	0.139	0.136	0.138	0.136	0.132	0.138	0.139
1.946	0.104	0.124	0.130	0.127	0.130	0.130	0.122	0.130	0.131
1.983	0.094	0.115	0.122	0.119	0.124	0.123	0.113	0.121	0.124
2.019	0.086	0.106	0.114	0.111	0.117	0.117	0.104	0.114	0.117
2.056	0.078	0.099	0.107	0.103	0.111	0.111	0.097	0.107	0.111
2.093	0.071	0.092	0.100	0.096	0.106	0.106	0.089	0.100	0.104
2.130	0.064	0.085	0.094	0.090	0.100	0.101	0.083	0.094	0.099
2.166	0.058	0.079	0.088	0.084	0.095	0.096	0.077	0.088	0.093
2.203	0.053	0.073	0.083	0.078	0.091	0.091	0.071	0.082	0.088
2.240	0.048	0.068	0.078	0.073	0.086	0.087	0.066	0.077	0.083
2.276	0.043	0.063	0.073	0.068	0.082	0.082	0.061	0.072	0.079
2.313	0.039	0.058	0.068	0.063	0.078	0.079	0.056	0.068	0.074
2.350	0.036	0.054	0.064	0.059	0.074	0.075	0.052	0.064	0.070
2.387	0.032	0.050	0.060	0.055	0.070	0.071	0.048	0.060	0.066
2.423	0.029	0.047	0.057	0.051	0.067	0.068	0.044	0.056	0.063
2.460	0.026	0.043	0.053	0.048	0.063	0.065	0.041	0.052	0.059
2.497	0.024	0.040	0.050	0.045	0.060	0.062	0.038	0.049	0.056
2.534	0.022	0.037	0.047	0.042	0.057	0.059	0.035	0.046	0.053
2.570	0.020	0.035	0.044	0.039	0.055	0.056	0.033	0.043	0.050
2.607	0.018	0.032	0.041	0.036	0.052	0.053	0.030	0.041	0.048
2.644	0.016	0.030	0.039	0.034	0.049	0.051	0.028	0.038	0.045
2.680	0.015	0.028	0.036	0.032	0.047	0.049	0.026	0.036	0.043
2.717	0.013	0.026	0.034	0.030	0.045	0.046	0.024	0.034	0.040
2.754	0.012	0.024	0.032	0.028	0.043	0.044	0.022	0.031	0.038
2.791	0.011	0.022	0.030	0.026	0.041	0.042	0.020	0.030	0.036
2.827	0.010	0.020	0.028	0.024	0.039	0.040	0.019	0.028	0.034
2.864	0.009	0.019	0.027	0.022	0.037	0.038	0.018	0.026	0.032
2.901	0.008	0.018	0.025	0.021	0.035	0.037	0.016	0.024	0.031
2.937	0.007	0.016	0.024	0.020	0.033	0.035	0.015	0.023	0.029
2.974	0.007	0.015	0.022	0.018	0.032	0.033	0.014	0.022	0.028
3.011	0.006	0.014	0.021	0.017	0.030	0.032	0.013	0.020	0.026
3.048	0.005	0.013	0.020	0.016	0.029	0.030	0.012	0.019	0.025
3.084	0.005	0.012	0.018	0.015	0.028	0.029	0.011	0.018	0.024
3.121	0.004	0.011	0.017	0.014	0.026	0.028	0.010	0.017	0.022
3.158	0.004	0.010	0.016	0.013	0.025	0.027	0.009	0.016	0.021
3.194	0.004	0.010	0.015	0.012	0.024	0.025	0.009	0.015	0.020
3.231	0.003	0.009	0.014	0.011	0.023	0.024	0.008	0.014	0.019
3.268	0.003	0.008	0.013	0.011	0.022	0.023	0.008	0.013	0.018
3.305	0.003	0.008	0.013	0.010	0.021	0.022	0.007	0.012	0.017
3.341	0.002	0.007	0.012	0.009	0.020	0.021	0.006	0.012	0.016
3.378	0.002	0.007	0.011	0.009	0.019	0.020	0.006	0.011	0.015
3.415	0.002	0.006	0.011	0.008	0.018	0.019	0.006	0.010	0.015
3.451	0.002	0.006	0.010	0.008	0.017	0.019	0.005	0.010	0.014
3.488	0.002	0.005	0.009	0.007	0.016	0.018	0.005	0.009	0.013
3.525	0.001	0.005	0.009	0.007	0.016	0.017	0.004	0.008	0.012
3.562	0.001	0.005	0.008	0.006	0.015	0.016	0.004	0.008	0.012
3.598	0.001	0.004	0.008	0.006	0.014	0.016	0.004	0.007	0.011

3.635	0.001	0.004	0.007	0.005	0.014	0.015	0.003	0.007	0.011
3.672	0.001	0.004	0.007	0.005	0.013	0.014	0.003	0.007	0.010
3.708	0.001	0.003	0.007	0.005	0.012	0.014	0.003	0.006	0.010
3.745	0.001	0.003	0.006	0.004	0.012	0.013	0.003	0.006	0.009
3.782	0.001	0.003	0.006	0.004	0.011	0.012	0.003	0.006	0.009
3.819	0.001	0.003	0.005	0.004	0.011	0.012	0.002	0.005	0.008
3.855	0.001	0.003	0.005	0.004	0.010	0.011	0.002	0.005	0.008
3.892	0.001	0.002	0.005	0.003	0.010	0.011	0.002	0.005	0.007
3.929	0.000	0.002	0.005	0.003	0.009	0.011	0.002	0.004	0.007
3.966	0.000	0.002	0.004	0.003	0.009	0.010	0.002	0.004	0.007
4.002	0.000	0.002	0.004	0.003	0.009	0.010	0.002	0.004	0.006
4.039	0.000	0.002	0.004	0.003	0.008	0.009	0.002	0.004	0.006
4.076	0.000	0.002	0.004	0.002	0.008	0.009	0.001	0.003	0.006
4.112	0.000	0.002	0.003	0.002	0.008	0.008	0.001	0.003	0.005
4.149	0.000	0.001	0.003	0.002	0.007	0.008	0.001	0.003	0.005
4.186	0.000	0.001	0.003	0.002	0.007	0.008	0.001	0.003	0.005
4.223	0.000	0.001	0.003	0.002	0.007	0.007	0.001	0.003	0.005
4.259	0.000	0.001	0.003	0.002	0.006	0.007	0.001	0.003	0.004
4.296	0.000	0.001	0.003	0.002	0.006	0.007	0.001	0.002	0.004
4.333	0.000	0.001	0.002	0.002	0.006	0.007	0.001	0.002	0.004
4.369	0.000	0.001	0.002	0.001	0.006	0.006	0.001	0.002	0.004
4.406	0.000	0.001	0.002	0.001	0.005	0.006	0.001	0.002	0.004
4.443	0.000	0.001	0.002	0.001	0.005	0.006	0.001	0.002	0.003
4.480	0.000	0.001	0.002	0.001	0.005	0.006	0.001	0.002	0.003
4.516	0.000	0.001	0.002	0.001	0.005	0.005	0.001	0.002	0.003
4.553	0.000	0.001	0.002	0.001	0.004	0.005	0.001	0.002	0.003
4.590	0.000	0.001	0.002	0.001	0.004	0.005	0.000	0.001	0.003
4.626	0.000	0.001	0.001	0.001	0.004	0.005	0.000	0.001	0.003
4.663	0.000	0.001	0.001	0.001	0.004	0.005	0.000	0.001	0.003
4.700	0.000	0.000	0.001	0.001	0.004	0.004	0.000	0.001	0.002
4.737	0.000	0.000	0.001	0.001	0.004	0.004	0.000	0.001	0.002
4.773	0.000	0.000	0.001	0.001	0.003	0.004	0.000	0.001	0.002
4.810	0.000	0.000	0.001	0.001	0.003	0.004	0.000	0.001	0.002
4.847	0.000	0.000	0.001	0.001	0.003	0.004	0.000	0.001	0.002
4.883	0.000	0.000	0.001	0.001	0.003	0.004	0.000	0.001	0.002
4.920	0.000	0.000	0.001	0.001	0.003	0.003	0.000	0.001	0.002
4.957	0.000	0.000	0.001	0.000	0.003	0.003	0.000	0.001	0.002
4.994	0.000	0.000	0.001	0.000	0.003	0.003	0.000	0.001	0.002
5.030	0.000	0.000	0.001	0.000	0.003	0.003	0.000	0.001	0.002

6" lab column

Lc (cm)	Jl (cm/s)	Jg (cm/s)	% Eg	τ* (min)	τ** (min)	N_d	KCl, (gr-min/l)	
							in	out
258	1.24	0.47	12.20	3.23	3.76	0.1219	0.91	0.65
258	1.23	1.12	24.60	2.99	3.23	0.1709	1.36	1.10
258	1.14	1.48	35.60	2.87	2.76	0.1904	1.09	0.95
173	1.06	0.47	14.40	2.22	2.46	0.1354	0.91	0.56
173	0.97	1.12	27.41	2.04	2.08	0.1953	0.91	0.63
173	0.94	1.47	38.70	2.01	1.76	0.2176	0.45	0.38
173	1.47	0.46	15.60	1.50	1.62	0.1164	0.91	0.77
173	1.55	0.97	28.40	1.39	1.37	0.1559	0.61	0.52
173	1.51	1.51	38.90	1.35	1.17	0.1824	0.61	0.51

* Nominal time, Volume of the column / liquid flowrate

** RTD data

Dimensionless RTD curve E(θ) vs. θ using 6" lab column

Nd =	0.1219	0.1709	0.1904	0.1354	0.1953	0.2176	0.1164	0.1559	0.1824
(θ)	E (θ)	E (θ))	E (θ)	E (θ)	E (θ)	E (θ)	E (θ)	E (θ)	E (θ)
0.000	0.000	0.000	0.000	0.000	0.000	0.000	0.000	0.000	0.000
0.037	0.000	0.000	0.000	0.000	0.000	0.000	0.000	0.000	0.000
0.073	0.000	0.000	0.000	0.000	0.000	0.000	0.000	0.000	0.000
0.110	0.000	0.001	0.002	0.000	0.002	0.005	0.000	0.000	0.001
0.147	0.001	0.010	0.020	0.002	0.023	0.041	0.000	0.005	0.015
0.184	0.007	0.048	0.077	0.014	0.086	0.129	0.005	0.030	0.064
0.220	0.031	0.126	0.179	0.050	0.193	0.261	0.024	0.091	0.157
0.257	0.083	0.240	0.312	0.121	0.330	0.412	0.069	0.187	0.283
0.294	0.167	0.374	0.455	0.222	0.474	0.558	0.146	0.310	0.422
0.330	0.278	0.511	0.590	0.345	0.609	0.686	0.250	0.444	0.559
0.367	0.404	0.638	0.709	0.476	0.725	0.790	0.373	0.575	0.681
0.404	0.534	0.747	0.805	0.604	0.818	0.867	0.503	0.693	0.783
0.441	0.658	0.836	0.879	0.719	0.887	0.921	0.630	0.794	0.863
0.477	0.769	0.903	0.930	0.818	0.935	0.953	0.746	0.874	0.920
0.514	0.863	0.949	0.962	0.898	0.964	0.968	0.846	0.933	0.958
0.551	0.938	0.977	0.977	0.957	0.976	0.969	0.927	0.973	0.978
0.587	0.993	0.990	0.979	0.998	0.975	0.959	0.988	0.996	0.984
0.624	1.029	0.990	0.969	1.022	0.964	0.940	1.031	1.005	0.978
0.661	1.049	0.979	0.951	1.030	0.945	0.915	1.056	1.001	0.963
0.698	1.054	0.960	0.927	1.027	0.919	0.886	1.065	0.987	0.940
0.734	1.047	0.934	0.898	1.013	0.889	0.853	1.061	0.965	0.912
0.771	1.029	0.904	0.865	0.990	0.856	0.818	1.046	0.938	0.880
0.808	1.004	0.870	0.830	0.961	0.821	0.782	1.023	0.905	0.846
0.845	0.972	0.834	0.794	0.927	0.784	0.746	0.992	0.870	0.810
0.881	0.935	0.797	0.757	0.890	0.748	0.710	0.955	0.833	0.772
0.918	0.895	0.759	0.720	0.850	0.711	0.674	0.915	0.794	0.735
0.955	0.852	0.721	0.683	0.809	0.675	0.639	0.872	0.755	0.698
0.991	0.809	0.683	0.647	0.768	0.639	0.606	0.828	0.715	0.661
1.028	0.765	0.646	0.612	0.726	0.605	0.573	0.783	0.677	0.626
1.065	0.721	0.610	0.579	0.685	0.571	0.542	0.738	0.639	0.591
1.102	0.678	0.576	0.546	0.645	0.539	0.512	0.693	0.602	0.558
1.138	0.636	0.542	0.515	0.605	0.509	0.483	0.650	0.566	0.526
1.175	0.595	0.510	0.485	0.568	0.480	0.456	0.607	0.532	0.495
1.212	0.556	0.480	0.457	0.532	0.452	0.430	0.567	0.500	0.466
1.248	0.518	0.451	0.430	0.497	0.425	0.405	0.528	0.469	0.438
1.285	0.483	0.423	0.404	0.464	0.400	0.382	0.491	0.439	0.412
1.322	0.449	0.397	0.380	0.433	0.376	0.360	0.456	0.411	0.387
1.359	0.417	0.372	0.357	0.403	0.354	0.339	0.423	0.385	0.363
1.395	0.387	0.349	0.336	0.376	0.333	0.320	0.392	0.360	0.341
1.432	0.359	0.327	0.315	0.350	0.313	0.301	0.363	0.336	0.320
1.469	0.332	0.306	0.296	0.325	0.294	0.284	0.335	0.314	0.300
1.505	0.308	0.287	0.278	0.302	0.276	0.268	0.310	0.293	0.282
1.542	0.285	0.268	0.261	0.281	0.260	0.252	0.286	0.274	0.264
1.579	0.263	0.251	0.245	0.260	0.244	0.237	0.264	0.255	0.248
1.616	0.243	0.235	0.230	0.242	0.229	0.224	0.243	0.238	0.232
1.652	0.224	0.220	0.216	0.224	0.215	0.211	0.224	0.222	0.218

1.689	0.207	0.206	0.203	0.208	0.202	0.199	0.206	0.207	0.204
1.726	0.191	0.192	0.191	0.193	0.190	0.187	0.190	0.193	0.191
1.762	0.176	0.180	0.179	0.179	0.179	0.176	0.175	0.180	0.179
1.799	0.163	0.168	0.168	0.166	0.168	0.166	0.161	0.168	0.168
1.836	0.150	0.157	0.158	0.153	0.158	0.157	0.148	0.156	0.158
1.873	0.138	0.147	0.148	0.142	0.148	0.148	0.136	0.146	0.148
1.909	0.127	0.138	0.139	0.131	0.139	0.139	0.125	0.136	0.139
1.946	0.117	0.129	0.130	0.122	0.131	0.131	0.115	0.127	0.130
1.983	0.108	0.120	0.123	0.113	0.123	0.124	0.105	0.118	0.122
2.019	0.099	0.113	0.115	0.104	0.116	0.117	0.097	0.110	0.114
2.056	0.091	0.105	0.108	0.097	0.109	0.110	0.089	0.102	0.107
2.093	0.084	0.099	0.101	0.089	0.102	0.104	0.082	0.095	0.100
2.130	0.077	0.092	0.095	0.083	0.096	0.098	0.075	0.089	0.094
2.166	0.071	0.086	0.090	0.077	0.090	0.093	0.069	0.083	0.088
2.203	0.065	0.081	0.084	0.071	0.085	0.087	0.063	0.077	0.083
2.240	0.060	0.075	0.079	0.066	0.080	0.083	0.058	0.072	0.078
2.276	0.055	0.071	0.074	0.061	0.075	0.078	0.053	0.067	0.073
2.313	0.051	0.066	0.070	0.056	0.071	0.074	0.049	0.062	0.068
2.350	0.047	0.062	0.066	0.052	0.066	0.069	0.045	0.058	0.064
2.387	0.043	0.058	0.062	0.048	0.062	0.066	0.041	0.054	0.060
2.423	0.040	0.054	0.058	0.044	0.059	0.062	0.038	0.051	0.057
2.460	0.036	0.051	0.054	0.041	0.055	0.059	0.034	0.047	0.053
2.497	0.034	0.047	0.051	0.038	0.052	0.055	0.032	0.044	0.050
2.534	0.031	0.044	0.048	0.035	0.049	0.052	0.029	0.041	0.047
2.570	0.028	0.042	0.045	0.033	0.046	0.049	0.027	0.038	0.044
2.607	0.026	0.039	0.043	0.030	0.043	0.047	0.024	0.036	0.041
2.644	0.024	0.036	0.040	0.028	0.041	0.044	0.022	0.033	0.039
2.680	0.022	0.034	0.038	0.026	0.039	0.042	0.020	0.031	0.036
2.717	0.020	0.032	0.035	0.024	0.036	0.039	0.019	0.029	0.034
2.754	0.019	0.030	0.033	0.022	0.034	0.037	0.017	0.027	0.032
2.791	0.017	0.028	0.031	0.020	0.032	0.035	0.016	0.025	0.030
2.827	0.016	0.026	0.030	0.019	0.030	0.033	0.014	0.023	0.028
2.864	0.015	0.025	0.028	0.018	0.029	0.032	0.013	0.022	0.027
2.901	0.013	0.023	0.026	0.016	0.027	0.030	0.012	0.020	0.025
2.937	0.012	0.022	0.025	0.015	0.025	0.028	0.011	0.019	0.023
2.974	0.011	0.020	0.023	0.014	0.024	0.027	0.010	0.018	0.022
3.011	0.010	0.019	0.022	0.013	0.023	0.025	0.009	0.016	0.021
3.048	0.010	0.018	0.021	0.012	0.021	0.024	0.009	0.015	0.019
3.084	0.009	0.017	0.019	0.011	0.020	0.023	0.008	0.014	0.018
3.121	0.008	0.016	0.018	0.010	0.019	0.021	0.007	0.013	0.017
3.158	0.007	0.015	0.017	0.009	0.018	0.020	0.007	0.012	0.016
3.194	0.007	0.014	0.016	0.009	0.017	0.019	0.006	0.012	0.015
3.231	0.006	0.013	0.015	0.008	0.016	0.018	0.006	0.011	0.014
3.268	0.006	0.012	0.014	0.007	0.015	0.017	0.005	0.010	0.013
3.305	0.005	0.011	0.014	0.007	0.014	0.016	0.005	0.009	0.013
3.341	0.005	0.011	0.013	0.006	0.013	0.016	0.004	0.009	0.012
3.378	0.004	0.010	0.012	0.006	0.013	0.015	0.004	0.008	0.011
3.415	0.004	0.009	0.011	0.006	0.012	0.014	0.004	0.008	0.011
3.451	0.004	0.009	0.011	0.005	0.011	0.013	0.003	0.007	0.010
3.488	0.004	0.008	0.010	0.005	0.011	0.013	0.003	0.007	0.009
3.525	0.003	0.008	0.009	0.004	0.010	0.012	0.003	0.006	0.009

3.562	0.003	0.007	0.009	0.004	0.009	0.011	0.003	0.006	0.008
3.598	0.003	0.007	0.008	0.004	0.009	0.011	0.002	0.005	0.008
3.635	0.003	0.006	0.008	0.003	0.008	0.010	0.002	0.005	0.007
3.672	0.002	0.006	0.008	0.003	0.008	0.010	0.002	0.005	0.007
3.708	0.002	0.006	0.007	0.003	0.007	0.009	0.002	0.004	0.006
3.745	0.002	0.005	0.007	0.003	0.007	0.009	0.002	0.004	0.006
3.782	0.002	0.005	0.006	0.003	0.007	0.008	0.002	0.004	0.006
3.819	0.002	0.005	0.006	0.002	0.006	0.008	0.001	0.004	0.005
3.855	0.002	0.004	0.006	0.002	0.006	0.007	0.001	0.003	0.005
3.892	0.001	0.004	0.005	0.002	0.006	0.007	0.001	0.003	0.005
3.929	0.001	0.004	0.005	0.002	0.005	0.007	0.001	0.003	0.005
3.966	0.001	0.004	0.005	0.002	0.005	0.006	0.001	0.003	0.004
4.002	0.001	0.003	0.004	0.002	0.005	0.006	0.001	0.003	0.004
4.039	0.001	0.003	0.004	0.002	0.004	0.006	0.001	0.002	0.004
4.076	0.001	0.003	0.004	0.001	0.004	0.005	0.001	0.002	0.004
4.112	0.001	0.003	0.004	0.001	0.004	0.005	0.001	0.002	0.003
4.149	0.001	0.003	0.004	0.001	0.004	0.005	0.001	0.002	0.003
4.186	0.001	0.002	0.003	0.001	0.004	0.005	0.001	0.002	0.003
4.223	0.001	0.002	0.003	0.001	0.003	0.004	0.001	0.002	0.003
4.259	0.001	0.002	0.003	0.001	0.003	0.004	0.000	0.002	0.003
4.296	0.001	0.002	0.003	0.001	0.003	0.004	0.000	0.002	0.002
4.333	0.001	0.002	0.003	0.001	0.003	0.004	0.000	0.001	0.002
4.369	0.000	0.002	0.002	0.001	0.003	0.004	0.000	0.001	0.002
4.406	0.000	0.002	0.002	0.001	0.003	0.003	0.000	0.001	0.002
4.443	0.000	0.002	0.002	0.001	0.002	0.003	0.000	0.001	0.002
4.480	0.000	0.001	0.002	0.001	0.002	0.003	0.000	0.001	0.002
4.516	0.000	0.001	0.002	0.001	0.002	0.003	0.000	0.001	0.002
4.553	0.000	0.001	0.002	0.001	0.002	0.003	0.000	0.001	0.002
4.590	0.000	0.001	0.002	0.000	0.002	0.003	0.000	0.001	0.002
4.626	0.000	0.001	0.002	0.000	0.002	0.002	0.000	0.001	0.001
4.663	0.000	0.001	0.002	0.000	0.002	0.002	0.000	0.001	0.001
4.700	0.000	0.001	0.001	0.000	0.002	0.002	0.000	0.001	0.001
4.737	0.000	0.001	0.001	0.000	0.002	0.002	0.000	0.001	0.001
4.773	0.000	0.001	0.001	0.000	0.001	0.002	0.000	0.001	0.001
4.810	0.000	0.001	0.001	0.000	0.001	0.002	0.000	0.001	0.001
4.847	0.000	0.001	0.001	0.000	0.001	0.002	0.000	0.001	0.001
4.883	0.000	0.001	0.001	0.000	0.001	0.002	0.000	0.001	0.001
4.920	0.000	0.001	0.001	0.000	0.001	0.002	0.000	0.000	0.001
4.957	0.000	0.001	0.001	0.000	0.001	0.002	0.000	0.000	0.001
4.994	0.000	0.001	0.001	0.000	0.001	0.001	0.000	0.000	0.001
5.030	0.000	0.001	0.001	0.000	0.001	0.001	0.000	0.000	0.001

20" pilot unit

Lc (cm)	Jl (cm/s)	Jg (cm/s)	% Eg	τ^* (min)	τ^{**} (min)	N_d	KCl, (gr-min/l)	
							in	out
430	0.92	2.72	9.47	9.05	8.54	0.7512	8.62	6.74
430	0.64	2.90	11.30	12.84	11.90	0.9850	8.62	7.64
430	0.73	3.01	11.56	11.20	12.01	0.7912	8.62	8.20
430	0.78	3.06	11.90	10.45	9.86	0.8522	7.84	7.77
430	0.51	3.18	13.70	15.77	15.14	1.2545	7.84	7.71
430	1.17	3.22	13.40	6.86	6.32	0.7608	7.84	7.75
430	0.59	3.26	14.80	13.38	14.32	1.1239	13.44	13.26
430	0.98	3.27	15.70	7.98	7.15	0.7595	13.44	13.44
430	0.83	3.28	15.45	9.46	9.30	0.7392	13.44	13.08
430	0.68	3.32	15.80	7.44	8.09	0.9536	10.73	10.46
430	1.20	3.32	17.24	11.52	11.94	0.6955	12.28	11.31
430	0.99	3.39	17.86	6.62	5.93	0.7657	12.28	12.34
430	1.13	3.39	19.72	7.69	7.19	0.6974	17.92	17.36

* Nominal time, Volume of the column / liquid flowrate

** RTD data

Dimensionless RTD curve E(θ) vs. θ using 20" pilot unit

Nd =	0.7512	0.9850	0.7912	0.8522	1.2545	0.7608	1.1239
(θ)	E (θ)	E (θ))	E (θ)	E (θ)	E (θ)	E (θ)	E (θ)
0.000	0.000	0.000	0.000	0.000	0.000	0.000	0.000
0.037	0.012	0.076	0.018	0.031	0.258	0.014	0.154
0.073	0.361	0.778	0.426	0.532	1.284	0.376	1.041
0.110	0.850	1.293	0.932	1.053	1.680	0.870	1.508
0.147	1.141	1.461	1.206	1.297	1.685	1.157	1.592
0.184	1.256	1.452	1.299	1.356	1.561	1.267	1.519
0.220	1.268	1.371	1.293	1.324	1.407	1.275	1.396
0.257	1.228	1.266	1.240	1.252	1.258	1.231	1.266
0.294	1.163	1.158	1.166	1.166	1.124	1.164	1.142
0.330	1.090	1.056	1.086	1.078	1.006	1.089	1.031
0.367	1.014	0.964	1.006	0.993	0.905	1.012	0.933
0.404	0.942	0.880	0.931	0.914	0.817	0.939	0.846
0.441	0.873	0.805	0.861	0.843	0.741	0.870	0.771
0.477	0.810	0.739	0.797	0.777	0.675	0.807	0.704
0.514	0.752	0.680	0.738	0.718	0.618	0.748	0.646
0.551	0.699	0.628	0.685	0.665	0.567	0.695	0.594
0.587	0.650	0.581	0.637	0.617	0.523	0.647	0.548
0.624	0.606	0.539	0.593	0.574	0.483	0.603	0.508
0.661	0.566	0.501	0.553	0.535	0.448	0.563	0.471
0.698	0.529	0.467	0.517	0.499	0.416	0.526	0.439
0.734	0.495	0.436	0.484	0.467	0.388	0.493	0.409
0.771	0.465	0.408	0.453	0.438	0.363	0.462	0.383
0.808	0.437	0.383	0.426	0.411	0.340	0.434	0.359
0.845	0.411	0.359	0.400	0.386	0.319	0.408	0.337
0.881	0.387	0.338	0.377	0.363	0.300	0.384	0.317
0.918	0.365	0.319	0.356	0.343	0.283	0.363	0.299
0.955	0.345	0.301	0.336	0.324	0.267	0.342	0.282
0.991	0.326	0.285	0.318	0.306	0.252	0.324	0.266
1.028	0.309	0.269	0.301	0.290	0.239	0.307	0.252
1.065	0.292	0.255	0.285	0.275	0.226	0.291	0.239
1.102	0.277	0.242	0.270	0.261	0.215	0.276	0.227
1.138	0.263	0.230	0.257	0.248	0.204	0.262	0.216
1.175	0.250	0.219	0.244	0.235	0.194	0.249	0.205
1.212	0.238	0.209	0.232	0.224	0.185	0.237	0.196
1.248	0.227	0.199	0.221	0.214	0.177	0.226	0.187
1.285	0.216	0.190	0.211	0.204	0.169	0.215	0.178
1.322	0.206	0.181	0.201	0.194	0.161	0.205	0.170
1.359	0.197	0.173	0.192	0.186	0.154	0.196	0.163
1.395	0.188	0.166	0.184	0.177	0.148	0.187	0.156
1.432	0.180	0.159	0.176	0.170	0.142	0.179	0.149
1.469	0.172	0.152	0.168	0.163	0.136	0.171	0.143
1.505	0.165	0.146	0.161	0.156	0.130	0.164	0.137
1.542	0.158	0.140	0.154	0.149	0.125	0.157	0.132
1.579	0.151	0.134	0.148	0.143	0.120	0.151	0.127
1.616	0.145	0.129	0.142	0.138	0.116	0.144	0.122
1.652	0.139	0.124	0.136	0.132	0.111	0.139	0.117

1.689	0.134	0.119	0.131	0.127	0.107	0.133	0.113
1.726	0.129	0.115	0.126	0.122	0.103	0.128	0.109
1.762	0.124	0.111	0.121	0.117	0.100	0.123	0.105
1.799	0.119	0.107	0.116	0.113	0.096	0.118	0.101
1.836	0.114	0.103	0.112	0.109	0.093	0.114	0.097
1.873	0.110	0.099	0.108	0.105	0.090	0.109	0.094
1.909	0.106	0.096	0.104	0.101	0.087	0.105	0.091
1.946	0.102	0.092	0.100	0.098	0.084	0.102	0.088
1.983	0.098	0.089	0.097	0.094	0.081	0.098	0.085
2.019	0.095	0.086	0.093	0.091	0.078	0.094	0.082
2.056	0.091	0.083	0.090	0.088	0.076	0.091	0.079
2.093	0.088	0.081	0.087	0.085	0.074	0.088	0.077
2.130	0.085	0.078	0.084	0.082	0.071	0.085	0.074
2.166	0.082	0.075	0.081	0.079	0.069	0.082	0.072
2.203	0.079	0.073	0.078	0.077	0.067	0.079	0.070
2.240	0.077	0.071	0.076	0.074	0.065	0.077	0.068
2.276	0.074	0.068	0.073	0.072	0.063	0.074	0.066
2.313	0.072	0.066	0.071	0.069	0.061	0.072	0.064
2.350	0.069	0.064	0.068	0.067	0.059	0.069	0.062
2.387	0.067	0.062	0.066	0.065	0.058	0.067	0.060
2.423	0.065	0.061	0.064	0.063	0.056	0.065	0.058
2.460	0.063	0.059	0.062	0.061	0.055	0.063	0.056
2.497	0.061	0.057	0.060	0.059	0.053	0.061	0.055
2.534	0.059	0.055	0.058	0.057	0.052	0.059	0.053
2.570	0.057	0.054	0.057	0.056	0.050	0.057	0.052
2.607	0.055	0.052	0.055	0.054	0.049	0.055	0.050
2.644	0.054	0.051	0.053	0.052	0.047	0.054	0.049
2.680	0.052	0.049	0.052	0.051	0.046	0.052	0.048
2.717	0.050	0.048	0.050	0.049	0.045	0.050	0.046
2.754	0.049	0.047	0.049	0.048	0.044	0.049	0.045
2.791	0.048	0.045	0.047	0.047	0.043	0.047	0.044
2.827	0.046	0.044	0.046	0.045	0.042	0.046	0.043
2.864	0.045	0.043	0.044	0.044	0.041	0.045	0.042
2.901	0.043	0.042	0.043	0.043	0.040	0.043	0.041
2.937	0.042	0.041	0.042	0.042	0.039	0.042	0.040
2.974	0.041	0.040	0.041	0.040	0.038	0.041	0.039
3.011	0.040	0.039	0.040	0.039	0.037	0.040	0.038
3.048	0.039	0.038	0.039	0.038	0.036	0.039	0.037
3.084	0.038	0.037	0.037	0.037	0.035	0.038	0.036
3.121	0.037	0.036	0.036	0.036	0.034	0.037	0.035
3.158	0.035	0.035	0.035	0.035	0.033	0.035	0.034
3.194	0.035	0.034	0.034	0.034	0.033	0.035	0.033
3.231	0.034	0.033	0.034	0.033	0.032	0.034	0.032
3.268	0.033	0.032	0.033	0.033	0.031	0.033	0.032
3.305	0.032	0.031	0.032	0.032	0.030	0.032	0.031
3.341	0.031	0.031	0.031	0.031	0.030	0.031	0.030
3.378	0.030	0.030	0.030	0.030	0.029	0.030	0.029
3.415	0.029	0.029	0.029	0.029	0.028	0.029	0.029
3.451	0.028	0.028	0.029	0.029	0.028	0.029	0.028
3.488	0.028	0.028	0.028	0.028	0.027	0.028	0.027
3.525	0.027	0.027	0.027	0.027	0.026	0.027	0.027

3.562	0.026	0.026	0.026	0.027	0.026	0.026	0.026
3.598	0.026	0.026	0.026	0.026	0.025	0.026	0.026
3.635	0.025	0.025	0.025	0.025	0.025	0.025	0.025
3.672	0.024	0.025	0.024	0.025	0.024	0.024	0.025
3.708	0.024	0.024	0.024	0.024	0.024	0.024	0.024
3.745	0.023	0.024	0.023	0.023	0.023	0.023	0.023
3.782	0.022	0.023	0.023	0.023	0.023	0.023	0.023
3.819	0.022	0.022	0.022	0.022	0.022	0.022	0.022
3.855	0.021	0.022	0.022	0.022	0.022	0.021	0.022
3.892	0.021	0.021	0.021	0.021	0.021	0.021	0.021
3.929	0.020	0.021	0.021	0.021	0.021	0.020	0.021
3.966	0.020	0.021	0.020	0.020	0.020	0.020	0.021
4.002	0.019	0.020	0.020	0.020	0.020	0.019	0.020
4.039	0.019	0.020	0.019	0.019	0.020	0.019	0.020
4.076	0.018	0.019	0.019	0.019	0.019	0.018	0.019
4.112	0.018	0.019	0.018	0.018	0.019	0.018	0.019
4.149	0.017	0.018	0.018	0.018	0.018	0.018	0.019
4.186	0.017	0.018	0.017	0.018	0.018	0.017	0.018
4.223	0.017	0.018	0.017	0.017	0.018	0.017	0.018
4.259	0.016	0.017	0.017	0.017	0.017	0.016	0.017
4.296	0.016	0.017	0.016	0.016	0.017	0.016	0.017
4.333	0.016	0.016	0.016	0.016	0.017	0.016	0.017
4.369	0.015	0.016	0.015	0.016	0.016	0.015	0.016
4.406	0.015	0.016	0.015	0.015	0.016	0.015	0.016
4.443	0.014	0.015	0.015	0.015	0.016	0.014	0.016
4.480	0.014	0.015	0.014	0.015	0.016	0.014	0.015
4.516	0.014	0.015	0.014	0.014	0.015	0.014	0.015
4.553	0.013	0.015	0.014	0.014	0.015	0.014	0.015
4.590	0.013	0.014	0.013	0.014	0.015	0.013	0.015
4.626	0.013	0.014	0.013	0.013	0.014	0.013	0.014
4.663	0.013	0.014	0.013	0.013	0.014	0.013	0.014
4.700	0.012	0.013	0.013	0.013	0.014	0.012	0.014
4.737	0.012	0.013	0.012	0.013	0.014	0.012	0.013
4.773	0.012	0.013	0.012	0.012	0.013	0.012	0.013
4.810	0.011	0.013	0.012	0.012	0.013	0.011	0.013
4.847	0.011	0.012	0.011	0.012	0.013	0.011	0.013
4.883	0.011	0.012	0.011	0.012	0.013	0.011	0.012
4.920	0.011	0.012	0.011	0.011	0.012	0.011	0.012
4.957	0.010	0.012	0.011	0.011	0.012	0.011	0.012
4.994	0.010	0.011	0.010	0.011	0.012	0.010	0.012
5.030	0.010	0.011	0.010	0.011	0.012	0.010	0.012

Nd =	0.7595	0.7392	0.9536	0.6955	0.7657	0.6974
(θ)	E (θ)	E (θ))	E (θ)	E (θ)	E (θ)	E (θ)
0.000	0.000	0.000	0.000	0.000	0.000	0.000
0.037	0.013	0.011	0.063	0.007	0.014	0.007
0.073	0.374	0.342	0.718	0.277	0.384	0.280
0.110	0.867	0.825	1.239	0.732	0.880	0.737
0.147	1.155	1.120	1.426	1.042	1.165	1.046
0.184	1.265	1.242	1.432	1.188	1.272	1.190
0.220	1.274	1.260	1.362	1.227	1.278	1.228
0.257	1.231	1.224	1.264	1.207	1.233	1.208
0.294	1.164	1.162	1.161	1.157	1.164	1.157
0.330	1.089	1.090	1.062	1.093	1.088	1.093
0.367	1.013	1.017	0.971	1.025	1.011	1.024
0.404	0.939	0.945	0.888	0.956	0.938	0.956
0.441	0.871	0.877	0.814	0.891	0.869	0.890
0.477	0.807	0.814	0.748	0.829	0.805	0.829
0.514	0.749	0.756	0.689	0.772	0.747	0.771
0.551	0.696	0.703	0.636	0.719	0.694	0.718
0.587	0.647	0.654	0.589	0.671	0.645	0.670
0.624	0.603	0.610	0.546	0.626	0.601	0.625
0.661	0.563	0.570	0.508	0.585	0.561	0.585
0.698	0.526	0.533	0.474	0.548	0.524	0.547
0.734	0.493	0.499	0.443	0.514	0.491	0.513
0.771	0.462	0.468	0.414	0.482	0.461	0.482
0.808	0.434	0.440	0.389	0.453	0.433	0.453
0.845	0.409	0.414	0.365	0.427	0.407	0.426
0.881	0.385	0.390	0.344	0.402	0.383	0.401
0.918	0.363	0.368	0.324	0.379	0.361	0.379
0.955	0.343	0.347	0.306	0.358	0.341	0.358
0.991	0.324	0.329	0.289	0.339	0.323	0.338
1.028	0.307	0.311	0.274	0.321	0.306	0.320
1.065	0.291	0.295	0.260	0.304	0.290	0.303
1.102	0.276	0.280	0.246	0.288	0.275	0.288
1.138	0.262	0.266	0.234	0.274	0.261	0.273
1.175	0.249	0.252	0.223	0.260	0.248	0.260
1.212	0.237	0.240	0.212	0.247	0.236	0.247
1.248	0.226	0.229	0.202	0.236	0.225	0.235
1.285	0.215	0.218	0.193	0.224	0.214	0.224
1.322	0.205	0.208	0.184	0.214	0.205	0.214
1.359	0.196	0.199	0.176	0.204	0.195	0.204
1.395	0.187	0.190	0.168	0.195	0.187	0.195
1.432	0.179	0.181	0.161	0.186	0.178	0.186
1.469	0.171	0.173	0.154	0.178	0.171	0.178
1.505	0.164	0.166	0.148	0.171	0.163	0.170
1.542	0.157	0.159	0.142	0.163	0.157	0.163
1.579	0.151	0.152	0.136	0.156	0.150	0.156
1.616	0.144	0.146	0.131	0.150	0.144	0.150
1.652	0.139	0.140	0.126	0.144	0.138	0.144
1.689	0.133	0.135	0.121	0.138	0.133	0.138

1.726	0.128	0.129	0.116	0.132	0.128	0.132
1.762	0.123	0.124	0.112	0.127	0.123	0.127
1.799	0.118	0.120	0.108	0.122	0.118	0.122
1.836	0.114	0.115	0.104	0.118	0.113	0.117
1.873	0.110	0.111	0.100	0.113	0.109	0.113
1.909	0.106	0.107	0.097	0.109	0.105	0.109
1.946	0.102	0.103	0.093	0.105	0.101	0.105
1.983	0.098	0.099	0.090	0.101	0.098	0.101
2.019	0.094	0.095	0.087	0.097	0.094	0.097
2.056	0.091	0.092	0.084	0.094	0.091	0.094
2.093	0.088	0.089	0.081	0.090	0.088	0.090
2.130	0.085	0.086	0.079	0.087	0.085	0.087
2.166	0.082	0.083	0.076	0.084	0.082	0.084
2.203	0.079	0.080	0.074	0.081	0.079	0.081
2.240	0.077	0.077	0.071	0.078	0.076	0.078
2.276	0.074	0.075	0.069	0.076	0.074	0.076
2.313	0.072	0.072	0.067	0.073	0.071	0.073
2.350	0.069	0.070	0.065	0.071	0.069	0.071
2.387	0.067	0.067	0.063	0.068	0.067	0.068
2.423	0.065	0.065	0.061	0.066	0.065	0.066
2.460	0.063	0.063	0.059	0.064	0.063	0.064
2.497	0.061	0.061	0.058	0.062	0.061	0.062
2.534	0.059	0.059	0.056	0.060	0.059	0.060
2.570	0.057	0.057	0.054	0.058	0.057	0.058
2.607	0.055	0.056	0.053	0.056	0.055	0.056
2.644	0.054	0.054	0.051	0.054	0.054	0.054
2.680	0.052	0.052	0.050	0.053	0.052	0.053
2.717	0.050	0.051	0.048	0.051	0.050	0.051
2.754	0.049	0.049	0.047	0.049	0.049	0.049
2.791	0.047	0.048	0.046	0.048	0.047	0.048
2.827	0.046	0.046	0.044	0.046	0.046	0.046
2.864	0.045	0.045	0.043	0.045	0.045	0.045
2.901	0.043	0.043	0.042	0.044	0.043	0.044
2.937	0.042	0.042	0.041	0.042	0.042	0.042
2.974	0.041	0.041	0.040	0.041	0.041	0.041
3.011	0.040	0.040	0.039	0.040	0.040	0.040
3.048	0.039	0.039	0.038	0.039	0.039	0.039
3.084	0.038	0.038	0.037	0.038	0.038	0.038
3.121	0.037	0.037	0.036	0.037	0.036	0.037
3.158	0.035	0.036	0.035	0.036	0.035	0.036
3.194	0.035	0.035	0.034	0.034	0.035	0.034
3.231	0.034	0.034	0.033	0.034	0.034	0.034
3.268	0.033	0.033	0.032	0.033	0.033	0.033
3.305	0.032	0.032	0.031	0.032	0.032	0.032
3.341	0.031	0.031	0.031	0.031	0.031	0.031
3.378	0.030	0.030	0.030	0.030	0.030	0.030
3.415	0.029	0.029	0.029	0.029	0.029	0.029
3.451	0.029	0.028	0.029	0.028	0.029	0.028
3.488	0.028	0.028	0.028	0.028	0.028	0.028
3.525	0.027	0.027	0.027	0.027	0.027	0.027
3.562	0.026	0.026	0.026	0.026	0.026	0.026

3.598	0.026	0.026	0.026	0.025	0.026	0.025
3.635	0.025	0.025	0.025	0.025	0.025	0.025
3.672	0.024	0.024	0.025	0.024	0.024	0.024
3.708	0.024	0.024	0.024	0.023	0.024	0.023
3.745	0.023	0.023	0.024	0.023	0.023	0.023
3.782	0.023	0.022	0.023	0.022	0.023	0.022
3.819	0.022	0.022	0.022	0.022	0.022	0.022
3.855	0.021	0.021	0.022	0.021	0.021	0.021
3.892	0.021	0.021	0.021	0.020	0.021	0.020
3.929	0.020	0.020	0.021	0.020	0.020	0.020
3.966	0.020	0.020	0.020	0.019	0.020	0.019
4.002	0.019	0.019	0.020	0.019	0.019	0.019
4.039	0.019	0.019	0.020	0.018	0.019	0.018
4.076	0.018	0.018	0.019	0.018	0.018	0.018
4.112	0.018	0.018	0.019	0.018	0.018	0.018
4.149	0.018	0.017	0.018	0.017	0.018	0.017
4.186	0.017	0.017	0.018	0.017	0.017	0.017
4.223	0.017	0.017	0.018	0.016	0.017	0.016
4.259	0.016	0.016	0.017	0.016	0.016	0.016
4.296	0.016	0.016	0.017	0.015	0.016	0.015
4.333	0.016	0.015	0.016	0.015	0.016	0.015
4.369	0.015	0.015	0.016	0.015	0.015	0.015
4.406	0.015	0.015	0.016	0.014	0.015	0.014
4.443	0.014	0.014	0.015	0.014	0.015	0.014
4.480	0.014	0.014	0.015	0.014	0.014	0.014
4.516	0.014	0.014	0.015	0.013	0.014	0.013
4.553	0.014	0.013	0.014	0.013	0.014	0.013
4.590	0.013	0.013	0.014	0.013	0.013	0.013
4.626	0.013	0.013	0.014	0.012	0.013	0.012
4.663	0.013	0.012	0.014	0.012	0.013	0.012
4.700	0.012	0.012	0.013	0.012	0.012	0.012
4.737	0.012	0.012	0.013	0.012	0.012	0.012
4.773	0.012	0.012	0.013	0.011	0.012	0.011
4.810	0.011	0.011	0.012	0.011	0.012	0.011
4.847	0.011	0.011	0.012	0.011	0.011	0.011
4.883	0.011	0.011	0.012	0.010	0.011	0.010
4.920	0.011	0.011	0.012	0.010	0.011	0.010
4.957	0.010	0.010	0.012	0.010	0.011	0.010
4.994	0.010	0.010	0.011	0.010	0.010	0.010
5.030	0.010	0.010	0.011	0.010	0.010	0.010

Result of the least square method.

	(D/L)*(Jg/Ul)	Nd				
n	X	Y	Ln X	Ln Y	(Ln X)^2	(ln X) (Ln Y)
1	0.0353	0.1349	-3.3446	-2.0032	11.1864	6.7000
2	0.0499	0.1590	-2.9980	-1.8391	8.9877	5.5137
3	0.0658	0.1853	-2.7218	-1.6856	7.4079	4.5877
4	0.0179	0.0756	-4.0255	-2.5823	16.2044	10.3950
5	0.0220	0.1013	-3.8158	-2.2896	14.5606	8.7368
6	0.0313	0.1146	-3.4651	-2.1664	12.0067	7.5067
7	0.0286	0.1342	-3.5539	-2.0084	12.6300	7.1374
8	0.0589	0.1819	-2.8325	-1.7041	8.0230	4.8269
9	0.0752	0.2187	-2.5879	-1.5201	6.6974	3.9338
10	0.0196	0.0975	-3.9336	-2.3276	15.4734	9.1560
11	0.0368	0.1423	-3.3019	-1.9498	10.9023	6.4381
12	0.0551	0.1829	-2.8994	-1.6986	8.4067	4.9249
13	0.0440	0.1593	-3.1242	-1.8367	9.7605	5.7383
14	0.0994	0.2678	-2.3086	-1.3175	5.3296	3.0416
15	0.1110	0.2888	-2.1985	-1.2420	4.8333	2.7306
16	0.0297	0.1354	-3.5178	-1.9995	12.3750	7.0340
17	0.0661	0.1792	-2.7160	-1.7191	7.3767	4.6691
18	0.0831	0.2250	-2.4882	-1.4917	6.1910	3.7115
19	0.0197	0.1219	-3.9293	-2.1042	15.4392	8.2681
20	0.0406	0.1709	-3.2051	-1.7665	10.2726	5.6617
21	0.0494	0.1904	-3.0081	-1.6584	9.0485	4.9887
22	0.0336	0.1354	-3.3944	-1.9997	11.5217	6.7878
23	0.0738	0.1953	-2.6059	-1.6332	6.7908	4.2560
24	0.0844	0.2176	-2.4716	-1.5253	6.1089	3.7699
25	0.0233	0.1164	-3.7608	-2.1504	14.1433	8.0870
26	0.0395	0.1559	-3.2322	-1.8585	10.4468	6.0070
27	0.0538	0.1824	-2.9220	-1.7013	8.5382	4.9714
28	0.3161	0.7512	-1.1516	-0.2860	1.3262	0.3294
29	0.4739	0.9850	-0.7467	-0.0151	0.5576	0.0113
30	0.4292	0.7912	-0.8459	-0.2342	0.7155	0.1981
31	0.4071	0.8522	-0.8987	-0.1600	0.8076	0.1438
32	0.6372	1.2545	-0.4506	0.2267	0.2031	-0.1022
33	0.2820	0.7608	-1.2659	-0.2734	1.6025	0.3461
34	0.5545	1.1239	-0.5898	0.1168	0.3478	-0.0689
35	0.3314	0.7595	-1.1043	-0.2752	1.2196	0.3039
36	0.3944	0.7392	-0.9305	-0.3022	0.8658	0.2812
37	0.4864	0.9536	-0.7208	-0.0475	0.5196	0.0342
38	0.2705	0.6955	-1.3075	-0.3632	1.7096	0.4748
39	0.3311	0.7657	-1.1054	-0.2670	1.2220	0.2952
40	0.2851	0.6974	-1.2547	-0.3604	1.5744	0.4522
		SUM =	-96.7349	-52.0196	283.3337	162.2787

$$A = \mathrm{Exp}\left[\frac{(283.33)*(-52.01)-(162.27)*(-96.73)}{40*(283.33)-(-96.73)^2}\right] = 0.67$$

$$B = \frac{40*(162.27)-(-96.73)*(-52.01)}{40*(283.33)-(-96.73)^2} = 1.296$$

$$N_d = 1.296*\left(\frac{D_c}{L_c}*\frac{J_g}{J_l}*\left(1-\varepsilon_g\right)\right)^{0.67}$$

Appendix E: Column Scale-Up

Experiments at Bowater

4" lab column: diameter = 10.16 cm, height = 440 cm

% Consistency = ~ 1.0 % (plant)

Froth Depth = zero cm

Sparger # 1 (0.5 μm)

T = 41 °C

Jg =	0.58	cm/s													
Q	Jl	% Eg	Vol	ERIC	ERIC	Brightness		%Consit.		time	B. gain	% Flot.	% Rec	a = 87%	
lpm	cm/s		liters	F	A	F	A	F	A	min		effic.		-ln (1-R/a)	k
0.00	0.00	0.00	0.00	0.00	0.00	0.00	0.00	0.000	0.000	0.00	0.00	0.00	0.00	0.000	
5.98	1.23	5.30	33.77	689.50	223.30	49.59	58.91	1.234	1.131	5.64	9.32	67.61	70.32	1.652	0.2927
8.12	1.67	5.45	33.72	632.55	270.60	49.14	57.64	1.353	1.212	4.15	8.50	57.22	61.70	1.235	0.2976
10.17	2.09	5.50	33.70	714.07	332.66	48.92	56.85	1.154	1.158	3.31	7.93	53.41	53.19	0.946	0.2851
12.65	2.60	5.60	33.66	708.74	369.80	49.03	55.92	1.244	1.150	2.66	6.89	47.82	51.76	0.904	0.3395

Jg =	1.16	cm/s													
Q	Jl	% Eg	Vol	ERIC	ERIC	Brightness		%Consit.		time	B. gain	% Flot.	% Rec	a = 87%	
lpm	cm/s		liters	F	A	F	A	F	A	min		effic.		-ln (1-R/a)	k
0.00	0.00	0.00	0.00	0.00	0.00	0.00	0.00	0.000	0.000	0.00	0.00	0.00	0.00	0.000	
5.40	1.11	10.84	31.79	689.50	155.60	51.48	61.67	1.320	1.232	5.89	10.19	77.43	78.94	2.379	0.404
5.89	1.21	10.90	31.77	689.50	168.50	51.19	61.30	1.234	1.218	5.40	10.11	75.56	75.88	2.057	0.381
8.22	1.69	11.20	31.67	632.55	205.60	49.14	58.38	1.353	1.263	3.85	9.24	67.50	69.67	1.613	0.419
10.17	2.09	11.10	31.70	714.07	265.80	48.92	57.80	1.154	1.136	3.12	8.88	62.78	63.36	1.303	0.418
13.04	2.68	11.30	31.63	708.74	312.50	50.1	58.40	1.304	1.286	2.43	8.30	55.91	56.51	1.048	0.432
14.06	2.89	11.35	31.61	707.80	335.48	49.98	57.36	1.325	1.296	2.25	7.38	52.60	53.64	0.959	0.426

Jg =	1.74	cm/s													
Q	Jl	% Eg	Vol	ERIC	ERIC	Brightness		%Consit.		time	B. gain	% Flot.	% Rec	a = 87%	
lpm	cm/s		liters	F	A	F	A	F	A	min		effic.		-ln (1-R/a)	k
0.00	0.00	0.00	0.00	0.00	0.00	0.00	0.00	0.000	0.000	0.00	0.00	0.00	0.00	0.000	
5.50	1.13	19.30	28.78	689.50	114.64	49.89	61.78	1.234	1.191	5.24	11.89	83.37	83.96	3.354	0.641
7.83	1.61	20.20	28.46	632.55	140.12	49.14	60.69	1.353	1.296	3.63	11.55	77.85	78.78	2.360	0.649
10.17	2.09	20.30	28.42	714.07	180.20	48.92	60.38	1.154	1.199	2.80	11.46	74.76	73.78	1.884	0.674
12.26	2.52	20.40	28.39	708.74	210.89	49.03	60.19	1.304	1.276	2.32	11.16	70.24	70.87	1.685	0.728

Experiments at Bowater

4" lab column: diameter = 10.16 cm, height = 440 cm

% Consistency = ~1.0 % (Plant)

Froth Depth = zero cm

Sparger # 2 (2 μm)

T = 41 °C

Jg =	1.53	cm/s														
Q	Jl	% Eg	Vol	ERIC	ERIC	Brightness		% Consit.		time	B. gain	% Flot.	% Rec	a = 87%	
lpm	cm/s		liters	F	A	F	A	F	A	min		effic.		-ln (1-R/a)	k
0.00	0.00	0.00	0.00	0.00	0.00	0.00	0.00	0.000	0.000	0.00	0.00	0.00	0.00	0.000	
6.10	1.25	12.98	31.03	723.50	149.23	46.78	57.90	1.120	1.110	5.09	11.12	79.37	79.56	2.459	0.483
8.03	1.65	13.20	30.95	723.50	193.56	46.78	58.12	1.120	1.104	3.85	11.34	73.25	73.63	1.873	0.486
10.63	2.19	13.70	30.77	723.50	235.60	46.78	57.68	1.120	1.116	2.90	10.90	67.44	67.55	1.498	0.517
12.45	2.56	13.80	30.74	723.50	305.78	46.78	57.12	1.120	1.010	2.47	10.34	57.74	61.89	1.243	0.503

Jg =	2.36	cm/s													
Q	Jl	% Eg	Vol	ERIC	ERIC	Brightness		% Consit.		time	B. gain	% Flot.	% Rec	a = 87%	
lpm	cm/s		liters	F	A	F	A	F	A	min		effic.		-ln (1-R/a)	k
0.00	0.00	0.00	0.00	0.00	0.00	0.00	0.00	0.000	0.000	0.00	0.00	0.00	0.00	0.000	
5.92	1.22	20.28	28.43	853.60	156.42	47.02	58.20	1.200	1.116	4.80	11.18	81.68	82.95	3.066	0.639
8.15	1.68	20.45	28.37	853.60	181.18	47.02	58.47	1.200	1.125	3.48	11.45	78.77	80.10	2.534	0.728
10.45	2.15	20.89	28.21	853.60	196.70	47.02	58.54	1.200	1.109	2.70	11.52	76.96	78.69	2.349	0.870
12.49	2.57	21.10	28.14	853.60	226.30	47.02	58.96	1.200	1.164	2.25	11.94	73.49	74.28	1.923	0.854

Jg =	2.83	cm/s													
Q	Jl	% Eg	Vol	ERIC	ERIC	Brightness		% Consit.		time	B. gain	% Flot.	% Rec	a = 87%	
lpm	cm/s		liters	F	A	F	A	F	A	min		effic.		-ln (1-R/a)	k
0.00	0.00	0.00	0.00	0.00	0.00	0.00	0.00	0.000	0.000	0.00	0.00	0.00	0.00	0.000	
6.25	1.28	24.49	26.93	745.65	153.20	46.94	58.39	1.244	1.102	4.31	11.45	79.45	81.79	2.816	0.654
8.27	1.70	25.10	26.71	745.65	162.35	46.94	58.20	1.244	1.153	3.23	11.26	78.23	79.81	2.493	0.772
10.36	2.13	25.40	26.60	745.65	171.52	46.94	58.10	1.244	1.208	2.57	11.16	77.00	77.66	2.231	0.869
12.64	2.60	25.76	26.47	745.65	186.98	46.94	57.98	1.244	1.167	2.09	11.04	74.92	76.46	2.111	1.008

Jg =	3.06	cm/s													
Q	Jl	% Eg	Vol	ERIC	ERIC	Brightness		% Consit.		time	B. gain	% Flot.	% Rec	a = 87%	
lpm	cm/s		liters	F	A	F	A	F	A	min		effic.		-ln (1-R/a)	k
0.00	0.00	0.00	0.00	0.00	0.00	0.00	0.00	0.000	0.000	0.00	0.00	0.00	0.00	0.000	
6.25	1.28	26.57	26.19	901.30	184.28	46.44	57.32	1.376	1.180	4.19	10.88	79.55	82.47	2.954	0.705
8.23	1.69	27.40	25.89	901.30	211.94	46.44	57.45	1.376	1.206	3.15	11.01	76.49	79.39	2.436	0.775
10.62	2.18	27.90	25.71	901.30	238.42	46.44	56.98	1.376	1.236	2.42	10.54	73.55	76.25	2.091	0.864
12.69	2.61	27.63	25.81	901.30	273.81	46.44	56.49	1.376	1.293	2.03	10.05	69.62	71.46	1.722	0.847

Jg =	3.30	cm/s													
Q	Jl	% Eg	Vol	ERIC	ERIC	Brightness		% Consit.		time	B. gain	% Flot.	% Rec	a = 87%	
lpm	cm/s		liters	F	A	F	A	F	A	min		effic.		-ln (1-R/a)	k
0.00	0.00	0.00	0.00	0.00	0.00	0.00	0.00	0.000	0.000	0.00	0.00	0.00	0.00	0.000	
6.28	1.29	28.75	25.41	895.60	198.23	46.56	57.05	1.351	1.097	4.05	10.49	77.87	82.03	2.862	0.707
8.44	1.74	29.12	25.28	895.60	233.12	46.56	57.04	1.351	1.030	2.99	10.48	73.97	80.16	2.542	0.849
10.61	2.18	29.76	25.05	895.60	245.92	46.56	56.57	1.351	1.268	2.36	10.01	72.54	74.23	1.919	0.813
12.72	2.61	29.98	24.97	895.60	263.43	46.56	56.16	1.351	1.306	1.96	9.60	70.59	71.57	1.729	0.881

Experiments at Bowater

4" lab column: diameter = 10.16 cm, height = 440 cm

% Consistency = ~ 1.0 % (Plant)

Froth Depth = zero cm

Sparger 5 (20 μm)

T = 41 °C

Jg =	1.16	cm/s													
Q	Jl	% Eg	Vol	ERIC	ERIC	Brightness		%Consit.		time	B. gain	% Flot.	% Rec	a = 87%	
lpm	cm/s		liters	F	A	F	A	F	A	min		effic.		-ln (1-R/a)	k
0.00	0.00	0.00	0.00	0.00	0.00	0.00	0.00	0.000	0.000	0.00	0.00	0.00	0.00	0.000	
5.35	1.10	5.85	33.51	594.00	215.80	48.60	58.76	1.289	1.015	6.26	10.16	63.67	71.39	1.718	0.2744
6.18	1.27	5.90	33.49	594.00	226.70	48.60	58.29	1.289	1.148	5.42	9.69	61.84	66.01	1.422	0.2623
8.07	1.66	5.90	33.49	594.00	263.80	48.60	57.40	1.289	1.168	4.15	8.80	55.59	59.76	1.161	0.2800
9.73	2.00	6.10	33.42	594.00	315.80	48.60	55.66	1.289	1.159	3.44	7.06	46.84	52.20	0.916	0.2667
12.45	2.56	6.20	33.38	594.00	361.50	48.60	53.91	1.289	1.139	2.68	5.31	39.14	46.22	0.758	0.2827
13.52	2.78	6.21	33.38	594.00	396.50	48.60	53.41	1.289	1.060	2.47	4.81	33.25	45.11	0.731	0.2961

Jg =	1.74	cm/s													
Q	Jl	% Eg	Vol	ERIC	ERIC	Brightness		%Consit.		time	B. gain	% Flot.	% Rec	a = 87%	
lpm	cm/s		liters	F	A	F	A	F	A	min		effic.		-ln (1-R/a)	k
0.00	0.00	0.00	0.00	0.00	0.00	0.00	0.00	0.00	0.00	0.00	0.00	0.00	0.00	0.00	0.00
5.30	1.09	8.25	32.65	671.50	198.50	47.86	58.96	1.312	1.126	6.16	11.10	70.44	74.63	1.951	0.317
5.93	1.22	8.30	32.64	661.17	225.60	47.86	57.82	1.312	1.158	5.50	9.96	65.88	69.89	1.626	0.296
7.73	1.59	8.50	32.56	661.17	288.90	47.86	56.78	1.312	1.188	4.21	8.92	56.30	60.43	1.186	0.282
9.63	1.98	8.90	32.42	661.17	332.50	47.86	55.53	1.312	1.191	3.37	7.67	49.71	54.34	0.980	0.291
12.40	2.55	9.10	32.35	661.17	374.90	49.58	56.20	1.312	1.151	2.61	6.62	43.30	50.28	0.863	0.331
13.33	2.74	9.12	32.34	661.17	395.60	49.58	55.78	1.312	1.162	2.43	6.20	40.17	47.01	0.777	0.320

Experiments at Bowater

20" pilot column: diameter = 50.8 cm, height = 540 cm

% Consistency = ~1.0 % (Plant)

Froth Depth = zero cm

T = 41 °C

Jg cm/s	Jl cm/s	% Eg	ERIC F	ERIC A	Brightness F	Brightness A	%Consit. F	%Consit. A	time min	B. gain	% Flot. effic.	% Rec	k
2.64	0.89	10.24	885	325	47.6	56.0	1.40	1.10	9.05	8.38	63.27	71.18	0.2923
2.81	0.62	11.30	989	230	46.7	57.0	1.43	1.15	12.84	10.30	76.74	81.29	0.4469
2.92	0.71	11.56	1083	310	46.3	56.4	1.45	1.13	11.20	10.14	71.37	77.71	0.3693
2.97	0.76	11.90	1083	285	46.3	55.3	1.45	1.25	10.45	9.03	73.68	77.31	0.3807
3.08	0.49	13.56	926	207	46.4	59.8	1.40	1.03	15.77	13.36	77.63	83.59	0.5203
3.12	1.13	13.84	895	365	47.6	54.9	1.50	1.12	6.86	7.26	59.27	69.47	0.3483
3.16	0.57	14.80	989	207	46.8	60.4	1.43	1.20	13.38	13.63	79.07	82.49	0.5083
3.17	0.95	15.70	877	233	46.8	59.1	1.43	1.19	7.98	12.35	73.38	77.93	0.5017
3.17	0.80	15.45	877	229	46.8	59.3	1.43	1.14	9.46	12.53	73.85	79.18	0.4811
3.22	0.66	15.80	989	245	46.8	59.4	1.43	1.10	11.52	12.62	75.22	81.03	0.4874
3.22	1.00	17.24	977	258	46.8	56.6	1.43	1.27	7.44	9.82	73.59	76.54	0.4839
3.28	0.96	17.12	956	246	46.4	57.6	1.41	1.21	7.76	11.15	74.25	77.87	0.5172
3.28	1.09	17.72	946	250	46.4	56.5	1.42	1.31	6.79	10.04	73.56	75.51	0.4907

4" lab column

SS #	Jg [cm/s]	Jl [cm/s]	% Eg	% Rec	Db [cm]	Sb [1/s]	K
1	0.58	1.23	5.30	70.32	0.0930	37.42	0.2927
1	0.58	1.67	5.45	61.70	0.0962	36.17	0.2976
1	0.58	2.09	5.50	53.19	0.0996	34.94	0.2851
1	0.58	2.60	5.60	51.76	0.1031	33.75	0.3395
1	1.16	1.11	10.84	78.94	0.1023	68.00	0.4040
1	1.16	1.21	10.90	75.88	0.1029	67.64	0.3811
1	1.16	1.69	11.20	69.67	0.1055	65.97	0.4188
1	1.16	2.09	11.10	63.36	0.1104	63.04	0.4179
1	1.16	2.68	11.30	56.51	0.1151	60.47	0.4321
1	1.16	2.89	11.35	53.64	0.1169	59.54	0.4263
1	1.74	1.13	19.30	83.96	0.0976	106.97	0.6406
1	1.74	1.61	20.20	78.78	0.0996	104.82	0.6494
1	1.74	2.09	20.30	73.78	0.0986	105.88	0.6739
1	1.74	2.52	20.40	70.87	0.0996	104.82	0.7278
2	1.53	1.25	12.98	79.56	0.1259	72.92	0.4834
2	1.53	1.65	13.20	73.63	0.1287	71.33	0.4859
2	1.53	2.19	13.70	67.55	0.1271	72.23	0.5175
2	1.53	2.56	13.80	61.89	0.1236	74.27	0.5033
2	2.36	1.22	20.28	82.95	0.1281	110.54	0.6385
2	2.36	1.68	20.45	80.10	0.1269	111.58	0.7281
2	2.36	2.15	20.89	78.69	0.1278	110.80	0.8701
2	2.36	2.57	21.10	74.28	0.1253	113.01	0.8537
2	2.83	1.28	24.49	81.79	0.1270	133.70	0.6535
2	2.83	1.70	25.10	79.81	0.1306	130.02	0.7719
2	2.83	2.13	25.40	77.66	0.1323	128.34	0.8689
2	2.83	2.60	25.76	76.46	0.1360	124.85	1.0080
2	3.06	1.28	26.57	82.47	0.1293	142.00	0.7051
2	3.06	1.69	27.40	79.39	0.1325	138.57	0.7745
2	3.06	2.18	27.90	76.25	0.1319	139.20	0.8636
2	3.06	2.61	27.63	71.46	0.1406	130.58	0.8470
2	3.30	1.29	28.75	82.03	0.1318	150.23	0.7074
2	3.30	1.74	29.12	80.16	0.1372	144.31	0.8490
2	3.30	2.18	29.76	74.23	0.1320	150.00	0.8127
2	3.30	2.61	29.98	71.57	0.1378	143.69	0.8810
5	1.16	1.10	5.85	71.39	0.1489	46.74	0.2744
5	1.16	1.27	5.90	66.01	0.1491	46.68	0.2623
5	1.16	1.66	5.90	59.76	0.1471	47.31	0.2800
5	1.16	2.00	6.10	52.20	0.1477	47.12	0.2667
5	1.16	2.56	6.20	46.22	0.1534	45.37	0.2827
5	1.16	2.78	6.21	45.11	0.1558	44.67	0.2961
5	1.74	1.09	8.25	74.63	0.1649	63.31	0.3167
5	1.74	1.22	8.30	69.89	0.1651	63.23	0.2958
5	1.74	1.59	8.50	60.43	0.1645	63.47	0.2817
5	1.74	1.98	8.90	54.34	0.1600	65.25	0.2911
5	1.74	2.55	9.10	50.28	0.1624	64.29	0.3307
5	1.74	2.74	9.12	47.01	0.1641	63.62	0.3203

20" pilot unit

Jg [cm/s]	Jl [cm/s]	% Eg	% Rec	Db [cm]	Sb [1/s]	K
2.64	0.89	10.24	71.18	0.2943	53.81	0.2923
2.81	0.62	11.30	81.29	0.2842	59.38	0.4469
2.92	0.71	11.56	77.71	0.2883	60.74	0.3693
2.97	0.76	11.90	77.31	0.2848	62.53	0.3807
3.08	0.49	13.56	83.59	0.2597	71.25	0.5203
3.12	1.13	13.84	69.47	0.2571	72.72	0.3483
3.16	0.57	14.80	82.49	0.2436	77.77	0.5083
3.17	0.95	15.70	77.93	0.2303	82.50	0.5017
3.17	0.80	15.45	79.18	0.2346	81.18	0.4811
3.22	0.66	15.80	81.03	0.2324	83.02	0.4874
3.22	1.00	17.24	76.54	0.2130	90.56	0.4839
3.28	0.96	17.12	77.87	0.2188	89.96	0.5172
3.28	1.09	17.72	75.51	0.2114	93.11	0.4907